

AN EXAMINATION OF STREAM REAERATION COEFFICIENTS AND
HYDRAULIC CONDITIONS IN A POOL-AND-RIFFLE STREAM

by

James Lloyd Smoot

Dissertation submitted to the Faculty of the
Virginia Polytechnic Institute and State University
in partial fulfillment of the requirements for the degree of
Doctor of Philosophy
in
Civil Engineering

APPROVED:

Robert C. Hoehn

Clifford W. Randall

John T. Novak

Chin Y. Kuo

James M. Wiggert

January, 1988

Blacksburg, Virginia

AN EXAMINATION OF STREAM REAERATION COEFFICIENTS AND
HYDRAULIC CONDITIONS IN A POOL-AND-RIFFLE STREAM

by

James Lloyd Smoot

Committee Chairman: Robert C. Hoehn
Civil Engineering

(ABSTRACT)

Oxygen transfer between flowing surface waters and the atmosphere can be mathematically described as a first-order reaction and is known as stream reaeration. The first-order rate coefficient or stream reaeration coefficient is a necessary input parameter to stream water-quality models and is partially controlled by the hydraulic conditions of the stream. These coefficients may vary for a given stream reach because of varying hydraulic characteristics brought about by streamflow changes.

Hydraulic measurements and reaeration coefficient determinations were made on four pool-and-riffle reaches of Middle Fork Beargrass Creek near Louisville, Kentucky using the hydrocarbon gas tracer technique. Measurements were made on each reach for up to seven streamflow conditions ranging from extremely low to medium. Contrary to published findings applicable to reaches not characterized by a series of pools and riffles, the reaeration coefficient was shown to increase with increasing streamflow for all four reaches studied. Therefore, stream water-quality models developed for these, or similar, stream reaches using reaeration coefficients determined at normal streamflow conditions

may over estimate the influence of atmospheric reaeration under a much lower flow condition, such as extreme low flow--the selected critical condition for which water-quality models are commonly developed.

Twenty-five published equations used for estimating stream reaeration coefficients were evaluated using the measured hydraulic and reaeration data and were shown to generate highly variable and generally inaccurate predictions. Over half of the equations generated mean prediction errors of more than 50 percent. The best equation overall generated a mean prediction error of 15 percent. The equations were also shown to be highly sensitive to the methods used for determining the input parameter values.

Four equations were statistically developed from the data collected in this research. Two of the equations provided more accurate estimates for the four studied reaches than any of the 25 published equations. Mean prediction errors for the two were 1.2 and 9.2 percent. For verification, the developed equations were also evaluated against the 25 published equations using published reaeration and hydraulic data from 39 hydrocarbon gas tracer measurements on other streams. The two developed equations which were most accurate for the four study reaches were also determined to be superior to all of the 25 published equations using the verification data. Mean prediction errors for the two equations using the verification data were 2.3 and 5.5 percent.

ACKNOWLEDGMENTS

Many persons have contributed to the successful completion of this dissertation. The author would first like to acknowledge the contributions made by his graduate committee chairman, Dr. Robert C. Hoehn. Dr. Hoehn provided the author a rich background for this research through coverage of related material in graduate coursework. He also gave freely of his time and provided direction and support throughout the research. The other members of the author's graduate committee, Drs. Clifford W. Randall, John T. Novak, Chin Y. Kuo, and James M. Wiggert, also contributed guidance and constructive criticism to the author during his research.

The author would also like to acknowledge the financial support provided by the U.S. Geological Survey throughout the author's doctoral coursework and research. They also contributed to this research by providing necessary equipment and support personnel for field measurements, laboratory analyses, and data reduction.

The most significant contribution to the author in completing this dissertation was made by his family (his wife, Chris, and children, Stacey, Heather, and Kyle). Chris typed much of this dissertation--from an almost-illegible hand-written draft. Sacrifices were also made by his children during the numerous evenings, weekends, holidays, and vacations when the author was busy working on this research rather than participating in family activities. Additionally, his family's love, support, and encouragement helped the author more than words can

express. Therefore, this dissertation is dedicated to them--Chris, Stacey, Heather, and Kyle.

TABLE OF CONTENTS

Abstract.....	ii
Acknowledgments.....	iv
Table of contents.....	vi
List of tables.....	x
List of figures.....	xiii
Introduction.....	1
Background.....	2
Research objectives.....	3
Literature review.....	5
Theory of reaeration through air-water interface.....	5
Film models.....	8
Surface-renewal models.....	11
Kinetic theory.....	14
Large eddy.....	15
Turbulent diffusion.....	15
Effect of hydraulic factors on the reaeration coefficient....	17
Effect of environmental factors on the reaeration coefficient.....	19
Temperature.....	19
Wind.....	21
Suspended sediment.....	23
Surfactants.....	24
Other.....	26
Effect of streamflow changes to the reaeration coefficient...	27

Methods for predicting reaeration coefficients.....	32
Theoretically based equations.....	33
Semiempirical equations.....	35
Empirical equations.....	39
Methods for measuring reaeration coefficients.....	44
Dissolved-oxygen balance.....	44
Disturbed equilibrium.....	49
Tracer gas.....	50
Materials and methods.....	58
Site selection and description.....	58
Field survey.....	62
Tracer-gas techniques.....	63
Slug injection.....	65
Steady-state injection.....	67
Tracer injection.....	69
Dye sampling and measurement.....	72
Gas sampling and measurement.....	74
Field measurements.....	76
Tracer computation.....	79
Hydraulic computation.....	81
Computation error analysis.....	86
Error analysis of prediction equations.....	88
Prediction equation development.....	89
Results and discussion.....	91
Measurements and conditions.....	91

Physical and hydraulic properties.....	91
Hydrocarbon gas tracer measurements.....	125
Example computations from hydrocarbon gas tracer measurements.....	136
Discussion.....	151
Effect of streamflow changes to the reaeration coefficient...	154
Comparative analysis.....	154
Discussion.....	158
Evaluation of published reaeration coefficient prediction equations.....	158
Comparative analysis.....	159
Sensitivity of predictions to the methods of parameter value determination.....	162
Discussion.....	175
Prediction equation development.....	176
Equation building and selection.....	177
Verification analysis.....	189
Discussion.....	195
Conclusions.....	197
References cited.....	200
Additional references.....	206
Appendices.....	210
Appendix A -- Analytical method for determination of propane in water.....	211

Appendix B -- Time-concentration data for dye and propane from field measurements.....	215
Appendix C -- Plots of reaeration coefficient versus selected hydraulic parameters.....	241
Appendix D -- Reaeration prediction equation verification data sets.....	249
Vita.....	253

LIST OF TABLES

Table 1 -- Summary of selected reaeration coefficient prediction equations from the literature.....	45
Table 2 -- Streamflow exceedance probabilities and 7-day lowflow return periods for flow conditions during hydrocarbon gas tracer measurements made on reaches of the Middle Fork Beargrass Creek.....	94
Table 3 -- Summary of cross section surveying of tracer measurement reaches of Middle Fork Beargrass Creek....	99
Table 4 -- Hydraulic parameter results from tracer measurements made on reaches of the Middle Fork Beargrass Creek....	101
Table 5 -- Hydraulic parameter results from tracer measurements made on reaches of the Middle Fork Beargrass Creek....	103
Table 6 -- Hydraulic parameter results from tracer measurements made on reaches of the Middle Fork Beargrass Creek....	104
Table 7 -- Selected characteristics of reaches of Middle Fork Beargrass Creek during hydrocarbon gas tracer measurements.....	105
Table 8 -- Environmental conditions during hydrocarbon gas tracer measurements made in Middle Fork Beargrass Creek.....	124
Table 9 -- Hydrocarbon gas tracer technique injections made in Middle Fork Beargrass Creek.....	126
Table 10 -- Reaeration and propane desorption coefficients and water temperatures from hydrocarbon gas tracer measurements made on reaches of the Middle Fork Beargrass Creek.....	134
Table 11 -- Error propagation through reaeration coefficient computations using a relative error common to all hydrocarbon gas tracer measurements.....	137
Table 12 -- Dye time-concentration data and computed areas, centroids, and masses for the upstream end of reach B during hydrocarbon gas tracer measurements made on reaches of the Middle Fork Beargrass Creek, May 16, 1985.....	139

Table 13 -- Dye time-concentration data and computed areas, centroids, and masses for the downstream end of reach B during hydrocarbon gas tracer measurements made on reaches of the Middle Fork Beargrass Creek, May 16, 1985.....	141
Table 14 -- Propane time-concentration data and computed areas, centroids, and masses for the upstream end of reach B during hydrocarbon gas tracer measurements made on reaches of the Middle Fork Beargrass Creek, May 16, 1985.....	143
Table 15 -- Propane time-concentration data and computed areas, centroids, and masses for the downstream end of reach B during hydrocarbon gas tracer measurements made on reaches of the Middle Fork Beargrass Creek, May 16, 1985.....	144
Table 16 -- Dye time-concentration data and computed areas, centroids, and masses for the upstream end of reach D during hydrocarbon gas tracer measurements made on reaches of the Middle Fork Beargrass Creek, May 7, 1985.....	148
Table 17 -- Dye time-concentration data and computed areas, centroids, and masses for the downstream end of reach D during hydrocarbon gas tracer measurements made on reaches of the Middle Fork Beargrass Creek, May 7, 1985.....	149
Table 18 -- Characteristics of simple linear regressions between the reaeration coefficient and discharge for hydrocarbon gas tracer measurements on reaches of Middle Fork Beargrass Creek.....	157
Table 19 -- Error analysis and relative ranking for selected reaeration coefficient predictive equations using hydrocarbon gas tracer measurements from reaches of Middle Fork Beargrass Creek.....	160
Table 20 -- Error analysis for selected reaeration coefficient predictive equations using three different methods of input parameter value determination for hydrocarbon gas tracer measurements on reaches of Middle Fork Beargrass Creek.....	173

Table 21 -- Summary of error analysis for selected reaeration coefficient predictive equations using three different methods of input parameter value determination for hydrocarbon gas tracer measurements on reaches of Middle Fork Beargrass Creek.....	174
Table 22 -- Statistical measures of fit for reaeration coefficient prediction equations developed from hydrocarbon gas tracer measurements on reaches of Middle Fork Beargrass Creek.....	184
Table 23 -- Verification error analysis and relative ranking for selected reaeration coefficient predictive equations using 39 hydrocarbon gas tracer measurements on 23 stream reaches in Massachusetts and Kentucky.....	193
Table 24 -- Verification data set from results of 39 hydrocarbon gas tracer measurements on 23 stream reaches in Kentucky and Massachusetts.....	250
Table 25 -- Reaeration coefficient prediction results for the Kentucky and Massachusetts verification data set.....	251

LIST OF FIGURES

Figure 1 -- Simplified dissolved-oxygen budget for a stream in contact with the atmosphere.....	6
Figure 2 -- Schematic of the surface film theory of gas transfer.	9
Figure 3 -- Stylized profiles for pool-and-riffle and channel-controlled stream reaches under various flow conditions.....	30
Figure 4 -- Middle Fork Beargrass Creek location map.....	61
Figure 5 -- Flow duration curve for daily mean discharges for Middle Fork Beargrass Creek, 1966-1985.....	93
Figure 6 -- Estimated return periods and 7-day annual low flows for Middle Fork Beargrass Creek, 1966-1985.....	96
Figure 7 -- Hydrograph of mean daily discharge for Middle Fork Beargrass Creek during the period of hydrocarbon gas tracer measurements, April through September, 1985...	98
Figure 8 -- Comparison of reach-averaged depth and reach-averaged hydraulic radius determined from length-weighted hydraulic measurements.....	107
Figure 9 -- Reach-averaged water-surface slope shown as a function of discharge for reaches of Middle Fork Beargrass Creek, from tracer measurements made from April 18, 1985 through September 18, 1985.....	108
Figure 10 -- Reach-averaged velocity shown as a function of discharge for reaches of Middle Fork Beargrass Creek, from tracer measurements made from April 18, 1985 through September 18, 1985.....	109
Figure 11 -- Reach-averaged depth shown as a function of discharge for reaches of Middle Fork Beargrass Creek, from tracer measurements made from April 18, 1985 through September 18, 1985.....	110
Figure 12 -- Reach-averaged width shown as a function of discharge for reaches of Middle Fork Beargrass Creek, from tracer measurements made from April 18, 1985 through September 18, 1985.....	111

Figure 13 -- Reach-averaged cross-sectional area shown as a function of discharge for reaches of Middle Fork Beargrass Creek, from tracer measurements made from April 18, 1985 through September 18, 1985.....	112
Figure 14 -- Reach-averaged Froude number shown as a function of discharge for reaches of Middle Fork Beargrass Creek, from tracer measurements made from April 18, 1985 through September 18, 1985.....	113
Figure 15 -- Reach-averaged shear velocity shown as a function of discharge for reaches of Middle Fork Beargrass Creek, from tracer measurements made from April 18, 1985 through September 18, 1985.....	114
Figure 16 -- Reach-averaged dispersion coefficient shown as a function of discharge for reaches of Middle Fork Beargrass Creek, from tracer measurements made from April 18, 1985 through September 18, 1985.....	115
Figure 17 -- Reach-averaged shear stress shown as a function of discharge for reaches of Middle Fork Beargrass Creek, from tracer measurements made from April 18, 1985 through September 18, 1985.....	116
Figure 18 -- Reach-averaged Reynolds number shown as a function of discharge for reaches of Middle Fork Beargrass Creek, from tracer measurements made from April 18, 1985 through September 18, 1985.....	117
Figure 19 -- Reach-averaged Manning "n" value shown as a function of discharge for reaches of Middle Fork Beargrass Creek, from tracer measurements made from April 18, 1985 through September 18, 1985.....	118
Figure 20 -- Coefficient of variation of cross-sectional area as a function of discharge for reaches of Middle Fork Beargrass Creek, from tracer measurements made from April 18, 1985 through September 18, 1985.....	122
Figure 21 -- Interquartile range divided by the median (expressed as a percent) value of cross-sectional area as a function of discharge for reaches of Middle Fork Beargrass Creek, from tracer measurements made from April 18, 1985 through September 18, 1985.....	123
Figure 22 -- Dye and propane concentration from hydrocarbon gas tracer measurements made on Middle Fork Beargrass Creek, upstream end of reach A (upstream end of reach C), May 16, 1985 tracer injection.....	127

Figure 23 -- Dye and propane concentration from hydrocarbon gas tracer measurements made on Middle Fork Beargrass Creek, downstream end of reach A (upstream end of reach B), May 16, 1985 tracer injection.....	128
Figure 24 -- Dye and propane concentration from hydrocarbon gas tracer measurements made on Middle Fork Beargrass Creek, downstream end of reach B (downstream end of reach C), May 16, 1985 tracer injection.....	129
Figure 25 -- Dye and propane concentration from hydrocarbon gas tracer measurements made on Middle Fork Beargrass Creek, upstream end of reach D, May 7, 1985 tracer injection.....	132
Figure 26 -- Dye and propane concentration from hydrocarbon gas tracer measurements made on Middle Fork Beargrass Creek, downstream end of reach D, May 7, 1985 tracer injection.....	133
Figure 27 -- Reaeration coefficient shown as a function of discharge for reaches of Middle Fork Beargrass Creek, from tracer measurements made from April 18, 1985 through September 18, 1985.....	135
Figure 28 -- Linear relations between the reaeration coefficient and discharge for reaches of Middle Fork Beargrass Creek, from hydrocarbon gas tracer measurements made from April 18, 1985 through September 18, 1985.....	156
Figure 29 -- Schematic box plots of reaeration coefficient estimates using selected prediction equations and hydrocarbon gas tracer measurement data from reaches of Middle Fork Beargrass Creek.....	161
Figure 30 -- Comparison of mean velocity determined by three different methods for reach A of the Middle Fork Beargrass Creek, from tracer measurements made between April 18, 1985 and September 18, 1985.....	164
Figure 31 -- Comparison of mean velocity determined by three different methods for reach B of the Middle Fork Beargrass Creek, from tracer measurements made between April 18, 1985 and September 18, 1985.....	165
Figure 32 -- Comparison of mean velocity determined by three different methods for reach C of the Middle Fork Beargrass Creek, from tracer measurements made between April 18, 1985 and September 18, 1985.....	166

Figure 33 -- Comparison of mean velocity determined by three different methods for reach D of the Middle Fork Beargrass Creek, from tracer measurements made between April 18, 1985 and September 18, 1985.....	167
Figure 34 -- Comparison of mean depth determined by three different methods for reach A of the Middle Fork Beargrass Creek, from tracer measurements made between April 18, 1985 and September 18, 1985.....	169
Figure 35 -- Comparison of mean depth determined by three different methods for reach B of the Middle Fork Beargrass Creek, from tracer measurements made between April 18, 1985 and September 18, 1985.....	170
Figure 36 -- Comparison of mean depth determined by three different methods for reach C of the Middle Fork Beargrass Creek, from tracer measurements made between April 18, 1985 and September 18, 1985.....	171
Figure 37 -- Comparison of mean depth determined by three different methods for reach D of the Middle Fork Beargrass Creek, from tracer measurements made between April 18, 1985 and September 18, 1985.....	172
Figure 38 -- Reaeration coefficient shown as a function of reach-averaged water-surface slope for reaches of Middle Fork Beargrass Creek, from tracer measurements made from April 18, 1985 through September 18, 1985.....	178
Figure 39 -- Reaeration coefficient shown as a function of reach-averaged velocity for reaches of Middle Fork Beargrass Creek, from tracer measurements made from April 18, 1985 through September 18, 1985.....	179
Figure 40 -- Reaeration coefficient shown as a function of reach-averaged depth for reaches of Middle Fork Beargrass Creek, from tracer measurements made from April 18, 1985 through September 18, 1985.....	180
Figure 41 -- Reaeration coefficient shown as a function of reach-averaged dispersion coefficient for reaches of Middle Fork Beargrass Creek, from tracer measurements made from April 18, 1985 through September 18, 1985.....	181
Figure 42 -- Comparison of field-measured reaeration coefficients with those predicted using developed equation, P1....	185
Figure 43 -- Comparison of field-measured reaeration coefficients with those predicted using developed equation, P2....	186

Figure 44 -- Comparison of field-measured reaeration coefficients with those predicted using developed equation, P3....	188
Figure 45 -- Comparison of field-measured reaeration coefficients with those predicted using developed equation, P4....	190
Figure 46 -- Schematic box plots of reaeration coefficient estimates using developed prediction equations and hydrocarbon gas tracer measurement data from reaches of Middle Fork Beargrass Creek.....	191
Figure 47 -- Dye and propane concentration from hydrocarbon gas tracer measurements made on Middle Fork Beargrass Creek, upstream end of reach A (upstream end of reach C), April 18, 1985 tracer injection.....	216
Figure 48 -- Dye and propane concentration from hydrocarbon gas tracer measurements made on Middle Fork Beargrass Creek, downstream end of reach A (upstream end of reach B), April 18, 1985 tracer injection.....	217
Figure 49 -- Dye and propane concentration from hydrocarbon gas tracer measurements made on Middle Fork Beargrass Creek, downstream end of reach B (downstream end of reach C), April 18, 1985 tracer injection.....	218
Figure 50 -- Dye and propane concentration from hydrocarbon gas tracer measurements made on Middle Fork Beargrass Creek, upstream end of reach A (upstream end of reach C), May 8, 1985 tracer injection.....	219
Figure 51 -- Dye and propane concentration from hydrocarbon gas tracer measurements made on Middle Fork Beargrass Creek, downstream end of reach A (upstream end of reach B), May 8, 1985 tracer injection.....	220
Figure 52 -- Dye and propane concentration from hydrocarbon gas tracer measurements made on Middle Fork Beargrass Creek, downstream end of reach B (downstream end of reach C), May 8, 1985 tracer injection.....	221
Figure 53 -- Dye and propane concentration from hydrocarbon gas tracer measurements made on Middle Fork Beargrass Creek, upstream end of reach A (upstream end of reach C), May 16, 1985 tracer injection.....	222

Figure 54 -- Dye and propane concentration from hydrocarbon gas tracer measurements made on Middle Fork Beargrass Creek, downstream end of reach A (upstream end of reach B), May 16, 1985 tracer injection.....	223
Figure 55 -- Dye and propane concentration from hydrocarbon gas tracer measurements made on Middle Fork Beargrass Creek, downstream end of reach B (downstream end of reach C), May 16, 1985 tracer injection.....	224
Figure 56 -- Dye and propane concentration from hydrocarbon gas tracer measurements made on Middle Fork Beargrass Creek, upstream end of reach A (upstream end of reach C), May 24, 1985 tracer injection.....	225
Figure 57 -- Dye and propane concentration from hydrocarbon gas tracer measurements made on Middle Fork Beargrass Creek, downstream end of reach A (upstream end of reach B), May 24, 1985 tracer injection.....	226
Figure 58 -- Dye and propane concentration from hydrocarbon gas tracer measurements made on Middle Fork Beargrass Creek, downstream end of reach B (downstream end of reach C), May 24, 1985 tracer injection.....	227
Figure 59 -- Dye and propane concentration from hydrocarbon gas tracer measurements made on Middle Fork Beargrass Creek, upstream end of reach A (upstream end of reach C), June 14, 1985 tracer injection.....	228
Figure 60 -- Dye and propane concentration from hydrocarbon gas tracer measurements made on Middle Fork Beargrass Creek, downstream end of reach A (upstream end of reach B), June 14, 1985 tracer injection.....	229
Figure 61 -- Dye and propane concentration from hydrocarbon gas tracer measurements made on Middle Fork Beargrass Creek, downstream end of reach B (downstream end of reach C), June 14, 1985 tracer injection.....	230
Figure 62 -- Dye and propane concentration from hydrocarbon gas tracer measurements made on Middle Fork Beargrass Creek, upstream end of reach A, August 19, 1985 tracer injection.....	231
Figure 63 -- Dye and propane concentration from hydrocarbon gas tracer measurements made on Middle Fork Beargrass Creek, downstream end of reach A, August 19, 1985 tracer injection.....	232

Figure 64 -- Dye and propane concentration from hydrocarbon gas tracer measurements made on Middle Fork Beargrass Creek, upstream end of reach A, September 17, 1985 tracer injection.....	233
Figure 65 -- Dye and propane concentration from hydrocarbon gas tracer measurements made on Middle Fork Beargrass Creek, downstream end of reach A, September 17, 1985 tracer injection.....	234
Figure 66 -- Dye and propane concentration from hydrocarbon gas tracer measurements made on Middle Fork Beargrass Creek, upstream end of reach D, April 19, 1985 tracer injection.....	235
Figure 67 -- Dye and propane concentration from hydrocarbon gas tracer measurements made on Middle Fork Beargrass Creek, downstream end of reach D, April 19, 1985 tracer injection.....	236
Figure 68 -- Dye and propane concentration from hydrocarbon gas tracer measurements made on Middle Fork Beargrass Creek, upstream end of reach D, May 7, 1985 tracer injection.....	237
Figure 69 -- Dye and propane concentration from hydrocarbon gas tracer measurements made on Middle Fork Beargrass Creek, downstream end of reach D, May 7, 1985 tracer injection.....	238
Figure 70 -- Dye and propane concentration from hydrocarbon gas tracer measurements made on Middle Fork Beargrass Creek, upstream end of reach D, September 18, 1985 tracer injection.....	239
Figure 71 -- Dye and propane concentration from hydrocarbon gas tracer measurements made on Middle Fork Beargrass Creek, downstream end of reach D, September 18, 1985 tracer injection.....	240
Figure 72 -- Reaeration coefficient shown as a function of reach-averaged width for reaches of Middle Fork Beargrass Creek, from tracer measurements made from April 18, 1985 through September 18, 1985.....	242
Figure 73 -- Reaeration coefficient shown as a function of reach-averaged cross-sectional area for reaches of Middle Fork Beargrass Creek, from tracer measurements made from April 18, 1985 through September 18, 1985.....	243

Figure 74 -- Reaeration coefficient shown as a function of reach-averaged Froude number for reaches of Middle Fork Beargrass Creek, from tracer measurements made from April 18, 1985 through September 18, 1985.....	244
Figure 75 -- Reaeration coefficient shown as a function of reach-averaged shear velocity for reaches of Middle Fork Beargrass Creek, from tracer measurements made from April 18, 1985 through September 18, 1985.....	245
Figure 76 -- Reaeration coefficient shown as a function of reach-averaged shear stress for reaches of Middle Fork Beargrass Creek, from tracer measurements made from April 18, 1985 through September 18, 1985.....	246
Figure 77 -- Reaeration coefficient shown as a function of reach-averaged Reynolds number for reaches of Middle Fork Beargrass Creek, from tracer measurements made from April 18, 1985 through September 18, 1985.....	247
Figure 78 -- Reaeration coefficient shown as a function of reach-averaged Mannings "n" values for reaches of Middle Fork Beargrass Creek, from tracer measurements made from April 18, 1985 through September 18, 1985.....	248

INTRODUCTION

Stream reaeration coefficients are necessary input parameters for stream water-quality models. Water-resource managers and scientists use these models to accurately simulate the in-stream water quality conditions resulting from a variety of existing or proposed land use and water- and waste-management practices. These simulations are useful tools for establishing permitted allocations for oxygen-demanding wastes which maintain water quality above mandated stream standards or for studying the complex processes affecting stream water quality. Generally, these wasteload allocation models are developed for some predetermined critical stream condition which is usually some combination of low flow (less dilution) and high water temperature (high chemical and biological reaction rates). The lowest flow which occurs for seven consecutive days on an average recurrence interval of ten years (7Q10) is often the flow criterion selected. Water-quality models are often most sensitive to the accuracy of the reaeration coefficient. However, because the reaeration process is quite complex and the reaeration coefficient varies over four-orders of magnitude, it is often the most difficult model input parameter to determine accurately.

BACKGROUND

Reaeration coefficients may vary for a given reach under differing hydraulic characteristics brought about by different streamflow conditions. This may introduce error to water-quality models developed for flow conditions other than that prevailing during the determination of the reaeration coefficient. This situation is common because models are developed for very infrequent low-flow conditions. In major rivers and streams with a nearly uniform rate of energy dissipation (channel-controlled), the reaeration coefficient usually decreases with increasing stream discharge. This leads to environmentally conservative model results at extreme low-flow conditions. This result is environmentally acceptable but financially wasteful because of the additional level of waste treatment required. In pool-and-riffle streams in which the hydraulic geometry varies significantly throughout a reach, the influence of flow condition to the reaeration coefficient is less clear.

Reaeration coefficients are usually determined by either field measurement, using surrogate gas tracer techniques, or by the use of prediction equations which relate stream physical and hydraulic parameters to the reaeration coefficient. The tracer-technique measurements are relatively difficult to make, are labor intensive, and are expensive. The resulting reaeration coefficients are valid only at the hydraulic and environmental conditions prevailing during measurement and, therefore, limit the usefulness of the determined values.

Prediction equations also have numerous drawbacks for use in determining reaeration coefficients for water quality model input. The theoretically derived equations, collectively, tend to be inadequate due to the manner in which equation parameters have been related to measurable bulk-flow hydraulic variables. Empirically derived equations tend to be useful only for application to physical and hydraulic conditions which are similar to those of the model development because the complex gas-tracer process has been simplified by the use of a few statistically selected surrogate variables. How these surrogate variables relate to the complex process appears to be site or at least stream-type specific. Additional errors may be introduced by the selection of methods used to measure the parameters that are input to the prediction equations which may differ from those methods used in the development of the equation.

RESEARCH OBJECTIVES

The broad objective of this research was to improve the understanding of the reaeration process occurring in pool-and-riffle streams and how it may be influenced by hydraulic changes associated with varying streamflow conditions. Specific objectives were as follows:

- (1) For selected pool-and-riffle stream reaches, evaluate the influence of streamflow-induced hydraulic changes to field measured reaeration coefficients.
- (2) Using the reaeration coefficients and hydraulic parameters measured to satisfy (1) above, evaluate the accuracy of selected theoretical and empirical prediction equations from the literature.
- (3) Determine the sensitivity of the prediction equations selected in (2) above to the methods used to determine the necessary input parameter values.
- (4) Using the field measured hydraulic parameters and reaeration coefficients, empirically develop equations which can be used to fit the measured data and predict reaeration coefficients for the reaches used in measurement as well as other similar pool-and-riffle streams.

LITERATURE REVIEW

THEORY OF REAERATION THROUGH AIR-WATER INTERFACE

Reaeration is the process whereby oxygen is exchanged between the atmosphere and a water body in contact with the atmosphere. The net direction of this transfer is usually from the atmosphere to the water body, because the dissolved oxygen concentrations in most water bodies is below saturation due to various in-stream uses of the oxygen. However, at times when photosynthetic activity in a water body creates a supersaturated oxygen condition, the net exchange then reverses and oxygen moves from the water to the atmosphere. A simplified dissolved oxygen budget for a stream in contact with the atmosphere is schematically shown in Figure 1.

The process of gas-absorption at the interface between a flowing liquid and a gas is very complicated and only superficially understood (Bennett and Rathbun, 1972). Early work by Adeney and Becker (1919) showed that the absorption of oxygen into water followed a first-order kinetic process. The rate of absorption is proportional to the oxygen deficit as follows:

$$\frac{dD_o}{dt} = -K_2 D_o \quad (1)$$

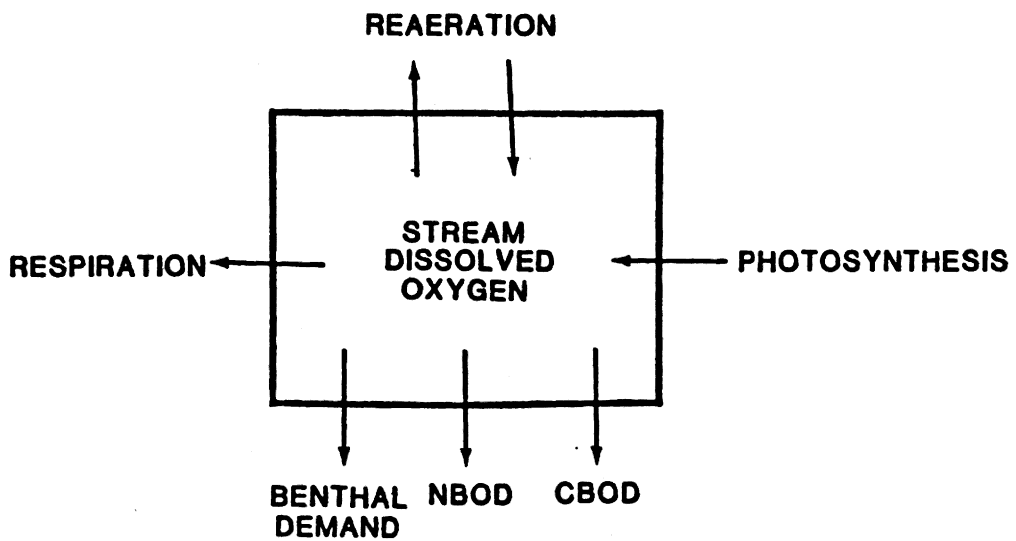


Figure 1 -- Simplified dissolved-oxygen budget for a stream in contact with the atmosphere

where D_o is the dissolved oxygen deficit (the difference between the saturation value of dissolved oxygen (C_s) and the concentration (C) at time, t), K_2 is the reaeration coefficient, and units are compatible. The above relation may also be expressed directly in terms of the dissolved oxygen concentration (C) as:

$$\frac{dC}{dt} = K_2(C_s - C) = \frac{K_L}{D} (C_s - C) \quad (2)$$

where K_L is the reaeration film coefficient, D is the depth of the liquid phase (stream), and units are compatible.

Generally, all subsequent research was conducted on the assumption that the Adeney and Becker (1919) first-order model was correct, and nearly all dispute by researchers was in selecting the reaeration coefficient. Streeter and Phelps (1925) presented the classical oxygen sag model which utilizes the first-order reaeration term but also a first order deoxygenation term. It is given as:

$$\frac{dD_o}{dt} = K_1 L - K_2 D_o \quad (3)$$

where K_1 is the deoxygenation coefficient, L is the ultimate biochemical oxygen demand, and units are compatible. The equation could be used in its integrated form along with field measurements and K_1 calculated from laboratory biochemical oxygen demand (BOD) tests to "back calculate" the

reaeration coefficient. Numerous conceptual models of the mass-transfer process at the gas-liquid interface have been proposed. The models can be divided into groups which include film, surface-renewal, kinetic theory, large eddy, and turbulent-diffusion models (Rathbun, 1977).

Film Models

Whitman (1923) led the field in film theory. He theorized that laminar films of gas and liquid exist at the interface between the two phases. Within the film, the mass transport is in a direction perpendicular to the streamflow and therefore by molecular diffusion alone following Fick's law. This process is much slower than the turbulent diffusion taking place within the remainder of the phases. The resistance to mass transfer is then concentrated in the two films. The interface between the liquid and gas film would offer no resistance to mass transfer. Because oxygen has a relatively low solubility in water, the resistance to mass transfer in the gas film is negligible (Holley, 1973). The model is then simplified to that shown in Figure 2, where the concentration of oxygen (C) throughout the gas film is nearly equal to the concentration in the gas phase (C_g), the concentration in the water phase is uniform, and all the concentration gradient (resistance to mass transfer) is in the liquid film. The concentration of oxygen in the water outside the liquid film is assumed to be kept

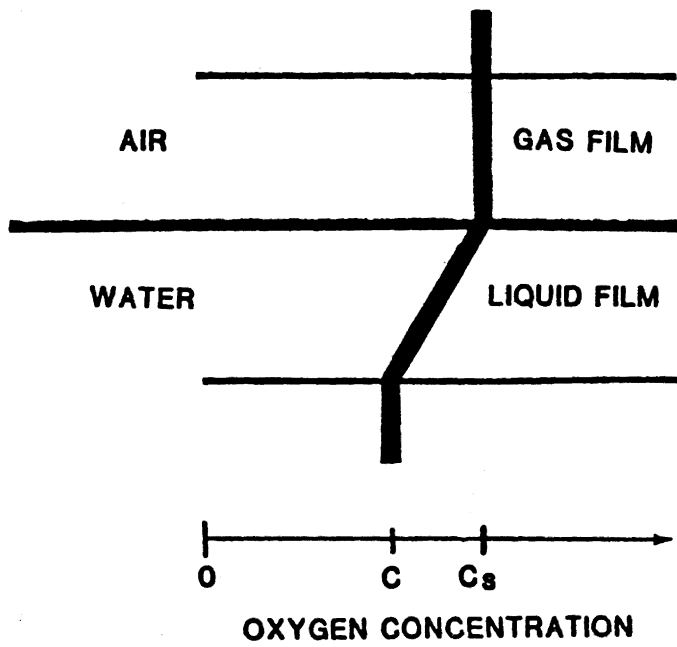


Figure 2 -- Schematic of the surface film theory of gas transfer

uniform by mixing caused by hydrodynamic turbulence. The mass transfer coefficient based on the liquid phase, K_L , is given by:

$$K_L = \frac{D_m}{L_f} \quad (4)$$

where D_m is the molecular diffusivity, L_f is the film layer thickness, and units are compatible. But $K_2 = K_L/D$ so:

$$K_2 = \frac{D_m}{L_f D} \quad (5)$$

where D is the mean depth of the liquid phase (stream) in compatible units.

Holley (1973) and Bennett and Rathbun (1972) pointed out the many shortcomings of the film model. The validity of the assumption that a stagnant film is present on the surface of a turbulent liquid is questionable for the field situation of open-channel flow. However, Bennett and Rathbun (1972) pointed out that the concept of diffusion into laminar patches of infinitesimal area existing for short periods of time on the water surface before being replaced by liquid from the bulk liquid has been used in further conceptual model development.

Surface-Renewal models

Renewal models include those of film-penetration, penetration, and surface-renewal-damped-eddy diffusivity models (Bennett and Rathbun, 1972). The renewal models assume molecular diffusion into a surface layer which is purely molecular. The surface layer may be of varying thickness. Below the layer, diffusivity in the liquid is assumed to be infinite, which would make the concentration independent of depth. After gas diffusion into a parcel within the surface layer for some time, the parcel is exchanged with one from the bulk liquid. The frequency of renewal is described by an assumed probability-density function.

According to Holley (1973) and Bennett and Rathbun (1972), Higbie (1935) and Danckwerts (1951) viewed the surface of the liquid as being a laminar film but that the thickness of the film was large with respect to the depth penetrated by the molecular diffusion during life of the film. The differences in their theories lies in how the parcels are replaced. Higbie (1935) theorized that all the parcels would be replaced after a uniform age, while Danckwerts (1951) thought that the ages would follow a distribution similar to a normal distribution. These two theories, like the film model, would relate the mass-transfer coefficient to molecular diffusivity and thickness of the surface layer, but also to an average renewal frequency. Danckwerts (1951) relation is given as:

$$K_L = (D_m s)^{0.5} \quad (6)$$

where s is the average rate of surface renewal in reciprocal time units compatible with D_m . A shortcoming of the two theories was that the authors did not attempt to relate surface renewal to open channel flow mechanics.

Danckwert's (1951) model was modified by Dobbins (1956) to account for a wide range of surface renewal rates. When s is small his model would approach the film model, and when s is large it would approach Danckwert's (1951) penetration model. Bennett and Rathbun (1972) presented later modifications to Dobbins (1956) model, but also stated that they were not widely accepted. O'Connor and Dobbins (1958) pointed out with their calculations that for open channel flow in rivers, the Dobbins (1956) model would usually reduce to the Danckwert's (1951) model. They also attempted to relate the Dobbins (1956) model parameters to those of open channel flow. The mean rate of surface renewal was then the only parameter needing relation. They recognized two classes of river turbulence: nonisotropic and isotropic. For nonisotropic (Chezy C less than 17 or mean depth less than about 5 feet) turbulence, s could be related to hydraulic terms by the Prandtl mixing length and the vonKarman logarithmic velocity law. For this nonisotropic turbulence case, the mass transfer coefficient is then given as:

$$K_L = c_1 \frac{D_m^{0.5} S^{0.25}}{D^{0.25}} \quad (7)$$

where c_1 is a constant and varies with different units used, and S is the channel slope. For isotropic turbulence O'Connor and Dobbins (1958) used field measurements which showed that the average rate of surface renewal, s , was equal to the average stream velocity divided by the mean depth. The mass-transfer coefficient was then given as:

$$K_L = c_2 (D_m V / D)^{0.5} \quad (8)$$

where c_2 varies with different units used and V is the mean stream velocity.

Additional efforts to combine the film model with the penetration concept have been made by many researchers (Bennett and Rathbun, 1972). These film-penetration models are idealized in that the process of gas transfer takes place in two separate steps - molecular diffusion and then turbulent diffusion. This idealization has resulted in some difficulties in relating model parameters to flow parameters. The O'Connor and Dobbins (1958) methods for evaluating these parameters is quite simplistic. Bennett and Rathbun (1972) reported efforts by other researchers which are more sophisticated but require the evaluation of additional experimental coefficients.

King (1966) proposed a surface-renewal-damped-eddy diffusivity

model which recognized that mass transport near the surface is due not only to molecular diffusion but also to turbulent diffusion caused by small-scale eddies. This theory results in three additional parameters which would need to be determined. Bennett and Rathbun (1972) reported follow-up work by other researchers which relates one of the three factors to energy dissipation, fluid viscosity and density. Even though King's (1966) model is physically more realistic, it has had little practical use because of the difficulty in obtaining input for the added parameters.

Kinetic Theory

Krenkel and Orlob (1963) presented a kinetic theory originally developed by Miyamoto (1932). The model is based on the velocity of molecules arriving at the interface from both the gas and the liquid phases. It also considers the frequency of the arrival.

Tsivoglou (1967) presented a kinetic-theory model which considered the rate of entry and loss of oxygen molecules from water. The resulting mass transfer coefficient, K_L was theorized to be a function of the surface layer thickness, number of new surface layers exposed per unit of time, and the proportion of molecules in the surface layer that escape. This model is of little practical use because the parameters can not be measured. Tsivoglou (1967) also presented an application of

Einstein's law of diffusion which stated that the mass-transfer coefficient for a gas is proportional to its molecular diameter. This finding has not been universally accepted because experimental evidence suggests a different relationship (Bennett and Rathbun, 1972).

Large Eddy

The large eddy model as developed by Fortescue and Pearson (1967) and presented by Bennett and Rathbun (1972) assumes that mass transfer at a turbulent liquid surface can be modeled by a series of steady-roll cells. The turbulence intensity and a scale factor for the roll cells are necessary parameters. Because these parameters can not be measured, the mean velocity and mean depth are substituted which results in an equation of the form of O'Connor and Dobbins (1958) for the case of isotropic turbulence.

Turbulent Diffusion

Many of the theoretical models presented assume some type of surface layer in which, at least near the interface, the molecular diffusion process is dominant. Bennett and Rathbun (1972) reference Kishinevsky (1955) as postulating his surface rejuvenation theory, that for high turbulence levels the turbulent diffusion process is not

damped-out at the water surface. He found that in open-channel flows the turbulence level is not high enough to make the turbulent diffusion model applicable. Only laboratory stirred-tank experiments generating a high level of turbulence could validate the model. It becomes evident then that each of the theoretical models discussed previously has a varying range of dependence on D_m in predicting the gas transfer coefficient. Therefore, each of the models should only be applicable for a range of turbulence conditions.

In turbulent free-surface flow, evidence indicates that turbulence exists at the water surface. However, the critical region in the absorption process for oxygen is in the region immediately below the surface which can be viewed as a film. The diffusion and boundary-layer concepts have been successfully used to represent the oxygen transport away from the water surface (Holly, 1973).

Reaeration of turbulent free-surface flows then appears to involve two physical processes--molecular diffusion of the oxygen and hydrodynamic mixing of the water. The mixing allows for the continuous replacement of the water near the surface layer and thus increases the rate of oxygen molecules entering the water and the subsequent rate at which the oxygen is distributed throughout the water phase.

EFFECT OF HYDRAULIC FACTORS ON THE REAERATION COEFFICIENT

As was presented in the previous section, many conceptual models have been developed over the years in attempts to explain the reaeration process. Many of these models contain parameters which are either impossible or at least difficult to quantify. Efforts have been made to relate the parameters in these models to some physical and hydraulic parameters that can be determined. Some researchers (Churchill and others, 1962), instead of trying to relate the physical and hydraulic parameters to parameters in conceptual models which oversimplify the reaeration process, develop empirical relations with measured parameters.

Tsivoglou and Neal (1976) carefully considered that reaeration is a direct function of the rate of water-surface renewal; therefore, it was necessary to distinguish between hydraulic properties that cause turbulence and those which only reflect turbulence. They also reconsidered the true meanings of simple terms such as velocity, depth, and roughness and how such terms should be measured. They saw the slope as the most basic of causative factors because the slope influences the velocity, depth, and turbulence. Because reaeration is a time-dependent process, the time of flow was also considered to be of great importance. These two factors taken together gives rise to their theory that the reaeration coefficient should be proportional to the rate of elevation change--or energy dissipation. Elevation change divided by travel time equals the slope multiplied by the mean velocity.

From the development of the O'Connor and Dobbins (1958) equations based on the film-penetration model, velocity, depth, and slope were shown to be key parameters for open-channel flow cases of nonisotropic and isotropic turbulence.

Isaacs and Gaudy (1968) used the reaeration coefficient, velocity, depth, molecular diffusivity, kinematic viscosity, and the gravitational constant and formed four dimensionless parameters. These included the Reynolds number, Froude number, Schmidt number, and a fourth consisting of the reaeration coefficient multiplied by the depth squared and divided by the molecular diffusivity. When combined and constrained by constant temperature they showed that K_2 should be a function of velocity and depth.

Churchill and others (1962) had previously formed five dimensionless groups. Their work had resulted in 19 regression models involving the dimensionless parameter groups. Their most promising models contained the parameters velocity, depth, or slope.

The physical and hydraulic parameters used by nearly all researchers to develop reaeration prediction models include some combination of velocity, mean depth, energy slope, channel slope, hydraulic radius, resistance coefficient, discharge, water density, viscosity, surface tension, temperature, molecular diffusion, and the turbulent diffusion coefficient. Additional parameters such as shear velocity, Reynolds number, and Froude number can be calculated from the above list.

The Environmental Protection Agency (1985) listed 27 common reaeration prediction models. Nineteen involved only some combination of the three parameters, velocity, slope, and depth.

Additional factors being included for reaeration studies in more recent literature (Parker and Gay, 1987; and Kilpatrick and others, 1987) include suspended sediment, conductivity, methylene blue active substances (MBAS) concentration, wind speed, and a wind sheltering factor. However, in most field studies these factors have not been reported to be dominant.

EFFECT OF ENVIRONMENTAL FACTORS ON THE REAERATION COEFFICIENT

Many researchers have been aware that environmental factors such as temperature, wind, suspended sediment concentration, dissolved solids concentration, and presence of surfactants can influence the gas transfer process of reaeration.

Temperature

One environmental factor which has been demonstrated to affect the reaeration process is temperature. The primary influence of temperature on the reaeration process is to speed up the movement of oxygen molecules in both the air and the water. It is then possible to

saturate the surface water film faster and possibly to a greater depth in an equal time. Therefore, it is expected that the reaeration coefficient would increase with temperature.

The first rigorous review of previous work done to determine the relation between the reaeration coefficient and temperature was presented by Elmore and West (1961). In that paper, the authors reported that all previous work had been completed under poorly controlled conditions and thus could not provide an accurate evaluation. This view, that all work prior to 1961 was suspect, was also expressed by Kramer (1974). After careful experimentation, Elmore and West (1961) concluded that the rate of reaeration increases at the geometric rate of 2.41 percent per degree Celsius throughout the temperature range normally found in natural streams (5-30 degrees). The general equation is presented as:

$$K_2(T) = K_2(20) \theta^{(T-20)} \quad (9)$$

where $\theta = 1.0241$. Churchill (1962) also found that θ was 1.0241. Previous studies reported a range for θ , from 1.008 to 1.047 (Kramer, 1974; Environmental Protection Agency, 1985). Wilson and Macleod (1974) verified the empirically derived θ of 1.0241 using a theoretical approach. Their work related the Reynolds and Schmidt numbers to the reaeration coefficient by using the O'Connor and Dobbins (1958) model for isotropic turbulence. They then used the known temperature dependency for the density, viscosity, and molecular diffusion terms in

the Reynolds and Schmidt numbers to arrive at the temperature dependency of the reaeration coefficient. Their findings over a temperature range of 0-30 degrees Celsius were in good agreement with those of Elmore and West (1961). The only other finding since the work of Elmore and West (1961) and Churchill (1962) that did not find θ to be approximately 1.0241 was that reported by Tsivoglou (1967) in which his experimentation resulted in a θ of 1.022. It has been fairly well accepted that the temperature dependency model described by Elmore and West (1961) is correct. Therefore a θ value of 1.0241 or 1.024 has been commonly used (Rathbun, 1977; Parker and Gay, 1987; and Yotsukura and others, 1984).

Wind

Wind blowing across the surface of a water body is an environmental factor that acts to increase the reaeration coefficient. Wilson and Macleod (1974) cited Penz (1963) as stating that because transport of oxygen into water by reaeration is controlled by the film on the water side of the water-air interface, winds or other air movements would not normally be expected to affect the reaeration coefficient. He continued to state that the limited influence could be in motion of the water and to increase the water's surface area. Experimental results presented by Eloubaidy and Plate (1972) indicated that the reaeration coefficient could be significantly increased by wind action and that the increase

was much larger than what could be accounted for by an increase in surface area. They concluded that the increase was due to increased turbulence in the water caused by the wind shear at the air-water interface.

Kramer (1974) cited Downing and Truesdale (1955) as performing laboratory experiments on the effect of wind. They found that below a wind speed of seven miles per hour, no apparent effect on the reaeration coefficient was observed. Eloubaidy and Plate (1972) determined that the significant increase in the reaeration coefficient coincided with the appearance of small waves which were wind generated. The corresponding wind speed ranged between 1.6 and 2.5 miles per hour. Environmental Protection Agency (1985) cites Mattingly (1977) as developing an empirical model to relate wind speed to the corresponding increase in reaeration coefficient for channels. His data suggests that the threshold of wind effect would be at a wind speed of about 5 miles per hour, but his data were very limited. Yotsukura and others (1984) found, in a study of reaeration on the Chenango River, that the reaeration coefficient appeared to increase by as much as 30 percent with a wind speed of 5.6 miles per hour.

Banks and Henera (1977) also studied the effect of wind on reaeration. In addition, they addressed the effect of rainfall on reaeration. They concluded that rainfall and wind could both affect reaeration, especially in lakes or lagoons.

Jirka and Brutsaert (1984) reported on two field studies of the effect of wind on reaeration in rivers. They concluded that the

micrometeorological effects of stream banks and vegetation appear to be important factors. They also concluded that, for wide and moderately flat-sloped (slope less than 0.0001) rivers, wind shear could play a significant role in reaeration.

Suspended Sediment

The effect of suspended sediment on the reaeration coefficient has been addressed by a few researchers. Because the reaeration process is partially controlled by turbulence on the water side of the water-air interface, any factor affecting the turbulence may effect the reaeration process. Alonso and others (1975), and Environmental Protection Agency (1985) citing Holley (1975) investigated the possibility that the suspended sediment concentration should somehow be related to the reaeration coefficient. Alonso and others (1975) noted that from laboratory studies a model could be developed relating an increase in average sediment concentration to a decrease in the reaeration coefficient. From their laboratory data it can be concluded that a sediment concentration of 1000 mg/L could reduce the reaeration coefficient about 1 percent from its value in water free from suspended sediment. A typical reaeration coefficient (base e) for their study was about 80 day⁻¹.

Kothandaraman (1973) also studied the effects of contaminants on the reaeration coefficients. Total suspended solids as determined from

multiple linear regression had a positive effect on the reaeration coefficient in his studies. He cautioned that his findings may be only applicable to his studies.

Bennett and Rathbun (1972) cited work by Poon and Campbell (1967) and McQuivey (1970) indicating that small concentrations of biologically inert suspended matter increased the reaeration coefficient. Their conclusion was that the suspended sediment increased the intensity of the turbulence.

Other researchers have included suspended sediment among the environmental factors to be collected during reaeration measurements (Yotsukua and others, 1984; Parker and Gay, 1987). Little has been done with the suspended sediment data in these studies other than a qualitative assessment and a verification that concentrations were characteristic of other water bodies of interest. Parker and Gay (1987), however, made attempts to include suspended sediment concentration as an regressor variable in developing multiple regression prediction equations from thirty reaeration measurements made in Massachusetts. They concluded it to be statistically insignificant in their empirical model building.

Surfactants

Numerous researchers have studied the effects of surfactants or surface-active agents on the oxygen-transfer process of reaeration. In

general, all researchers have qualitatively demonstrated to one degree or another that the addition of surfactants such as detergents and soap in sewage decreased the reaeration coefficient. Bennett and Rathbun (1972) cite five separate studies which were conducted and published between 1954 and 1959, all concluding to a varying degree that the presence of surfactants could cause a reduction in oxygen transfer. Mancy and Okum (1965) were able to relate the reduction to the intensity of turbulence. They observed that in streams with little turbulence (more laminar) and ones with very turbulent flows that surfactants had little effect on reaeration. The streams with mild turbulence were the ones most affected. Kehr (1938) studied the effect of various substances found in sewage on the reaeration process. He noted that soap, fatty acids, and oils could depress the reaeration coefficient to 40 percent of its tap-water value.

Rand (1959) also studied the effects of sewage on the reaeration process. He concluded that the reaeration coefficient for raw domestic sewage was about 60 percent of a clean water value. He concluded that polluted streams are likely to contain enough sewage to depress the reaeration coefficient to less than 95 percent of the clean water rate.

Kothandaraman (1971) measured the MBAS concentrations in laboratory studies of reaeration on Illinois River water. His findings were not conclusive and he presented statistically conflicting results on the effect of surfactants on reaeration. Parker and Gay (1987) also used MBAS concentration as a measure of surfactants. Their studies also failed to show a statistically-significant effect of surfactants in

predicting stream reaeration coefficients.

After much review of previous work on the subject, Wilson and Macleod (1974) concluded that there was considerable uncertainty regarding the quantitative effect of surfactants on reaeration rates. However, they believed that qualitatively there was experimental evidence to support the conclusion that reaeration coefficients for surfactant-contaminated waters tend to be lower than for uncontaminated water.

Other

In addition to the effects of temperature, wind, suspended sediment, and surfactants, other environmental factors playing a role in reaeration have been addressed. Some of these factors include salinity, total dissolved solids, oils and gasolines, and rainfall. Bennett and Rathbun (1972) cited work by Ogden, Gibbs, and Gameson (1959) which specifically addressed the effects of salinity on the reaeration coefficient. Their work resulted in a mathematical relation relating the percent reduction of the reaeration coefficient to the salinity. A 10 percent reduction, they noted, would be caused by a 2.8 parts per thousand salinity. Bennett and Rathbun (1972) also cited work by Downing and Truesdale (1955) which showed the effects of oil films. They concluded that oil film would not pose a significant influence on reaeration because little effect was measured until the oil-film

thickness exceeded 0.0001 centimeters and films of that thickness would not persist for long in natural streams. Earlier work by Kehr (1938) showed that a reduction of about 60 percent could be experienced by oil and gasoline films 0.01 centimeters thick. Multiple regression analysis by Kothanderaman (1971) and Parker and Gay (1987) showed that neither total dissolved solids nor specific conductance to be statistically meaningful in predicting the reaeration coefficient.

EFFECT OF STREAMFLOW CHANGES TO THE REAERATION COEFFICIENT

As previously discussed, many hydraulic factors have been demonstrated to have an influence on the gas-transfer process of reaeration. Some of the more common factors related to the reaeration coefficient, either theoretically or empirically, include the depth of flow and velocity. However, it is generally well known that depth and velocity increase with discharge. Examples of this knowledge includes work presented by Leopold and Maddock (1953), Langbein and Durum (1967), Bansal (1973), Brown (1974), and other researchers. Much of the work did not involve reach-averaged values but rather addressed the relations between flow and both depth and velocity at a single cross-section on the stream or river.

Leopold and Maddock (1953) observed that both depth and velocity varied logarithmically with discharge. The forms of these relations were shown as:

$$D = C_1 (Q)^{C_2} \quad (10)$$

and

$$V = C_3 (Q)^{C_4} \quad (11)$$

where C_2 and C_4 are constants for a given river gaging station and C_1 and C_3 vary with units selected. They noted that for twenty rivers studied in the Great Plains region of the United States that C_2 averaged 0.40 and C_4 averaged 0.34. Based on a review of previous work Langbein and Durum (1967) drew similar conclusions and noted C_2 and C_4 to both be about 0.40. Morel-Seytoux and Lau (1975) evaluated similar formulas from measurements on the Mississippi River and noted similar values. St. John and others (1984) also demonstrated a similar logarithmic relation between discharge and both depth and velocity.

Langbein and Durum (1967), Bansal (1973), Zogorski and Faust (1973), Morel-Seytoux and Lau (1975), and St. John and others (1984) all utilized relations similar to those of Leopold and Maddock (1953) along with selected theoretical and empirical reaeration prediction equations to demonstrate that the reaeration coefficient should be inversely related to stream discharge. Brown (1974) cited laboratory flume experimental results by Isaacs (1967) which also demonstrated an inverse relation between the reaeration coefficient and discharge. However, the inference that reaeration is inversely related to discharge was based

either on reach-averaged depths and velocities in a flume which had constant geometric properties or on geometric properties measured at only a single cross-section on the stream. The single, cross-section measurement would be representative of the entire reach (reach-averaged) only if the geometric and hydraulic cross-sectional characteristics were uniform along the entire reach. Channel-controlled reaches and reaches of major rivers do more closely fit these conditions than pool-and-riffle reaches common to many small and medium-sized streams. Therefore, for major rivers and channel-controlled stream reaches, the reaeration coefficient would be expected in some way to be inversely related to discharge as was found from flume- and single-cross-section stream determinations. However, in small- and medium-sized streams in which pool-and-riffle reaches are common (or in which there exists a longitudinal variability in hydraulic geometric properties) it is less clear from the literature that the reaeration coefficient would either increase or decrease with increasing discharge. The contrast of pool-and-riffle and channel-control streams under varying flow conditions is shown in Figure 3.

Langbein and Durum (1967) studied pool-and-riffle reaches of the Kansas River under various low, medium, and high flows. They concluded that within the riffles the reaeration coefficient would decrease with discharge in much the way as it was anticipated from the previous study of channel-controlled streams. However, within the pooled sections the reaeration coefficient would increase with increasing discharge--the opposite from riffle sections. They also presented evidence that the

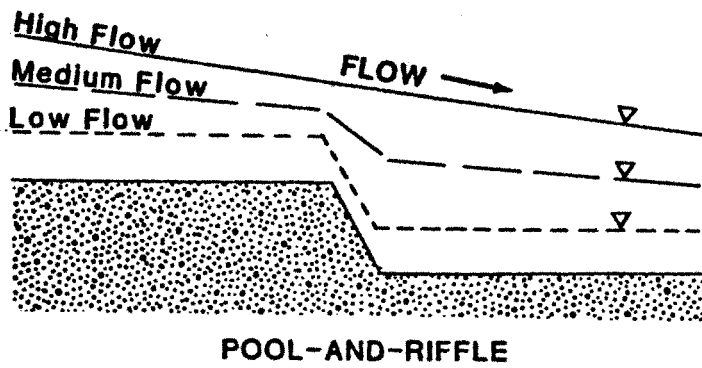
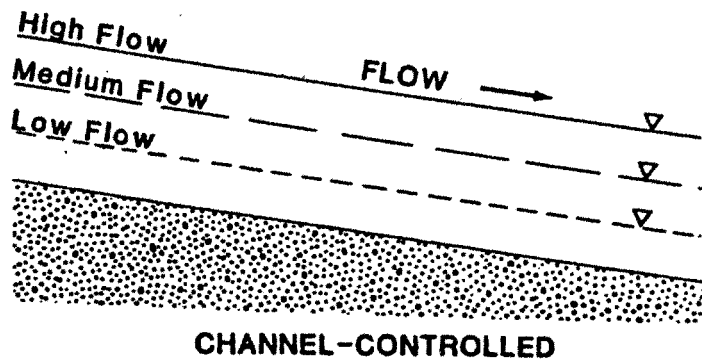


Figure 3 -- Stylized profiles for pool-and-riffle and channel-controlled stream reaches under various flow conditions

difference between the reaeration coefficient in the riffles and the pools was greatest under low flow and diminished with increasing flow until the effect was "drowned out" at near bankfull conditions. It appeared clear to Langbein and Durum (1967) that the reach-averaged reaeration coefficient would fall somewhere between the values for the riffle and that of the pool. However, it was not clear to them where the reach averaged value would fall or how it would be related to discharge. Miller and Wenzel (1985) also studied how geometric and hydraulic properties change under varying flow conditions in pool-and-riffle streams. As was previously reported (Langbein and Durum, 1967), they also found that differences between pooled and riffle sections were greatest under low flow and were "drowned out" with increasing discharges. They also looked at how energy was lost in the pool-and-riffle sequences under different flow conditions.

Tsivoglou and Neal (1976) used three measurements (using the radioactive tracer method) to show that the reaeration coefficient for the Canandaigua Outlet increased with discharge. These measurements suggested that the reaeration coefficient increased at the 0.26 power of the discharge. Measurements made at two flow conditions on three stream reaches in Ohio also indicated in each case that the reaeration coefficient increased with discharge (Ohio Environmental Protection Agency, 1983). In reaeration measurements made on 13 reaches in Massachusetts at two or more flow conditions, Parker and Gay (1987) compiled data that indicated a positive relation between the reaeration coefficient and discharge in all but one reach. Ruhl and Smoot (1987)

measured reaeration coefficients using tracer methods on several streams in Kentucky. On two reaches, two measurements were made at different flow conditions. Only one reach showed a positive relation between the reaeration coefficient and discharge. The other--a channel controlled reach--showed an inverse relation to exist as would be expected.

METHODS FOR PREDICTING REAERATION COEFFICIENTS

The methods used for predicting reaeration coefficients for use in water-quality models consist of applying a equation which relates the reaeration coefficient to some combination of physical and hydraulic stream parameters. These methods are in contrast to measurement methods to be discussed in a following section. The input physical and hydraulic parameter values are either field measured at the flow condition to be modeled or are estimated on the basis of empirically derived relations with more easily determined variables. The development of reaeration coefficient prediction equations have followed either the path of theoretical, empirically-based, or a combination of the two (Rathbun, 1977). The equations presented in the following sections are for "base e" reaeration coefficients and have been adjusted for comparison purposes to a temperature of 20 degrees Celsius, where needed.

Theoretically Based Equations

Many conceptual models have been developed to describe the gas-transfer process of reaeration at the air-water interface. Included are film, surface-renewal, kinetic theory, large eddy, and turbulent diffusion models. These models, generally, are not useful for prediction of the reaeration coefficients of streams because the input parameters such as film thickness, renewal rates, and eddy sizes have not and may not be quantifiable for streams. However, a few theoretically based equations have been developed which are considered useful for prediction purposes.

Nemerow (1974) reported on work done by O'Connor and Dobbins (1956) in which they presented two equations for predicting reaeration coefficients. One equation, for streams exhibiting a pronounced vertical velocity gradient, was derived using the assumption of nonisotropic turbulence and was based on the film-penetration conceptual model. The equation is given as:

$$K_2 = 21.16(S)^{0.25}(D)^{-1.25} \quad (12)$$

where K_2 is in days^{-1} , S is in feet per foot, and D is in feet. The coefficient given is valid for the molecular diffusivity value at 20 degrees Celsius. Nemerow (1974) reported that O'Connor and Dobbins (1956) had stated that turbulence is assumed nonisotropic when Chezy's C (C_c) = $V/((RS)^{0.5})$ is less than 14-20, where R is the hydraulic radius

in feet. For most natural streams this turbulence break occurs at a mean depth equal to about five feet.

O'Connor and Dobbins (1958) endorsed the prediction equation which they had originally developed for isotropic turbulence for use in both isotropic and nonisotropic turbulence. This multipurpose theoretical equation is also based on the concept of film penetration and is given as:

$$K_2 = 12.81(V)^{0.5}(D)^{-1.5} \quad (13)$$

where K_2 is in days^{-1} , V is in feet per second, and D is in feet. Again the molecular diffusivity is contained within the coefficient and is valid for a temperature of 20 degrees Celsius. The above formulation is probably the most widely used reaeration coefficient prediction equation (Environmental Protection Agency, 1985).

Another theoretically based equation was developed by Dobbins (1965) but generally has not received wide usage. The formulation was developed using experimental data and is expressed as:

$$K_2 = 116.6 \frac{(1 + F^2)^{0.375}}{(0.9 + F)^{1.5}} \frac{(VS)^{0.375}}{D} \coth \frac{4.1 (VS)^{0.125}}{(0.9 + F)^{0.5}} \quad (14)$$

where K_2 is in days^{-1} , V is in feet per second, S is in feet per foot, D is in feet, F is the Froude number = $V/(gD)^{0.5}$ (g is the acceleration due to gravity), and \coth is the hyperbolic cotangent function. Grant

and Skavroneck (1980) and Ruhl and Smoot (1987) found prediction errors using the equation to be highly variable.

Semiempirical Equations

Many equations have been developed which fall into the category of semiempirical. This category includes equations based on the rate of energy dissipation or in which the reaeration coefficient is correlated with the longitudinal dispersion coefficient (Rathbun, 1977). The rate of energy dissipation can be expressed as the change in energy head per unit time. If we assume that the velocity head is negligible or that at least the velocity head at the upstream and downstream end of a reach is the same, then the rate of energy dissipation can be expressed as SL/t where S is the water-surface slope, L is the reach length, and t is the reach mean travel time. But because L/t is simply the mean velocity in the reach, the rate of energy dissipation can be expressed as the product of V and S .

Krenkel and Orlob (1963) developed an energy dissipation type reaeration equation based on measurements made in a small laboratory flume. The equation has received wide use (EPA, 1985; Rathbun, 1977; and Ruhl and Smoot, 1987) and is given as:

$$K_2 = 234.5(VS)^{0.408}(D)^{-0.66} \quad (15)$$

where K_2 is in days^{-1} , V is in feet per second, S is in feet per foot, and D is in feet.

Cadwallader and McDonnell (1969) developed an equation based on the concept of energy dissipation using field stream data obtained from Owens and others (1964) and Churchill and others (1962). Their equation is given as:

$$K_2 = 336.8(VS)^{0.5}(D)^{-1.0} \quad (16)$$

where K_2 is in days^{-1} , V is in feet per second, S is in feet per foot, and D is in feet.

Parkhurst and Pomeroy (1972) collected reaeration data from the study of sewers as well as in small streams. Their resulting empirically fit equation is for prediction use where Reynolds numbers are greater than 5,000. The equation is given as:

$$K_2 = 48.4(1 + 0.17(F)^{2.0})(VS)^{0.375}(D)^{-1.0} \quad (17)$$

where K_2 is in days^{-1} , V is in feet per second, S is in feet per foot, and D is in feet.

One of the simplest semiempirical equations in common usage (Environmental Protection Agency, 1985) was developed by Tsivoglou and Wallace (1972) using radioactive tracer measurement data from five rivers. The equation is given as:

$$K_2 = 4133(VS) \quad (18)$$

where K_2 is in days^{-1} , V is in feet per second, and S is in feet per foot. Tsivoglou and Neal (1976) later used radioactive-tracer measurements on 24 different streams to develop the following prediction equation:

$$K_2 = (c)(V)(S) \quad (19)$$

where K_2 is in days^{-1} , $c = 9500$ for discharges less than 10 cubic feet per second and 6860 for discharges greater than 10 cubic feet per second, V is in feet per second, and S is in feet per foot. Grant (1978) used a similar formulation also based on field radioactive tracer measurements. His equation was empirically determined to be:

$$K_2 = 4591(VS) \quad (20)$$

where K_2 is in days^{-1} , V is in feet per second, and S is in feet per foot.

Krenkel and Orlob (1962) also used the longitudinal dispersion coefficient D_L measured from laboratory flume experiments in developing a reaeration prediction equation. The dispersion coefficients from their flume experiments, however, were generally much lower than those

commonly determined for natural streams. The equation developed is given as:

$$K_2 = 4.18(D_L)^{1.321}(D)^{-2.32} \quad (21)$$

where K_2 is in days⁻¹, D_L is in square feet per second, and D is in feet.

Other equations closely related to the semiempirical ones include the shear velocity (u_*). One such equation developed by Thackston and Krenkel (1969) from flume measurements has compared well to other prediction equations in studies by Grant and Skavroncek (1980) and Ruhl and Smoot (1987). It is given as:

$$K_2 = 24.94(1 + F^{0.5})u_* (D)^{-1.0} \quad (22)$$

where K_2 is in days⁻¹, $u_* = (gRS)^{0.5}$ and is expressed in feet per second, and D is in feet. Lau (1972) used the same data as Thackston and Krenkel (1969) and developed another equation containing shear velocity. It is given as:

$$K_2 = 2515(u_*/V)^{3.0} (V/D) \quad (23)$$

where K_2 is in days⁻¹, $u_* = (gRS)^{0.5}$ and is expressed in feet per second, V is in feet per second, and D is in feet. In studies which compared the accuracy of prediction equations performed by Grant and

Skavroneck (1980) and Ruhl and Smoot (1987), the equation developed by Lau (1972) was concluded to be highly imprecise and inaccurate.

Empirical Equations

Empirical equations for predicting reaeration coefficients generally relate the dependent variable (reaeration coefficient) to one or more independent variables (hydraulic parameters). The relation is usually developed by linear or non-linear regression of the variables or transforms of the variables. Most empirical prediction equations in the literature have the reaeration coefficient directly proportional to one or more hydraulic parameters, each raised to some power (Rathbun, 1977). This form of equation results from applying linear regression on logarithmic transforms of the variables. The reaeration process is complex, and theoretically based equations have been generally shown to be inadequate; therefore, empirical equations are gaining in usage because of the ability of parameters within these equations to act as surrogates for others not included (Bennett and Rathbun, 1972):

Some of the first and most complete development of empirical prediction equations was presented by Churchill and others (1962). They developed 19 equations from oxygen-balance measurements made in rivers. Two of their equations have been used by others (Grant and Skavroneck, 1980; and Ruhl and Smoot, 1987) and are given as:

$$K_2 = 0.03453(V)^{2.695}(D)^{-3.085}(S)^{-0.823} \quad (24)$$

and

$$K_2 = 11.573(V)^{0.969}(D)^{-1.673} \quad (25)$$

where K_2 is in days⁻¹, V is in feet per second, D is in feet, and S is in feet per foot.

Owens and others (1964) measured oxygen recovery in six streams. They developed two equations from their data. They are given as:

$$K_2 = 23.23(V)^{0.73}(D)^{-1.75} \quad (26)$$

and

$$K_2 = 21.74(V)^{0.67}(D)^{-1.85} \quad (27)$$

where K_2 is in days⁻¹, V is in feet per second, and D is in feet.

Langbein and Durum (1967) synthesized data from O'Connor and Dobbins (1958), Churchill and others (1962), Krenkel and Orlob (1963), and Streeter and others (1936) and proposed the following equation:

$$K_2 = 7.61(V)(D)^{-1.33} \quad (28)$$

where K_2 is in days⁻¹, V is in feet per second, and D is in feet.

Isaacs and Gaudy (1968) developed an equation from measurements using a laboratory recirculating tank. The equation is given as:

$$K_2 = 8.61(V)(D)^{-1.5} \quad (29)$$

where K_2 is in days⁻¹, V is in feet per second, and D is in feet. The equation's accuracy ranged from fair to poor compared with other equations in studies performed by Grant and Skavroneck (1980) and Ruhl and Smoot (1987).

Nemerow (1974) reported on work by Isaacs and others (1969) in which they proposed an equation similar to that of Isaacs and Gaudy (1968) but with a different coefficient. The refined equation is presented as:

$$K_2 = 6.523(V)(D)^{-1.5} \quad (30)$$

where K_2 is in days⁻¹, V is in feet per second, and D is in feet.

At about the same time, measurements were conducted in a laboratory flume by Negulescu and Rojanski (1969). They proposed the following prediction equation:

$$K_2 = 10.91(V/D)^{0.85} \quad (31)$$

where K_2 is in days⁻¹, V is in feet per second, and D is in feet.

Padden and Gloyna (1971) used linear regression analysis of river and stream reaeration measurement data and developed a prediction equation. It is given as:

$$K_2 = 6.864(V)^{0.703}(D)^{-1.054} \quad (32)$$

where K_2 is in days⁻¹, V is in feet per second, and D is in feet.

Bennett and Rathbun (1972) used linear regression on 172 river and flume data sets obtained from the literature. They developed two equations which have been used (Grant and Skavroneck, 1980 and Ruhl and Smoot, 1987). The equations are given as:

$$K_2 = 106.16(V)^{0.413}(S)^{0.273}(D)^{-1.408} \quad (33)$$

and

$$K_2 = 20.19(V)^{0.607}(D)^{-1.689} \quad (34)$$

where K_2 is in days⁻¹, V is in feet per second, S is in feet per foot, and D is in feet.

Bansal (1973) reevaluated the field data collected by Churchill and others (1962) and earlier results of O'Connor and Dobbins (1956) and developed the following prediction equation:

$$K_2 = 4.67(V)^{0.6}(D)^{-1.40} \quad (35)$$

where K_2 is in days⁻¹, V is in feet per second, and D is in feet.

Parker and Gay (1987) used the hydrocarbon gas tracer technique on 30 stream reaches in Massachusetts. They empirically developed the following prediction equation from their field data:

$$K_2 = 252.2(D)^{-0.176}(V)^{0.355}(S)^{0.438} \quad (36)$$

where K_2 is in days⁻¹, D is in feet, V is in feet per second, and S is in feet per foot.

Ruhl and Smoot (1987) also used the hydrocarbon gas tracer technique to measure the reaeration coefficient on five streams in eastern Kentucky. They found simple regression equations did well in fitting the measured data. These simple equations were given as:

$$K_2 = 3.72(D)^{-1.358} \quad (37)$$

and

$$K_2 = 815(S)^{0.733} \quad (38)$$

where K_2 is in days⁻¹, D is in feet, and S is in feet per foot.

Some studies have been done to compare the accuracy of predictions

based on the literature equations presented in this paper as well as others. These studies include ones by Bennett and Rathbun (1972); Lau (1972); Wilson and MacLeod (1974); Rathbun (1977); Rathbun and Grant (1978); Grant and Skavroneck (1980); Ohio EPA (1983); Parker and Gay (1986); and Ruhl and Smoot (1987). No one prediction equation was found to be "best" in each of these studies. Common conclusions from all the studies were that the prediction equations are most applicable over the range in variables for which they were developed and, outside that range, errors may be great. Some of these equations are summarized in Table 1.

METHODS FOR MEASURING REAERATION COEFFICIENTS

All methods which have been used to field measure stream reaeration coefficients can be classified as dissolved-oxygen balance, disturbed equilibrium, or tracer techniques (Rathbun, 1977 and EPA, 1985).

Dissolved-Oxygen Balance

Streeter and Phelps (1925) introduced the use of a dissolved-oxygen balance to derive reaeration coefficients in their study of the Ohio River. The general approach is to measure the dissolved-oxygen concentration changes along the stream reach under steady-state

Table 1 -- Summary of selected reaeration coefficient prediction equations from the literature

DEVELOPER	EQUATION
<u>Theoretically Based Equations</u>	
1. O'Connor and Dobbins (1956) (Nemerow, 1974)	$K_2 = 21.16(S)^{0.25}(D)^{-1.25}$
2. O'Connor and Dobbins (1958)	$K_2 = 12.81(V)^{0.5}(D)^{-1.5}$
3. Dobbins (1965)	$K_2 = 116.6 \frac{(1 + F^2)}{(0.9 + F)^{1.5}} \frac{(VS)^{0.375}}{D} \coth \frac{4.1(VS)^{0.125}}{(0.9 + F)^{0.5}}$
<u>Semiempirical Equations</u>	
4. Krenkel and Orlob (1963)	$K_2 = 234.5(VS)^{0.408}(D)^{-0.66}$
5. Cadwallader and McDonnell (1969)	$K_2 = 336.8(VS)^{0.5}(D)^{-1.0}$
6. Parkhurst and Pomeroy (1972)	$K_2 = 48.4(1 + 0.17(F)^{2.0})(VS)^{0.375}(D)^{-1.0}$
7. Tsivoglou and Wallace (1972)	$K_2 = 4133(VS)$
8. Tsivoglou and Neal (1976)	$K_2 = (c)(V)(S)$
where: c=9500 for Q<10 and c=6860 for Q>10	
9. Grant (1978)	$K_2 = 4591(VS)$
10. Thackston and Krenkel (1969)	$K_2 = 24.94(1 + F^{0.5})u_* (D)^{-1.0}$

(continued)

Table 1 (continued) -- Summary of selected reaeration coefficient prediction equations from the literature

DEVELOPER	EQUATION
<u>Empirical Equations</u>	
11. Churchill and others I (1962)	$K_2 = 0.03453(V)^{2.695}(D)^{-3.085}(S)^{-0.823}$
12. Churchill and others II (1962)	$K_2 = 11.573(V)^{0.969}(D)^{-1.673}$
13. Owens and others I (1964)	$K_2 = 23.23(V)^{0.73}(D)^{-1.75}$
14. Owens and others II (1964)	$K_2 = 21.74(V)^{0.67}(D)^{-1.85}$
15. Langbein and Durum (1967)	$K_2 = 7.61(V)(D)^{-1.33}$
16. Isaacs and Gaudy (1968)	$K_2 = 8.61(V)(D)^{-1.5}$
17. Isaacs and others (1969) (Nemerow, 1974)	$K_2 = 6.523(V)(D)^{-1.5}$
18. Negulescu and Rojanski (1969)	$K_2 = 10.91(V/D)^{0.85}$
19. Padden and Gloyna (1971)	$K_2 = 6.864(V)^{0.703}(D)^{-1.054}$
20. Bennett and Rathbun I (1972)	$K_2 = 106.16(V)^{0.413}(S)^{0.273}(D)^{-1.408}$
21. Bennett and Rathbun II (1972)	$K_2 = 20.19(V)^{0.607}(D)^{-1.689}$
22. Bansal (1973)	$K_2 = 4.67(V)^{0.6}(D)^{-1.40}$
23. Parker and Gay (1986)	$K_2 = 252.2(D)^{-0.176}(V)^{0.355}(S)^{0.438}$

(continued)

Table 1 (continued) -- Summary of selected reaeration coefficient prediction equations from the literature

DEVELOPER	EQUATION
24. Ruhl and Smoot I (1987)	$K_2 = 3.72(D)^{-1.358}$
25. Ruhl and Smoot II (1987)	$K_2 = 815(S)^{0.733}$

- Where:
- K_2 = Reaeration coefficient (base e), in days⁻¹
 - S = Reach water-surface slope, in feet per foot
 - D = Mean depth in reach, in feet
 - V = Mean velocity in reach, in feet per second
 - F = Mean Froude number in reach
 - u_* = Mean shear velocity in reach, in feet per second
 - Q = Mean discharge in reach, in cubic feet per second

conditions, measure or calculate all sources and sinks of dissolved oxygen (except reaeration), and calculate the reaeration as the difference between the accounted-for sources and sinks and the measured dissolved oxygen concentration changes (Rathbun, 1977 and Holley and Yotsukura, 1984). In the Streeter and Phelps (1925) one-dimensional consideration, only one source term (reaeration) and one sink term (carbonaceous biochemical oxygen demand) were included in the balance. Later, oxygen-balance applications utilized more complete formulations. A fairly complete formulation discussed by Holley and Yotsukura (1984) contains terms for: 1) reaeration, 2) carbonaceous biochemical oxygen demand, 3) nitrogenous biochemical oxygen demand, 4) benthic oxygen demand, 5) photosynthetic oxygen production, and 6) plant respiration.

The major drawbacks in using the dissolved-oxygen balance technique for determining the reaeration coefficient were presented by Bennett and Rathbun (1972) and Holley and Yotsukura (1984). They concluded that potentially serious errors could result from the method. The errors result from the difficulty in determining the rates of the source and sink terms and in applying rates determined for one location to the entire reach. In addition to error considerations, to acquire the input data needed for solution to a fairly complete formula describing a dissolved oxygen balance is extremely labor-intensive and costly. Another drawback is that the assumption of a purely one-dimensional, steady-state process is poor. Because of these drawbacks, the technique is seldom used except under specialized conditions where many of the

source and sink terms can be eliminated and the technique could be effectively used (Rathbun, 1977).

Disturbed Equilibrium

Gameson and others (1955) first presented the disturbed equilibrium technique for measuring the reaeration coefficient. It has been applied by numerous researchers including Owens and others (1964) and Zogorski and Faust (1973) with minor modification. The technique consists of measuring the dissolved oxygen concentrations at each end of the reach being measured for two different levels of dissolved oxygen concentration. One level used is the natural condition. The other is usually established by reducing the dissolved oxygen concentration by the injection of sodium sulfite and a cobalt catalyst into the stream. If all the variables in the dissolved oxygen budget (photosynthesis, respiration, benthic demand, reaeration coefficient, velocity, carbonaceous BOD rate coefficient, nitrogenous BOD rate coefficient, oxygen saturation concentration, etc.) are constant during the measurements, then the reaeration coefficient can be computed. The original application used a steady-state injection of sodium sulfite but was later modified to use short-duration releases (Zogorski and Faust, 1973).

This technique is generally used only in laboratory flumes and small streams because it is difficult to artificially produce a

dissolved-oxygen deficit in a major stream or river. Some of the other drawbacks of the method arise from the assumptions that all variables in the dissolved oxygen budget are constant with time. Another assumption, which is questionable, is that the respiration is completely independent of the dissolved oxygen concentration (Rathbun, 1977).

Again, because of the many assumptions needed, the potential for significant errors, and the practicality of creating artificial deficits, the method has lost popularity in favor of tracer techniques, except in well-controlled conditions, such as in flumes.

Tracer Gas

The dissolved-oxygen balance and disturbed-equilibrium techniques depend on determinations of dissolved oxygen concentrations within the measurement stream reach and can be affected by other dissolved oxygen source and sink processes within the stream. The tracer-gas technique for measuring the reaeration coefficient, in contrast, does not require any of these determinations. Tsivoglou and others (1965, 1968) proposed the use of surrogate gas tracers which are artificially added to the stream water. The basis of the technique is that a relationship exists between the rate coefficient for the desorption of the gas tracer and the rate coefficient for the absorption of atmospheric oxygen (reaeration coefficient). This relationship needs to be independent of mixing conditions, water quality conditions, and temperature.

Additional conditions for the method to be accurate include: 1) the tracer gas should have no sources or sinks other than surface transfer, 2) the tracer gas should not be present in the water naturally, 3) the tracer gas should be able to be measured in the microgram-per-liter range, and 4) the tracer gas should have a mass-transfer rate coefficient approximately in the same range as that of oxygen (Holley and Yotsukura, 1984).

Radioactive Gas

Tsivoglou and others (1965) concluded that the monatomic or "noble" gases were the most promising for use as tracers because of their chemical inertness. They also thought that the radioactive isotopes of these gases would allow for simple and highly sensitive measurement methods. In laboratory studies both Krypton-85 (Kr^{85}) and Radon-222 (Rn^{222}) were evaluated for use as reaeration tracers. They demonstrated that both Kr^{85} and Rn^{222} had mass-transfer rate coefficients in the same range as oxygen and that a relation between the coefficients for both tracers and oxygen were independent of temperature and mixing conditions.

Field tests by Tsivoglou and others (1968) on the Jackson River in West Virginia and Virginia demonstrated that the tracer technique with radioactive krypton gas could be used to obtain reproducible field determinations of the reaeration coefficient. In their field tests the

measurement method which has since been applied widely (Environmental Protection Agency, 1985) consisted of instantaneously injecting a homogeneous mixture of dissolved Kr⁸⁵ gas, tritium, and rhodamine-WT dye. Each of the three tracers would undergo the same convection, dispersion, and dilution processes. Sampling for the tracers at downstream cross-sections was guided by field fluorometer measurements of rhodamine-WT dye. The tritium was used as a conservative tracer to account for dispersion and dilution. The krypton gas was used as the oxygen surrogate. Tritium and krypton concentrations were determined by liquid scintillation counting.

In the radioactive tracer gas technique, the desorption coefficient for krypton gas is determined by:

$$K_{Kr} = \frac{1}{t_d - t_u} \log_e \frac{(C_{Kr}/C_{Tr})_u}{(C_{Kr}/C_{Tr})_d} \quad (39)$$

where K_{Kr} is the first-order desorption coefficient for krypton, t is the elapsed time to the peak value of dye concentration, C_{Kr} and C_{Tr} are the concentrations of krypton and tritium corresponding to the time of the peak value of dye concentration, the subscripts u and d refer to upstream and downstream ends of the measurement stream reach, and units are compatible. The reaeration coefficient is then determined by:

$$K_2 = 1.20 K_{Kr} \quad (40)$$

where K_2 and K_{Kr} are in consistent units.

The radioactive tracer technique using Kr^{85} has received wide attention and, as of 1985, was still being recommended by the U.S. Environmental Protection Agency (Environmental Protection Agency, 1985). The major drawbacks of the technique are that it requires a release of radioactive material into the environment and the difficulties and safety issues related to obtaining and handling radioactive materials (Rathbun and Grant, 1978).

Hydrocarbon Gas

Responding to some of the drawbacks of using radioactive tracers, Rathbun and others (1975) began some preliminary tests with non-radioactive gas for use in tracers. Their preliminary testing showed that low molecular weight hydrocarbon gases may be desirable substitutes for the radioactive gases previously used. More extensive laboratory testing was performed with ethylene and propane gases. Later, Rathbun and others (1978) presented evidence that both these gases were acceptable substitutes for radioactive gases in a modified, gas-tracer method for determining stream reaeration coefficients. The ratio of the mass-transfer coefficient for oxygen to either ethylene or propane was determined to be independent of temperature and mixing conditions. These ratios were laboratory determined to be 1.15 and 1.39 for ethylene and propane respectively. Rainwater and Holley (1983) later duplicated

these findings in independent laboratory tests.

Following the development of the hydrocarbon gas tracer technique, numerous field tests have been conducted to compare its results with those from the more widely established radioactive gas tracer technique. The comparisons have been favorable and are presented in publications by Rathbun and Grant (1978) and Grant and Skavroneck (1980).

In the modified, gas-tracer technique (later referred to as the "hydrocarbon gas tracer technique") either ethylene or, more commonly, propane is introduced to the stream through diffusers as the surrogate gas for oxygen. Rhodamine-WT dye is simultaneously injected as a dispersion-dilution tracer and as a field indicator. Because of the low solubility of either propane or ethylene in water, an instantaneous injection into the stream is not possible--instead a constant rate, short duration injection is used (Rathbun, 1979). As with the radioactive gas tracer method, sampling for the tracers downstream is guided by field determinations of the dye concentration. Hydrocarbon gas concentrations are laboratory determined by a gas chromatography method.

The mathematical methods used to determine the tracer gas desorption coefficient and, ultimately, the reaeration coefficient are similar to those used in the radioactive gas tracer technique (Rathbun and Grant, 1978). In what has been referred to as the "peak method", the desorption coefficient is determined by:

$$K_t = \frac{1}{t_d - t_u} \log_e \frac{(RC_t/C_d)_u}{(RC_t/C_d)_d} \quad (41)$$

where K_t is the tracer gas desorption coefficient, R is the portion of the dye recovered, C_t is the peak concentration of the tracer gas, C_d is the peak concentration of the dye, and all units are compatible. The desorption coefficient can also be determined by what has been referred to as the "area method" by using a ratio of the areas under the time-concentration curves at each end of the measurement reach. The calculation is given as:

$$K_t = \frac{1}{t_d - t_u} \log_e \frac{(AQ)_u}{(AQ)_d} \quad (42)$$

where A is the area under the time concentration curve, Q is the stream discharge, and all units are compatible.

In a modification to the hydrocarbon gas tracer technique, Yotsukura and others (1983) applied the principle of superposition and developed the steady-state hydrocarbon gas tracer technique. In their technique, the tracer gas is injected at a constant rate for a period long enough to achieve a "plateau" concentration on the time-concentration curve for the downstream end of the measurement reach. Only a single slug injection of dye is used at the initiation of gas injection and allows for travel time computation and an indication of the establishment of a gas-concentration plateau (the plateau is

developed at the end of the passage of the dye cloud). The desorption coefficient for the tracer gas is determined by:

$$K_t = \frac{1}{\tau_d - \tau_u} \log_e \frac{(C_p Q)_u}{(C_p Q)_d} \quad (43)$$

where C_p is the plateau concentration of tracer gas and all units are compatible. Because of slight adjustments sometimes desired because of longitudinal dispersion, Yotsukura and others (1984) suggested that the above formulation be modified using a trial-and-error solution to the following equation:

$$\frac{(C_p Q)_u}{(C_p Q)_d} = \frac{(\int (C_d / A_d \exp(K_t t)) dt)_u}{(\int (C_d / A_d \exp(K_t t)) dt)_d} \quad (44)$$

where the initial value of K_t is derived from the equation above, A_d is the area under the dye time-concentration curve calculated by:

$$A_d = \int C_d dt \quad (45)$$

and all units are compatible.

The hydrocarbon gas tracer technique, using both slug-injection and steady-state injection schemes, has received wide usage and has been successful under a variety of stream conditions. Publications referencing these applications include Bauer and others (1979), Crawford (1985), EPA (1985), Grant and Skavroneck (1980), Hren (1984), Parker and

Gay (1987), Rathbun and Grant (1978), Ruhl and Smoot (1987), Yotsukura and others (1983), and Yotsukura and others (1984).

METHODS AND MATERIALS

In this chapter, the details of the methods used for data collection, analysis, and interpretation are presented. The methods included cover all significant aspects of site selection, experiment design, measurement, sampling, sample analysis, computation, and interpretation in investigating the relation of stream reaeration coefficients to hydraulic conditions in a pool-and-riffle stream.

SITE SELECTION AND DESCRIPTION

The criteria in selecting a stream to perform a series of reaeration/hydraulic measurements were many and included the following:

Field access - The stream reaches needed to be accessible under all anticipated flow conditions by field vehicle to transport the necessary equipment and samples to and from the stream and to make the necessary in-stream measurements.

Proximity - The stream reaches needed to be close enough to the author's residence or workplace in Louisville, Kentucky so that daily checks of the flow conditions could be made.

Hydraulic records - The stream should be one on which an extensive stage and streamflow record had been established. This enabled monitoring of flow conditions prior to and during field experiments. It also allowed flow duration and flow recurrence

information to be computed or determined for each of the experimental measurements.

Pool-and-riffle - It was desirable that the stream be one characterized by a series of pools and riffles under low-flow conditions and become more channel-controlled under higher flow conditions.

Multiple Reaches - A series of three or four reaches on the same stream were desired. This would enable multiple measurements in close proximity. The reaches need to be long enough to allow for appreciable loss of tracer gas but short enough so that the tracer gas is not entirely desorbed. This length consideration needed to be met under all expected flow conditions. The reaches should be hydraulically different from one another. For example depth, slope, velocity, and degree of pool and riffle development should be different. Each reach should also not be dominated by a single feature such as a major pool or major riffle.

Relation to other streams - The stream selected should be typical of small streams which would receive point-source waste and be modeled for determination of a wasteload allocation. This would facilitate the transferability of the findings to other streams of interest.

Size - The stream should be small enough so that very complete hydraulic/reaeration measurements can be accomplished by a field party of limited size (typically 3-4 persons).

The stream which met the above criteria and was selected for study was the Middle Fork Beargrass Creek in the suburban Louisville, Kentucky area in east Jefferson County. The stream location is shown in Figure 4. Middle Fork Beargrass Creek is typical of small streams in north-central Kentucky as well as elsewhere (Melcher and Ruhl, 1984).

The U.S. Geological Survey has maintained a continuous-record stage/discharge station (# 03293000) on Middle Fork Beargrass Creek at Cannons Lane, Louisville, Kentucky since 1939. The station is located 7.0 miles above the Ohio River confluence at 38 degrees, 14 minutes, 14 seconds latitude and 085 degrees, 39 minutes, 53 seconds longitude in hydrologic unit # 05140101. The stream at this station drains an 18.9 square mile area. The stage measurements have been made at the site with a nitrogen-gas bubbler in conjunction with a mercury manometer and a continuous analog recorder (Stevens, model A35) and also with a digital-tape recorder (Fischer-Porter) that records every hour. Discharge has been estimated and published for the station following methods by Buchanan and Somers (1969). These methods include current-meter measurements on a routine (monthly-bimonthly) and extreme-flow (flood or drought) basis and the development of a stage-discharge relationship used with the mean daily stage to determine mean daily discharge. The location of the gaging station is shown in Figure 4.

After extensive field reconnaissance, three reaches (four if two were considered jointly) were selected on the Middle Fork Beargrass Creek. Each met the criteria previously discussed, and two of the reaches were in series which would allow for dual-reach measurements

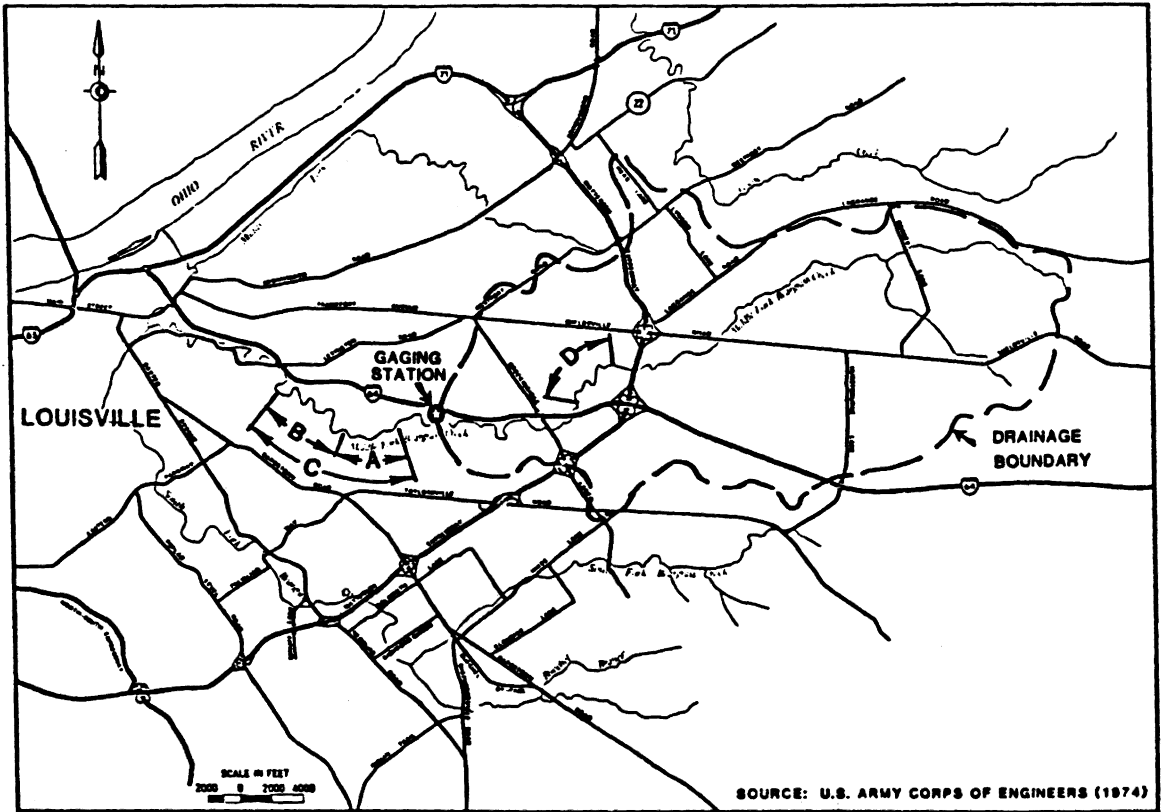


Figure 4 -- Middle Fork Beargrass Creek location map

from a single injection of tracers. The reaches were each preceded by a mixing reach which was selected so as to provide adequate lateral and vertical mixing of the tracers prior to measurement at the upstream end of the test reach. The length of the mixing reach was selected to provide optimum (95 percent) mixing as described by Kilpatrick and Cobb (1984) from a single midstream injection of reaeration tracers. The locations of the four reaches (termed A,B,C, and D) are also shown in Figure 4.

FIELD SURVEY

Prior to carrying out any reaeration measurements, a detailed physical survey of the selected reaches was made. For each reach, stream cross-sectioning was performed. Cross-sections were selected within each reach at a fixed interval (100 or 200 feet). At each of these, located in the field by taping along the centerline of flow, survey instruments consisting of a self-leveling optical level (Zeiss, model Ni-2), a telescoping survey rod capable of readings on the order of 0.001 foot, and a 100-foot metal tape were used to measure and delineate the stream bed and bank cross-sectionally following methods described by Benson and Dalrymple (1967) which were similar to methods used by Leopold and Maddock (1953). The right- and left-bank, water-surface elevations were measured at each selected cross-section. Minor modifications to the preselected cross-section locations were made in

the field if the selected cross-section was located under a bridge or within heavy bank vegetation which would prohibit level observation of the cross-section. In these cases, the section was moved slightly upstream or downstream to an acceptable location. All reach elevation measurements were tied to a single datum.

In addition to determinations of the cross-sectional characteristics and the water-surface profile of the selected reaches during the field survey, the establishment of a network of reference points was required from which these characteristics and profile could be determined (synthesized) under all flow conditions experienced during field reaeration measurements. The reference points were established by driving a nail in a sturdy overhanging tree or chiseling a mark on a rock in the stream and leveling to a common datum. The locations for the reference points were selected generally at natural breaks in the water-surface profile--above and below riffles and supplementally to maintain good resolution. The water surface would then be taped from each of these reference points during subsequent field reaeration measurements.

TRACER GAS TECHNIQUES

Reaeration coefficients for this study were determined using hydrocarbon gas-tracer techniques described by Rathbun (1979) and Yotsukura and others (1983) which were adapted from radioactive gas-

tracer techniques developed by Tsivoglou and others (1968). The hydrocarbon gas tracer technique is based on the assumption that the reaeration process can be related to the process of desorption of a selected hydrocarbon gas. It is further assumed that the first-order reaeration coefficient (K_2) can be mathematically related to the first-order desorption coefficient for the hydrocarbon gas (K_t). In stirred-tank experiments conducted by Rathbun and others (1978) and repeated by Rainwater and Holley (1983), it was shown that a linear relation exists between K_2 and K_t and is independent of mixing conditions or temperature. For propane, the surrogate gas used in all measurements, the relation was found to be:

$$K_2 = 1.39 K_t \quad (46)$$

where K_2 and K_t are in consistent units.

Because the tracer-gas desorption coefficient and the reaeration coefficient both change in response to temperature, adjustment of the coefficients determined by the tracer techniques to a standard temperature is needed if comparisons of measured values to each other or to predicted values is desirable. The temperature adjustment is given by Rathbun (1977) as:

$$K_{2-20} = K_2 1.024^{(20 - T)} \quad (47)$$

where K_{2-20} is the base-e reaeration coefficient at 20 degrees Celsius

in days⁻¹ and T is the mean reach water temperature in degrees Celsius.

Two strategies are available for the injection of the surrogate tracer gas. One, a near slug injection, leads to the peak- and total-weight methods of calculation. The other, a steady-state injection, leads to a different method of calculation.

Slug Injection

In this procedure the tracer gas along with a conservative dispersion-dilution tracer (rhodamine-WT) are injected simultaneously in the stream at a constant rate for a short duration--typically 15-30 minutes. The injection of the tracers is made far enough upstream of the reach of interest so that nearly complete lateral and vertical mixing of the tracers is achieved. Sampling for both propane and dye is conducted at both the upstream and downstream ends of the reach. Time-concentration (breakthrough) curves are then prepared from the data for both sampled cross-sections. Eighteen of the twenty reach reaeration determinations resulted from the slug-injection procedure.

In the peak method, the desorption coefficient for propane was calculated on the basis of the ratio of the peak propane and dye concentrations of the upstream and downstream samples cross-sections:

$$K_t = \frac{1}{t_d - t_u} \log_e \frac{(RC_t/C_d)_u}{(RC_t/C_d)_d} \quad (48)$$

where K_t is the desorption coefficient, in days^{-1} , t is the elapsed time of the centroid (or alternately, peak) of the dye time-concentration curve, in days, R is the portion of the dye recovered, C_t is the peak concentration of gas tracer, in micrograms per liter, C_d is the peak concentration of dye in micrograms per liter, and u and d denote the upstream and downstream sampling cross-sections of the reach. The portion of dye recovered is needed to account for minor losses in what theoretically should be a conservative tracer and is calculated by first determining the mass of dye represented by the time-concentration curve and dividing by the mass of dye initially injected. The mass of dye represented by the time-concentration curve (M_R) was determined by integrating the product of discharge (Q) and dye concentration with respect to time over the duration of the time-concentration curve:

$$M_R = \int Q C_d dt \quad (49)$$

The mass of dye injected (M_I) was determined as the product of the volume, purity, and density of a liquid dye solution. The rhodamine-WT dye used in all tracer measurements was 20-percent pure and had a density of 1.19 grams per milliliter.

The peak method assumes that a constant relation exists between the propane desorption coefficient and the reaeration coefficient and that the propane undergoes the same dispersion and dilution processes as the dye does. Another assumption is that the minor losses to the dye can be corrected and uniformly distributed across the time-concentration curve.

This adjustment does not change the shape of the curve and, hence, moment computations but does change the magnitude of each ordinate.

Because the complete dye time-concentration curve is normally sampled to facilitate computation of dye recovery and location of the centroid, the complete propane-recovery curve may be defined with some additional field and laboratory effort. This leads to the total weight method of computation:

$$K_t = \frac{1}{\tau_d - \tau_u} \log_e \frac{(\int C_t Q dt)_u}{(\int C_t Q d\tau)_d} \quad (50)$$

where all units are compatible. No additional assumptions are needed for the total-weight method and the dye time-concentration curve is needed only for calculation of mean travel time.

Steady-State Injection

In the steady-state procedure used for two of the twenty reach-re-aeration determinations, the tracer gas is injected into the stream at a constant rate for a long duration. The long-duration injection allows, under steady flow conditions, the in-stream gas concentration at the downstream end of the test reach to attain and maintain, for a predetermined period, a constant or plateau value. Based on the principle of superposition described by Yotsukura and others (1983),

this desired plateau concentration is achieved when the injection duration exceeds the passage time at the sampled cross-section for a tracer cloud resulting from a slug injection. The slug injection of dye is also made at the gas injection location simultaneously with the initiation of steady-gas injection. Sampling of the gas plateau concentration at the downstream cross-sections follows the complete passage of the dye tracer which signals the complete plateau development. Again, as with the slug-gas-injection procedure, the steady-state gas and slug-dye injection is made far enough upstream of the reach of interest to allow for adequate lateral and vertical mixing to be achieved. Sampling for dye at the upstream and downstream ends of the reach are needed to determine the mean (centroid) travel time in the reach and to signal the time to initiate sampling to define the plateau gas concentration at both ends of the reach.

The determination of the tracer gas desorption coefficient by the steady-state method follows a two-step procedure. The initial approximation of K_t is calculated similarly to that for the slug injection procedures. It is given by the following equation:

$$K_t = \frac{1}{t_d - t_u} \log_e \frac{(C_p Q)_u}{(C_p Q)_d} \quad (51)$$

where C_p is the plateau concentration of tracer gas in micrograms per liter and all other units are compatible. Because the above initial approximation of K_t may be corrected for possible minor effects of

longitudinal dispersion (Yotsukura and others, 1984), the more-accurate tracer gas desorption coefficient is determined through trial-and-error solution of the following equation for K_t :

$$\frac{(C_p Q)_u}{(C_p Q)_d} = \frac{(\int (C_d / A_d \exp(K_t t)) dt)_u}{(\int (C_d / A_d \exp(K_t t)) dt)_d} \quad (52)$$

where the initial value of K_t is derived from equation 51, above and all units are compatible.

The assumptions necessary for the steady state procedure are that flow is steady, that the tracer gas undergoes the same dispersion as the dye tracer, and that losses of dye can be corrected by multiplying all ordinates of the time-concentration curve by a loss factor.

Tracer Injection

For all injections by the slug-injection and steady-state procedures, propane gas was used as the surrogate tracer gas for oxygen. The propane gas was of a commercial grade obtained from local suppliers and stored in 20-pound tanks (barbeque-grill type). No more than one tank was used for a single injection so that the purity of the propane-gas mixture would be uniform. The injection rate of gas, which ranged from 10.0 to 15.0 liters per minute for slug injections and 2.0 liters per minute for steady-state injections, was provided by a single-stage

regulator (Union Carbide, model Purox W1-SSB-608-510) and maintained by a direct-reading rotometer (Union Carbide, model FM4348) calibrated for carbon dioxide (similar to propane). The injection rates were initially computed by methods suggested by Rathbun (1979). Later, injection rates were dictated by experience of what had previously been successful. The propane tank was kept on the stream bank on a scale during injection. Timed scale readings were used to verify the flow rate constancy as read on the rotometer. Gas injection was into the 50 percent of flow streamline through flexible, plastic tubing (Tygon, 0.25-inch I.D.) and either a single or dual, flat-plate diffuser positioned longitudinally on the streambed. The flat-plate, tile diffusers, which each measured 3 by 40 inches, had a nominal pore-size of 2 microns. The diffusers were positioned in a relatively deep section which allowed for maximum water-coverage and, hence, maximum gas absorption efficiency. Prior to injection, the tubing and diffusers were purged of air and filled with propane.

All injections utilized rhodamine-WT fluorescent dye as the conservative dispersion-dilution tracer. The dye was manufactured by Crompton and Knowles Corporation. For the slug-injection, gas-tracer tests, dye was injected during the same period as the propane. The quantity of dye used for each tracer test was calculated from methods described by Rathbun (1979) so as not to exceed the downstream limit for dye concentration of 10 micrograms per liter, which is recommended by the U.S. Geological Survey. The dye quantity ranged from 50 to 150 milliliters of 20-percent dye. The dye injection duration was dictated

by the propane injection duration. The injection rate of dye solution (20-percent dye mixed with distilled water) was chosen so as to be in an accurate range for the battery-powered laboratory-grade metering pump (Fluid Metering, model RP-BG75-2SSY) used to inject the solution. The rate for all such injections was set at 40 milliliters per minute. The dilution requirements for the dye solution were calculated such that the desired mass of dye would all be injected over the selected duration of the injection at the selected constant rate of the metering pump. For example, for a 30-minute injection at 40 milliliters per minute, the selected dye volume would be diluted with distilled water to a volume of 1200 milliliters. The injection of the dye solution into the stream, as with the propane, was made through flexible, plastic tubing (Tygon, 0.125-inch I.D.) from the metering pump positioned on the stream bank. The dye solution entered the stream at the water surface directly above the diffuser plate in the 50 percent of flow streamline. The injection tubing was purged of air prior to injection and filled with dye solution. The dye solution was pumped from a graduated cylinder so that timed readings of dye-solution usage could be made throughout each injection to ensure a constant delivery rate.

Dye injection as part of the steady-state, gas-tracer procedure was made as an instantaneous slug injection. The dye quantity was calculated as previously described. The dye was then carefully measured with a pipette or graduated cylinder and then mixed with about three gallons of stream water in a five-gallon, plastic bucket. The dye solution was then poured into the stream directly above the gas diffuser

plate at the time the steady-state propane injection was started.

All persons involved either in handling the dye or dye solutions, or in equipment cleanup following injection wore disposable plastic gloves. These persons were preferably not involved in later dye-sampling operations downstream. All cleanup was performed up the stream bank, well away from the water's edge, to prevent accidental release of additional dye.

Dye Sampling and Measurement

At the first sampling cross-section (upstream end of the measurement reach), which was located far enough downstream to ensure adequate lateral and vertical mixing, a discharge measurement was first performed. From the discharge measurement, the lateral location of the center of flow (50-percent of flow) was determined and marked by flagging the position on a tape (tagline) stretched across the stream. Additionally, the centers of the left and right thirds of flow were flagged. These locations were determined from the discharge measurement at the lateral points which corresponded to the 16.7 and 83.3 percent of cumulative discharge. Dye samples were collected at each of the three points in the sampling cross-section at mid-depth by hand. Glass vials (8-dram) with screw-caps were used to contain each sample. The vials were laboratory cleaned and rinsed with distilled water and rinsed again with stream water at the time of sampling. One or two samples from each

point taken prior to the arrival of the dye cloud were retained for determination of background fluorescence. This background is usually due to the presence of algae or other organics. Sampling intervals varied but, ideally, 30 to 45 samples from each sampling point were taken so that the time-concentration curve could be accurately defined. Generally, sampling intervals were shortest on the rising limb and at the peak of the curve and longest to define the falling limb and tail portions of the curve. The tail portions of some of the dye recovery curves were sampled using an automatic sampling device. Two types were used. One was a floating "dye boat" described by Kilpatrick (1972) and enabled dye sampling using 24 syringes which were spring-loaded and mechanically tripped sequentially at a pre-determined interval, which could range from 10 to 45 minutes. The other was a bank-mounted, pumping-type, sequential-sampler (Isco, model 1640) with a programmable sampling interval. Samples were taken again at the 50-percent streamline. After sample collection with the automatic sampler was complete, the syringes or sampler bottles were emptied into the 8-dram glass vials and treated in the same manner as those collected manually.

A portable, filter-fluorometer (Turner Designs, model 10 equipped with a rhodamine filter kit) was used in the field to detect the presence of the dye tracer. These field dye determinations were used to direct the frequency of dye sampling and to initiate and terminate propane sampling. The remaining dye sample was retained in the glass vial and stored in an insulated, light-proof box and transported back to a laboratory for final dye analysis. The fluorometer was calibrated for

direct reading in micrograms per liter using procedures described by Wilson and others (1984). Care was taken to ensure that the dye used for standards and for field injection was from the same lot. A dye standard was also used in the field to constantly check the calibration of the fluorometer. Final dye concentration determinations were made on dye samples in the laboratory after all samples were temperature equilibrated with the fresh dye standards. Fluorometer calibration was checked approximately after every five determinations. Dye concentration-time data was recorded on specially prepared field forms and then entered into the U.S. Geological Survey computer for storage and subsequent computation.

Sampling for dye at other sampling cross-sections downstream followed the same procedures. However, because there was additional lateral mixing afforded by the additional length of travel, only the center of flow streamline was sampled.

Gas Sampling and Measurement

At each of the sampling cross-sections, gas sampling was done at middepth along only the center of flow streamline. However, during one tracer measurement, the upstream cross-section was also sampled within the right, middle, and left thirds of flow along with the dye. The sampling interval for propane gas was determined from real-time analysis of the dye sampling. For the slug-injection procedure, the dye and gas

clouds are assumed to be in the same location, so gas sampling to define the gas time-concentration curve can be based on the measured dye concentrations. For the steady-state procedure, the gas sampling to define the plateau concentration follows the complete (dye concentrations less than two percent of the peak concentration) passage of the dye cloud. Gas sampling intervals varied, but the majority of samples were collected so as to most accurately define the peak portion of the breakthrough curve. This provided the greatest accuracy for both the peak method and the total-weight method because most of the mass is transported nearer the peak. Generally, 20-30 gas samples were collected at each sampling point for the slug-injection procedure and 10-15 for the steady-state procedure. However, because gas analysis is expensive, not all samples were analyzed. Based on the prepared dye recovery curve, gas samples for analysis were selected from those collected which best defined the gas, time-concentration curve or plateau.

The gas samples were collected in 40-milliliter septum vials with small, sewage-type, dissolved-gas samplers. The samplers filled in approximately 20 to 25 seconds and allowed approximately 4 to 5 exchanges of the water in the 40-milliliter vial. The propane samples were preserved (to avoid possible biological decay) with one milliliter of 37-percent, reagent-grade formaldehyde which was injected into the sample by pipette. The glass vials were then sealed air-tight with plastic screw caps containing teflon liners. To maintain the samples air-tight until analysis, the sample vials were kept at near sampling

temperature (to prevent excessive expansion or contraction) in an insulated, light-proof box. The samples selected for analysis were packed in commercial coolers kept close to the sampling temperature and sent by overnight mail to the U.S. Geological Survey laboratory in Atlanta, Georgia for analysis.

Determination of propane gas concentrations were made using a procedure described by Shultz and others (1976). The method uses a stripping line and cold-trap apparatus in conjunction with a gas chromatograph equipped with a flame ionization detector (FID). A detailed description of the procedure is presented in Appendix A.

As with the dye concentration data, the gas concentration-time data were also entered and stored in the USGS computer.

Field Measurements

As was previously mentioned, prior to any field reaeration measurements, a field survey was carried out in which reference points were installed or marked along each of the reaches to be tested. During the tracer studies the water-surface elevation at each of the reference points was measured and recorded using a folding engineer's rule and a line level where needed. The measurements were made along the reach and followed the cloud of tracers as closely as possible. These measurements, along with the surveyed cross-sections, could provide a water-surface profile of the reach during each tracer measurement.

Additionally, the cross-section geometry could be synthesized using the reference point measurements and later used for analysis.

Discharge measurements were made at each sampling cross-section prior to the arrival of the tracers. These measurements were made with a cup-type current meter (Price, Pygmy model) and methods described by Buchanan and Somers (1969). At the time of the discharge measurement, the water-surface elevation at the reference point nearest the sampling cross-section was measured and used in developing a stage-discharge relation. Throughout the passage of the tracers past the sampling cross-section, multiple measurements of the water surface elevation at the reference point were made. If any appreciable change in stage was detected, additional current-meter discharge measurements were made. In this way, a time-discharge curve would be available along with the time-concentration curves prepared from tracer sampling.

Water temperature was recorded at each sampling cross-section during the time of passage of the tracer cloud through the test reach. These measurements were made with a laboratory-grade mercury thermometer placed in a flowing portion of the stream. The measurements were recorded to 0.1 degree Celsius at a frequent interval--typically every 15 to 30 minutes. The mean water temperature to be used in standardizing each reach reaeration coefficient calculation was time-weighted. This time-weighted mean was made by tracking the water temperature during the period that the centroid of the tracer cloud was within the measurement reach. Correction of the reaeration and

desorption coefficients to a standard of 20 degrees Celsius was made using equation 47.

Field notes detailing flow conditions, weather, air temperature, and other environmental and hydrologic observations were kept. These notes could be used later qualitatively to aid in the interpretation of the research findings. Additional environmental support variables occasionally measured included suspended sediment concentration, specific conductivity, and wind speed. Suspended sediment samples were collected with a hand-held sediment sampler (U.S. Geological Survey, model DH-48). Methods described by Guy and Norman (1970) were used to obtain a 300 to 400 milliliter sediment/water sample which was representative of the sampling cross-section. Analysis of the sample followed the procedure described by Guy (1969). Specific conductivity was measured in-stream using a field conductance meter (Beckman, model RB-3 or RB-5) equipped with temperature compensation and a dip-type cell. Wind speed above the water surface was measured and recorded using a cup-type anemometer equipped with a digital totalizer (Belfort Instruments, model S-349A) and mounted on a tripod. Readings were taken from the totalizer at intervals during the passage of the tracer cloud through the measurement reach. The anemometer cups were positioned at a height averaging 2.5 feet above the water surface during the measurements. These environmental variables were included for qualitative assessment purposes only.

Tracer Computation

Similar computational procedures were used for dye data collected for both slug-injection and steady-state gas tracer techniques. Methods suggested by Grant and Skavroneck (1980) were used to adjust measured dye concentrations to what they would have been if the dye had been completely conservative. This procedure is handled directly in the computational scheme used for determining first-order desorption coefficients (equation 48). The background fluorescence or equivalent background dye concentration was determined for each set of dye samples collected at each sample cross-section from samples collected prior to the passage of the dye cloud. This background value, which ranged from 0.02 to 0.20 micrograms per liter, was subtracted from each concentration value prior to development of the dye time-concentration curve. The lateral mixing completeness for each study in which three sampling points in the sampling cross-section were taken was determined. This was done by comparing the fractional recovery of dye at each point with that injected. Because each of the three sampling points represented one-third of the total flow, one third of the dye mass recovered should have been represented by the dye recovery curve at each point. Where the mass recoveries varied by less than ten percent, the center sampling point dye recovery curve alone was used for further computation. Where this variance was more than ten percent, each of the ordinates of the dye recovery curves were averaged to produce an average response curve for the cross-section.

The time of travel or mean reach travel time was calculated as the difference in the centroids for the dye response curve upstream and downstream. The centroids were calculated for each time-concentration curve using a specially prepared computer program utilizing the moment method. The moment method follows the following calculation:

$$\bar{t} = \frac{\int C t dt}{\int C dt} \quad (53)$$

where \bar{t} is the elapsed time from start of dye injection to the centroid of the time-concentration curve, C is the dye concentration, and t is the time since dye injection initiation.

The longitudinal dispersion coefficient was also calculated from the dye time-concentration curves based on a method described by Fischer (1973). The relation is given as:

$$D_L = \frac{(S_t)_d^2 - (S_t)_u^2}{t_d - t_u} \frac{V^2}{2} \quad (54)$$

where D_L is the longitudinal dispersion coefficient, in square feet per second, $(S_t)^2$ is the variance of the time-concentration curve, and V is the mean reach velocity in feet per second, which is given as the reach length, L , in feet divided by travel time, $t_d - t_u$, in seconds.

Hydraulic Computation

A time-discharge curve for each trace at each sampling cross-section was developed from the stages measured before, during, and following the passage of the tracer cloud along with the developed stage-discharge relationship. The rating was shifted following procedures described by Buchanan and Somers (1969) so as to pass through the measured discharge values from the period of the trace. This accounted for minor shifts occurring in the stage-discharge relation due to control changes between periods of discharge measurement. The mean discharge corresponding to each trace for each sampling cross-section was calculated on the basis of weighted dye concentrations determined from the dye time-concentration curve. The mean discharge for each reach for each tracer study was determined from simple averaging of the upstream and downstream cross-sectional mean discharges. Where contiguous reaches were combined into one, the mean discharge for the combined reached was determined by travel-time weighting the mean reach discharges for each reach being composited. All discharges were measured and recorded to three significant figures.

Cross-sectional characteristics of the reaches under the flow conditions during tracer measurement were determined using field measurements made during the tracer measurement in conjunction with surveyed cross-sections. The measured water surface elevations at the surveyed reference points were utilized with the surveyed cross-sections and a discharge determination to generate a complete set of physical and

hydraulic characteristics for each surveyed cross-section. Reach-averaged values for each characteristic were calculated using a length weighting scheme. The length weighting utilized the effective length determined from the midpoint of the increment upstream to the midpoint of the increment downstream.

The reach-averaged hydraulic parameters to be used in reaeration coefficient predictive equation evaluation and development are given below.

- (1) Mean reach discharge (Q), in cubic feet per second, was determined as previously described.
- (2) Reach length (L), in feet, was determined by taping the longitudinal distance along the 50-percent-of-flow streamline from the upstream to downstream ends of each reach.
- (3) Mean width (W), in feet, was determined by using the computed length-weighted mean widths.
- (4) Mean velocity (V), in feet per second, was determined as the reach length, L , in feet divided by the mean travel time (difference in the upstream and downstream dye cloud centroid times, $t_d - t_u$), in seconds.
- (5) Mean depth (D), in feet, was determined as the discharge, Q , divided by the mean velocity, V , and the mean width, W .
- (6) Mean cross-sectional area (A), in square feet, was determined as the product of the mean width, W , and mean depth, D .

- (7) Water-surface slope (S), in feet per foot, was determined by dividing the difference between water surface elevations at the upstream and downstream ends of the reach by the reach length, L .
- (8) Froude number (F) is a dimensionless quantity determined by dividing the mean velocity, V , by the square root of the product of the acceleration due to gravity, g , and the mean depth, D .
- (9) Hydraulic radius (R), in feet, is normally determined as the mean cross-sectional area divided by the mean wetted perimeter. However, in this research, cross-sectional measurements indicated that in all cases it was approximately equal to the mean depth, so for computational purposes it was assumed to be equivalent to the mean depth, D .
- (10) Mean shear velocity (u_*), in feet per second, was determined as the square root of the product of the acceleration due to gravity, g , the hydraulic radius, R , and the water-surface slope, S .
- (11) Longitudinal dispersion coefficient (D_L), in square feet per second, was determined as previously discussed.
- (12) Mean shear stress (SS), in pounds per square foot, was determined as the product of the unit weight of water (62.31 pounds per cubic foot), the hydraulic radius, R , and the water surface slope, S .

(13) Mean Reynolds number (N_R) is dimensionless and was determined as the product of the mean velocity, V , and the hydraulic radius, R , divided by the kinematic viscosity of water at the mean reach water temperature, T .

(14) Mannings roughness coefficient (n) was determined by solving Mannings equation ($V = (1.486 / n) R^{0.667} S^{0.5}$) for n using the mean velocity, V , hydraulic radius, R , and the water-surface slope, S .

Alternate formulations to those just described were used in evaluating the sensitivity of reaeration coefficient predictive equations to the methods used in determining the input parameter values.

In the simplest method (method 1) the following approaches were used:

- (1) Mean depth (D_1), in feet, was estimated using the average of the mean depths computed for each of the upstream and downstream ends of the measurement reach.
- (2) Mean velocity (V_1), in feet per second, was estimated using a regression equation by Boning (1974) in which $V_1 = 0.38 Q^{0.4} S^{0.2}$.

The other necessary parameters were computed from the depth and velocity estimates along with the water-surface slope calculated as previously presented. Another method used for parameter value estimation (method 2) included:

(1) Mean depth (D_2), in feet, was estimated using the length-weighted average of cross-sectional mean depths for all cross-sections in the measurement reach.

(2) Mean Velocity (V_2) was determined in the same manner as V_1 .

Again, the other parameters necessary for input into the prediction equations were calculated from the depth and velocity estimates and water-surface slope as previously defined. The original method previously presented was termed "method 3."

Parametric and non-parametric statistics were developed and applied so that the degree of pool-and-riffling for each reach and under different flow conditions could be objectively measured. Intuitively, pool-and-riffling should be related to the variability of the depth and cross-sectional area longitudinally along each reach. In a completely channel-controlled reach with no pool-and-riffling, the variability in the depth and cross-sectional area would be small, approaching zero. In contrast, in a highly pooled-and-riffled reach large variability would be expected. The depths and cross-sectional areas used in the measurement were determined from the cross-sections for each trace for each flow condition which were synthesized using both field measurements and surveyed cross-sections. A parametric statistic--the coefficient of variation (C.V.) of the depths and cross-sectional areas--were determined and used as pool-and-riffling statistics. Alternately, a non-parametric statistic was developed because the distributions of depths and cross-sectional areas were not normal, but skewed. The non-parametric statistic was calculated as the interquartile range (the 75-

percentile value minus the 25-percentile value) divided by the median value expressed as a percent (IQR/M).

It was desirable to estimate the flow duration and recurrence interval for each flow condition observed during tracer measurement. These were determined for the historical gaged discharge record from the USGS Middle Fork Beargrass Creek station using conventional U.S. Geological Survey procedures. Only the period of record from 1966 to 1985 was used because it most closely represented the current conditions. Significant land-use changes occurred during the period of record prior to 1966. From field observations under low and medium flow conditions, it is evident that parts of the Middle Fork Beargrass Creek basin were sources and parts were sinks for streamflow. Therefore, no modifications to the durations or recurrence intervals were made for the studied reaches based on contributing drainage basin areas. This assumption considered that the drainage areas for the stream reaches studied and for the Middle Fork Beargrass Creek gage location are not significantly different.

Computation Error Analysis

An examination of equations 48, 50, and 51 shows that errors in the determination of factors in those equations will propagate to the calculated K_t value. Yotsukura and others (1983) demonstrated that the error propagation will be controlled by the nondimensional number $K_t(\bar{\epsilon}_d - \bar{\epsilon}_u)$. If this product is less than one, then the error in K_t will be

less than the errors in determining the gas concentrations and masses as well as discharge. It also follows, then, that for $K_t(\bar{E}_d - \bar{E}_u)$ values greater than one, the error in the computed K_t could be greater than that of the input values. It is then desirable to compute a relative error (E_R) of K_t and K_2 values from an assumed error (E_A) in the input concentrations and discharge. The assumed error was set as a coefficient of variation of two percent. The corresponding relative error in K_t and K_2 were then determined and expressed as a coefficient of variation and 95-percent confidence bands. The relative error of the K_t values (E_R) is calculated by:

$$E_R = E_A / K_t(\bar{E}_d - \bar{E}_u) \quad (55)$$

If the relative error is assumed normally distributed, the 95-percent confidence bands are calculated by:

$$K_{2-U95} = K_2 + (K_2)(E_R)(1.96) \quad (56)$$

where K_{2-U95} is the upper 95-percent confidence band on K_2 , and

$$K_{2-L95} = K_2 - (K_2)(E_R)(1.96) \quad (57)$$

where K_{2-L95} is the lower 95-percent confidence band on K_2 .

ERROR ANALYSIS OF PREDICTION EQUATIONS

In evaluating the performance of prediction equations in providing reaeration coefficient estimates predicted values are compared to measured values under the same hydraulic conditions. Statistics need to be used which can measure both the precision and the accuracy of these predictions. The precision of estimates generally measures the scatter. A precise model may also provide biased results. A model which always over predicts the reaeration coefficient by a nearly constant percentage is said to be precise, but not necessarily accurate. However, if on average the model predicts the coefficient closely then the model is said to be accurate but not necessarily precise.

Two statistics were used for assessing the errors of prediction equations (Rathbun, 1977; and Krenkel and Novotny, 1980). The standard error (SE) which is sensitive to the issue of precision is calculated as:

$$SE = \frac{(\sum(\hat{K}_2 - K_2)^2)^{0.5}}{N^{0.5}} \quad (58)$$

where \hat{K}_2 is the predicted reaeration coefficient and N is the number of observations or tracer measurements. The normalized mean error (NME) is sensitive to the issue of accuracy and is calculated as:

$$NME = \frac{(\sum(\hat{K}_2 - K_2) / K_2) 100}{N} \quad (59)$$

Each statistic was considered equally important because prediction models need to be both precise and accurate. The models were ranked based on each statistic separately and combined with a equal weighting to produce an overall rank. The models were ranked from best to worst. Additionally, box plots were used to show schematically the performance of each prediction equation. Both precision and accuracy can be seen on a box plot.

PREDICTION EQUATION DEVELOPMENT

The development of semiempirical and empirical prediction equations first required the selection of candidate independent variables to be considered. Initially, all variables measured or calculated were included for consideration. The general sequence of steps was as follows: (1) Scatterplots of all independent variables against the dependent variable, the reaeration coefficient were developed. These were used to identify variables which visually correlated with the reaeration coefficient. Also the appropriateness of a linear relation or the need for variable transformation (inverse, logarithm, or powers) was evaluated. (2) A correlation matrix with all the non-transformed variables was developed in order to look for early evidence of

multicollinearity. This was desirable because, generally, highly correlated variables are not used together in multiple regression model building. (3) An "all possible models" computer routine to identify the better possible model combinations was executed. (4) Model building techniques including stepwise, forward, and backward schemes also were used to identify statistically superior models. (5) Simple and multiple linear-regressions were used to evaluate the characteristics of each of the better models considered. (6) Fit-statistics, as well as colinearity diagnostics, were used in the model evaluation process.

RESULTS AND DISCUSSION

In this chapter, the results of all measurements, computations, and interpretations are presented and discussed.

MEASUREMENTS AND CONDITIONS

In this section, the results of field measurements and laboratory determinations will be presented. Additionally, the hydrologic and environmental conditions existing during the period of field measurements will also be included. The field measurements and laboratory determinations were used in computational schemes which resulted in summarized data, which also are presented.

Physical and Hydraulic Properties

Streamflow Conditions

The selected reaches of Middle Fork Beargrass Creek were in close proximity to the U.S. Geological Survey gaging station (see Figure 4). The gaging station record used to characterize the long-term flow variability was selected as the period 1966-1985. Records prior to 1966

were not considered because land-use and stream characteristics were quite different than they were during the period of this field investigation.

One useful way to characterize streamflow is by a flow-duration analysis. In this analysis, each observation in the period of record is sorted and percentiles are computed for each observed value. This procedure was applied to an analysis of mean daily discharge values for the selected period of record. A plot of the results is presented in Figure 5. In the figure, each value of mean daily discharge is plotted with the corresponding percentage of the observations in the record which equaled or exceeded that value. Note that the mean daily discharge was less than about 15 cubic feet per second about half the time. Also for the period of record used, Figure 5 can be used to find that a probability of the daily discharge being between 6.0 and 27 cubic feet per second (75-percentile and 25-percentile values) is 0.50.

For each tracer measurement made on Middle Fork Beargrass Creek, a corresponding flow-duration percentage was determined for the measured discharge. These probabilities ranged from 29.4 to 99.9 percent and are shown in Table 2. The 99.9 percent value roughly means that probably for only one day in 1000 days would the mean daily discharge be as low or lower than that measured. From the probability of exceedance values given in Table 2 it can be seen that the tracer measurements made were during roughly medium to low flow. No tracer measurements were made during the upper 29.4 percent of flows.

Modeling of stream water quality is frequently performed, for

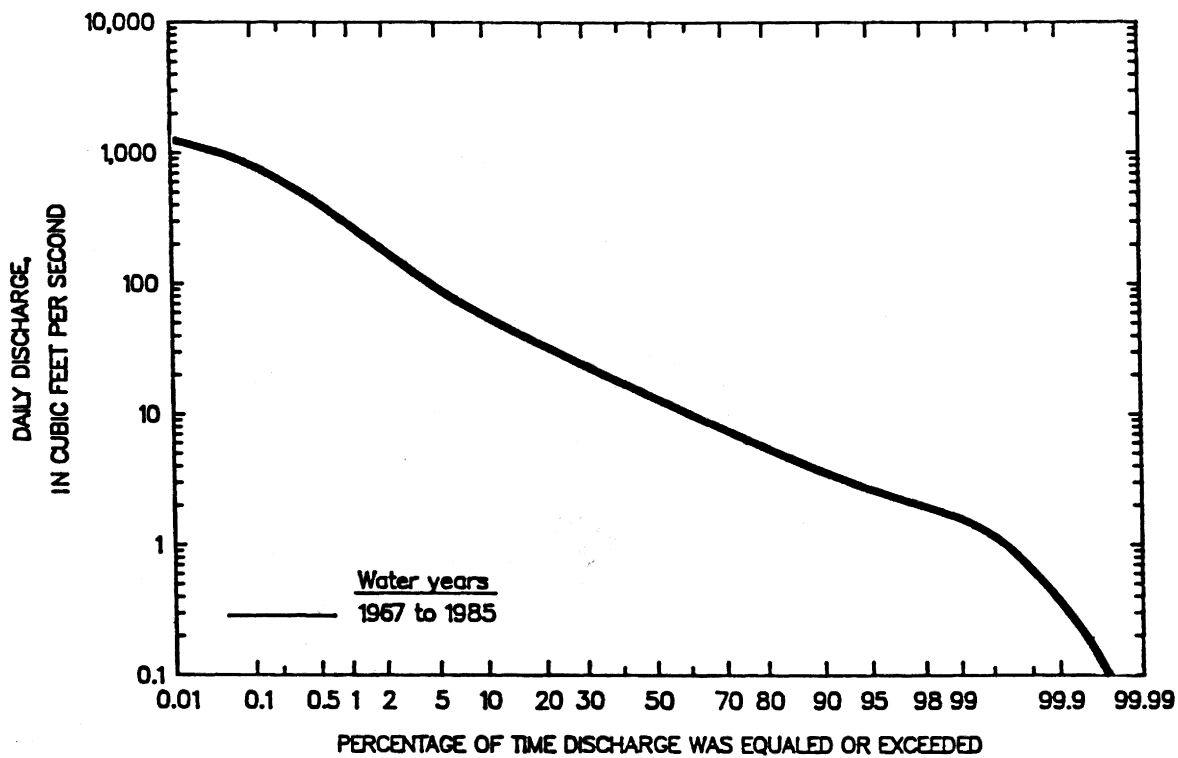


Figure 5 -- Flow duration curve for daily mean discharges for Middle Fork Beargrass Creek, 1966-1985

Table 2 -- Streamflow exceedance probabilities and 7-day lowflow return periods for flow conditions during hydrocarbon gas tracer measurements made on reaches of the Middle Fork Beargrass Creek

REACH	DATE (mmddy)	DISCHARGE (ft ³ /s)	PROBABILITY OF EXCEEDANCE ^{1,2} (percent)	7-DAY LOW-FLOW RETURN PERIOD ^{1,3} (years)
A	041885	12.100	51.9	---
A	050885	2.910	93.1	1.6
A	051685	8.830	63.5	---
A	052485	22.800	29.4	---
A	061485	13.000	49.1	---
A	081985	4.160	85.3	---
A	091785	0.509	99.9	94
B	041885	12.400	51.9	---
B	050885	2.920	93.1	1.6
B	051685	7.220	69.6	---
B	052485	21.800	32.4	---
B	061485	12.700	51.9	---
C	041885	12.300	51.9	---
C	050885	2.920	93.1	1.6
C	051685	7.690	67.7	---
C	052485	22.100	30.6	---
C	061485	12.800	51.9	---
D	041985	7.770	67.7	---
D	050785	3.070	92.6	1.4
D	091885	0.628	99.8	56

¹Both probabilities and return periods were determined from daily discharge records for U.S. Geological Survey station 03293000 for water years 1966-1985.

²Values shown are for the probabilities that the discharges measured would have been equaled or exceeded.

³The values shown result from a fitted Log Pearson Type III distribution of annual 7-day low-flow discharges. Values of return period less than 1.01 years are omitted in the table.

wasteload allocation purposes, at some prescribed low-flow condition. The common condition selected is for the lowest average flow over seven consecutive days which is expected to occur, on average, once in ten years. This condition is commonly called the "7-day, 10-year" low flow or 7Q10 value.

For each year in the flow record (for which record was complete) the lowest 7-day discharge was found. These values were then fit to a Log Pearson type III distribution to relate the values to a recurrence probability. The recurrence probabilities were converted to return periods and are shown graphically in Figure 6. The individual annual data points, plotted using Cunnane plotting positions, along with the smoothed curve are presented. From the data used to plot Figure 6, the 7Q10 could be estimated to be about 1.3 cubic foot per second.

As was done in the flow duration analysis, each flow condition measured during tracer measurements was evaluated using the data presented graphically in Figure 6. Only values of return periods greater than 1.01 years are presented in Table 2. Six of the tracer measurements were made at discharges with a longer return period than 1.01 years. Note that two of the measurements were made at discharges with return periods of substantially longer than the usually modeled 10-year low flow event. These two return periods were estimated at 56 and 94 years from the fitted data used to plot the curve in Figure 6.

In interpretation of a tracer measurement result, it was not entirely satisfactory to determine only the discharge during the measurement and its corresponding flow-duration and equivalent 7-day,

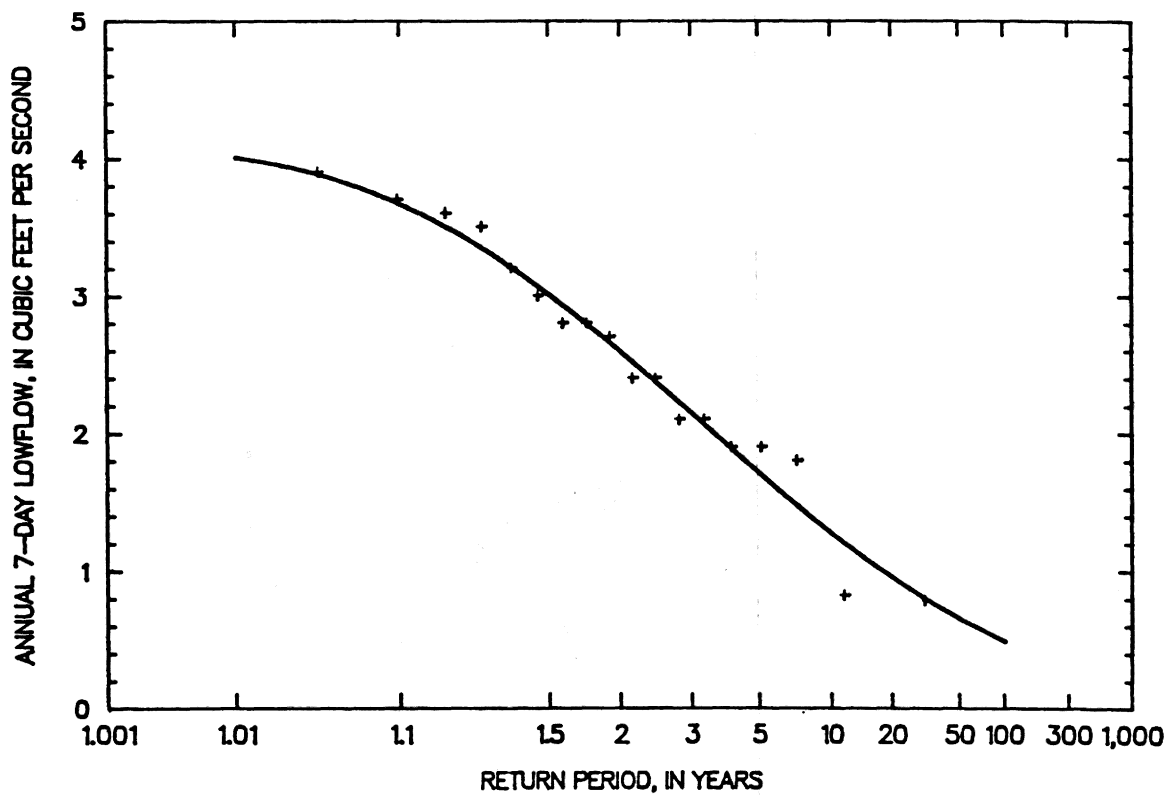


Figure 6 -- Estimated return periods and 7-day annual low flows for Middle Fork Beargrass Creek, 1966-1985

low-flow return period. Additionally, it was desirable to determine the flow conditions between, and just prior to, the tracer measurements. Therefore, the mean daily discharge values for the entire period of field measurements were computed and plotted as a continuous hydrograph for the period of April through September, 1985. This hydrograph is presented in Figure 7. Note that the range of mean daily discharges for that period was from a low of about 0.23 cubic feet per second during September to a high of about 130 cubic feet per second during August.

Hydraulic Characteristics

As an important adjunct to the desorption/reaeration measurements made, accurate and detailed hydraulic measurements were desired. As discussed in the Materials and Methods chapter, a preliminary field survey was performed on April 11, 1985 on four selected reaches. Elevation reference points were installed along each reach from which the water-surface elevation could be measured during each tracer measurement. These reference points were installed above and below obvious breaks in the water-surface profile rather than spaced equally. The number of reference points installed in each reach is shown in Table 3.

A detailed field survey was performed between May 30 and June 3, 1985 in which the previously installed reference points were leveled and when equally spaced cross-sections of each reach were measured and

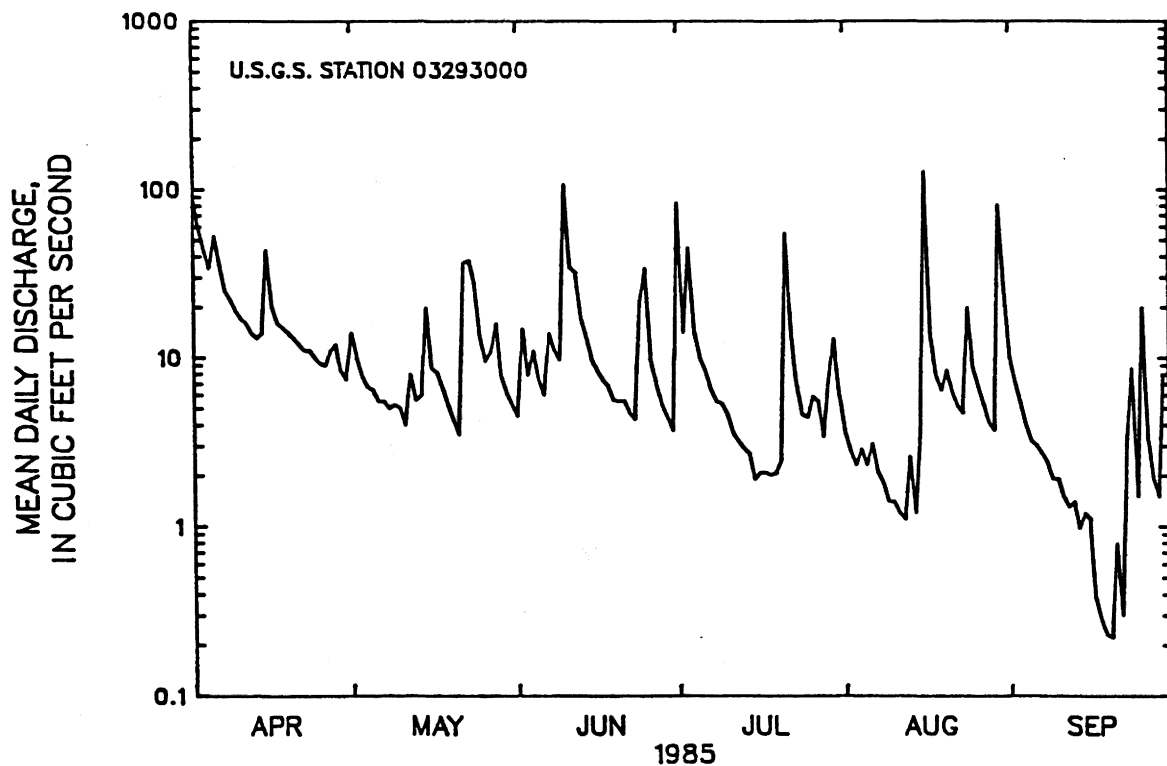


Figure 7 -- Hydrograph of mean daily discharge for Middle Fork Beargrass Creek during the period of hydrocarbon gas tracer measurements, April through September, 1985

Table 3 -- Summary of cross section surveying of tracer measurement reaches of Middle Fork Beargrass Creek

REACH	LENGTH (ft)	WATER-SURFACE SLOPE (ft/ft)	NUMBER OF CROSS SECTIONS	NUMBER OF REFERENCE POINTS
A	3040	0.0047	30	21
B	5035	0.00060	27	16
C	8075	0.0021	56	36
D	3825	0.0016	38	26

leveled. The survey data were incorporated into a computer program which could be used to synthesize the water surface profile and length-weighted cross-section and hydraulic parameter values. The number of cross-sections within each reach varied from 27 to 56. The actual number in each reach, along with the reach length, is given in Table 3.

The hydraulic parameters selected for use were presented in the Materials and Methods chapter. The reach-averaged hydraulic parameter values during each tracer measurement were computed from the tracer results, measured stream discharge, and application of the above-described cross-section computer program.

Discharge, slope, velocity, reach length, and stream width corresponding to each set of tracer measurements are shown in Table 4. Discharge ranged from 0.509 to 22.8 cubic feet per second. The slope was nearly constant for each reach. The variation shown within each reach was caused by upstream and downstream velocity-head differences and minor measurement errors. The slopes among reaches ranged over one order of magnitude from 3.1 to 25 feet per mile. The reach-averaged velocity was widely variable. It ranged from 0.018 feet per second during low flow conditions in reach A to 0.626 feet per second in the same reach under the highest flow conditions experienced during tracer measurements. The same length of each reach was used for all tracer measurements. The stream width did not vary much between reaches or for the same reach under different flow conditions. The reach-averaged width range as shown in Table 4 is from 24.7 to 42.3 feet.

The reach-averaged depth, Froude number, cross-sectional area,

Table 4 -- Hydraulic parameter results from tracer measurements made on reaches of the Middle Fork Beargrass Creek

REACH	DATE (mmddyy)	DISCHARGE (ft ³ /s)	SLOPE (ft/ft)	VELOCITY (ft/s)	LENGTH (ft)	WIDTH (ft)
A	041885	12.100	0.004670	0.3840	3040	39.9
A	050885	2.910	0.004710	0.1030	3040	35.8
A	051685	8.830	0.004690	0.2710	3040	40.0
A	052485	22.800	0.004650	0.6260	3040	42.3
A	061485	13.000	0.004680	0.4190	3040	40.6
A	081985	4.160	0.004700	0.1820	3040	33.8
A	091785	0.509	0.004720	0.0180	3040	27.4
B	041885	12.400	0.000597	0.2910	5035	28.9
B	050885	2.920	0.000603	0.0827	5035	27.5
B	051685	7.220	0.000599	0.1850	5035	28.8
B	052485	21.800	0.000601	0.4660	5035	29.9
B	061485	12.700	0.000589	0.3130	5035	29.1
C	041885	12.300	0.002130	0.3200	8075	33.0
C	050885	2.920	0.002150	0.0894	8075	30.6
C	051685	7.690	0.002140	0.2100	8075	33.0
C	052485	22.100	0.002130	0.5160	8075	34.6
C	061485	12.800	0.002130	0.3460	8075	33.4
D	041985	7.770	0.001590	0.3910	3825	30.0
D	050785	3.070	0.001600	0.1840	3825	27.9
D	091885	0.628	0.001560	0.0501	3825	24.7

Reynolds number, shear velocity, longitudinal dispersion coefficient, shear stress, and reach composite Manning's "n" values for each of the tracer measurements are shown in Tables 5 and 6. The calculated depth of each reach did not vary greatly between tracer measurements. For example, in reach A the range of computed depth was from 0.675 to 0.862 feet. The Froude number was highly variable as was the velocity. The reach-averaged cross-sectional area, while more variable than width, was not highly variable either for a reach during different flow conditions or between reaches. The Reynold's number varied by over an order of magnitude. The lowest values corresponding to more-laminar values of less than 2000 to values of over 60,000 corresponding to more turbulent conditions. Shear velocity as well as shear stress was nearly constant for each reach but varies markedly between reaches. The dispersion coefficient, calculated from the time-concentration curves for injected conservative tracers, varied over an order of magnitude and ranged from less than 9 to greater than 90 square feet per second. The reach composite Manning's "n" values were computed using the assumptions that all energy loss within each reach was lost at a constant rate and could be attributable to channel frictional losses. Note that high "n" values appear associated with low-flow conditions and low "n" values correspond to high-flow conditions.

A comparative summary of the key reach and hydraulic parameters of reach length, slope, velocity, depth, discharge, and Froude number is given by reach in Table 7. It is evident that the variability of these measures is more pronounced for measurements from reach A and less

Table 5 -- Hydraulic parameter results from tracer measurements made on reaches of the Middle Fork Beargrass Creek

REACH	DATE (mmddy)	DISCHARGE (ft ³ /s)	DEPTH (ft)	FROUDE NUMBER	CROSS- SECTION AREA (ft ²)	REYNOLDS NUMBER
A	041885	12.100	0.790	0.07610	31.5	28337.1
A	050885	2.910	0.789	0.02040	28.3	7665.6
A	051685	8.830	0.815	0.05290	32.6	20429.8
A	052485	22.800	0.862	0.11900	36.5	44510.3
A	061485	13.000	0.764	0.08450	31.0	27527.7
A	081985	4.160	0.675	0.03900	22.8	13087.7
A	091785	0.509	1.030	0.00313	28.3	1719.1
B	041885	12.400	1.470	0.04220	42.6	41434.6
B	050885	2.920	1.280	0.01290	35.3	9456.6
B	051685	7.220	1.360	0.02800	39.1	23732.5
B	052485	21.800	1.560	0.06580	46.8	62192.3
B	061485	12.700	1.390	0.04670	40.6	39258.1
C	041885	12.300	1.160	0.05230	38.4	35526.1
C	050885	2.920	1.070	0.01520	32.7	8696.4
C	051685	7.690	1.110	0.03510	36.6	21827.3
C	052485	22.100	1.240	0.08170	42.8	54035.2
C	061485	12.800	1.110	0.05970	37.0	34223.6
D	041985	7.770	0.662	0.08470	19.9	22315.8
D	050785	3.070	0.597	0.04200	16.7	9494.8
D	091885	0.628	0.507	0.01240	12.5	2257.8

Table 6 -- Hydraulic parameter results from tracer measurements made on reaches of the Middle Fork Beargrass Creek

REACH	DATE (mmddy)	DISCHARGE (ft ³ /s)	SHEAR VELOCITY (ft/s)	DISPERSION COEFFICIENT (ft ² /s)	SHEAR STRESS (lb/ft ²)	MANNINGS N
A	041885	12.100	0.345	39.80	0.229880	0.22598
A	050885	2.910	0.346	25.30	0.231556	0.84536
A	051685	8.830	0.351	46.60	0.238171	0.32763
A	052485	22.800	0.359	94.00	0.249757	0.14661
A	061485	13.000	0.339	59.70	0.222791	0.20275
A	081985	4.160	0.320	27.40	0.197678	0.43067
A	091785	0.509	0.396	9.22	0.302926	5.78469
B	041885	12.400	0.168	17.30	0.054683	0.16133
B	050885	2.920	0.158	17.30	0.048093	0.52021
B	051685	7.220	0.162	22.30	0.050760	0.24134
B	052485	21.800	0.174	49.10	0.058419	0.10517
B	061485	12.700	0.162	35.20	0.051014	0.14352
C	041885	12.300	0.282	23.00	0.153956	0.23662
C	050885	2.920	0.272	19.90	0.143344	0.80631
C	051685	7.690	0.277	28.50	0.148011	0.35094
C	052485	22.100	0.292	61.40	0.164573	0.15342
C	061485	12.800	0.276	42.30	0.147320	0.21250
D	041985	7.770	0.184	53.80	0.065586	0.11509
D	050785	3.070	0.175	20.00	0.059519	0.22900
D	091885	0.628	0.160	8.62	0.049282	0.74470

Table 7 -- Selected characteristics of reaches of Middle Fork Beargrass Creek during hydrocarbon gas tracer measurements

CHARACTERISTIC	REACH			
	A	B	C	D
Reach length (ft)	3040	5035	8075	3825
Slope (ft/ft)	.0047	.00060	.0021	.0016
Mean velocity (ft/s)	.0190-.626	.0827-.466	.0894-.516	.0501-.391
Mean depth (ft)	.675-1.03	1.28-1.56	1.07-1.24	.507-.662
Mean discharge (ft ³ /s)	.509-22.8	2.92-21.8	2.92-22.1	.628-3.07
Mean Froude number	.00313-.119	.0129-.0658	.0152-.0817	.0124-.0847

pronounced for measurements for the other reaches--especially reach B.

For computational purposes, the assumption was made that there was no significant difference between the reach-averaged depth and reach-averaged hydraulic radius. This was made, in part, because a reach-averaged hydraulic radius could not be back-calculated in the same manner as the depth. To check to see how valid this assumption was, the length-weighted average reach depth and hydraulic radius values, generated by the cross-section program, were compared. This comparison is presented in Figure 8. It is evident from the plotted data that, as expected, under lower flow conditions generally corresponding to lesser depths, the values are closer to one another (points plot closer to the depth equals hydraulic radius line) and deviate more at higher flow conditions. At greater depths, corresponding to higher flow conditions, the data points diverge from the depth equals hydraulic radius line.

If channel roughness, flow constrictions, water quality, and environmental conditions were identical for every tracer measurement for a given reach, then the resulting hydraulic parameter values determined would be expected to vary in a smooth continuous manner with reach discharge. The reach-averaged hydraulic parameters determined are presented as a function of discharge in Figures 9 through 19. Figure 9 shows that the overall reach water-surface slope varied markedly from reach to reach but varied almost undetectably for the same reach under different flow conditions. The reach velocity increased uniformly with discharge in all four reaches (Figure 10). Note that apparent outliers do exist for reach A, B, and C at discharges of about 4, 12, and 13

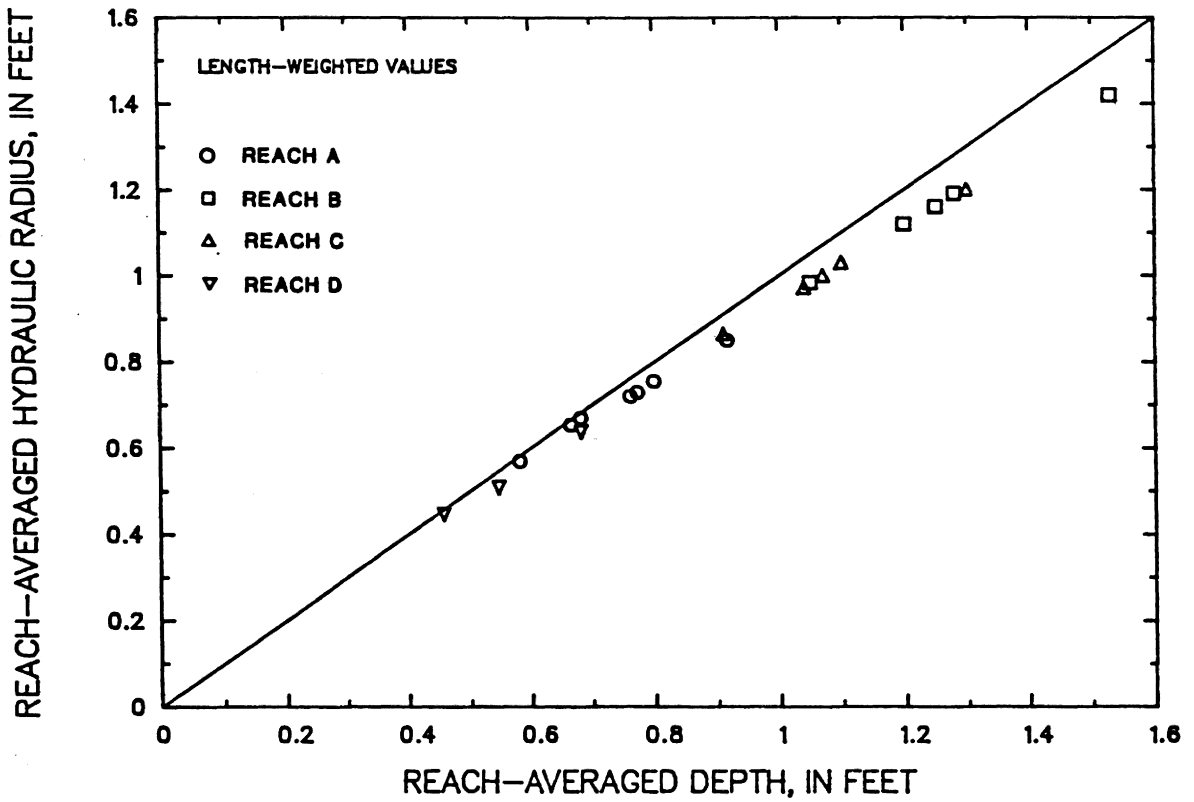


Figure 8 -- Comparison of reach-averaged depth and reach-averaged hydraulic radius determined from length-weighted hydraulic measurements

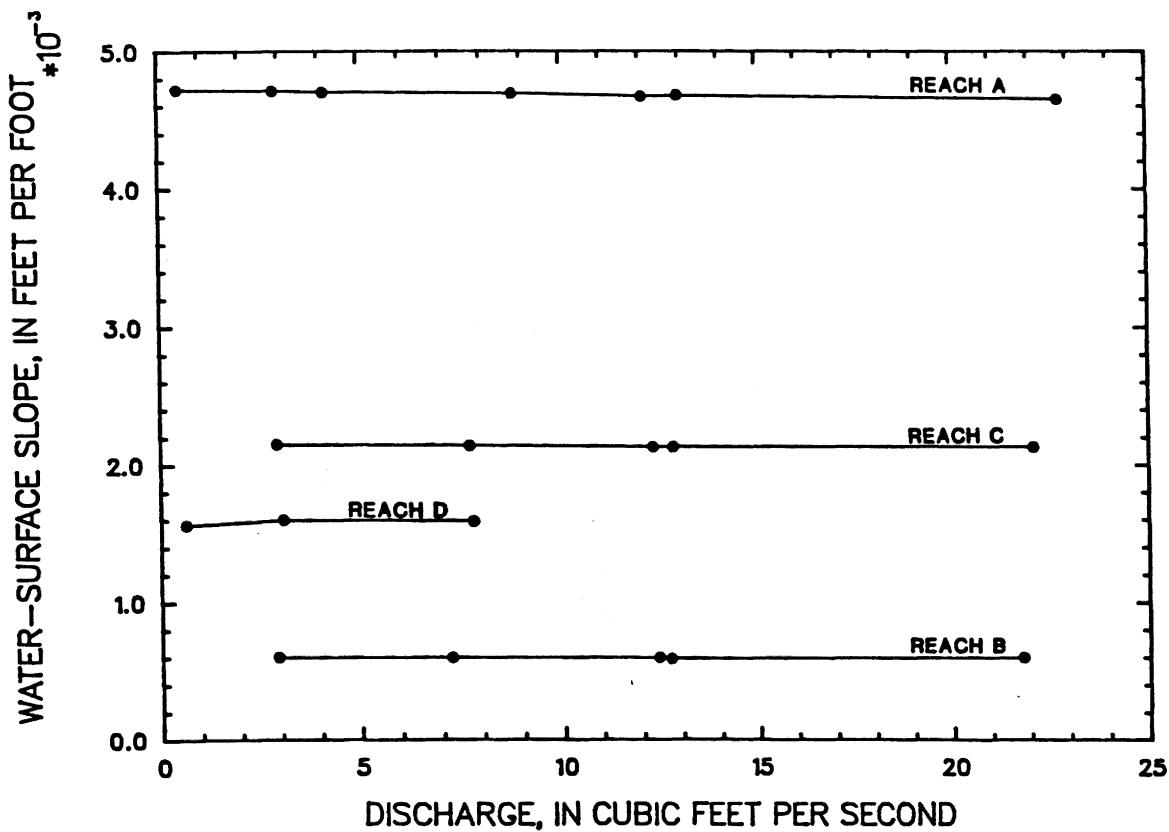


Figure 9 -- Reach-averaged water-surface slope shown as a function of discharge for reaches of Middle Fork Beargrass Creek, from tracer measurements made from April 18, 1985 through September 18, 1985

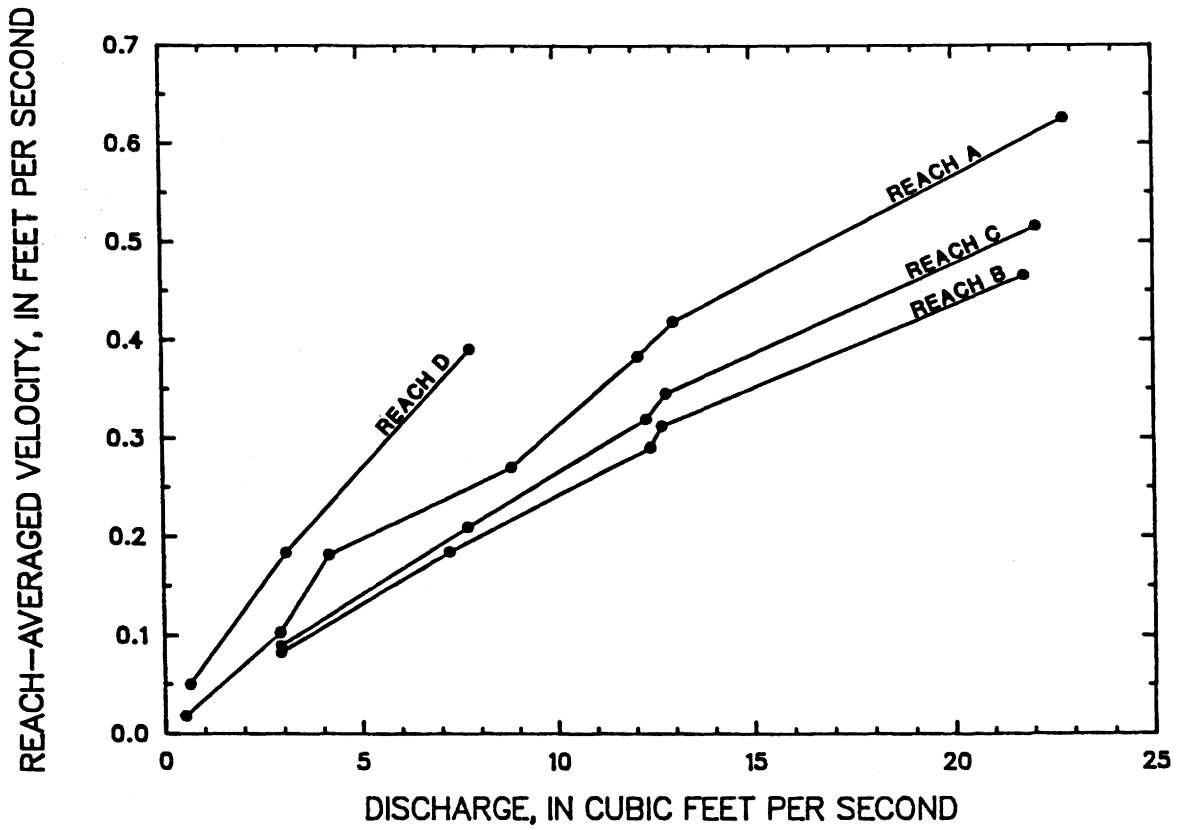


Figure 10 -- Reach-averaged velocity shown as a function of discharge for reaches of Middle Fork Beargrass Creek, from tracer measurements made from April 18, 1985 through September 18, 1985

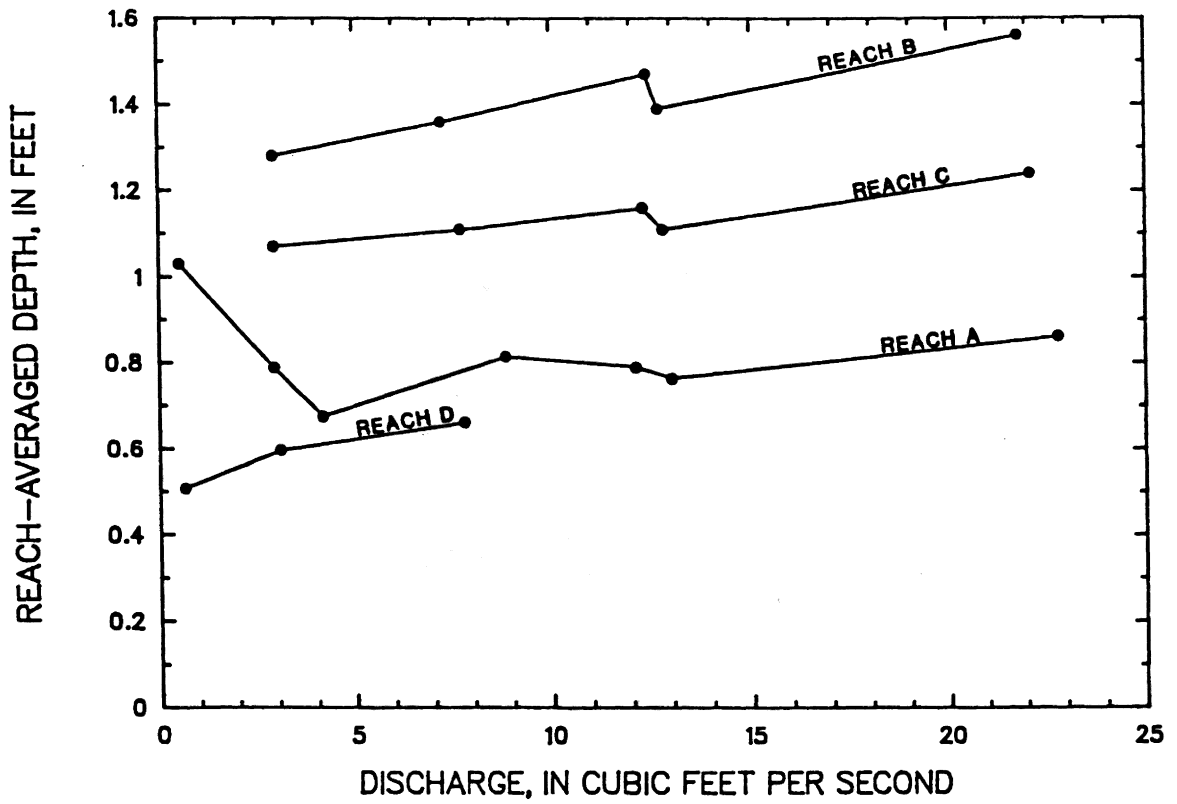


Figure 11 -- Reach-averaged depth shown as a function of discharge for reaches of Middle Fork Beargrass Creek, from tracer measurements made from April 18, 1985 through September 18, 1985

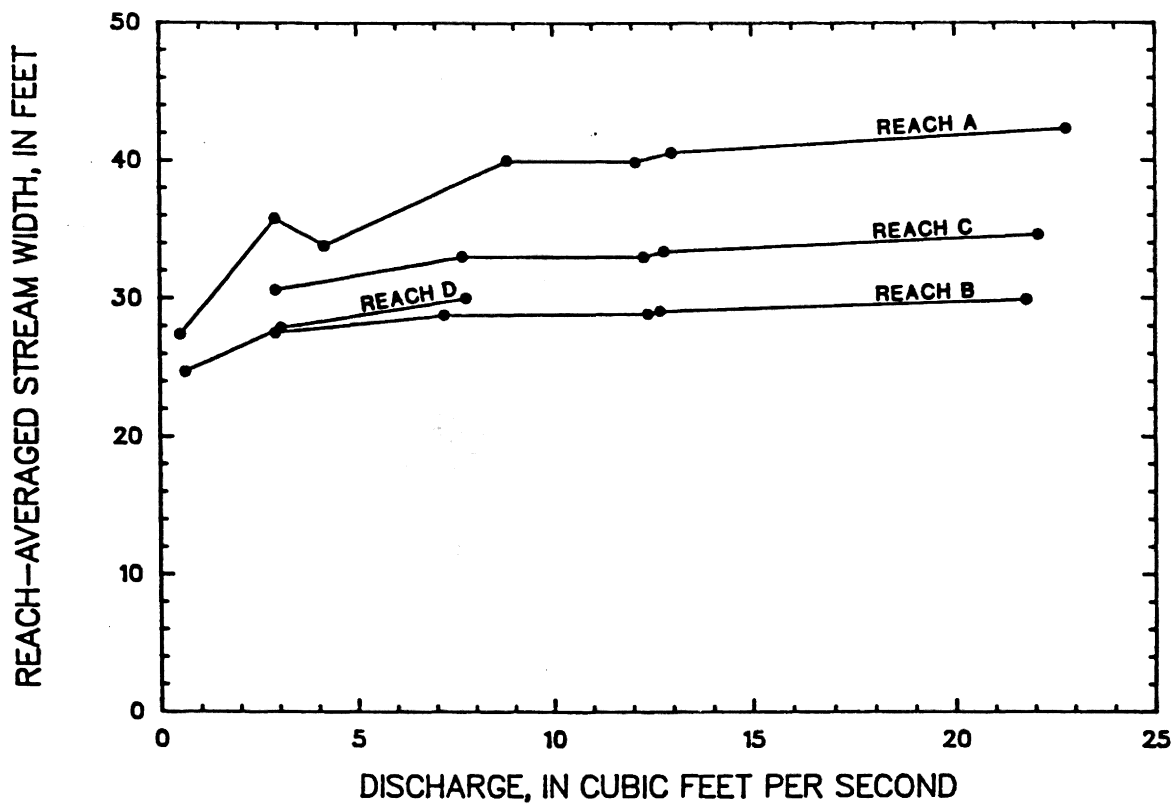


Figure 12 -- Reach-averaged width shown as a function of discharge for reaches of Middle Fork Beargrass Creek, from tracer measurements made from April 18, 1985 through September 18, 1985

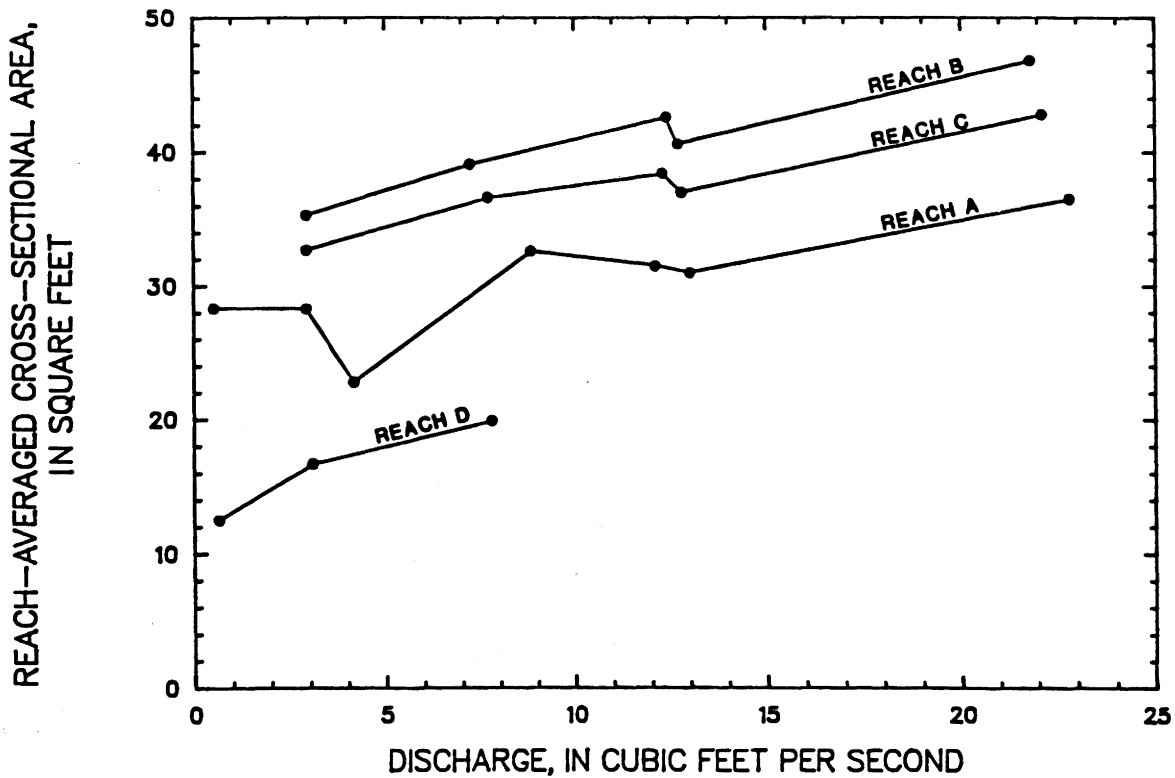


Figure 13 -- Reach-averaged cross-sectional area shown as a function of discharge for reaches of Middle Fork Beargrass Creek, from tracer measurements made from April 18, 1985 through September 18, 1985

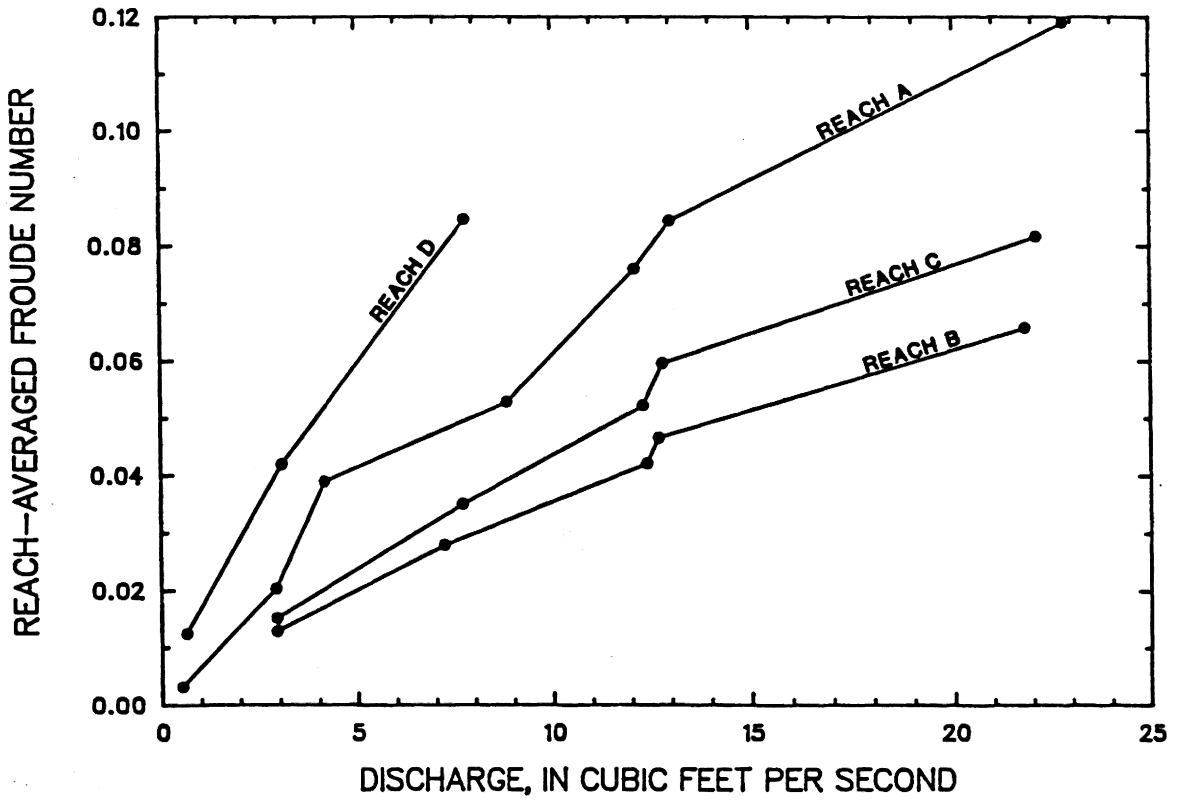


Figure 14 -- Reach-averaged Froude number shown as a function of discharge for reaches of Middle Fork Beargrass Creek, from tracer measurements made from April 18, 1985 through September 18, 1985

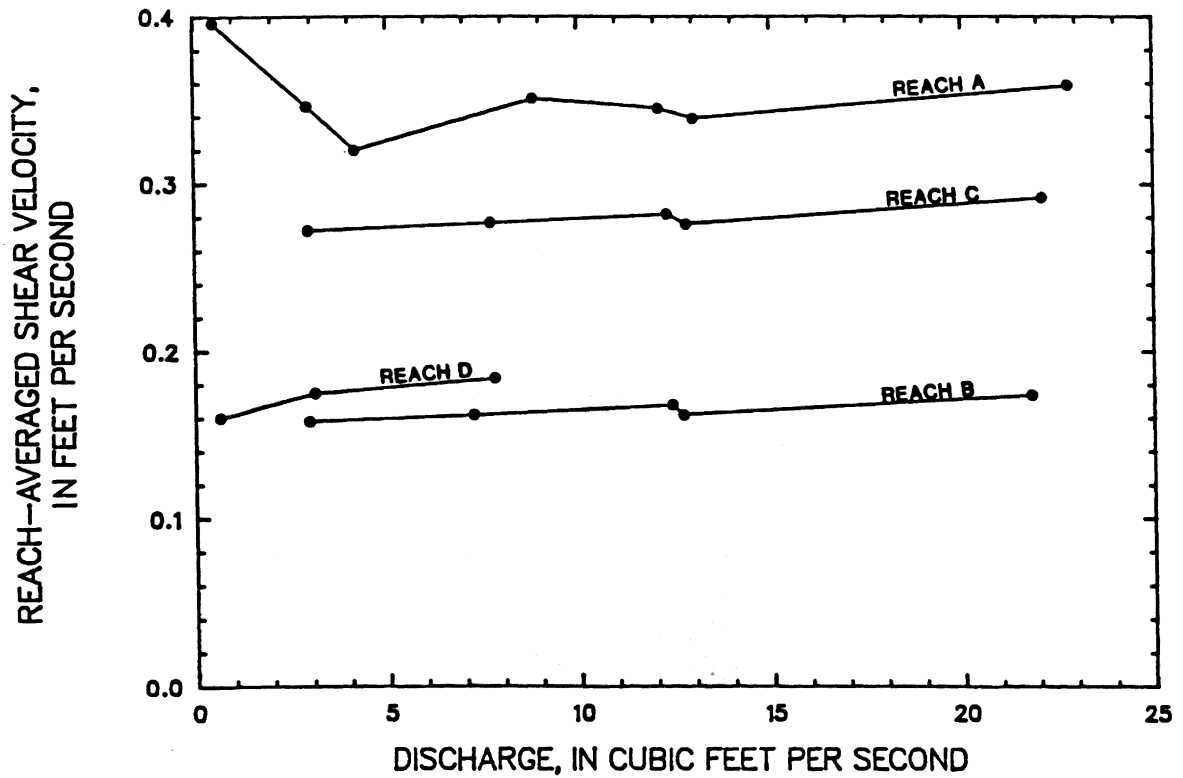


Figure 15 -- Reach-averaged shear velocity shown as a function of discharge for reaches of Middle Fork Beargrass Creek, from tracer measurements made from April 18, 1985 through September 18, 1985

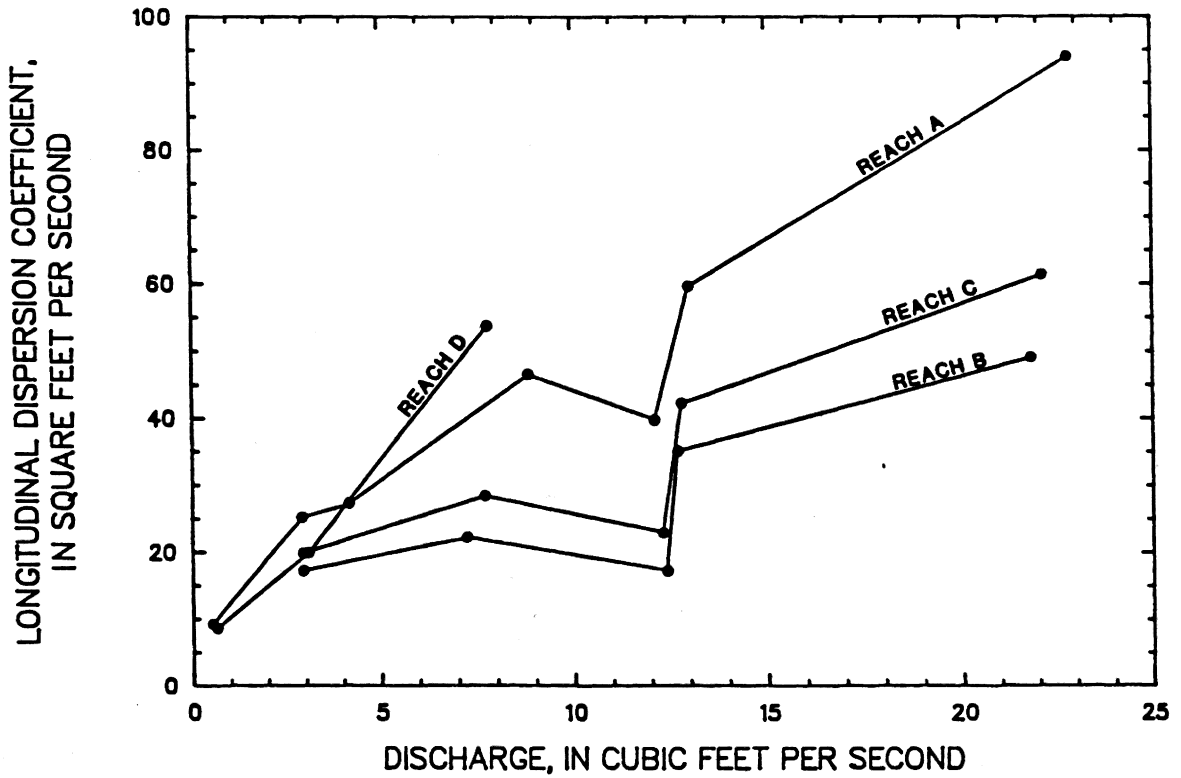


Figure 16 -- Reach-averaged dispersion coefficient shown as a function of discharge for reaches of Middle Fork Beargrass Creek, from tracer measurements made from April 18, 1985 through September 18, 1985

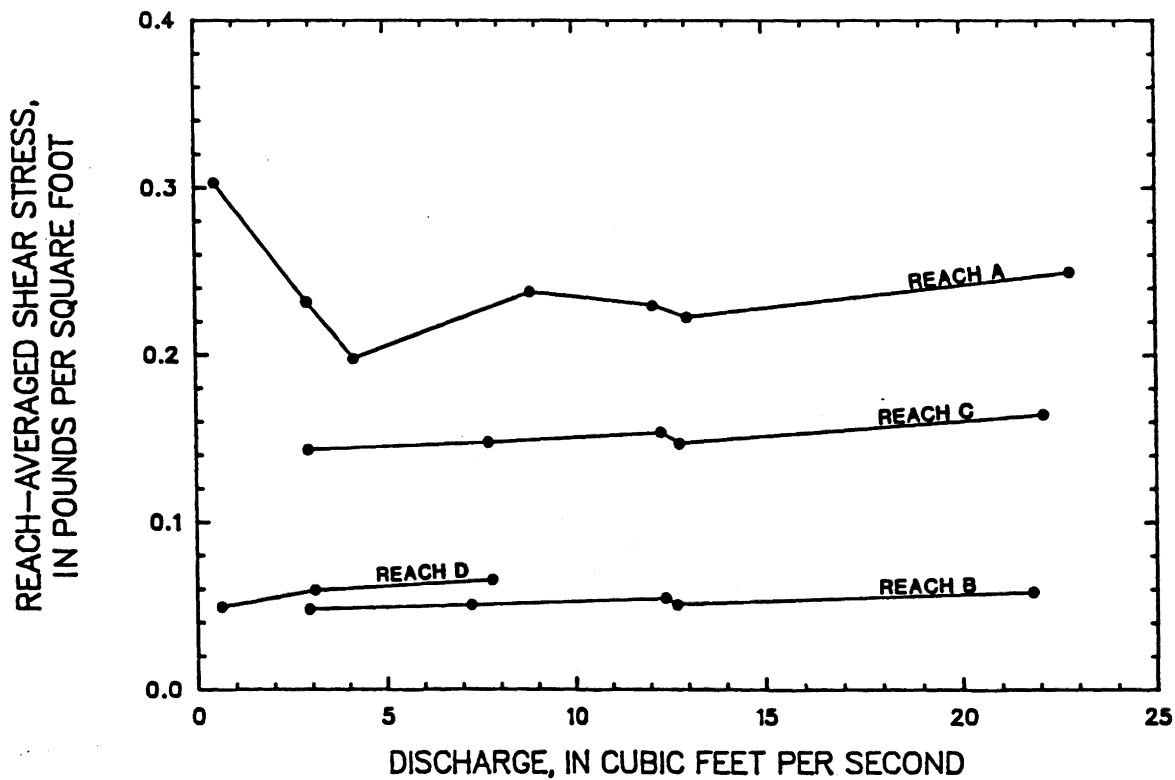


Figure 17 -- Reach-averaged shear stress shown as a function of discharge for reaches of Middle Fork Beargrass Creek, from tracer measurements made from April 18, 1985 through September 18, 1985

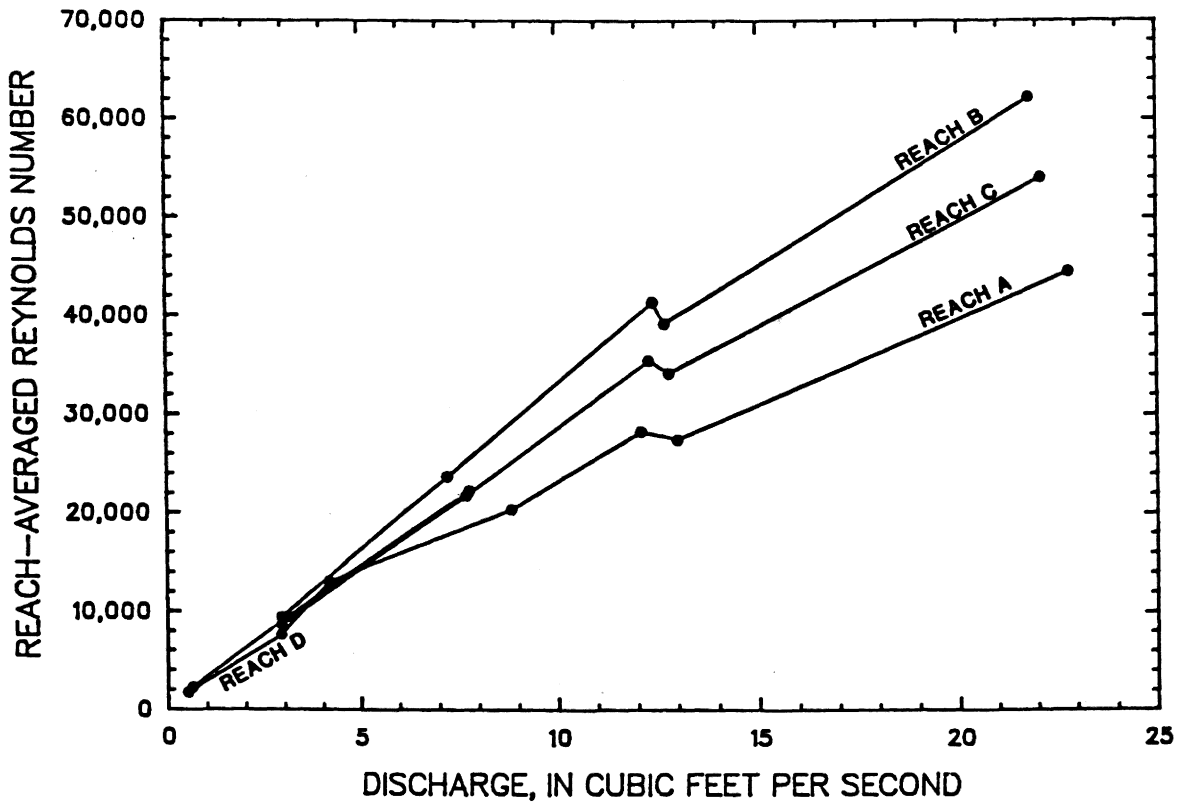


Figure 18 -- Reach-averaged Reynolds number shown as a function of discharge for reaches of Middle Fork Beargrass Creek, from tracer measurements made from April 18, 1985 through September 18, 1985

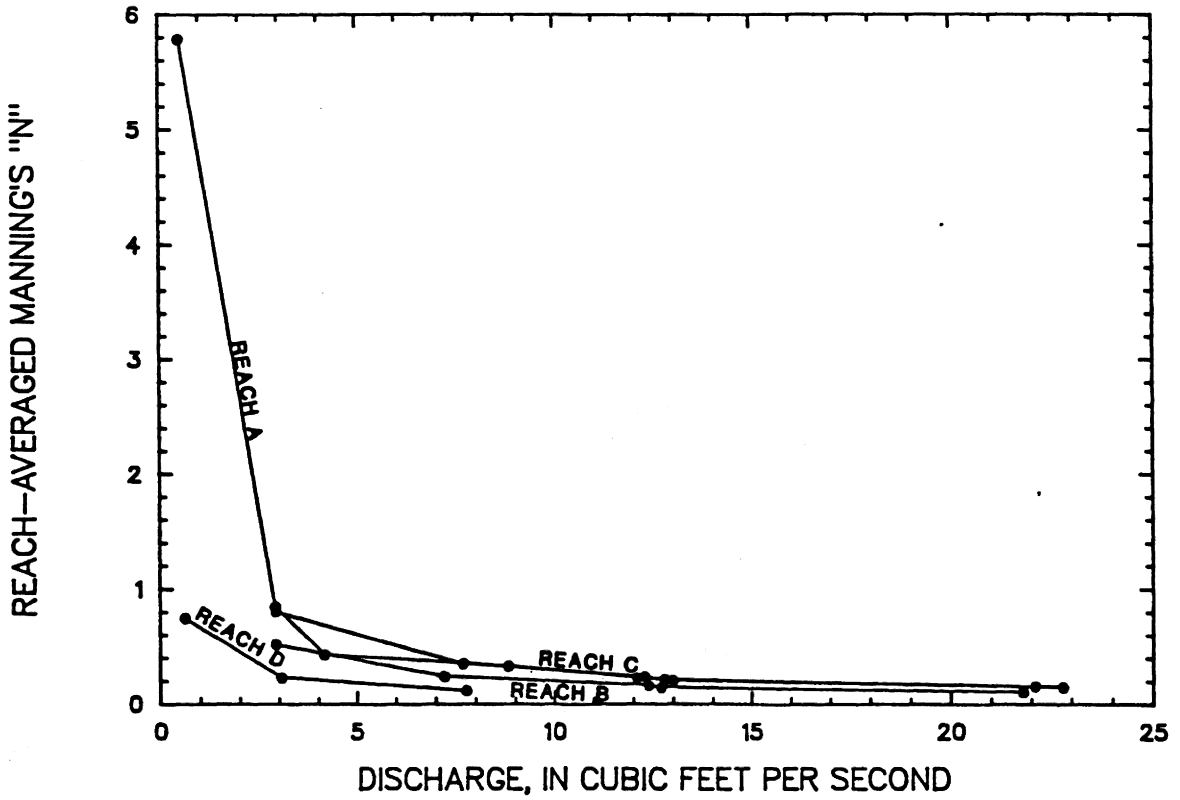


Figure 19 -- Reach-averaged Manning "n" value shown as a function of discharge for reaches of Middle Fork Beargrass Creek, from tracer measurements made from April 18, 1985 through September 18, 1985

cubic feet per second. The reach-averaged depths presented in Figure 11 vary little for each reach with changes in discharge. Note the discontinuity in the plot for reaches B and C again at discharge of about 12-13 cubic feet per second. Also notice that for reach A for low discharges the depth appears to decrease with increasing discharge. Figure 12 displays the reach-averaged width as a function of discharge. As would have been expected for an entrenched stream channel such as for Middle Fork Beargrass Creek, the variability in width was greater between reaches than for the same reach under different flow conditions. Again note the discontinuity of the plot for reach A at about 3 to 4 cubic feet per second. Because of the method used to calculate the reach-averaged cross-sectional areas, the values do not vary drastically for any one reach, as is shown in Figure 13. Again note the outlier value for reach A at about 4 cubic feet per second. The Froude number, because it is determined from the reach velocity and the reach depth (which varied little for any given reach) shows a similar relation to that of velocity in Figure 10 (see Figure 14). The same outlier measurements as those for the velocity are again apparent. The shear velocity, shown in Figure 15, varied little with discharge. This could have been expected because the shear velocity was computed from the slope and depth neither which varied significantly with discharge. The time-concentration dye curves were used to compute an equivalent longitudinal dispersion coefficient. The longitudinal dispersion coefficient was calculated as if all the longitudinal spreading of the dye cloud was due to turbulent dispersion. The values for each reach

are plotted as a function of discharge in Figure 16. The obvious outliers are for tracer measurements made on reaches A,B, and C at about 12 cubic feet per second. The shear stress, computed from the slope and depth, plots similarly to the shear velocity and shows little variability with discharge (Figure 17). The Reynolds number values plotted with discharge show a strong increasing trend with discharge for all four reaches (Figure 18). Again as with velocity, a discontinuity is seen for reach A at a discharge of about 4 cubic feet per second, and for reaches A, B, and C for discharge values of about 12-13 cubic feet per second. The Manning's "n" value decreased with discharge for all reaches (Figure 19). This is partly attributable to the condition where, in an entrenched channel, as depth increases the relative channel roughness decreases. Also under lower flow conditions in a pool-and-riffle stream, the reach composite "n" value accounts for energy losses (occurring mostly in riffles) using a velocity which is highly influenced by the presence of pools.

In a highly pooled and riffled reach the cross-sectional area would change dramatically between cross-sections measured in pools and those in riffles. However, in a reach with little pool-and-riffle development or in one in which the pool-and-riffing was "drowned out" the cross-sectional area variability within the reach would be small. To evaluate the effect of changing discharge conditions on the hydraulic characteristics of the pool-and-riffle sequences within each reach, two statistics were developed and computed. These statistics measured the relative variability of the cross-sectional area within each reach for

each tracer measurement. The cross-sectional areas were determined from the synthesized water surface profiles using the computational cross-section program previously described. The coefficient of variation of these cross-sectional areas is shown as a function of discharge in Figure 20. It can be seen that as discharge increases the variability in cross-sectional area decreases as the pool-and-riffle sequences are "drowned out". A non-parametric measure of the variability--the interquartile range divided by the median--shown in Figure 21, illustrates the same trend with discharge and is less affected by non-normally distributed data. Note on both figures the same discontinuities are present as were shown for velocity in Figure 10.

Environmental Conditions

In the Literature Review chapter the relation between environmental conditions and gas-transfer processes was discussed. For qualitative purposes stream conductivity, suspended-sediment concentration, and wind speed were recorded during tracer measurements. These values along with average water temperature are presented in Table 8. Note that no anomalous environmental conditions, which would be expected to influence gas tracer measurements, were evident. However, a periphyton bloom was observed along reaches A,B, and C during the April 18, 1985 and May 8, 1985 field measurements and could have had a hydraulic influence.

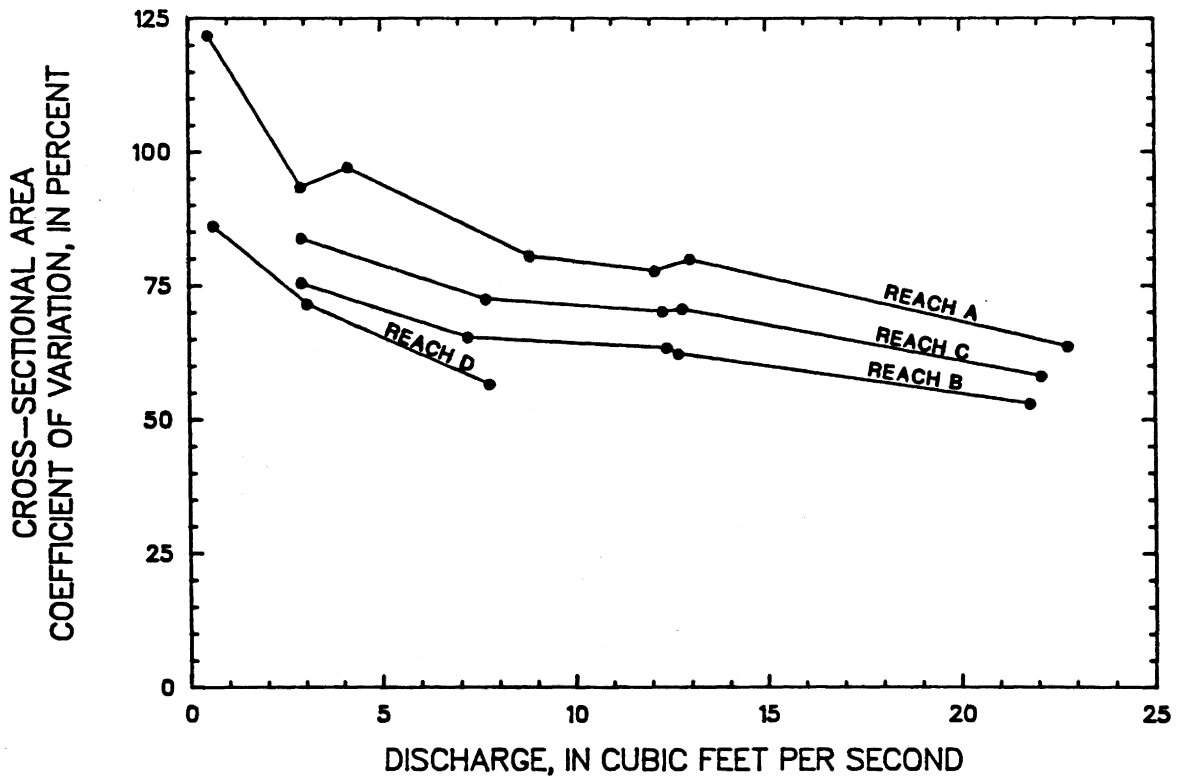


Figure 20 -- Coefficient of variation of cross-sectional area as a function of discharge for reaches of Middle Fork Beargrass Creek, from tracer measurements made from April 18, 1985 through September 18, 1985

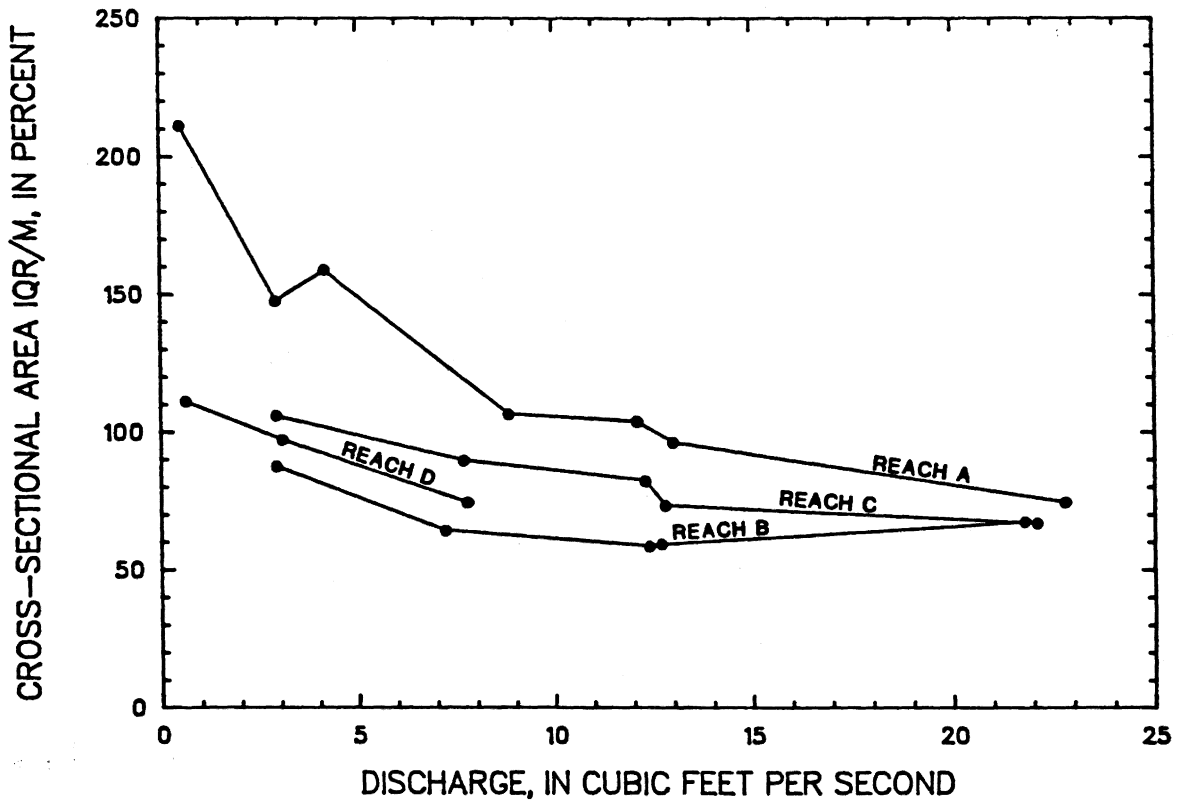


Figure 21 -- Interquartile range divided by the median (expressed as a percent) value of cross-sectional area as a function of discharge for reaches of Middle Fork Beargrass Creek, from tracer measurements made from April 18, 1985 through September 18, 1985

Table 8 -- Environmental conditions during hydrocarbon gas tracer measurements made in Middle Fork Beargrass Creek

DATE (mmddy)	MEASUREMENT REACH	WATER TEMPERATURE (degrees Celsius)	CONDUCTANCE (uS/cm)	WIND ¹	SUSPENDED SEDIMENT ² (mg/L)
041885	A,B,C	20.4, 21.9, 21.3	---	light	clear
041985	D	17.2	---	light	clear
050785	D	17.3	570	light	clear
050885	A,B,C	20.8, 18.6, 19.4	---	calm	clear
051685	A,B,C	20.0, 20.8, 20.5	420	slight	clear
052485	A,B,C	15.5, 16.9, 16.4	330	calm	16.0
061485	A,B,C	17.1, 19.0, 18.3	610	calm	23.0
081985	A	26.0	575	light	6.0
091785	A	20.1	575	light	1.0
091885	D	18.4	650	light	2.0

¹Wind speed estimates were based on the Beaufort Scale (Petterssen, 1958). Calm, light, and slight convert to <1, 1-3, and 4-7 miles per hour, respectively. For comparability, anemometer measurement results were converted to the Beaufort Scale.

²Field estimates of suspended sediment concentration which were less than 20 mg/L are shown as clear.

Hydrocarbon Gas Tracer Measurements

Stream Desorption and Reaeration

Ten hydrocarbon gas tracer injections were made in Middle Fork Beargrass Creek during the period April 18 - September 18, 1985. Pertinent information relating to the tracer injections is shown in Table 9. The quantity of dye used per injection ranged from 50 to 150 milliliters of 20-percent solution of rhodamine-WT. Propane was injected at a rate of 2 liters per minute for steady-state measurements and at 10 liters per minute for the slug-injection technique. An exception to this was during the May 8, 1985 measurement in which 15 liters per minute was selected. The injection period was variable as is seen in the table. The 16 minute injection of 80 milliliters of dye solution on June 14, 1985 resulted from a ruptured propane injection tube which necessitated the early stoppage of a planned 30-minute, 150-milliliter injection.

The time-concentration curves resulting from field measurements and laboratory determinations of both dye and propane concentrations are presented for all tracer measurements in Appendix B. A typical set of time-concentration curves for reaches A, B, and C, for use with the peak and total-weight method computations, are shown in Figures 22, 23, and 24. In Figure 22 for the tracer measurement made on May 16, 1985, note the maximum concentrations observed at the upstream end of reach A and C

Table 9 -- Hydrocarbon gas tracer technique injections made in Middle Fork Beargrass Creek

DATE (mmddy)	MEASUREMENT REACH	INJECTION TIME	INJECTION METHOD ¹	INJECTION PERIOD (min) ²	DYE QUANTITY (mL)	PROPANE RATE (L/min)
041885	A,B,C	1045	S.D.	30	150	10
041985	D	0830	S.S.	300	50	2
050785	D	0930	S.S.	487	50	2
050885	A,B,C	0810	S.D.	30	150	15
051685	A,B,C	0853	S.D.	30	150	10
052485	A,B,C	0945	S.D.	30	150	10
061485	A,B,C	0900	S.D.	16	80	10
081985	A	1247	S.D.	30	150	10
091785	A	1034	S.D.	30	150	10
091885	D	0938	S.D.	20	100	10

¹S.D. denotes short duration for use in the slug injection procedure; S.S. denotes steady-state for use in the steady-state injection procedure.

²For steady-state injections, injection period is for propane--dye injection was instantaneous.

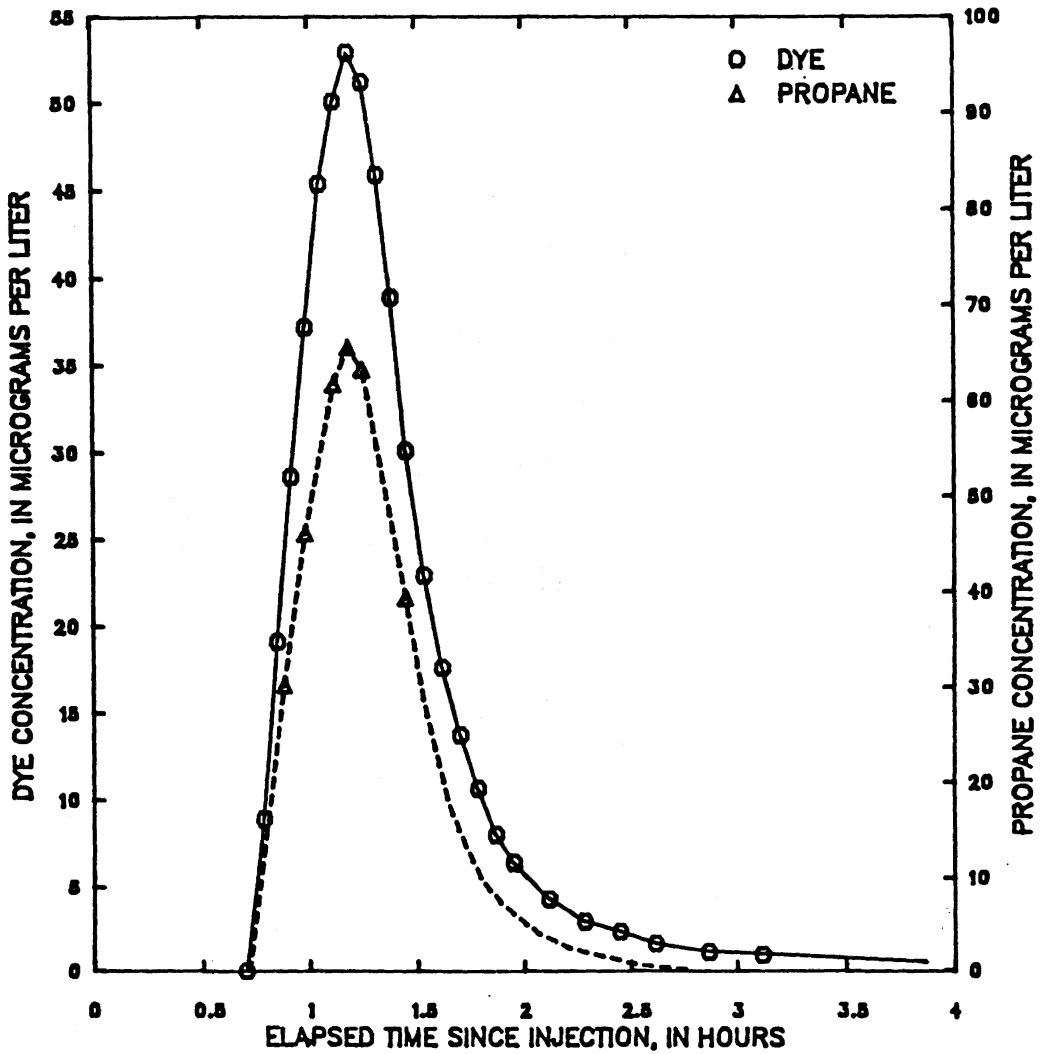


Figure 22 -- Dye and propane concentration from hydrocarbon gas tracer measurements made on Middle Fork Beargrass Creek, upstream end of reach A (upstream end of reach C), May 16, 1985 tracer injection

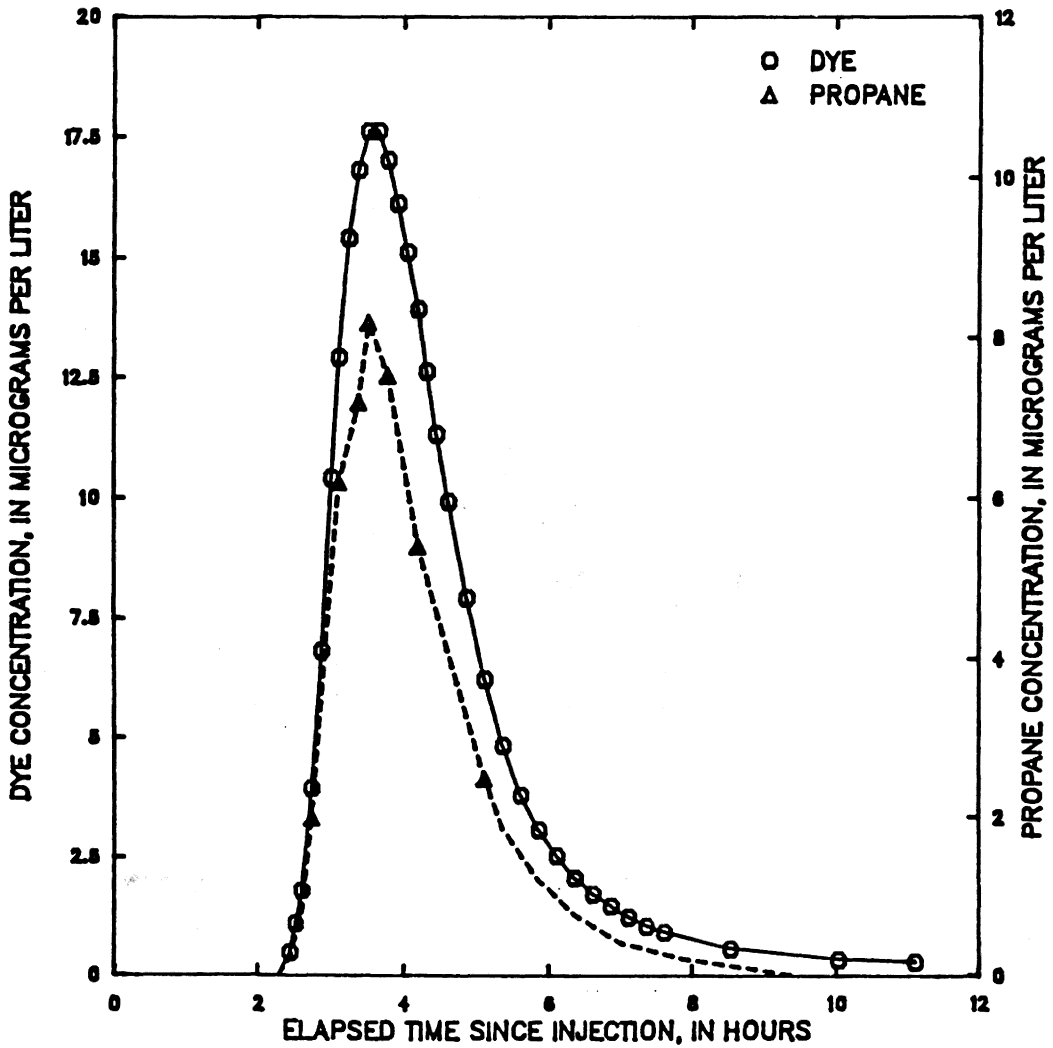


Figure 23 -- Dye and propane concentration from hydrocarbon gas tracer measurements made on Middle Fork Beargrass Creek, downstream end of reach A (upstream end of reach B), May 16, 1985 tracer injection

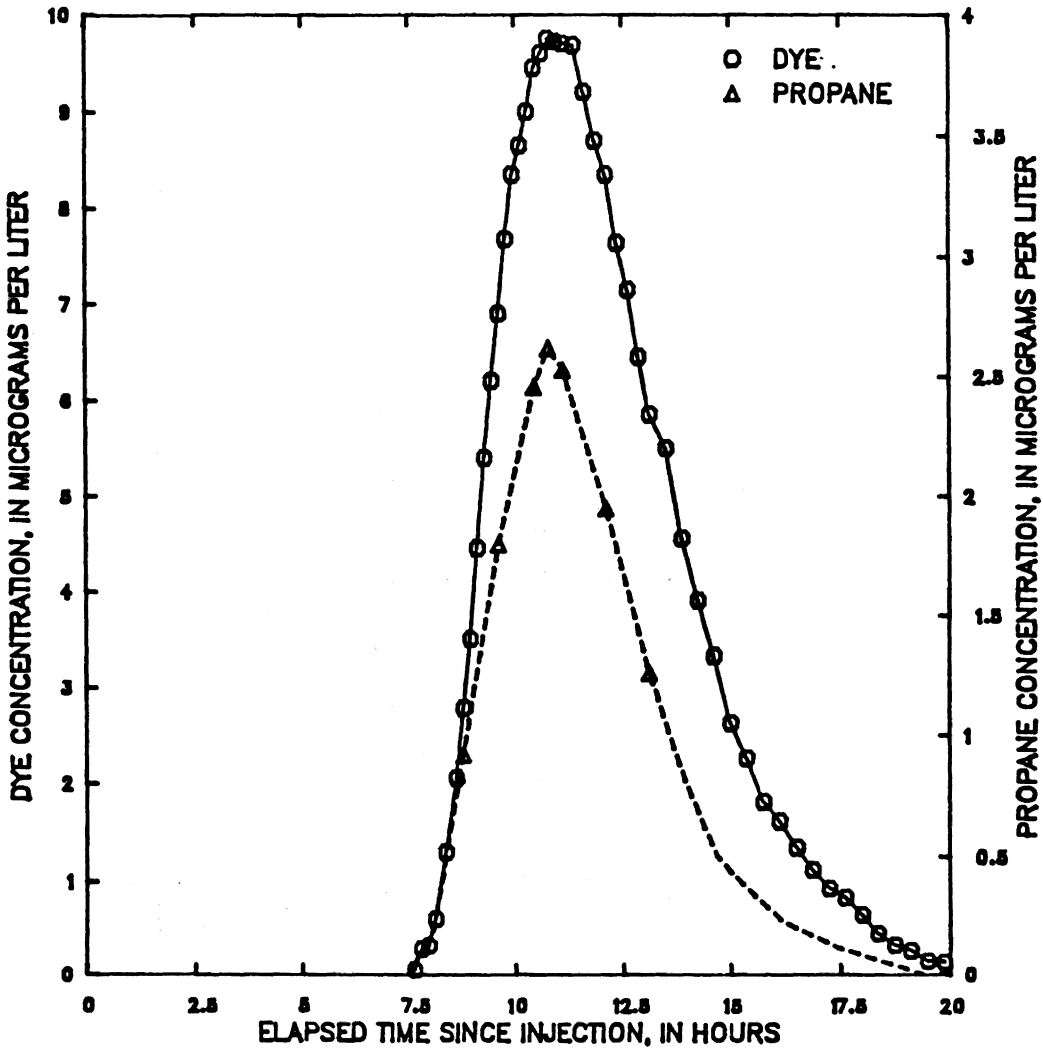


Figure 24 -- Dye and propane concentration from hydrocarbon gas tracer measurements made on Middle Fork Beargrass Creek, downstream end of reach B (downstream end of reach C), May 16, 1985 tracer injection

for dye and propane were approximately 53 and 65 micrograms per liter, respectively. The ratio of the two then is about 0.8 to 1.0. Note in Figure 23 that by the time the tracers arrived at the downstream end of reach A (upstream end of reach B) that the peak concentrations of dye and propane were lower due to dispersion but then the ratio of their peak concentrations was about 2.2 to 1.0 because of desorption of the propane gas. By the time the tracers had moved through reach B (end of reach C) the concentrations were reduced further by dispersion and now the ratio of their peak concentrations is about 3.7 to 1.0 because of continued desorption of the propane gas (Figure 24). This trend is also evident for all the other tracer measurements made for the same reaches. However, because the discharge and travel times were varying, the change in the ratios of peak dye concentrations to propane concentrations was also variable. Note that from the curves (Figures 22 through 24), the sampling coverage of the dye cloud passage was relatively complete. This was also true for most of the other tracer measurements. The exception was for the tracer measurement on September 17, 1985 at the downstream end of reach A. Because of a drastic change in flow conditions, the receding portions of both dye and propane curves had to be synthesized using logarithmic decay and logarithmic decay coupled with a desorption estimate for the two curves, respectively. Note that this extrapolation would have little influence on the peak method computations. In general, the coverage of the propane curves was not as complete as for the dye because of the budget consideration for the relatively expensive propane analysis. However, in all cases, the peak

values of propane were well-sampled and would lead to unaffected desorption computations. For use in total weight calculations, the propane curve recessions were determined using the measured dye recession curves coupled with desorption estimates. For the steady-state measurements on reach D, April 19 and May 7, 1985, the propane plateau concentration was determined using the average of five samples each. The May 7, 1985 reach D dye and propane data plots are shown in Figures 25 and 26.

The computations of propane desorption and equivalent reaeration coefficients were made using the peak, total weight, and steady-state techniques. The resulting desorption coefficients and temperature-corrected reaeration coefficients are presented in Table 10. Note that generally there is good agreement between the coefficients determined by the peak and the total-weight method. The averaged, temperature-corrected reaeration coefficients are plotted with discharge in Figure 27. In general, there was an increasing trend shown for each reach. The anomalous data points identified on the plot of velocity versus discharge (Figure 10) also correspond to outlier values on Figure 27.

Error Propagation

In the types of computations made in calculating desorption coefficients, errors in determining values for input can propagate in the computed desorption coefficients. This potential for error

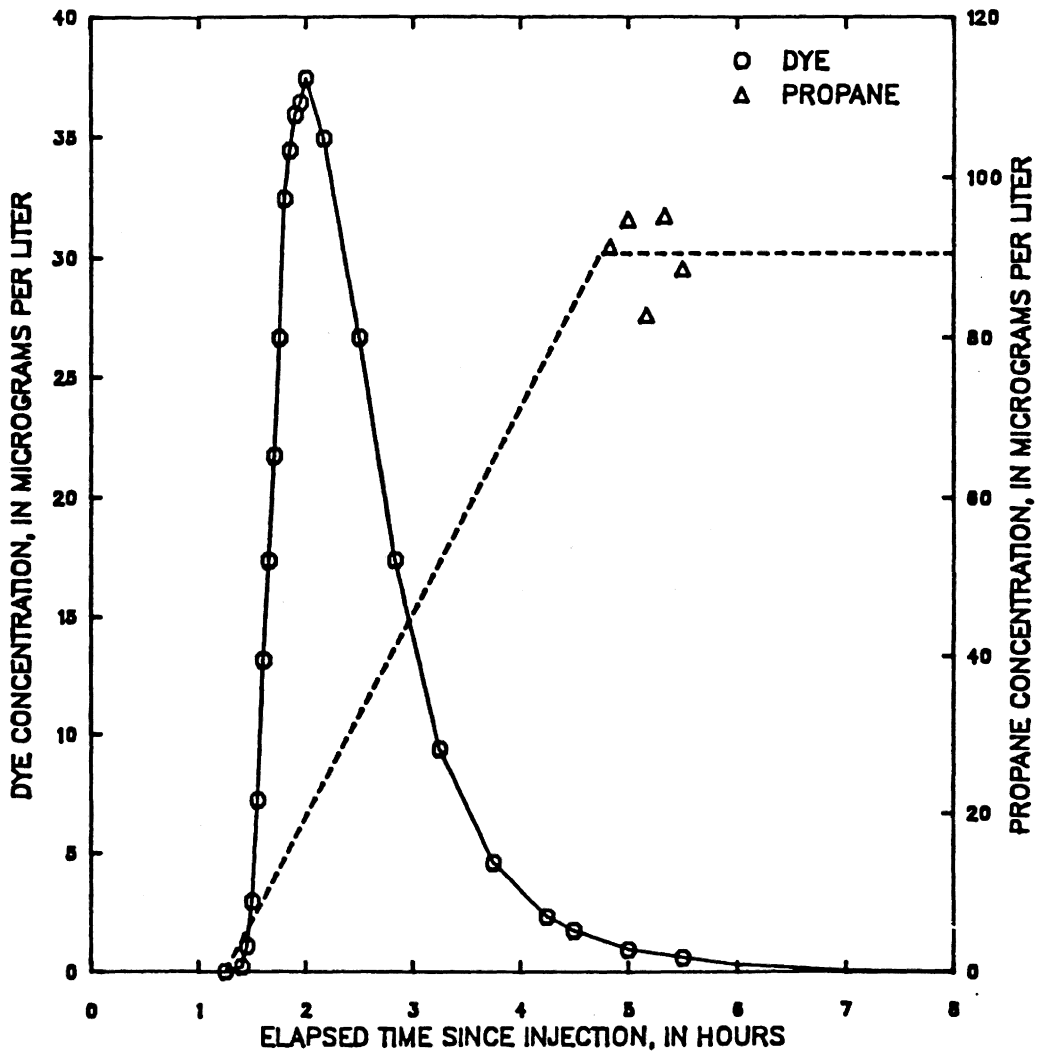


Figure 25 -- Dye and propane concentration from hydrocarbon gas tracer measurements made on Middle Fork Beargrass Creek, upstream end of reach D, May 7, 1985 tracer injection

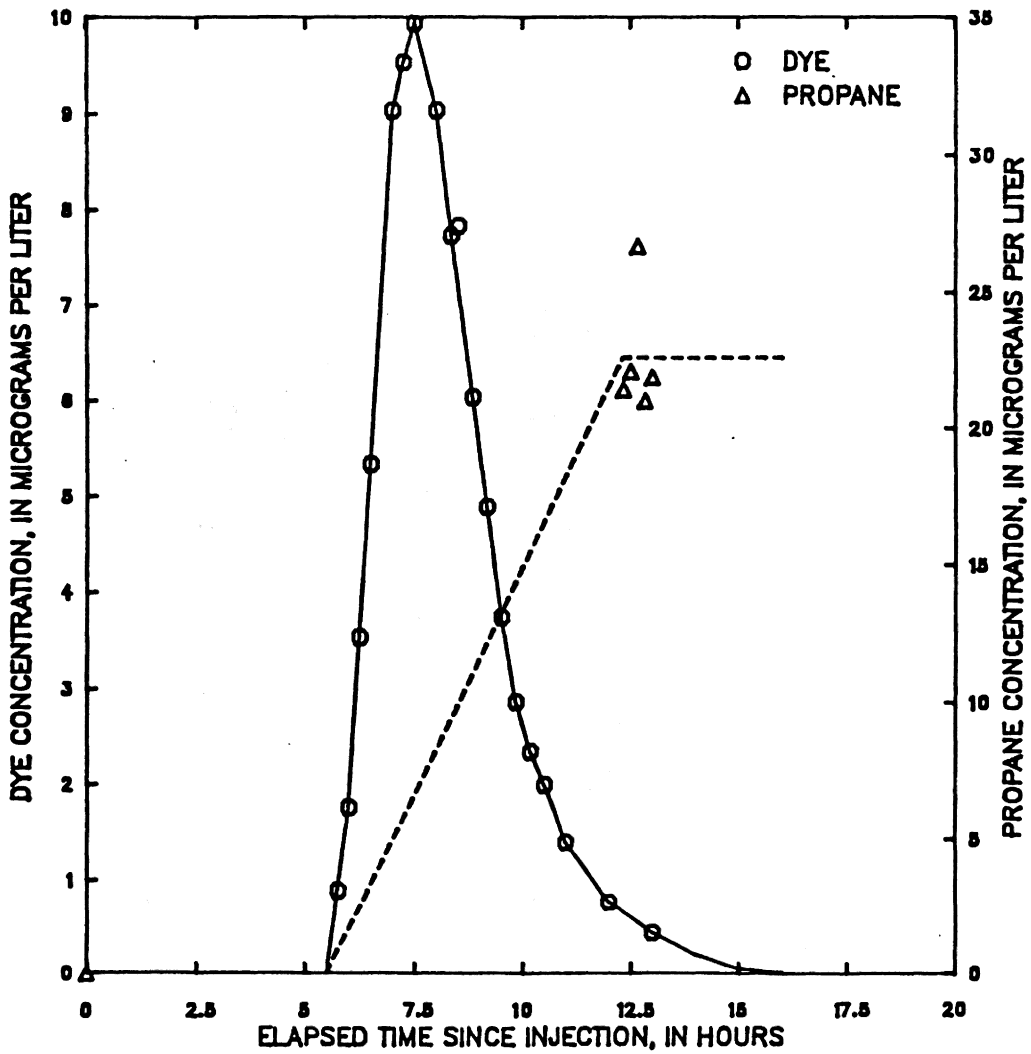


Figure 26 -- Dye and propane concentration from hydrocarbon gas tracer measurements made on Middle Fork Beargrass Creek, downstream end of reach D, May 7, 1985 tracer injection

Table 10 -- Reaeration and propane desorption coefficients and water temperatures from hydrocarbon gas tracer measurements made on reaches of the Middle Fork Beargrass Creek

REACH	DATE	DISCHARGE TEMP.		REAERATION COEFFICIENT ¹				DESORPTION ²
				(day ⁻¹)				COEF.
(mmddyy)	(ft ³ /s)	(deg.C.)	PEAK	T. WEIGHT	S.S.	AVERAGE	(day ⁻¹)	
A	041885	12.100	20.4	16.60	16.60	---	16.60	12.100
A	050885	2.910	20.8	8.30	8.66	---	8.48	6.230
A	051685	8.830	20.0	11.30	11.60	---	11.50	8.240
A	052485	22.800	15.5	23.70	23.10	---	23.40	15.200
A	061485	13.000	17.1	21.30	21.30	---	21.30	14.300
A	081985	4.160	26.0	11.20	11.50	---	11.40	9.440
A	091785	0.509	20.1	3.20	3.28	---	3.24	2.340
B	041885	12.400	21.9	2.04	1.99	---	2.02	1.520
B	050885	2.920	18.6	1.22	1.27	---	1.25	0.867
B	051685	7.220	20.8	2.85	2.87	---	2.86	2.100
B	052485	21.800	16.9	2.60	3.19	---	2.90	1.940
B	061485	12.700	19.0	4.23	3.17	---	3.70	2.600
C	054185	12.300	21.4	6.50	6.50	---	6.50	4.840
C	050885	2.920	19.3	3.62	3.77	---	3.70	2.620
C	051685	7.690	20.5	5.29	5.38	---	5.34	3.890
C	052485	22.100	16.4	8.99	9.29	---	9.14	6.040
C	061485	12.800	18.5	9.34	8.61	---	8.98	6.240
D	041985	7.770	17.2	---	---	11.80	11.80	7.970
D	050785	3.070	17.3	---	---	6.07	6.07	4.090
D	091885	0.628	18.4	4.34	4.38	---	4.36	3.030

¹Reaeration coefficients shown are adjusted to 20 degrees Celsius.

²Desorption coefficients for propane are for temperatures given in the table.

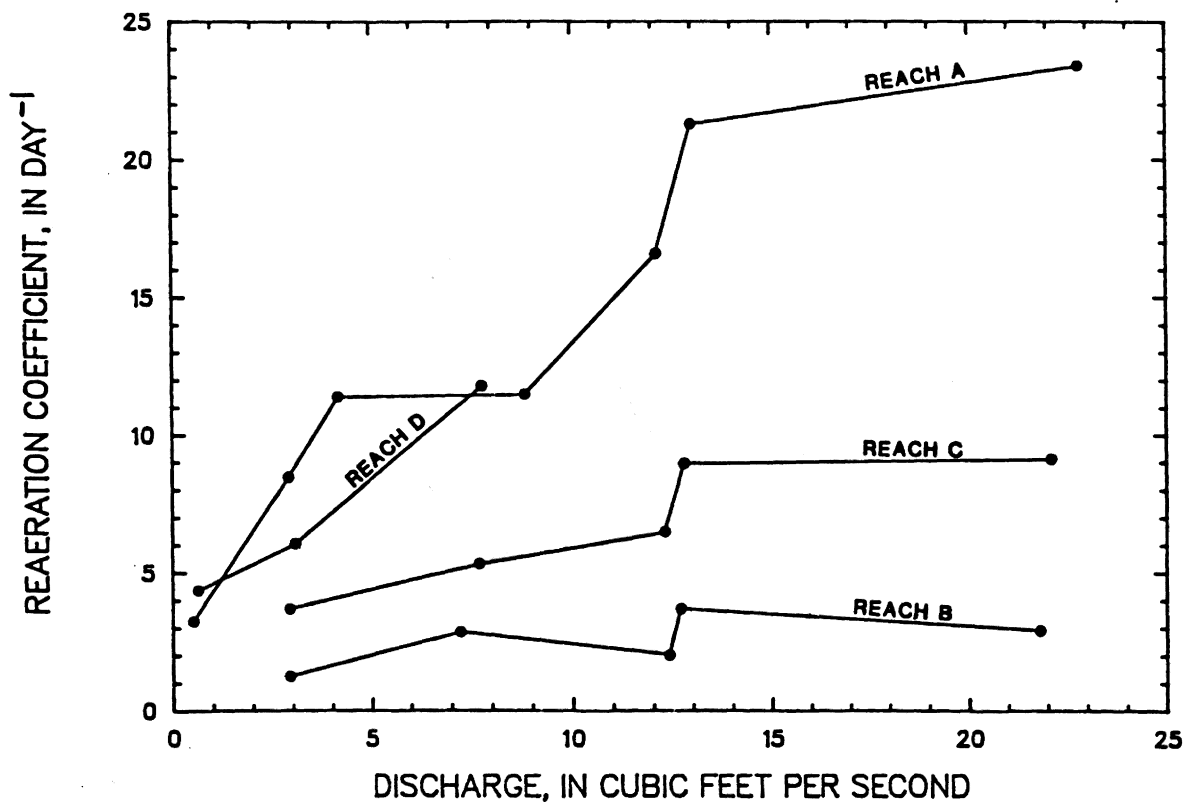


Figure 27 -- Reaeration coefficient shown as a function of discharge for reaches of Middle Fork Beargrass Creek, from tracer measurements made from April 18, 1985 through September 18, 1985

propagation was considered to be a major concern of Parker and Gay (1987) and Yotsukura and others (1983) in interpreting their tracer measurements.

It was desirable to compare the likelihood for these type propagation errors for computed reaeration coefficients from tracer measurements on Middle Fork Beargrass Creek. In doing so, an assumed error of 2.0 percent (coefficient of variation) was used. From the 2.0 percent error, a relative error was calculated and the corresponding 95-percent confidence bands (assuming a normal distribution) were determined for each of the calculated reaeration coefficients. These confidence bands of the reaeration coefficient and the relative error are presented in Table 11. Note that the relative error values are useful for intermeasurement comparability only and are not reflective of the true but unknown errors made in measurement. From Table 11, it can be seen that the highest relative errors are for measurements made during higher flows and the lower relative errors relate to measurements made during lower flow conditions.

Example Computations from Hydrocarbon Gas Tracer Measurements

For purposes of demonstration, computations by both the peak and total-weight methods using a slug or short-duration injection procedure as well as by the steady-state procedure are presented. The tracer measurement of reach B on May 16, 1985 will be used to demonstrate the

Table 11 -- Error propagation through reaeration coefficient computations using a relative error common to all hydrocarbon gas tracer measurements

REACH	DATE (mmddy)	DISCHARGE (ft ³ /s)	REAERATION COEFFICIENT (day ⁻¹)			RELATIVE ERROR (percent)
			UPPER BAND ¹	MEDIAN VALUE ²	LOWER BAND ³	
A	041885	12.100	17.18	16.60	16.01	1.8
A	050885	2.910	8.63	8.48	8.32	0.93
A	051685	8.830	11.92	11.50	11.07	1.9
A	052485	22.800	24.47	23.40	22.32	2.3
A	061485	13.000	21.99	21.30	20.60	1.7
A	081985	4.160	11.64	11.40	11.15	1.1
A	091785	0.509	3.26	3.24	3.21	0.44
B	041885	12.400	2.28	2.02	1.75	6.6
B	050885	2.920	1.33	1.25	1.16	3.3
B	051685	7.220	3.02	2.86	2.69	3.0
B	052485	21.800	3.36	2.90	2.43	8.2
B	061485	12.700	3.99	3.70	3.40	4.1
C	041885	12.300	6.68	6.50	6.31	1.4
C	050885	2.920	3.75	3.70	3.64	0.73
C	051685	7.690	5.46	5.34	5.21	1.2
C	052485	22.100	9.46	9.14	8.81	1.2
C	061485	12.800	9.18	8.98	8.77	1.2
D	041985	7.770	12.31	11.80	11.28	2.2
D	050785	3.070	6.31	6.07	5.82	2.0
D	091885	0.628	4.42	4.36	4.29	0.75

¹The upper 95-percent confidence band for the temperature corrected reaeration coefficient assuming a common relative error for all tracer computations equal to a two-percent coefficient of variation. Based on equation 56.

²The computed, temperature-corrected reaeration coefficient.

³The lower 95-percent confidence band for the temperature corrected reaeration coefficient assuming a common relative error for all tracer computations equal to a two-percent coefficient of variation. Based on equation 57.

⁴Relative error is computed from equation 55 with as assumed error of two percent.

slug injection procedure and associated computations.

From Table 9, it can be seen that the tracer injection was initiated at 0853 for a period of 30 minutes using 150 milliliters of rhodamine-WT dye and propane at a delivery rate of 10 liters per minute. Samples for both dye and propane were collected at the upstream and downstream ends of reach B, so as to define the time-concentration relation for each tracer. The raw data along with computations resulting from application of the computerized centroid program are shown in Tables 12-15. The time-concentration plots for dye and propane at each end of reach B are additionally shown in Figures 23 and 24.

The mass of dye injected can be determined as the product of the volume, purity, and density (Dye mass injected = 150 milliliters x 0.20 x 1.19 grams per milliliter = 35.7 grams). The mass recovered at each end of reach B is determined by: Dye mass recovered = $\int QCdt$, or by computations by the centroid program (Tables 12 and 13). The mass recovered is then 32.869 grams and 29.606 grams for the upstream and downstream ends of reach B, respectively. The percent dye recovery can be computed by dividing each of these values by the mass of dye injected and results in 92.1 percent and 82.9 percent.

The dye concentration weighted-mean discharge for each end of reach B is determined by:

$$Q = \frac{\int Q C dt}{\int C dt} \quad (60)$$

Table 12 -- Dye time-concentration data and computed areas, centroids, and masses for the upstream end of reach B during hydrocarbon gas tracer measurements made on reaches of the Middle Fork Beargrass Creek, May 16, 1985

TIME (hhmm)	CONCENTRATION (ug/L)	DISCHARGE (ft ³ /s)
0853	0.070	9.560
1110	0.070	9.020
1120	0.540	9.020
1125	1.150	9.020
1130	1.850	9.020
1138	4.000	9.020
1146	6.900	9.020
1154	10.500	9.020
1200	13.000	9.020
1208	15.500	9.020
1216	16.900	9.020
1224	17.700	9.020
1232	17.700	9.020
1240	17.100	9.020
1248	16.200	9.020
1256	15.200	9.020
1305	14.000	9.020
1312	12.700	9.020
1320	11.400	9.020
1330	10.000	9.020
1345	8.000	7.470
1400	6.300	7.470
1415	4.900	7.500
1430	3.850	7.500
1445	3.120	7.500
1500	2.580	7.000
1515	2.120	7.000
1530	1.770	7.000
1545	1.520	6.500
1600	1.280	6.500
1615	1.090	6.500
1630	0.970	6.500
1725	0.620	6.000
1855	0.390	5.000
2000	0.340	4.000

(continued)

Table 12 (continued) -- Dye time-concentration data and computed areas, centroids, and masses for the upstream end of reach B during hydrocarbon gas tracer measurements made on reaches of the Middle Fork Beargrass Creek, May 16, 1985

TIME (hhmm)	CONCENTRATION (ug/L)	DISCHARGE (ft ³ /s)
2100	0.240	4.000
2200	0.140	4.000
2300	0.070	4.000
INTEGRATED AREA = 38.338 ug/L-hr		
CENTROID = 4.499 hr		
MASS = 32.869 g		

Table 13 -- Dye time-concentration data and computed areas, centroids, and masses for the downstream end of reach B during hydrocarbon gas tracer measurements made on reaches of the Middle Fork Beargrass Creek, May 16, 1985

TIME (hhmm)	CONCENTRATION (ug/L)	DISCHARGE (ft ³ /s)
0853	0.090	9.560
1620	0.090	8.400
1630	0.140	8.400
1640	0.360	8.400
1650	0.400	8.400
1700	0.680	8.400
1715	1.390	8.400
1730	2.150	7.100
1740	2.880	7.100
1750	3.600	7.100
1800	4.550	7.100
1810	5.500	7.100
1820	6.300	7.100
1830	7.000	7.100
1840	7.780	6.600
1850	8.450	6.600
1900	8.750	6.600
1910	9.100	6.600
1920	9.550	6.600
1930	9.700	6.300
1940	9.850	6.300
1950	9.820	6.100
2000	9.800	6.100
2015	9.780	6.100
2030	9.300	5.900
2045	8.800	5.900
2100	8.450	5.900
2115	7.740	5.600
2130	7.250	5.600
2145	6.550	5.400
2200	5.950	5.400
2223	5.600	5.400
2245	4.650	5.100
2308	4.000	5.100
2330	3.420	5.100
2353	2.720	5.100
0015	2.350	5.500
0038	1.900	5.500

(continued)

Table 13 (continued) -- Dye time-concentration data and computed areas, centroids, and masses for the downstream end of reach B during hydrocarbon gas tracer measurements made on reaches of the Middle Fork Beargrass Creek, May 16, 1985

TIME (hhmm)	CONCENTRATION (ug/L)	DISCHARGE (ft ³ /s)
0100	1.700	5.500
0123	1.430	5.500
0145	1.200	5.500
0208	1.000	5.700
0230	0.900	5.700
0253	0.720	5.900
0315	0.520	5.900
0338	0.400	5.900
0400	0.340	5.900
0423	0.230	6.200
0445	0.220	6.200
0530	0.190	6.200
0630	0.160	6.500
0730	0.140	6.500
0800	0.120	6.500
0900	0.090	6.500

INTEGRATED AREA = 48.220 ug/L-hr

CENTROID = 12.073 hr

MASS = 29.606 g

Table 14 -- Propane time-concentration data and computed areas, centroids, and masses for the upstream end of reach B during hydrocarbon gas tracer measurements made on reaches of the Middle Fork Beargrass Creek, May 16, 1985

TIME (hhmm)	CONCENTRATION (ug/L)	DISCHARGE (ft ³ /s)
0853	0.000	9.560
1110	0.000	9.020
1120	0.200	9.020
1125	0.500	9.020
1130	0.750	9.020
1138	1.980	9.020
1200	6.200	9.020
1216	7.200	9.020
1224	8.190	9.020
1240	7.530	9.020
1305	5.400	9.200
1400	2.480	7.470
1415	1.850	7.500
1445	1.200	7.500
1515	0.750	7.000
1553	0.400	6.500
1645	0.200	6.500
1815	0.000	4.000
2300	0.000	4.000

INTEGRATED AREA = 15.559 ug/L-hr

CENTROID = 4.208 hr

MASS = 13.579 g

Table 15 -- Propane time-concentration data and computed areas, centroids, and masses for the downstream end of reach B during hydrocarbon gas tracer measurements made on reaches of the Middle Fork Beargrass Creek, May 16, 1985

TIME (hhmm)	CONCENTRATION (ug/L)	DISCHARGE (ft ³ /s)
0853	0.000	9.530
1620	0.000	8.400
1657	0.190	8.400
1740	0.920	7.100
1830	1.800	7.100
1920	2.460	6.600
1940	2.620	6.300
2000	2.530	6.100
2100	1.950	5.900
2200	1.260	5.400
2250	0.810	5.100
2335	0.500	5.100
0020	0.350	5.500
0105	0.220	5.500
0220	0.110	5.700
0415	0.000	6.200
0900	0.000	6.500

INTEGRATED AREA = 11.113 ug/L-hr

CENTROID = 11.609 hr

MASS = 7.008 g

or by dividing the computed mass by the integrated area under the time-concentration curve from Tables 12 and 13 and providing appropriate units conversion. In Tables 12 and 13 the computed mass is given in grams and the area under the time-concentration curve is given in microgram per liter-hours. The weighted discharges are then computed by:

$$Q = \text{Mass}(9.804)/\text{Area}$$

where 9.804 is a conversion factor. The resulting weighted discharges were 8.41 and 6.02, respectively, for the upstream and downstream ends of reach B. The mean reach discharge for the tracer measurement is then just the average of these two values, or 7.22 cubic feet per second.

The reach travel time was computed as the difference between the time of the centroid of the dye time-concentration curve (or more accurately the centroid of the dye time-mass curve) for each end of the reach. The elapsed time from tracer injection to the dye time-concentration curve centroid for each end of reach B was calculated using the method of moments centroid program and is shown in Tables 12 and 13 as 4.499 and 12.073 hours. The travel time through the reach was then 7.574 hours or 454 minutes.

The peak values of both dye and propane for each end of reach B are determined from either Figures 23 and 24 or Tables 12-15.

The water temperature for reach B was determined from field observations to be 20.8 degrees Celsius.

The peak method computation for the desorption coefficient follows equation 48:

$$K_t = \frac{1440 \text{ min/d}}{454 \text{ min}} \log_e \frac{(8.19(.921))/17.7}{(2.62(.829))/9.85} = 2.09 \text{ day}^{-1}$$

The corresponding reaeration coefficient is computed by equation 46 as:

$$K_2 = 1.39(2.09) = 2.90 \text{ day}^{-1}$$

The reaeration coefficient is then standardized to 20 degrees Celsius by equation 47 as:

$$K_{2-20} = 2.90(1.024)^{(20-20.8)} = 2.85 \text{ day}^{-1}$$

The mass of propane passing each end of reach B is computed in the same manner as the dye, again by the use of the centroid program. The resulting masses are listed in Tables 14 and 15 and are 13.579 and 7.008 grams for the upstream and downstream ends of reach B, respectively.

The total weight method computation for the desorption coefficient follows equation 50:

$$K_t = \frac{1440 \text{ min/d}}{454 \text{ min}} \log_e \frac{13.579}{7.008} = 2.10 \text{ day}^{-1}$$

The corresponding reaeration coefficient is computed as it was for the peak method to be 2.92 day^{-1} . When adjusted to 20 degrees Celsius, the reaeration coefficient is 2.87 day^{-1} , which compares closely to the

value computed by the peak method procedure. The two values are averaged and the resulting reaeration coefficient for reach B is 2.86 day^{-1} (Table 10).

An example of steady-state procedure computations will be made on results from the May 7, 1985 steady state injection for reach D.

From Table 9 it can be seen that the tracer injection was initiated at 0930 for 487 minutes using 2.0 liters per minute of propane and an instantaneous injection of 50 milliliters of rhodamine-WT dye. Samples for dye were collected at the upstream and downstream ends of reach D so as to define the time-concentration relation and to indicate the proper time to sample for propane to define the steady-state plateau concentrations. The raw data along with dye computations resulting from application of the centroid program are shown in Tables 16 and 17. The propane concentration values were simply averaged to determine the plateau concentration. The time-concentration plots for dye and plateau concentration values for propane are additionally shown in Figures 25 and 26.

The dye masses or percent recoveries are not usually needed for desorption coefficient computations using the steady state procedure. The reach travel time is computed from the dye time-concentration curve centroids as was done using the slug injection procedures. The travel time, 346 minutes, was determined from the differences of the values shown in Tables 16 and 17.

The discharges were constant at the upstream and downstream ends of reach D at 2.42 and 3.71 cubic feet per second, respectively. The

Table 16 -- Dye time-concentration data and computed areas, centroids, and masses for the upstream end of reach D during hydrocarbon gas tracer measurements made on reaches of the Middle Fork Beargrass Creek, May 7, 1985

TIME (hhmm)	CONCENTRATION (ug/L)	DISCHARGE (ft ³ /s)
0930	0.040	2.420
1045	0.040	2.420
1054	0.250	2.420
1057	1.100	2.420
1100	3.020	2.420
1103	7.250	2.420
1106	13.200	2.420
1109	17.400	2.420
1112	21.800	2.420
1115	26.700	2.420
1118	32.500	2.420
1121	34.500	2.420
1124	36.000	2.420
1127	36.500	2.420
1130	37.500	2.420
1140	35.000	2.420
1200	26.700	2.420
1220	17.400	2.420
1245	9.400	2.420
1315	4.600	2.420
1345	2.340	2.420
1400	1.750	2.420
1430	0.950	2.420
1500	0.610	2.420
1530	0.300	2.420
1600	0.180	2.420
1630	0.080	2.420
1700	0.040	2.420
1730	0.040	2.420

INTEGRATED AREA = 48.726 ug/L-hr

CENTROID = 2.545 hr

MASS = 12.020 g

Table 17 -- Dye time-concentration data and computed areas, centroids, and masses for the downstream end of reach D during hydrocarbon gas tracer measurements made on reaches of the Middle Fork Beargrass Creek, May 7, 1985

TIME (hhmm)	CONCENTRATION (ug/L)	DISCHARGE (ft ³ /s)
0930	0.060	3.710
1500	0.060	3.710
1515	0.950	3.710
1530	1.820	3.710
1545	3.600	3.710
1600	5.400	3.710
1630	9.100	3.710
1645	9.600	3.710
1700	10.000	3.710
1730	9.100	3.710
1750	7.800	3.710
1820	6.100	3.710
1840	4.950	3.710
1900	3.800	3.710
1920	2.920	3.710
1940	2.400	3.710
2000	2.050	3.710
2030	1.450	3.710
2130	0.820	3.710
2230	0.490	3.710
2330	0.250	3.710
0030	0.100	3.710
0130	0.060	3.710

INTEGRATED AREA = 30.463 ug/L-hr

CENTROID = 8.315 hr

MASS = 11.521 g

plateau concentration of propane as shown in Figures 25 and 26 are 90.6 and 22.6 micrograms per liter.

The initial computation of the propane desorption coefficient follows equation 51:

$$K_t = \frac{1440 \text{ min/d}}{346 \text{ min}} \log_e \frac{90.6(2.42)}{22.6(3.71)} = 4.00 \text{ day}^{-1}$$

A refined value for the desorption coefficient, which accounts for possible minor effects of dispersion, can be determined from equation 52 by trial and error, starting with the value initially computed. These successive calculations were made by computer program and result in a slight adjustment to the desorption coefficient to 4.09 day^{-1} .

The corresponding reaeration coefficient is computed by equation 46 as:

$$K_2 = 1.39(4.09) = 5.69 \text{ day}^{-1}$$

The reaeration coefficient is then standardized from the mean field water temperature of 17.3 to 20 degrees Celsius by equation 47 as:

$$K_{2-20} = 5.69(1.024)^{(20-17.3)} = 6.07 \text{ day}^{-1}$$

Again, the mean reach discharge is calculated as the average of the discharge of the upstream and downstream ends of reach D. The mean discharge was determined to be 3.07 cubic feet per second.

Discussion

If channel roughness, water quality, and environmental conditions were the same for all measurements made in a reach and if there were no errors in measurement computation, the relations between the various hydraulic parameters and stream discharge would be expected to be smooth and continuous. However, due to seasonal changes and changes in antecedent flow conditions, suggested by Figure 7, the relations of the hydraulic parameters with discharge would not be expected to be totally smooth and continuous.

One of the measurements which stands out as an anomaly in Figures 9-19 is the one made on reaches A,B, and C on April 18, 1985 at a discharge of 12.1-12.4 cubic feet per second. This measurement shows sharp differences from one made at a slightly higher discharge (12.7-13.0 cubic feet per second) on June 14, 1985. Field observations on April 18, 1985 indicated that there was a periphytic algae bloom which resulted in mossy growths on all exposed surfaces throughout the reaches. In contrast, there was a major runoff event just prior to the June 14, 1985 measurements (see Figure 7) which apparently scoured the exposed surfaces clean (little periphyton was observed during the measurements). One possible explanation for the noted discontinuities in Figures 9-19 could be the presence of excessive periphyton. The presence of the periphyton may have retarded the velocity, somewhat, increased the depth of flow, and increased the cross-sectional area. Additionally, it may have dampened the turbulence of flow by smoothing

out otherwise irregular surfaces which could have accounted for the lower-than-expected longitudinal dispersion coefficient. Because the velocity and turbulence were apparently reduced, the lower, desired reaeration coefficients (Figure 27) are also in line with expectations.

Another anomaly shown in Figures 9-19 is for the measurements made on reach A at 2.91 cubic feet per second (May 8, 1985) as compared to the ones made at 4.16 cubic feet per second (August 19, 1985). Again, antecedent conditions were greatly different prior to each of these measurements. Prior to May 8, 1985, conditions were dry (Figure 7) and during measurements a periphyton bloom was again observed. The August 19, 1985 measurement followed shortly after the highest magnitude runoff-event of the measurement period (Figure 7), and, as would have been expected, the reach was notably free of periphytic growth. The presence of periphyton could again be expected to retard the velocity somewhat, increase the depth of flow, and increase the cross-sectional area. In contrast, the near total absence of periphyton could have the opposite effect as compared to typical stream conditions. Again this suggested scenario could account for all the anomalies associated with these two measurements shown in the previously discussed figures.

In Table 10 and Figure 27 it can be seen that the highest variability in the measured reaeration coefficients is associated with reach A which is also the reach shown in Figures 20 and 21 to exhibit the most pool-and-riffle development under low flow conditions. Under these low-flow conditions the reach velocity is also quite low because of the long travel times through each of the well-developed pools. It

then seems evident that the pools would influence the outcome of the reach-averaged, hydraulic-parameter values and reduce the velocity and maintain a nearly constant weighted reach depth. These both serve to negatively impact on the reaeration coefficient. Therefore, it appears that the more pool-and-riffle development in a reach, the more dramatic the decline in the reaeration coefficient under a discharge decline or the more positive the relation between the reaeration coefficient and discharge would be.

From an evaluation of the propagation of errors in computing reaeration coefficients, it appears clear that larger errors would have been expected for higher discharge conditions (with everything else the same). This is explained by the fact that higher discharge conditions lead to higher velocities and, therefore, shorter travel times. Because desorption or reaeration is a time-dependent process, a shorter travel time allows for less gas transfer with the atmosphere. Therefore, the peak or plateau concentrations or total weight of propane used in the computation is less different downstream as compared to upstream as it would be for a longer travel time. This similarity of values upstream and downstream is, therefore, what accounts for larger relative errors in computed coefficients.

EFFECT OF STREAMFLOW CHANGES TO THE REAERATION COEFFICIENT

One significant question which was addressed by the design of this research was "would the reaeration coefficient increase or decrease with discharge in a given reach characterized by pool-and-riffle development?" The four reaches chosen for study all differed in their overall water-surface slopes (Figure 9) and in the level of pool-and-riffle development present at similar flow conditions (Figures 20 and 21).

Comparative Analysis

The most straight-forward approach to testing how the reaeration coefficient is affected by hydraulic changes brought about by changes in discharge is to fit a linear regression to the measured reaeration coefficient and discharge data for each reach. A two-sided t-test would then be used to evaluate the significance of the slope parameter in each of the regressions. The null hypothesis of the t-test is that there is no relation between the reaeration coefficient and discharge. The tested hypothesis is that the slope of the regression is non-zero, the direction of the relation given by the sign of the fitted regression slope.

The reaeration coefficient-discharge values for each reach were fitted, using simple linear regression (least-squares method) with the

lines shown in Figure 28. The equations for the lines along with the corresponding fit statistics are presented in Table 18. Note that the fit of each line in Figure 28 appears reasonable. The residuals (difference between fitted and measured values) appear to be somewhat randomly distributed for each line. This suggests that a linear fit is not inappropriate and major variable transformation is not indicated. From the t-test significance probability values presented in Table 18, it can be seen that the probability of there not being a relationship between the reaeration coefficient and discharge (based on the measurements) in reach A is only 0.21 percent. However, for the lowest-slope reach (reach B), exhibiting the least degree of pool-and-riffle development, the probability of there not being a relationship between the reaeration coefficient and discharge (based on the measurements) is 34.7 percent. Also note that for each of the reaches the relation is positive as is indicated in Table 18 from the positive regression slopes. The values shown in Table 18 for the coefficient of determination (R^2), root mean square error, and coefficient of variation are presented for the purpose of characterizing the statistical fit but are not strictly used in testing the hypothesis of whether the reaeration coefficient varies with discharge.

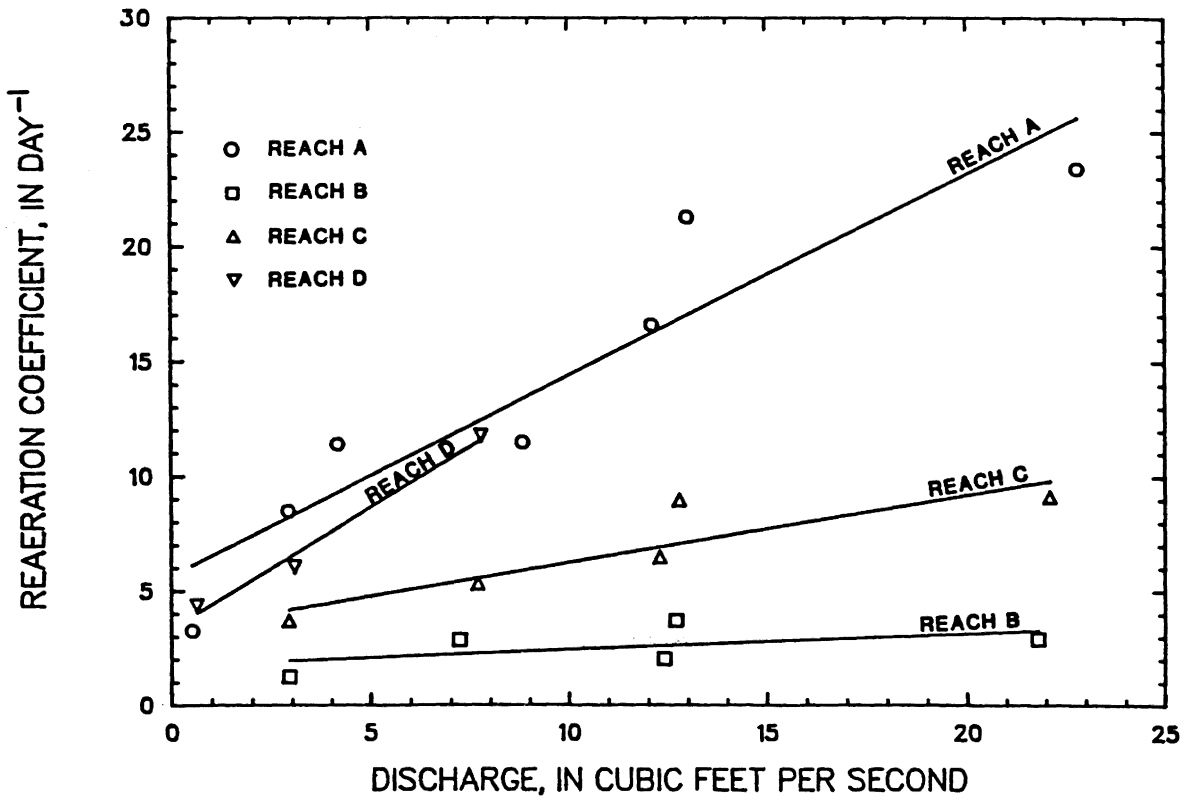


Figure 28 -- Linear relations between the reaeration coefficient and discharge for reaches of Middle Fork Beargrass Creek, from hydrocarbon gas tracer measurements made from April 18, 1985 through September 18, 1985

Table 18 -- Characteristics of simple linear regressions between the reaeration coefficient and discharge for hydrocarbon gas tracer measurements on reaches of Middle Fork Beargrass Creek

REACH	LINEAR EQUATION ¹	STATISTICAL MEASURE			
		R ²	ROOT M.S.E. (day ⁻¹)	C.V. (percent)	T-TEST SIGNIF.
A	$K_2 = 5.652 + 0.8763(Q)$	0.872	2.81	20.5	0.0021
B	$K_2 = 1.729 + 0.0716(Q)$	0.292	0.910	35.8	0.3470
C	$K_2 = 3.335 + 0.2938(Q)$	0.794	1.23	18.3	0.0424
D	$K_2 = 3.337 + 1.066(Q)$	0.985	0.670	9.04	0.0776

¹Where K_2 is in days⁻¹ and Q is in cubic feet per second.

Discussion

It is evident from the presented data that the reaeration coefficient does increase with increasing discharge (over the range of discharges measured) in the four studied reaches. However, if one arbitrarily selected a significance level (alpha) of 10 percent, then only the relations for reaches A, C, and D would be found to be significant. The regression slope for reach B likely would have been significant if there had been more observations or less measurement scatter. Note that the root mean square error for measurements on reach A and C were greater than for reach B but because the measured reaeration values and slope were higher, the regressions on those reaches were significant at the 0.10 level.

EVALUATION OF PUBLISHED REAERATION COEFFICIENT PREDICTION EQUATIONS

One of the significant objectives of this research was to evaluate the quality of reaeration coefficient predictions derived from the application of some of the numerous equations found in published literature and which are commonly used. Twenty-five of the best equations presented and discussed in the Literature Review chapter were selected for comparative analysis using reaeration and hydraulic data determined from this research. Of these equations, three were theoretically based, seven were semiempirical in nature, and the

remaining ones were strictly empirically developed using either stream or laboratory flume data. They were presented in Table 1.

Comparative Analysis

The statistics chosen for analysis were the normalized mean error and the standard error. The normalized mean error is sensitive to the issue of accuracy and the standard error is sensitive to precision. The standard error, because of the use of squared differences, is highly influenced by both upper and lower extreme values. Each of the 25 equations were ranked by each of the statistics. The overall performance rank was calculated as the ranked average of the ranks for each of the two statistics. The summarized errors and the relative ranking are presented in Table 19. The variability for the reaeration coefficient estimation errors are presented graphically by schematic box-and-whisker plots for each of the equations in Figure 29. The lower and upper ends of the box correspond to the lower and upper quartile value, respectively. The line across the box corresponds to the median value. The lines extending from both ends of box extend to the lowest and highest, respective value, which are less than 150 percent of the interquartile value away from the box. Other values shown are outliers. For normally distributed data, the box represents 50 percent of the observations and only 0.7 percent of the observations would be shown as outliers.

Table 19 -- Error analysis and relative ranking for selected reaeration coefficient predictive equations using hydrocarbon gas tracer measurements from reaches of Middle Fork Beargrass Creek

EQUATION NUMBER ¹	NORMALIZED MEAN ERROR		STANDARD ERROR		OVERALL RANK ²
	(percent)	RANK	(day ⁻¹)	RANK	
<u>Theoretically Based Equations</u>					
1	-12.5	2	5.94	14	7
2	9.05	1	3.99	7	3
3	30.1	5	2.95	2	2
<u>Semiempirical Equations</u>					
4	65.1	17	3.61	6	11.5
5	15.0	3	1.64	1	1
6	-55.3	14	6.80	18	16
7	-69.7	22	6.22	16	20.5
8	-41.7	8	3.31	4	5
9	-66.3	20	5.80	13	17
10	36.3	6	3.76	5	4
<u>Empirical Equations</u>					
11	-95.8	25	9.82	25	25
12	-51.2	12	6.02	15	14.5
13	39.0	7	4.05	8	6
14	43.4	9	4.48	10	8.5
15	-69.1	21	7.67	22	23
16	-65.2	18	7.25	20	20.5
17	-73.6	23	7.96	24	24
18	-44.2	10	6.42	17	14.5
19	-57.2	15	7.32	21	18.5
20	79.5	24	5.76	12	18.5
21	45.8	11	4.18	9	10
22	-66.2	19	7.87	23	22
23	61.5	16	3.05	3	8.5
24	-22.7	4	6.97	19	11.5
25	54.9	13	4.66	11	13

¹Equation numbers refer to the equation numbers presented in table 1.

²The overall rank is calculated as the ranked average of the normalized mean error rank and the standard error rank.

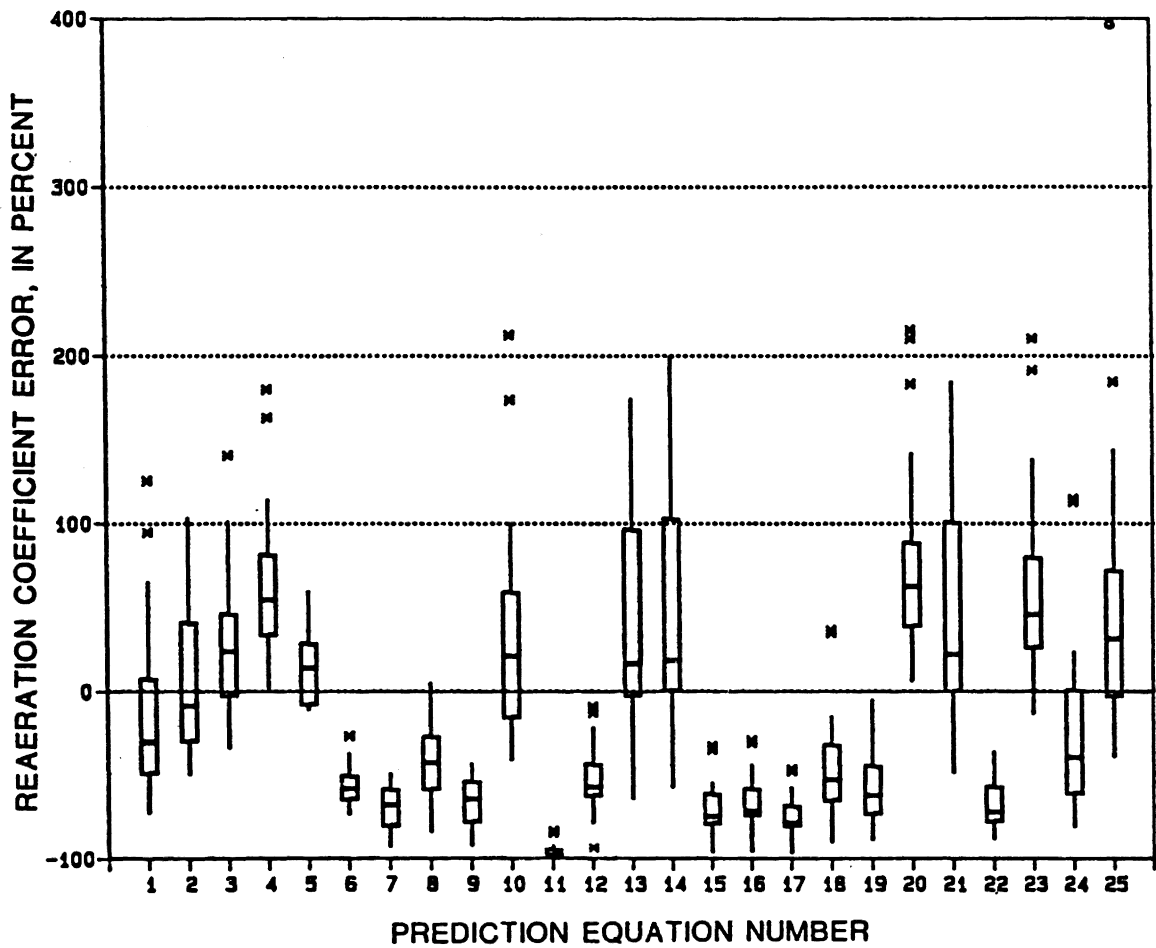


Figure 29 -- Schematic box plots of reaeration coefficient estimates using selected prediction equations and hydrocarbon gas tracer measurement data from reaches of Middle Fork Beargrass Creek

The normalized mean errors shown in Table 19 range from -95.8 to 79.5 percent. These errors are not expected to be normally distributed but rather should be described by a Couchee distribution because they are bounded on the lower side by a -100 percent value. The three theoretically based equations all ranked in the top five equations. The semiempirical equations can be seen to have done slightly better than the empirical equations.

The ranking using the standard error is somewhat different. The highest-ranked equation was semiempirical in nature corresponding to a standard error of 1.64 day^{-1} . The standard error of the lowest-ranked was almost 10.0 day^{-1} .

The best-overall equation was found to be a semiempirical equation developed by Cadwallader and McDonnell (1969) using velocity, depth, and slope as independent parameters. The next two, best-ranked equations were both theoretically based. They were the complex Dobbins (1965) equation; which uses Froude number, velocity, slope, and depth as input parameters; and the commonly used formulation by O'Connor and Dobbins (1958), which uses only velocity and depth.

Sensitivity of Predictions to the Methods of Parameter Value Determination

In addition to evaluating the performance of the selected reaeration coefficient prediction equations, it was also desired to

determine how sensitive the predictions were to the choice of the method used for input parameter value determination. The simplest technique which was evaluated was termed "method 1" and consisted of determining the depth only at the upstream and downstream ends of the stream reach. The slope was determined from differential leveling with survey instruments. The velocity was determined from the measured slope and discharge by use of an equation presented by Boning (1974). "Method 2" used the same methods except that the depth for the reach was determined by averaging depths taken at numerous, uniformly spaced cross-sections in the reach. "Method 3" is the more involved method which was used for nearly all other aspects of this research. It involved using a reach velocity determined from dye tracing and a depth determined by use of the continuity principle using the discharge, velocity, and reach averaged stream width. The slope was again field-measured using surveying methods.

Comparisons of velocities developed using the three methods is presented in Figures 30 through 33 and are shown as a function of discharge for each of the four reaches. In all reaches, methods 1 and 2 yielded higher velocities than are determined by the dye tracing technique of method 3 for low discharges. Both methods 1 and 2 underpredict the reach velocities at higher discharge conditions. Under low flow, the pools highly influence the reach velocity, but the overall reach slope, which is input to the Boning (1974) equation, is highly influenced by the presence of riffles.

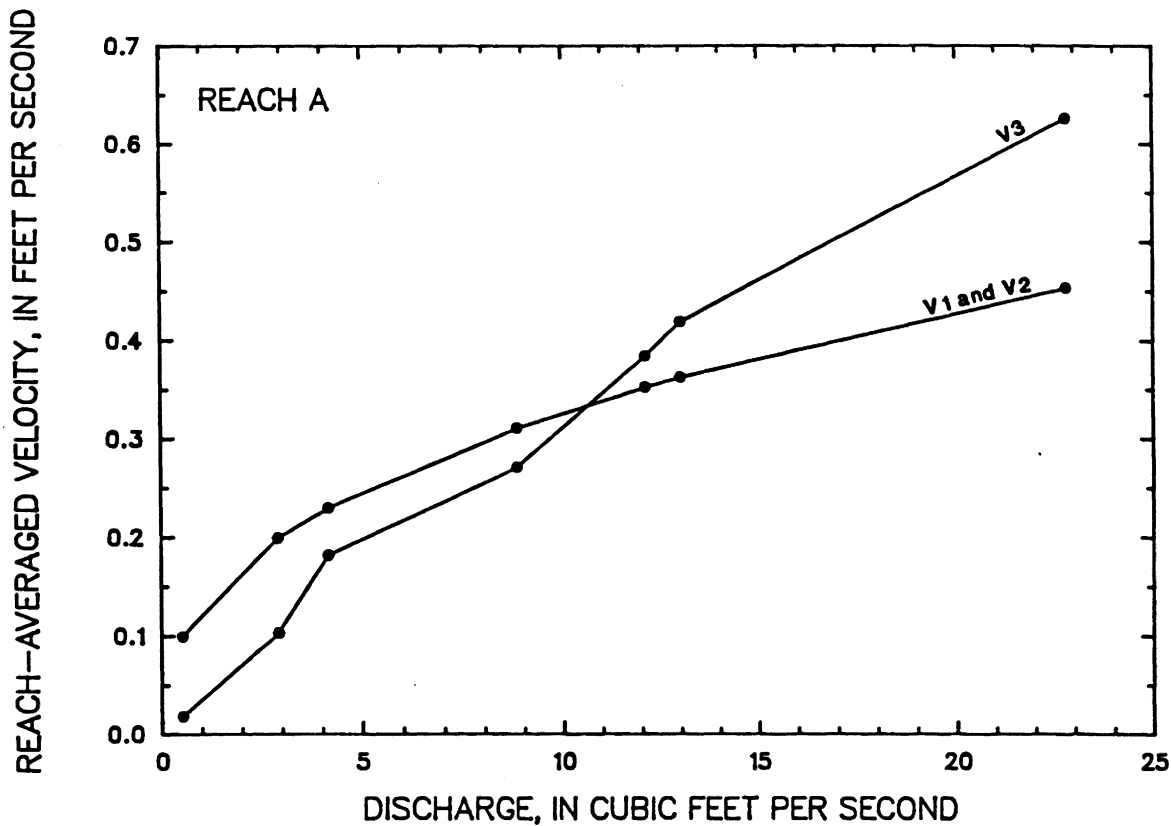


Figure 30 -- Comparison of mean velocity determined by three different methods for reach A of the Middle Fork Beargrass Creek, from tracer measurements made between April 18, 1985 and September 18, 1985

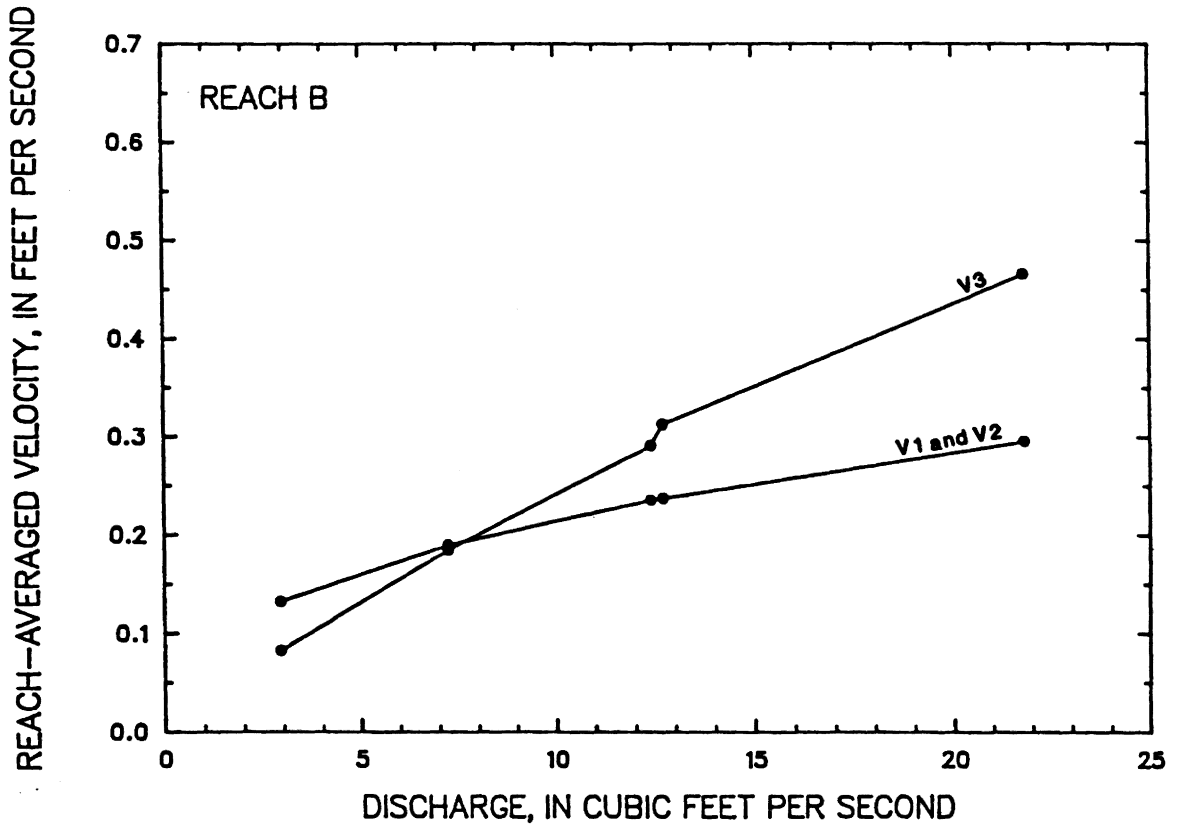


Figure 31 -- Comparison of mean velocity determined by three different methods for reach B of the Middle Fork Beargrass Creek, from tracer measurements made between April 18, 1985 and September 18, 1985

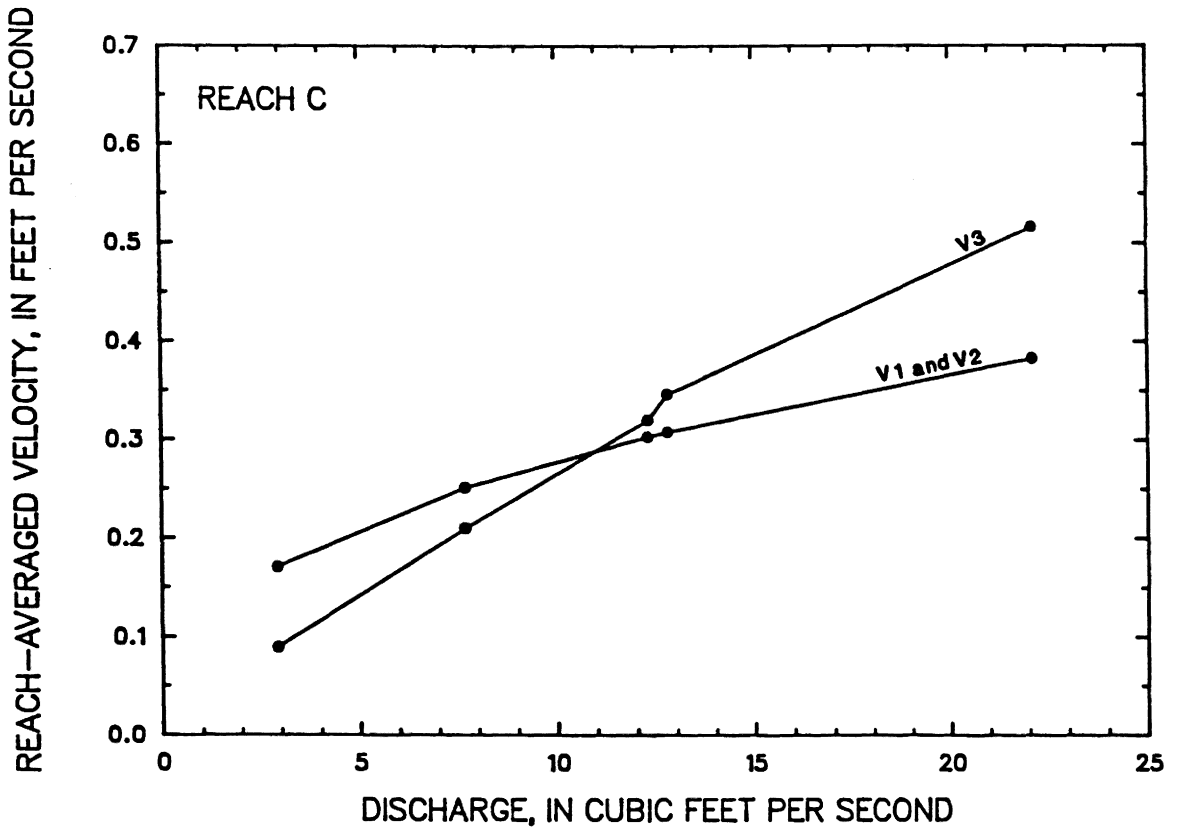


Figure 32 -- Comparison of mean velocity determined by three different methods for reach C of the Middle Fork Beargrass Creek, from tracer measurements made between April 18, 1985 and September 18, 1985

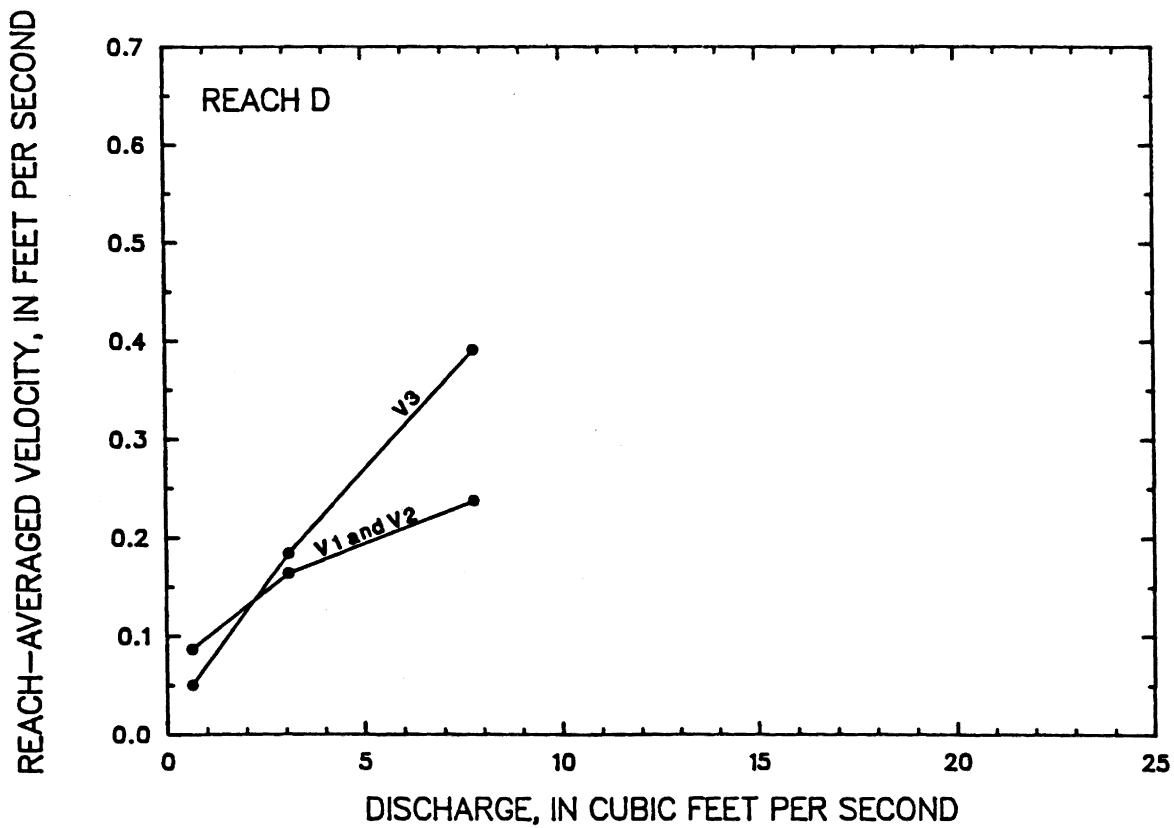


Figure 33 -- Comparison of mean velocity determined by three different methods for reach D of the Middle Fork Beargrass Creek, from tracer measurements made between April 18, 1985 and September 18, 1985

A similar comparison for depths determined by each of the three methods is presented in Figures 34 through 37 and are plotted as a function of discharge for each of the four reaches. In general, no similar relation with discharge was found as it was for velocity. However, it is clear that the simpler techniques tend to underestimate the depth as compared to the weighted value calculated in method 3. The dominance of residence time in the reach is in the pools. Therefore, particularly at low flow, the depth determined by method 3 would tend to be higher than the depth determined by either methods 1 or 2.

The same selected reaeration coefficient prediction equations were again used to evaluate prediction errors for each of the three data sets (from application of the three methods of determination). The normalized mean error and the standard error for each equation for each method are presented in Table 20. The simpler methods 1 and 2 resulted in generally higher predictions as can be seen from the normalized mean error. For the most part this arises from the overestimation of reach velocities and underestimation of reach depth previously presented. In nearly all cases the standard error was higher for predictions using either method 1 or 2 as compared to method 3. The mean, median, and extremes for values shown in Table 20 are presented in condensed form in Table 21. Using either the mean, or the more robust median, it can be seen in Table 21 that method 3 derived parameter estimates which, overall, resulted in less prediction errors than either method 1 or 2.

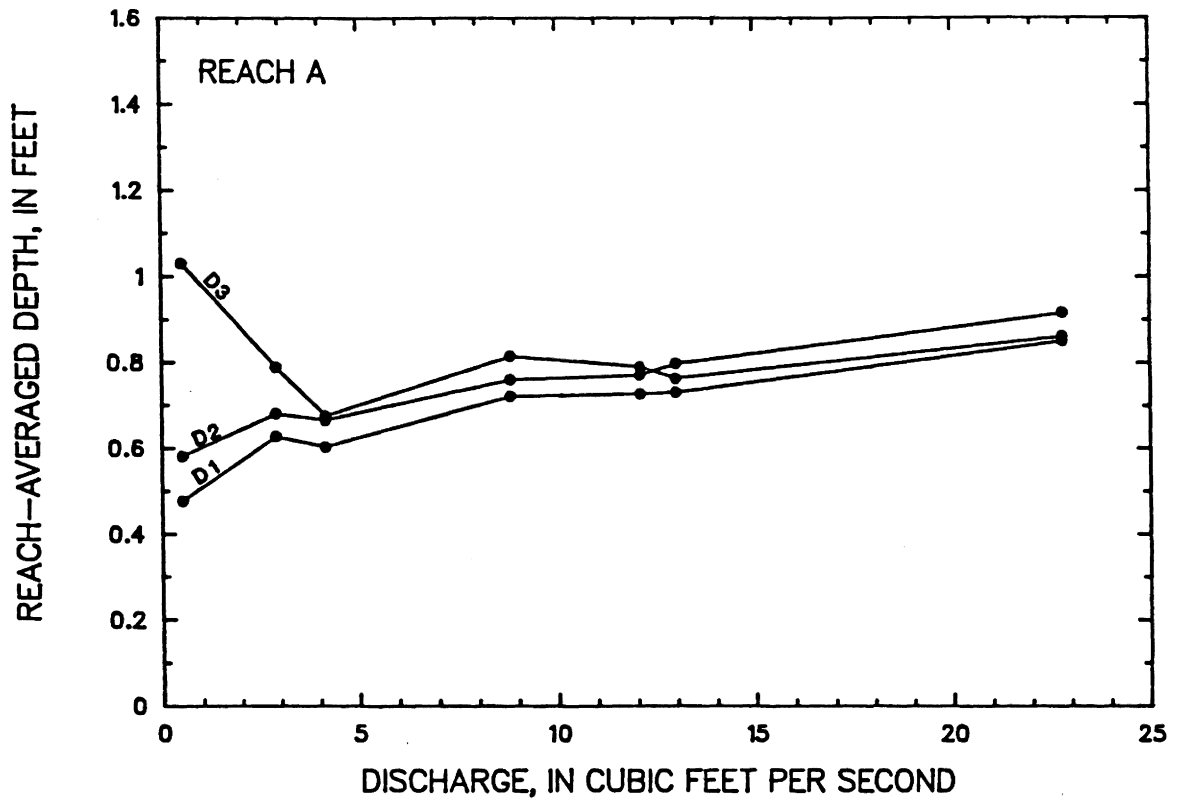


Figure 34 -- Comparison of mean depth determined by three different methods for reach A of the Middle Fork Beargrass Creek, from tracer measurements made between April 18, 1985 and September 18, 1985

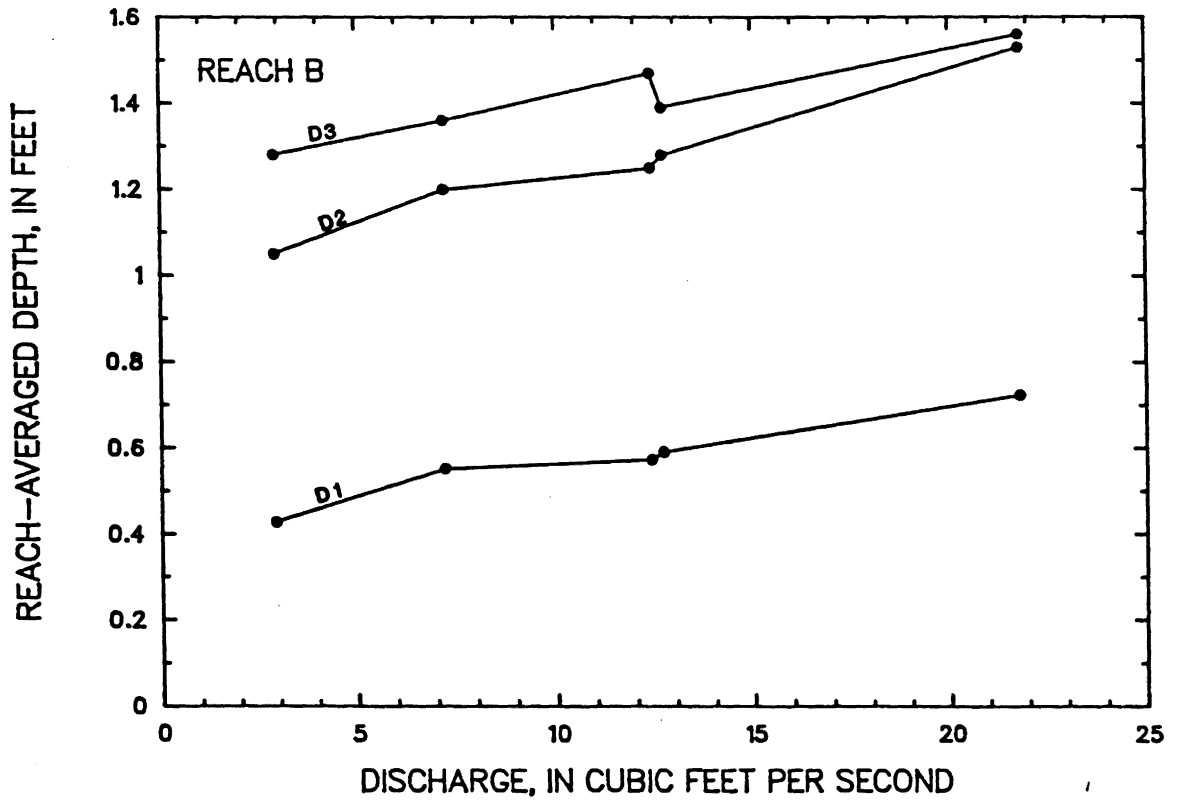


Figure 35 -- Comparison of mean depth determined by three different methods for reach B of the Middle Fork Beargrass Creek, from tracer measurements made between April 18, 1985 and September 18, 1985

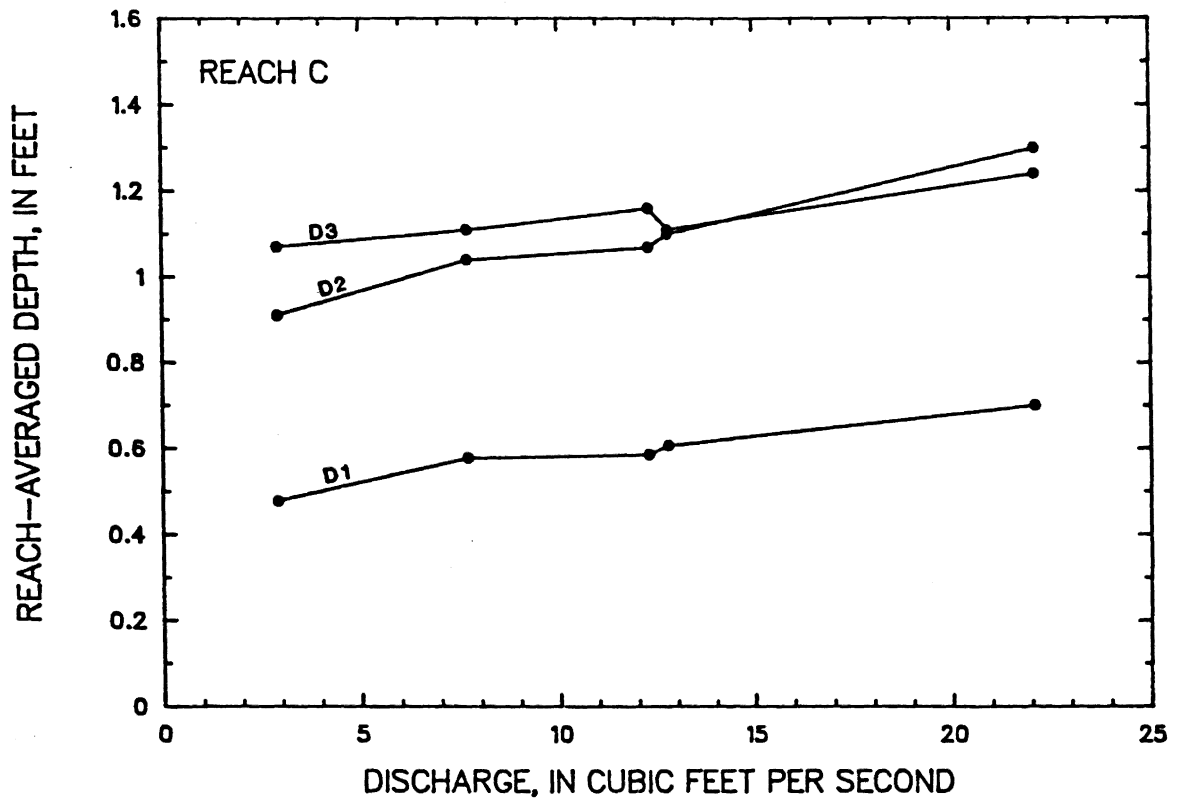


Figure 36 -- Comparison of mean depth determined by three different methods for reach C of the Middle Fork Beargrass Creek, from tracer measurements made between April 18, 1985 and September 18, 1985

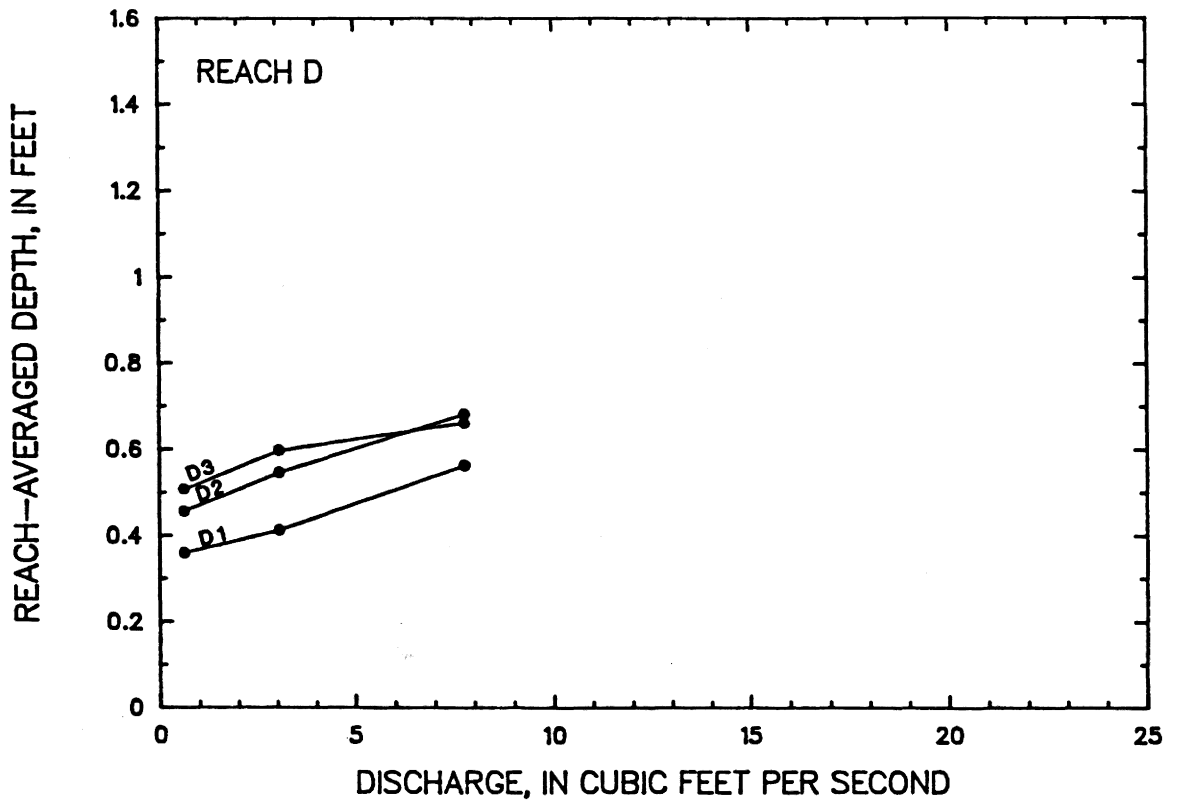


Figure 37 -- Comparison of mean depth determined by three different methods for reach D of the Middle Fork Beargrass Creek, from tracer measurements made between April 18, 1985 and September 18, 1985

Table 20 -- Error analysis for selected reaeration coefficient predictive equations using three different methods of input parameter value determination for hydrocarbon gas tracer measurements on reaches of Middle Fork Beargrass Creek

EQUATION NUMBER ¹	NORMALIZED MEAN ERROR ² (percent)			STANDARD ERROR ² (day ⁻¹)		
	1	2	3	1	2	3
<u>Theoretically Based Equations</u>						
1	96.5	6.27	-12.5	7.15	20.1	5.94
2	215	40.2	9.05	9.40	5.08	3.99
3	157	60.1	30.1	7.38	4.75	2.95
<u>Semiempirical Equations</u>						
4	167	93.9	65.1	7.89	5.33	3.61
5	126	43.2	15.0	6.31	3.95	1.64
6	-10.9	-44.9	-55.3	6.45	6.94	6.80
7	-67.2	-67.2	-69.7	6.65	6.65	6.22
8	-33.9	-33.9	-41.7	4.19	4.19	3.31
9	-63.6	-63.6	-66.3	6.27	6.27	5.80
10	93.2	50.0	36.3	5.56	4.71	3.76
<u>Empirical Equations</u>						
11	-79.7	-97.0	-95.8	9.75	10.0	9.82
12	46.7	-40.1	-51.2	6.15	6.48	6.02
13	358	80.5	39.0	14.8	5.34	4.05
14	405	90.6	43.4	16.7	6.15	4.48
15	-25.7	-64.2	-69.1	7.40	7.97	7.67
16	- 6.74	-58.6	-65.2	6.94	7.59	7.25
17	-29.3	-68.6	-73.6	7.62	8.22	7.96
18	0.929	-37.5	-44.2	6.43	6.77	6.42
19	- 9.05	-49.5	-57.2	7.09	7.52	7.32
20	363	133	79.5	16.2	8.42	5.76
21	369	90.8	45.8	15.2	5.91	4.18
22	- 8.89	-57.5	-66.2	7.47	7.99	7.87
23	92.5	76.5	61.5	4.67	4.14	3.05
24	96.2	- 5.57	-22.7	7.87	7.15	6.97
25	54.9	54.9	54.9	4.66	4.66	4.66

¹Equation numbers refer to the equation numbers presented in table 1.

²Methods 1, 2, and 3 refer to the methods described within the text.

Table 21 -- Summary of error analysis for selected reaeration coefficient predictive equations using three different methods of input parameter value determination for hydrocarbon gas tracer measurements on reaches of Middle Fork Beargrass Creek

ERROR MEASURE	METHOD ¹		
	1	2	3
Normalized mean error (percent)			
Mean absolute value	119.	60.3	50.9
Median absolute value	79.7	58.6	54.9
Minimum absolute value	0.929	5.57	9.05
Maximum absolute value	405.	133.	95.8
Standard error (day ⁻¹)			
Mean value	8.25	6.89	5.50
Median value	7.15	6.65	5.80
Minimum value	4.19	3.95	1.64
Maximum value	16.7	20.1	9.82

¹Methods 1, 2, and 3 refer to the methods described within the text.

Discussion

The results of error analysis for reaeration coefficient predictions using the 25 equations presented in Table 19 indicate that most all of the equations generate significant error. As an example, even the equation which was ranked second overall--the Dobbins (1965) equation--generated a mean error of over 30 percent. For all the equations taken collectively, the mean absolute error (Table 21) was over 50 percent. These levels of reaeration coefficient error may not be acceptable to a water-quality modeller developing a wasteload allocation. The introduction of a 50 or even a 30 percent error may drastically change the modeling output.

An additional error in predicting the reaeration coefficient could arise from the application of simpler techniques to determine the input parameter values. As an example, if the Dobbins (1965) equation (number 3) was selected and the velocity and depth determined using method 2, the resultant mean error would be about 60 percent--about double that obtained with the more involved method 3. If the reach depth was estimated from only two cross-sections, as was done in method 1, the Dobbins (1965) equation would have generated an average error of 157 percent (Table 20).

It is evident that existing reaeration coefficient prediction equations do not generate reliable values for Middle Fork Beargrass Creek using any of the input parameter determination schemes. However, it is clear that from the summary presented in Table 21 that the

prediction errors can likely be reduced significantly by using the parameter determination techniques referred to as method 3. If highly accurate reaeration coefficients are needed, it appears that additional work is needed to develop more accurate predictive capabilities. An additional alternative would be to field-measure the reaeration coefficient using either the hydrocarbon or radioactive gas tracer techniques.

It should be noted that reaeration coefficients that are determined either by field measurement or by the application of predictive equations may be valid only for the hydraulic conditions prevailing during measurement. As was presented in Figure 28, it was found that in Middle Fork Beargrass Creek that reaeration coefficients do vary under different flow conditions. The reaeration coefficient at the 7-day, 10-year low flow would be significantly lower than for more probable higher flows.

PREDICTION EQUATION DEVELOPMENT

One of the objectives of this research was to develop one or a series of reaeration coefficient prediction equations, if the best published ones were found to be inaccurate. As was discussed in the previous chapter, all the selected prediction equations generated significant errors in predicting the reaeration coefficients measured in Middle Fork Beargrass Creek. Therefore, efforts were made to develop a

few equations which could more accurately predict the coefficients measured. Additionally, the developed equations were verified using compatibly collected reaeration data in Massachusetts (Parker and Gay, 1987) and elsewhere in Kentucky (Ruhl and Smoot, 1987).

Equation Building and Selection

One of the first steps taken in developing prediction equations for the reaeration coefficient was to plot all possible raw independent variables with the dependent variable (reaeration coefficient). The raw (non-transformed) independent variables consisted of all the hydraulic parameters determined from the tracer measurements. Some of these scatterplots are presented in Figures 38 through 41 and in Appendix C. By analyzing the scatterplots it can be initially determined which independent variables correlate well with the reaeration coefficient and which may need transformation. In addition, consideration was given to the conceptual physical basis for gas exchange processes as was presented in the Literature Review chapter. In other words, the pattern displayed in the scatterplot would be expected to follow a conceptual model of the gas exchange process.

In Figure 38, the slope does appear to be related positively to the reaeration coefficient. Conceptually though, slope does not enter into the gas exchange process so it appeared to be acting as a surrogate variable for velocity or turbulence which was included in a conceptual

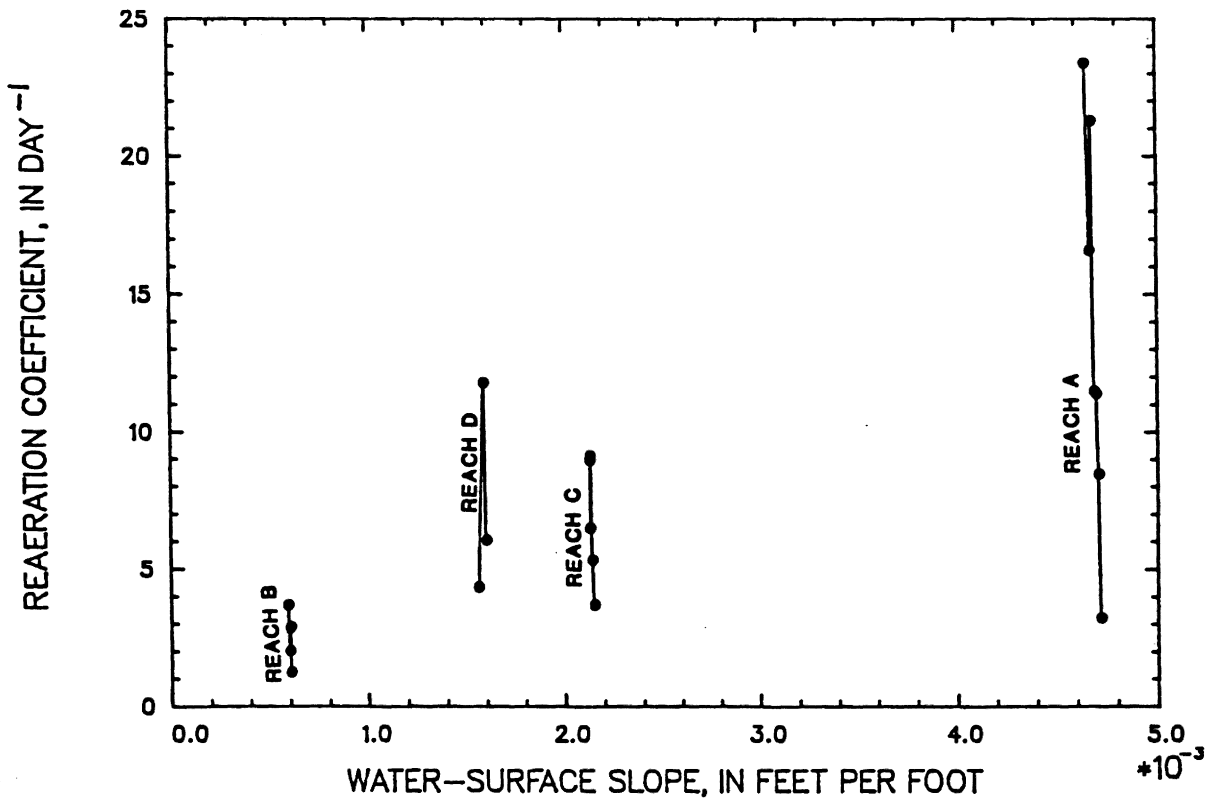


Figure 38 -- Reaeration coefficient shown as a function of reach-averaged water-surface slope for reaches of Middle Fork Beargrass Creek, from tracer measurements made from April 18, 1985 through September 18, 1985

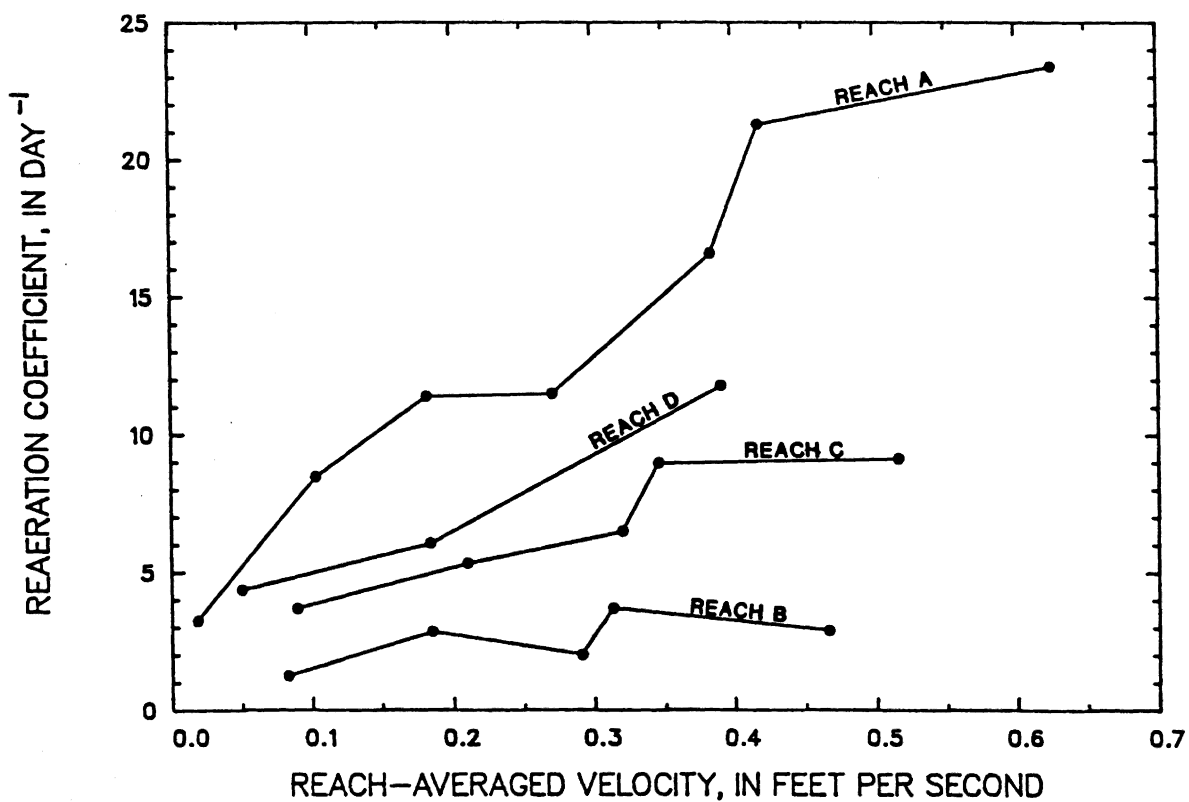


Figure 39 -- Reaeration coefficient shown as a function of reach-averaged velocity for reaches of Middle Fork Beargrass Creek, from tracer measurements made from April 18, 1985 through September 18, 1985

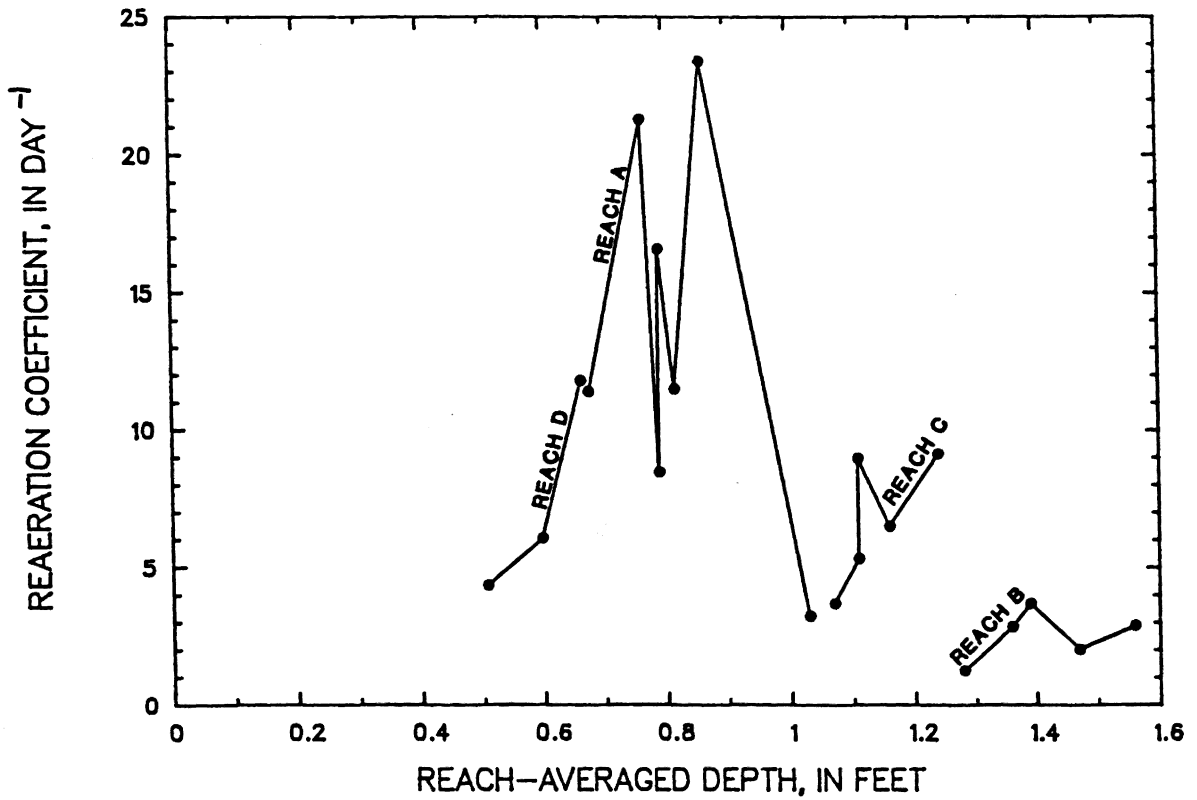


Figure 40 -- Reaeration coefficient shown as a function of reach-averaged depth for reaches of Middle Fork Beargrass Creek, from tracer measurements made from April 18, 1985 through September 18, 1985

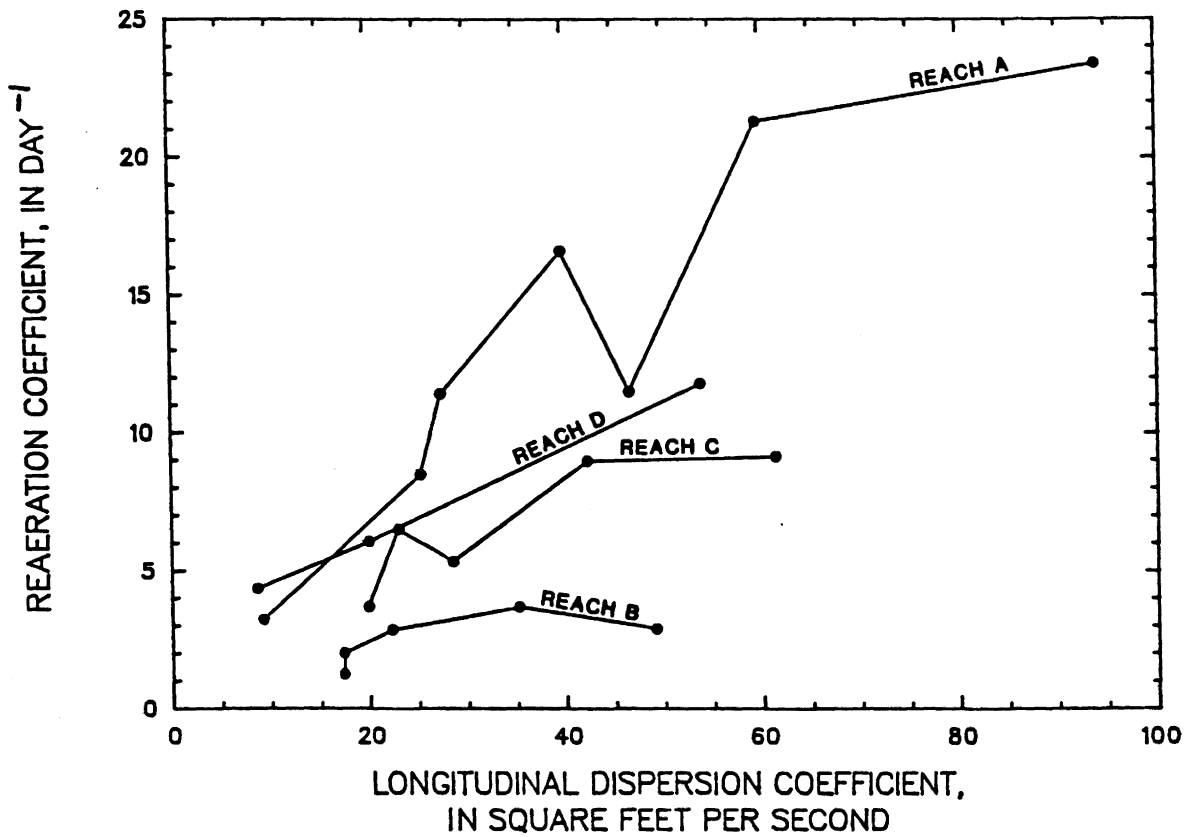


Figure 41 -- Reaeration coefficient shown as a function of reach-averaged dispersion coefficient for reaches of Middle Fork Beargrass Creek, from tracer measurements made from April 18, 1985 through September 18, 1985

model. Also note that from a comparison of Figure 21 with Figure 38 that slope could be used as a surrogate variable for the intensity or characteristics of pool and riffing. A strong relation is evident between velocity and the reaeration coefficient for each reach (Figure 39). The plots of depth with the reaeration coefficient (Figure 40) appear, for each reach, contrary to the conceptual gas transfer model. However, taken collectively the data show the expected inverse relation with the reaeration coefficient. The longitudinal dispersion coefficient (Figure 41) appears to be a possible surrogate variable for velocity.

Prior to invoking sophisticated computer based algorithms for building linear regression models, selected hydraulic parameters and their transforms, along with dimensionless and dimensionally homogeneous combinations of the parameters were isolated for analysis. In addition, the forms of some of the best equations presented in Table 19 were used. In general, the energy dissipation equations which fell under the category of semiempirical equations did better than most. These equations used the product of velocity and slope as the energy dissipation parameter. The simplest form of these equations follows the forms used by Tsivoglou and Wallace (1972) and Grant (1978). Equation P1 was developed using a zero-intercept, simple-linear regression and the velocity-slope product as the independent variable. The resulting equation is given as:

$$K_2 = 9630(VS) \quad (61)$$

where K_2 is in days^{-1} , V is in feet per second, and S is in feet per foot. The statistical fit measures are presented in Table 22. The plotted predictions are shown as a function of discharge for each of the reaches in Figure 42. Equation P1 appears to significantly underpredict the reaeration coefficient for reach D and slightly underpredict it for reach B.

The next equation developed, equation P2, followed the same form as the equation presented by Cadwallader and McDonnell (1969) which was ranked best overall in Table 19. Only the coefficient was fit with a zero-intercept simple linear regression as was done for equation P1. The resulting equation is given as:

$$K_2 = 319.7(VS)^{0.5}(D)^{-1.0} \quad (62)$$

where K_2 is in days^{-1} , V is in feet per second, S is in feet per foot, and D is in feet. The normalized mean error was found to be a little less than 10 percent (Table 22). From the R^2 value it can be seen that equation P2 accounted for 93.6 percent of the variability in the reaeration coefficients measured in all four reaches. From Figure 43 it can be seen that equation P2 predicts values for reaches A, B, and C well, but slightly overpredicts values for reach D.

The third equation developed, equation P3, was similar in form to P1 except an exponent on the velocity-slope product was fitted. The model was developed using log transforms and simple linear regression.

Table 22 -- Statistical measures of fit for reaeration coefficient prediction equations developed from hydrocarbon gas tracer measurements on reaches of Middle Fork Beargrass Creek

STATISTIC	VALUE FOR FITTED EQUATION			
	P1	P2	P3	P4
Coefficient of determination ² , R ²	0.821	0.936	0.851	0.959
Coefficient of variation, in percent	32.2	19.3	17.2	9.52
Root mean squared error, in day ⁻¹	2.65	1.59	1.37	1.19
Normalized mean error, in percent	-29.4	9.17	4.56	1.19
Standard error, in day ⁻¹	2.59	1.55	1.88	1.28
Maximum variance inflation factor	---	---	---	1.56

¹ P1: $K_2 = 9630(VS)$

P2: $K_2 = 319.7 \frac{(VS)^{0.5}}{D}$

P3: $K_2 = 840.8(VS)^{0.6284}$

P4: $K_2 = 683.8(V)^{0.5325}(D)^{-0.7258}(S)^{0.6236}$

² For equation P1 and P2 the coefficient of determination presented is a corrected coefficient of determination.

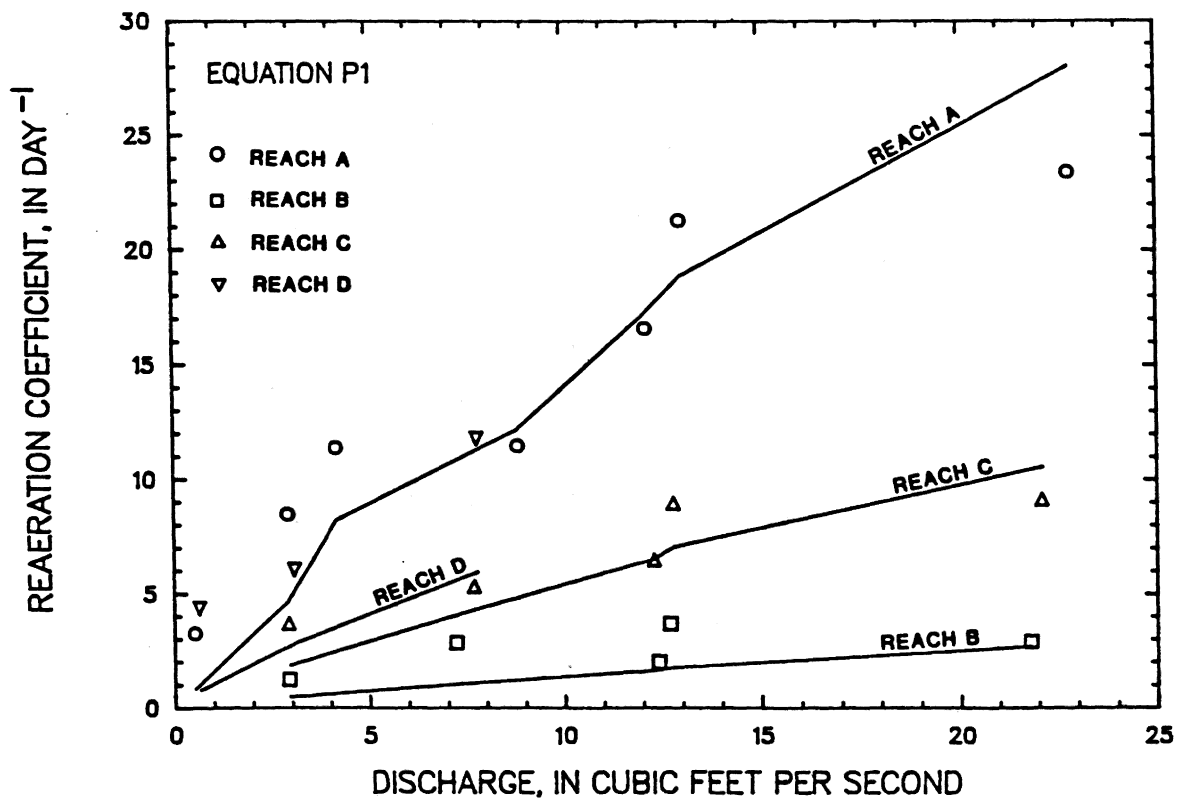


Figure 42 -- Comparison of field-measured reaeration coefficients with those predicted using developed equation, P1

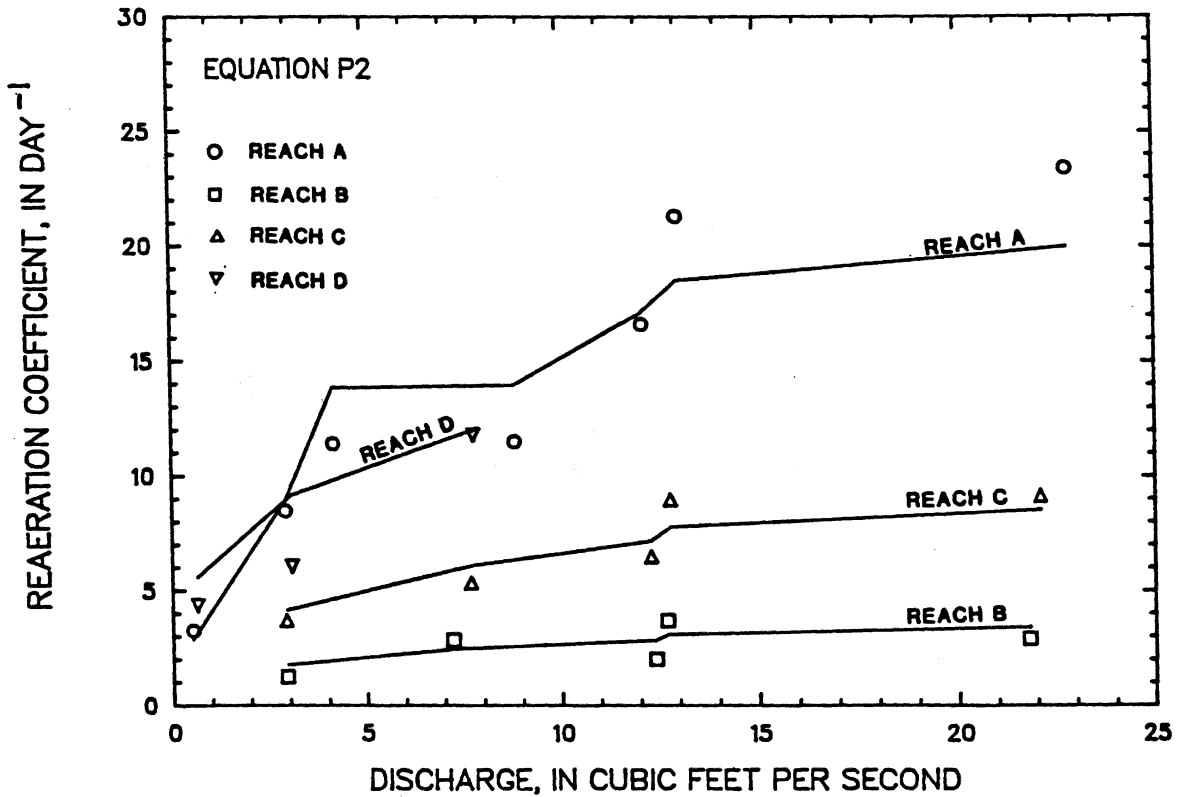


Figure 43 -- Comparison of field-measured reaeration coefficients with those predicted using developed equation, P2

The resulting equation is given as:

$$K_2 = 840.8(VS)^{0.6284} \quad (63)$$

where K_2 is in days^{-1} , V is in feet per second, and S is in feet per foot. The statistical characteristics of the fit, presented in Table 22, indicate that while the R^2 was not as high as for equation P2, the coefficient of variation and normalized mean error were significantly less. The fit of the equation is shown in Figure 44. Note that it overpredicts values for reach B and C and underpredicts the values for reach D.

Multiple linear regression model building techniques (stepwise, forward, and backward procedures) were used on the independent variables along with log transformations of the variables. Resulting models expressing a high degree of multicollinearity (two or more independent variables correlate highly with some combination of each other) were eliminated. The best model selected utilized log transformations of velocity, depth, and slope. Each variable was significant at the 0.0002 probability level. The resulting equation is termed equation P4 and is given as:

$$K_2 = 683.8(V)^{0.5325}(D)^{-0.7258}(S)^{0.6326} \quad (64)$$

where K_2 is in days^{-1} , V is in feet per second, D is in feet, and S is in feet per foot. The equation showed little evidence of

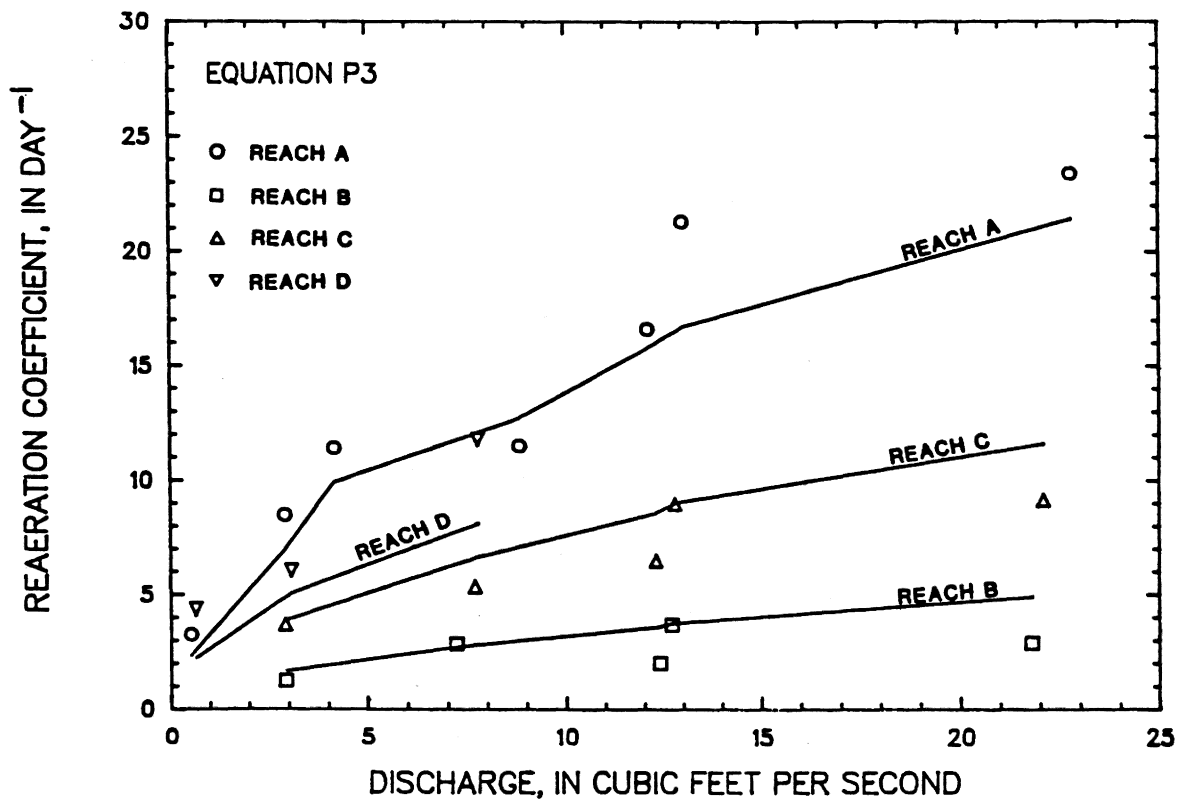


Figure 44 -- Comparison of field-measured reaeration coefficients with those predicted using developed equation, P3

multicollinearity (variance inflation factors less than 1.56) and a high coefficient of determination of 0.959. Additional fit statistics are presented in Table 22.

The fit of equation P4, shown in Figure 45, can be seen to be fairly good for all four reaches. Another equation containing velocity, depth, and slope and additionally the dispersion coefficient was superior to equation P4 based on fit statistics. However, it was not selected for presentation because the indicator of multicollinearity--the variance inflation factor--was significantly higher. This would render the equation less useful for predictions using other data sets. The prediction errors for equations P1 to P4 are presented using schematic box plots in Figure 46. Note that, graphically, equation P4 produces less scattered observations than the other equations.

Verification Analysis

To be useful, a reaeration coefficient prediction equation needs to be accurate not only in accounting for the variability of values contained in the development data set but also in predicting coefficient values for other data sets. Therefore, it was desirable to compare the performance of the four developed equations (P1, P2, P3, and P4) with the 25 selected equations from the literature (Table 1) using compatibly collected data elsewhere. The selected verification data were collected using the hydrocarbon gas tracer method on 23 different stream reaches

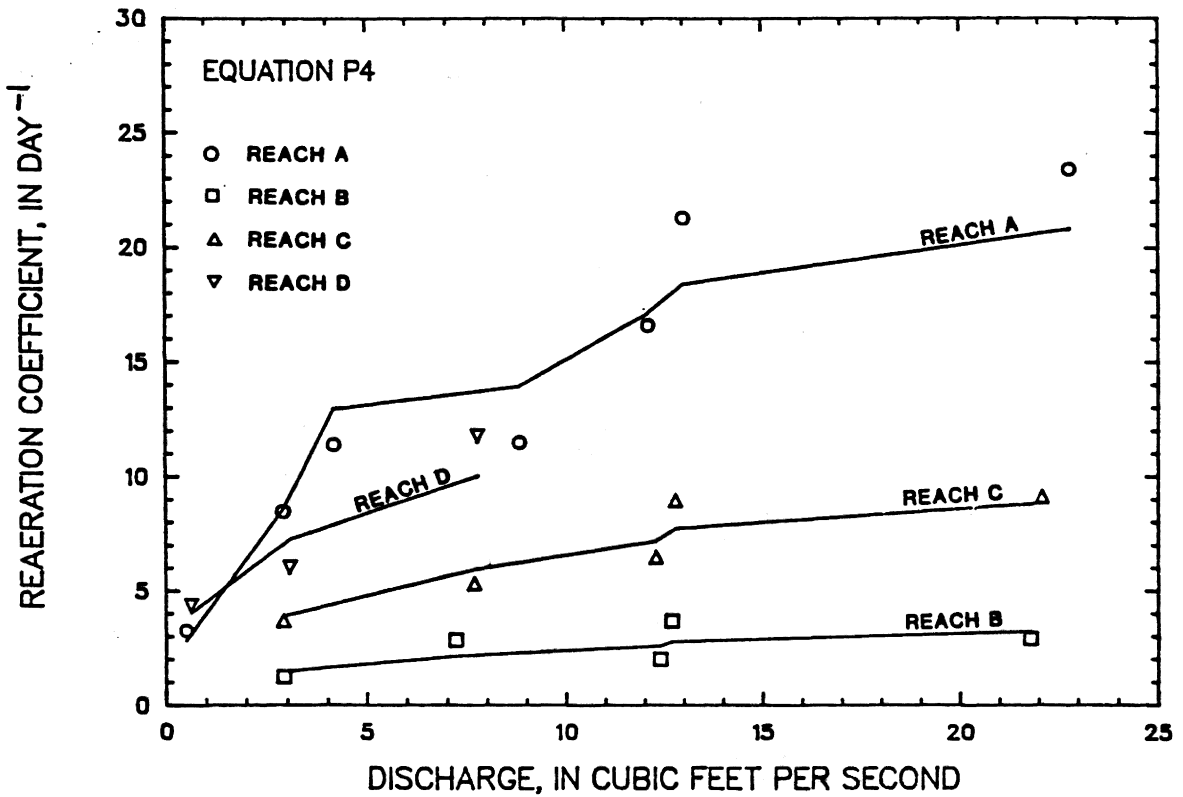


Figure 45 -- Comparison of field-measured reaeration coefficients with those predicted using developed equation, P4

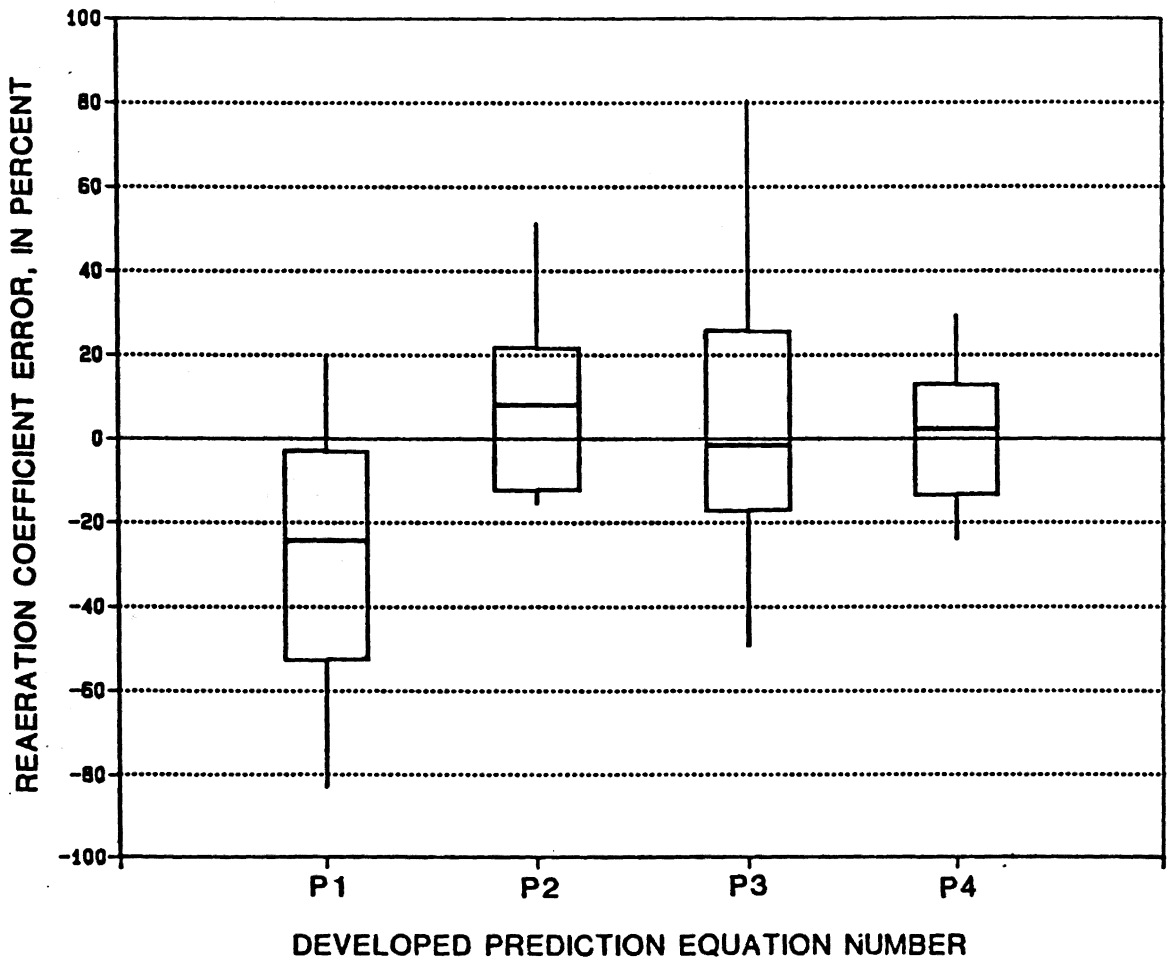


Figure 46 -- Schematic box plots of reaeration coefficient estimates using developed prediction equations and hydrocarbon gas tracer measurement data from reaches of Middle Fork Beargrass Creek

in Massachusetts and Kentucky (Parker and Gay, 1987; and Ruhl and Smoot, 1987). The data set consisted of discharge, slope, velocity, depth, width, and the reaeration coefficient--all determined in a manner similar to method 3 of this research. The data set contained 39 observations, some of which contained parameter values outside the range of values generated from this research found in Tables 4,5,6 and 10. The verification data set is contained in Appendix D. The highest variability in the predictions, using equations P1 to P4, appears to be for observations where the discharge is either significantly higher or lower than those observed during the measurements made on Middle Fork Beargrass Creek. The normalized mean error and standard error were again selected as the statistics to use to compare the accuracy of various literature equations and the ones developed in this research. The error summaries are presented in Table 23. The normalized mean error ranged from a low of -84.2 percent to a high of 80.3 percent. The Dobbins (1965) equation ranked highest for normalized mean error with an overall error of less than one percent. However, the scatter of its predictions inflated the standard error up to 11.9 day^{-1} , which ranked number 11. Note that two of the four equations developed in this research ranked in the top five based on either error statistic. The best, overall equation considering both error statistics was equation P4. The next best was equation P2 which was essentially the Cadwallader and McDonnell (1969) equation with a newly fitted coefficient. The third-best equation was the Dobbins (1965) equation, which was previously ranked two for the Middle Fork Beargrass Creek data set.

Table 23 -- Verification error analysis and relative ranking for selected reaeration coefficient predictive equations using 39 hydrocarbon gas tracer measurements on 23 stream reaches in Massachusetts and Kentucky¹

EQUATION NUMBER ²	NORMALIZED MEAN ERROR		STANDARD ERROR		OVERALL RANK ³
	(percent)	RANK	(day ⁻¹)	RANK	
<u>Theoretically Based Equations</u>					
1	-51.6	18	17.0	17	17
2	- 4.39	4	14.4	12	7
3	0.465	1	11.9	11	3
<u>Semiempirical Equations</u>					
4	56.5	23	8.27	3	12
5	7.79	6	10.5	9	6
6	-62.8	25	16.5	15	21.5
7	-34.2	13	9.99	6	9
8	14.5	7	17.5	20	13
9	-26.9	10	10.4	8	8
10	- 3.76	3	11.0	10	4
<u>Empirical Equations</u>					
11	-84.2	29	21.1	26	29
12	-41.4	15	15.1	13	14
13	37.6	14	18.9	25	20
14	33.4	12	21.0	28	21.5
15	-58.2	24	17.3	18	23
16	-55.3	22	16.6	16	18.5
17	-66.1	26	17.8	22	26.5
18	-17.3	8	15.8	14	10
19	-48.1	17	17.7	21	18.5
20	42.8	16	20.7	27	24
21	32.9	11	17.4	19	16
22	-66.8	27	18.6	24	28
23	80.3	28	7.32	1	15
24	-55.2	21	18.4	23	25
25	20.2	9	9.04	5	5

(continued)

Table 23 (continued) -- Verification error analysis and relative ranking for selected reaeration coefficient predictive equations using 39 hydrocarbon gas tracer measurements on 23 stream reaches in Massachusetts and Kentucky¹

EQUATION NUMBER ²	NORMALIZED MEAN ERROR		STANDARD ERROR		OVERALL RANK ³	
	(percent)	RANK	(day ⁻¹)	RANK		
		<u>Developed Equations</u>				
P1	53.4	19	29.8	29	26.5	
P2	2.32	2	10.1	7	2	
P3	54.5	20	8.92	4	11	
P4	5.54	5	7.81	2	1	

¹Reaeration and hydraulic data taken from reports by Parker and Gay (1987) and Ruhl and Smoot (1987).

²Equation numbers refer to the equation numbers presented in table 1 and table 25.

³The overall rank is calculated as the ranked average of the normalized mean error rank and the standard error rank.

Note that the best rated equation for standard error alone was developed by Parker and Gay (1987) on the Massachusetts observations of the verification data set. However, due to a poor normalized mean error ranking of last, its overall rank was fairly poor at 15.

Discussion

It was evident that from the results presented in the previous chapter, that the development of statistically better reaeration coefficient prediction equations was desirable. Of four equations developed, equations P2 and P4 were shown in Table 22 to have extremely high R^2 values while maintaining coefficients of variation of less than 20 percent. From the results of the verification analysis (Table 23), it is evident that equations P2 and P4 provided the most accurate and the most precise predicted reaeration coefficients of any of the equations evaluated. Both equations produced a normalized mean error of less than six percent.

Equations P2 and P4 appear not only to describe the variability of the developmental data set well but also to provide useful reaeration coefficient predictions for other stream reaches and hydraulic conditions. Caution should be exercised in applying the equations to streams in which the input parameters are significantly different from the range of those used in the equations' development.

Additional verification would be desirable prior to more general application of the equations. Refinement of the equations using a much larger, compatible, development data base, followed by extensive verification would also be desirable.

CONCLUSIONS

The broad objective of this research was to add to the understanding of the reaeration process occurring in pool-and-riffle streams and relate this process to the hydraulic conditions and changes associated with varying streamflow conditions. This objective was met. Several specific conclusions are warranted from the results of this research:

- (1) In four studied reaches of a pool-and-riffle stream (Middle Fork Beargrass Creek) the reaeration coefficient decreased with decreasing streamflow. From the results, the explanation appears to be that in pool-and-riffle streams the reaeration coefficient for the pools is dominant over the coefficient for the riffles because of the longer relative residence time in the pools. As flow decreases, the relative residence time in the pools would increase, thereby, decreasing the reaeration coefficient for the entire reach. The practical implication is that wasteload allocation models for pool-and-riffle streams, developed with reaeration coefficients for higher streamflow conditions, may not be environmentally conservative.

- (2) Reaeration coefficients for Middle Fork Beargrass Creek calculated on the basis of 25 selected published equations were highly variable and generally did not compare well to measured reaeration coefficients. The equations that ranked best and second best produced errors of about 15 and 30 percent, respectively. Collectively, the theoretically based equations performed better than either the semiempirical or empirical equations. However, the best ranked equation was found to be an energy dissipation (semiempirical) formulation.
- (3) The selected reaeration coefficient prediction equations were highly sensitive to the methods used for input parameter value determination. Three methods were evaluated and compared. In general, the two, simpler approaches to determining reach-averaged input values resulted in predictions which were much more variable and biased.
- (4) Four reaeration coefficient prediction equations were developed and presented from the data collected using simple or multiple linear regression procedures. Two of the equations not only provided reaeration coefficient estimates which were more accurate than any of the 25 selected published equations, but also provided more accurate predictions overall based on 39 tracer measurements on 23 stream reaches in Massachusetts and Kentucky. These two best equations each used velocity, depth, and slope as input parameters. One of the equations was an empirical modification of the energy dissipation model

presented by Cadwallader and McDonnell (1969). The other was entirely empirically derived using the field-collected tracer data. Each of these two equations were demonstrated to have applicability to stream reaches other than those of Middle Fork Beargrass Creek. However, the equations would likely be most accurate when used for streams in which the input parameter values fall within the range of those observed for Middle Fork Beargrass Creek during tracer measurements.

REFERENCES CITED

Adeney, W.E., and Becker, H.G., "The Determination of the Rate of Solution of Atmospheric Nitrogen and Oxygen by Water." Philosophical Magazine, 38, 317-338 (1919).

Alonso, C.V., McHenry, J.R., and Hong, J.C.S., "The Influence of Suspended Sediment on the Reaeration of Uniform Streams." Water Research, 9, 695-700 (1975).

Banks, R.B., and Herrera, F.F., "Effect of Wind and Rain on Surface Aeration." Journal of the Environmental Engineering Division, American Society of Civil Engineers, 103(EE3), 489-504 (1977).

Bansal, M.K., "Atmospheric Reaeration in Natural Streams." Water Research, 7(5), 769-782 (1973).

Bennett, J.P., and Rathbun, R.E., "Reaeration in Open-Channel Flow." Professional Paper 737, U.S. Geological Survey, Washington, D.C., 75 p. (1972).

Benson, M.A., and Dalrymple, T., "General Field and Office Procedures for Indirect Discharge Measurements." Techniques of Water-Resources Investigations, Chapter A1, Book 3, U.S. Geological Survey, Washington, D.C., 30 p. (1967).

Boning, C.W., "Generalization of Stream Travel Rates and Dispersion Characteristics from Time-of-Travel Measurements." U.S. Geological Survey Journal of Research, 2(4), 495-499 (1974).

Brown, L.C., "Statistical Evaluation of Reaeration Prediction Equations." Journal of the Environmental Engineering Division, American Society of Civil Engineers, 100(EE5), 1051-1068 (1974).

Buchanan, T.J., and Somers, W.P., "Discharge Measurements at Gaging Stations." Techniques of Water-Resources Investigations, book 3, chapter A8, U.S. Geological Survey, Washington, D.C., 65 p. (1969).

Cadwallader, T.E., and McDonnell, A.J., "A Multivariate Analysis of Reaeration Data." Water Research, 3, 731-742 (1969).

Churchill, M.A., Buckingham, R.A., and Elmore, H.L., The Prediction of Stream Reaeration Rates. Tennessee Valley Authority, Division of Health and Safety, Chattanooga, Tennessee, 98 p. (1962).

Danckwerts, P.V., "Significance of Liquid-Film Coefficients in Gas Absorption." Industrial and Engineering Chemistry, 41(6), 1460-1467 (1951).

Dobbins, W.E., "The Nature of the Oxygen Transfer Coefficient in Aeration Systems." in Biological Treatment of Sewage and Industrial Wastes, J. McCabe and W.W. Eckenfelder, Jr., editors, Volume 1, Reinhold Publishing Company, New York, New York, pp. 141-148 (1956).

Downing, A.L., and Truesdale, G.A., "Some Factors Affecting the Rate of Solution of Oxygen in Water." Journal of Applied Chemistry, 5, 570-581 (1955).

Elmore, H.L., and West, W.F., "Effect of Water Temperature on Stream Reaeration." Journal of the Sanitary Engineering Division, American Society of Civil Engineers, 87(SA-6), 59-71 (1961).

Eloubaidy, A.F., and Plate, E.J., "Wind Shear-Turbulence and Reaeration Coefficient." Journal of the Hydraulics Division, American Society of Civil Engineers, 98(HY-1), 153-170 (1972).

Environmental Protection Agency. "Rates, Constants, and Kinetics Formulations in Surface Water Quality Modeling." Second Edition, Research and Development Series Number EPA/600/3-85/040, U.S. Environmental Protection Agency, Athens, Georgia, 455 p. (1985).

Grant, R.S. and Skavronek, S., "Comparison of Tracer Methods and Predictive Equations for Determination of Stream-Reaeration Coefficients on Three Small Streams in Wisconsin." Water Resources Investigations Report 80-19, U.S. Geological Survey, Madison, Wisconsin, 36 p. (1980).

Grant, R.S., "Reaeration Capacity of the Rock River Between Lake Koshkonong, Wisconsin, and Rockton, Illinois." Water-Resources Investigations Report 77-128, U.S. Geological Survey, Madison, Wisconsin, 38 p. (1978).

Guy, H.P., "Laboratory Theory and Methods for Sediment Analysis." Techniques of Water-Resources Investigation, Book 5, Chapter C1, U.S. Geological Survey, Washington, D.C., 58 p. (1969).

Guy, H.P. and Norman, V.W., "Field Methods for Measurement of Fluvial Sediment." Techniques of Water-Resources Investigation, Book 3, Chapter C2, U.S. Geological Survey, Washington, D.C., 59 p. (1970).

Higbie, R., "The Rate of Absorption of a Pure Gas into a Still Liquid During Short Periods of Exposure." American Institute of Chemical Engineers Transactions, 31, 265-390 (1935).

Holley, E.R., "Diffusion and Boundary Layer Concepts in Aeration Through Liquid Surfaces." Water Research, 7, 559-573 (1973).

Isaacs, W.P., and Gaudy, A.F., "Atmospheric Oxygenation in a Simulated Stream." Journal of the Sanitary Engineering Division, American Society of Civil Engineers, 94(SA2), 319-344 (1968).

Jirka, G.H. and Brutsaert, w., "Measurements of Wind Effects on Water-Side Controlled Gas Exchange in Riverine Systems." in Gas Transport at Water Surfaces, W. Brutsaert and G.H. Jirka editors, D. Reidel Publishing Company, Dordrecht, Holland, pp. 437-446 (1984).

Kehr, R.W., "Measures of Natural Oxidation in Polluted Streams: Part IV -- Effect of Sewage on Atmospheric Reaeration Rates under Streamflow Conditions." Sewage Works Journal, 10(2), 228-240 (1938).

Kilpatrick, F.A., "Automatic Sampler for Dye Tracer Studies." Water Resources Research, 8(3), 737-742 (1972).

Kilpatrick, F.A., Rathbun, R.E., Yotsukura, N., Parker, G.W., and DeLong, L.L., "Determination of Stream Reaeration Coefficients by Use of Tracers." Open-File Report 87-245, U.S. Geological Survey, Reston, Virginia, 84 p. (1987).

King, C.J., "Turbulent Liquid Phase Mass Transfer at a Free Gas-Liquid Interface." Industrial and Engineering Chemistry Fundamentals, 5(1), 1-8 (1966).

Kothandaraman, V., "Effects of Contaminants on Reaeration Rates in River Water." Water Pollution Federation Journal, 43(5), 806-817 (1973).

Kramer, G.R., "Predicting Reaeration Coefficients for Polluted Estuaries." Journal of the Environmental Engineering Division, American Society of Civil Engineers, 100(EE1), 77-92 (1974).

Krenkel, P.A. and Novotny, V., Water Quality Management. Academic Press, New York, New York, 671 p. (1980).

Krenkel, P.A. and Orlob, G.T., "Turbulent Diffusion and the Reaeration Coefficient." Journal of the Sanitary Engineering Division, American Society of Civil Engineers, 88(3), 53-83 (1962).

Krenkel, P.A., and Orlob, G.T., "Turbulent Diffusion and the Reaeration Coefficient." Transactions of the American Society of Civil Engineers, 128(III), 293-334 (1963).

Langbein, W.B., and Durum, W.H., "The Aeration Capacity of Streams." Circular Number 542, U.S. Geological Survey, Washington, D.C., 6 p. (1967).

Lau, L.Y., "Prediction Equation for Reaeration in Open-Channel Flow." Journal of the Sanitary Engineering Division, American Society of Civil Engineers, 98(SA6), 1063-1068 (1972).

Leopold, L.B., and Maddock, T., Jr., "The Hydraulic Geometry of Stream Channels and Some Physiographic Implications." Professional Paper 252, U.S. Geological Survey, Washington, D.C., 59 p. (1953).

Mancy, K.H., and Okun, D.A., "The Effects of Surface Active Agents on Aeration." Water Pollution Control Federation Journal, 37(2), 212-227 (1965).

Miller, B.A., and Wenzel, H.G., "Analysis and Simulation of Low Flow Hydraulics." Journal of the Hydraulic Engineering Division, American Society of Civil Engineers, 111(12), 1429-1446 (1985).

Miyamoto, S., "A Theory of the Rate of Solution of Gas into Liquid." Chemical Society of Japan Bulletin, 7, 8-17 (1932).

Morel-Seytoux, H.J., and Lau, D.H., Discussion of "Statistical Evaluation of Reaeration Prediction Equations." by L.C. Brown, Journal of the Environmental Engineering Division, American Society of Civil Engineers, 10(EE5), 859-861 (1975).

Negulescu, M., and Rojanski, V., "Recent Research to Determine Reaeration Coefficient." Water Research, 3(3), 189-202 (1969).

Nemerow, N.L., Scientific Stream Pollution Analysis, McGraw-Hill Book Company, New York, New York, 358 p. (1974).

Ohio Environmental Protection Agency, Determining the Reaeration Coefficient for Ohio Streams, Water Quality Planning and Assessment Section, Ohio Environmental Protection Agency, Columbus, Ohio, (1983).

O'Connor, D.J., and Dobbins, W.E., "Mechanism of Reaeration in Natural Streams." Transactions of the American Society of Civil Engineers, 123, 641-666 (1958).

Owens, M., Edwards, R.W., and Gibbs, J.W., "Some Reaeration Studies in Streams." International Journal of Air and Water Pollution, 8, 469 (1964).

Padden, T.J. and Gloyna, E.F., "Simulation of Stream Processes in a Model River." University of Texas Report Number EHE-70-23, CRWR-72, Austin, Texas, 130 p. (1971).

Parker, G.W., and Gay, F.B., "A Procedure for Estimating Reaeration Coefficients for Massachusetts Streams." Water Resources Investigations Report 86-4111, U.S. Geological Survey, Boston, Massachusetts, 34 p. (1987).

Parkhurst, J.D., and Pomeroy, R.D., "Oxygen Absorption in Streams." Journal of the Sanitary Engineering Division, American Society of Civil Engineers, 98(SA1), 101-124 (1972).

Petterssen, S., Introduction to Meteorology. McGraw-Hill Book Company, New York, New York, 327 p. (1958).

Rainwater, K.A., and Holley, E.R., "Laboratory Studies on the Hydrocarbon Gas Tracer Technique for Reaeration Measurement." Center for Research in Water Resources, Report 189, University of Texas, Austin, Texas, 143 p. (1983).

Rand, M.C., "Laboratory Studies of Sewage Effects on Atmospheric Reaeration." Water Pollution Control Federation Journal, 31(10), 1197-1212 (1959).

Rathbun, R.E., "Reaeration Coefficients of Streams - State of the Art." Journal of the Hydraulics Division, American Society of Civil Engineers, 103(HY4), 409-424 (1977).

Rathbun, R.E., "Estimating the Gas and Dye Quantities for Modified Tracer Technique Measurement of Stream Reaeration Coefficients." Water Resources Investigations Report 79-27, U.S. Geological Survey, NSTL Station, Mississippi, 42 p. (1979).

Ruhl, K.J., and Smoot, J.L., "Mean Velocity, Longitudinal Dispersion, and Reaeration Characteristics of Selected Streams in the Kentucky River Basin." Water Resources Investigations Report 87-4179, U.S. Geological Survey, Louisville, Kentucky, 61 p. (1987).

Shultz, D.J., Pankow, J.F., Tai, D.Y., Stephens, D.W., and Rathbun, R.E., "Determination, Storage, and Preservation of Low Molecular Weight Hydrocarbon Gases in Aqueous Solution." U.S. Geological Survey Journal of Research, 4(2), 247-251 (1976).

St. John, J.P., Gallagher, T.W., and Paquin P.R., "The Sensitivity of the Dissolved Oxygen Balance to Predictive Reaeration Equations." in Gas Transfer at Water Surfaces, W. Brutsaert and G.H. Jirka, editors, D. Reidel Publishing Company, Dordrecht, Holland, pp. 557-588 (1984).

Streeter, H.W., and Phelps, E.B., "A Study of the Pollution and Natural Purification of the Ohio River." Public Health Bulletin 146, U.S. Public Health Service, 75 p. (1925).

Thackston, E.L., and Krenkel, P.A., "Reaeration Prediction in Natural Streams." Journal of the Sanitary Engineering Division, American Society of Civil Engineers, 95(SA1), 65-94 (1969).

Tsivoglou, E.C., "Tracer Measurement of Stream Reaeration." Federal Water Pollution Control Administration, U.S. Department of the Interior, Washington, D.C., 86 p. (1967).

Tsivoglou, E.C., Cohen, J.B., Shearer, S.D., and Godsil, P.J., "Tracer Measurement of Stream Reaeration: Part II -- Field Studies." Water Pollution Control Federation Journal, 40(2), 285-305 (1968).

Tsivoglou, E.C., and Neal, L.A., "Tracer Measurement of Reaeration: Part III -- Predicting the Reaeration Capacity of Inland Streams." Water Pollution Control Federation Journal, 48(12), 2669-2689 (1976).

Tsivoglou, E.C., and Wallace, J.R., "Characterization of Stream Reaeration Capacity." Report USEPA-R3-72-012, U.S. Environmental Protection Agency, Washington, D.C., Washington, D.C., 317 p. (1972).

Whitman, W.G., "Two-Film Theory of Gas Absorption." Chemical and Metallurgical Engineering, 29, 146 (1923).

Wilson, G.T., and Macleod, N., "A Critical Appraisal of Empirical Equations and Models for the Prediction of Reaeration of Deoxygenated Water." Water Research, 8(6), 341-366 (1974).

Yotsukura, N., Stedfast, D.A., Draper, R.E., and Brutsaert, W.H., "An Assessment of Steady-State Propane-Gas Tracer Method for Reaeration Coefficients -- Cowaselon Creek, New York." Water Resources Investigations Report 83-4183, U.S. Geological Survey, Reston, Virginia, 88 p. (1983).

Yotsukura, N., Stedfast, D.A., Jirka, G.H., "Assessment of a Steady-State Propane-Gas Tracer Method for Determining Reaeration Coefficients -- Chenango River, New York." Water Resources Investigations Report 84-4368, U.S. Geological Survey, Reston, Virginia, 69 p. (1984).

Zogorski, J.S., and Faust, S.D., "Atmospheric Reaeration Capacity of Streams: Part I -- Critical Review of Methods Available to Measure and to Calculate the Atmospheric Reaeration Rate Constant." Environmental Letters, 4(1), 35-39 (1973).

ADDITIONAL REFERENCES

Bauer, D.P., Rathbun, R.E., and Lowham, H.W., "Traveltime, Unit-Concentration, Longitudinal-Dispersion, and Reaeration Characteristics of Upstream Reaches of the Yampa and Little Snake Rivers, Colorado and Wyoming." Water-Resources Investigations Report 78-122, U.S. Geological Survey, Reston, Virginia, 66 p. (1979).

Bencala, K.E., and Walters, R.A., "Simulation of Solute Transport in a Mountain Pool-and-Riffle Stream--a Transient Storage Model." Water Resources Research, 19(3), 718-724 (1983).

Boyle, W.C., Berthouex, P.M., and Rooney, T.C., "Pitfalls in Parameter Estimation for Oxygen Transfer Data." Journal of the Environmental Engineering Division, American Society of Civil Engineers, 100(EE2), 391-408 (1974).

Churchill, M.A., Elmore, H.L., and Buckingham, R.A., "Prediction of Stream Reaeration Rates." American Society of Civil Engineers Transactions, 129, 24-26 (1964).

Cobb, E.D., "Constant-Rate-Injection Equipment for Dye-Dilution Discharge Measurements." in Selected Techniques in Water-Resources Investigations, 1966-67, Water-Supply Paper 1892, U.S. Geological Survey, Washington, D.C., pp. 15-23 (1967).

Crawford, C.G., "Measurement of Reaeration in the Wabash River near Lafayette and Terre Haute, Indiana, by the Modified Tracer Technique" in Selected Papers in the Hydrologic Sciences, Water Supply Paper 2270, pp. 69-81 (1985).

Dobbins, W.E., "BOD and Oxygen Relationships in Streams." Journal of the Sanitary Engineering Division, American Society of Civil Engineers, 91(SA-5), 49-55 (1965).

Fischer, H.B., "Longitudinal Dispersion and Turbulent Mixing in Open-Channel Flow." Annual Review of Fluid Mechanics, Volume 5, Annual Review Inc., Palo Alto, California, pp.59-78 (1973).

Foree, E.G., "Reaeration and Velocity Prediction for Small Streams." Journal of the Environmental Engineering Division, American Society of Civil Engineers, 102(EE5), 937-952 (1976).

Foree, E.G., "Low-Flow Reaeration and Velocity Characteristics of Kentucky Streams." Technical Report Number UKY-TR99-76-CE27, College of Engineering, University of Kentucky, Lexington, Kentucky, 81 p. (1976).

Gameson, A.L.H., Truesdale, G.A., and Downing, A.L., "Reaeration Studies in a Lakeland Beck." Journal of the Institution of Water Engineers, 9(7), 571-594 (1955).

Grant, R.S., "Reaeration-Coefficient Measurements of 10 Small Streams in Wisconsin Using Radioactive Tracers with a Section on the Energy-Dissipation Model." Water-Resources Investigations Report 76-96, U.S. Geological Survey, Madison, Wisconsin, 50 p. (1976).

Holley, E.R. and Yotsukura, N., "Field Techniques for Reaeration Measurement in Rivers." in Gas Transfer at Water Surfaces, W. Brutsaert and G.H. Jirka, editors, D. Reidel Publishing Company, Dordrecht, Holland, pp. 381-401 (1984).

Hren, J., "Determination of Reaeration Coefficients for Ohio Streams." Water Resources Investigations Report 84-4139, U.S. Geological Survey, Columbus, Ohio, 12 p. (1984).

Hubbard, E.F., Kilpatrick, F.A., Martens, L.A., and Wilson, J.F., Jr., "Measurement of Time of Travel and Dispersion in Streams by Dye Tracing." Techniques of Water-Resources Investigations, Book 3, Chapter A9, U.S. Geological Survey, Reston, Virginia, 44 p. (1982).

Kilpatrick, F.A., "Dosage Requirements for Slug Injections of Rhodamine BA and WT Dyes." in Geological Survey Research, 1970, Professional Paper 700-B, U.S. Geological Survey, Washington, D.C., pp.250-253 (1970).

Kilpatrick, F.A., and Cobb, E.D., "Measurement of Discharge Using Tracers." Open-File Report 84-136, U.S. Geological Survey, Reston, Virginia, 74 p. (1984).

McAuliffe, C., "Solubility in Water of Paraffin, Cycloparaffin, Olefin, Acetylene, Cycloolefin, and Aromatic Hydrocarbons." Journal of Physical Chemistry, 70(4), 1267-1275 (1966).

Melcher, N.B., and Ruhl, K.J., "Streamflow and Basin Characteristics at Selected Sites in Kentucky." Open-File Report 84-704, U.S. Geological Survey, Louisville, Kentucky, 80 p. (1984).

Neal, L.A., "Reaeration Measurement in Swamp Streams: Radiotracer Case Studies." in Gas Transfer at Water Surfaces, W. Brutsaert and G.H. Jirka, editors, D. Reidel Publishing Company, Dordrecht, Holland, pp. 381-401 (1984).

Quinones, F., Kiesler, J., and Macy, J., "Flow Duration at Selected Stream-Sites in Kentucky." Open-File Report 80-1221, U.S. Geological Survey, Louisville, Kentucky, 143 p. (1980).

Rathbun, R.E., Shultz, D.J., and Stephens, D.W., "Preliminary Experiments with a Modified Tracer Technique for Measuring Stream Reaeration Coefficients." Open-File Report 75-256, U.S. Geological Survey, Washington, D.C., 36 p. (1975).

Rathbun, R.E., Stephens, D.W., Shultz, D.J., and Tai, D.Y., "Laboratory Studies of Gas Tracers for Reaeration." Journal of the Environmental Engineering Division, American Society of Civil Engineers, 104(E2), 215-229 (1978).

Rathbun, R.E., and Grant, R.S., "Comparison of the Radioactive and Modified Techniques for Measurement of Stream Reaeration Coefficients." Water-Resources Investigations Report 78-68, NSTL Station, Mississippi, 57 p. (1978).

Smart, P.L., and Laidlaw, I.M.S., "An Evaluation of Some Fluorescent Dyes for Water Tracing." Water Resources Research, 13(1), 15-33 (1977).

Smoot, J.L., "Effect of Streamflow Conditions on Gas-Transfer Coefficients." in Hydraulic Engineering--Proceedings of the 1987 National Conference on Hydraulic Engineering, R.M. Ragan, editor, American Society of Civil Engineers, New York, New York, pp. 980-985 (1987).

Streeter, H.W., Wright, C.T., and Kehr, R.W., "An Experimental Study of Atmospheric Reaeration Under Stream-Flow Conditions--Part III of Measures of Natural Oxidation in Polluted Streams." Sewage Works Journal, 8(2), 282-316 (1936).

Sullivan, John N., "Low-Flow Characteristics of Kentucky Streams, 1984." Open- File Report 84-705, U.S. Geological Survey, Louisville, Kentucky, 1 p. (1984)

Tsivoglou, E.C., Discussion of "Laboratory Studies of Gas Tracers for Reaeration." by R.E. Rathbun, D.W. Stephens, D.J. Shultz, and D.Y. Tai. Journal of the Environmental Engineering Division, American Society of Civil Engineers, 105(E2), 426-428 (1979).

Tsivoglou, E.C., O'Connell, R.L., Walter, C.M., Godsil, P.J., and Logsdon, G.S., "Tracer Measurements of Atmospheric Reaeration: Part I -- Laboratory Studies." Water Pollution Control Federation Journal, 37(1), 1343-1362 (1965).

Velz, C.J., Applied Stream Sanitation. second edition:, John Wiley & Sons, New York, New York, 800 p. (1984).

Ware, R.W., and Foree, E.G., "Reaeration Characteristics of Low Level In-Channel Dams and Waterfalls in Kentucky Streams." Technical Report UKY-TR98-76-CE25, University of Kentucky, College of Engineering, Lexington, Kentucky, 19 p. (1976).

Wilcock, R.J., "Reaeration Studies on Some New Zealand Rivers Using Methyl Chloride as a Gas Tracer." in Gas Transfer at Water Surfaces, W. Brutsaert and G.H. Jirka, editors, D. Reidel Publishing Company, Dordrecht, Holland, pp. 413-420 (1984).

Wilson, J.F., Jr., Cobb, E.D., and Kilpatrick, F.A., "Fluorometric Procedures for Dye Tracing." Open-File Report 84-234, U.S. Geological Survey, Reston, Virginia. 53 p. (1984).

Witherspoon, P.A., and Saraf, U.N., "Diffusion of Methane, Ethane, Propane, and n-Butane in Water From 25 to 43 Degrees." The Journal of Physical Chemistry, 69(11), 3752-3755 (1965).

Yotsukura, N., and Sayre, W.W., "Transverse Mixing in Natural Channels." Water Resources Research, 12(4), 695-704 (1976).

APPENDICES

APPENDIX A
ANALYTICAL METHOD FOR DETERMINATION OF PROPANE IN WATER

Propane, Total Purgeable (ug/L)
Gas Chromatographic/Purge and Trap Technique

Reference: Shultz and Others (1976)

1. APPLICATION

This method is suitable for the determination of purgeable propane in waters or water-sediment mixtures generally containing between 0.1 and 100 ug/L. Higher concentrations may be determined by analyzing a smaller aliquot of the sample.

2. SUMMARY OF METHOD

Ten milliliters of a formalin-preserved sample are injected into a stripping chamber and sparged with nitrogen. The effluent gas stream is dried and passed through an alumina trap at -95 degrees Celsius where propane is isolated. The trap is heated to expel the adsorbed gas which is analyzed by gas chromatography using a flame ionization detector.

3. INTERFERENCES

No interferences have been observed. However, volatile compounds which have a retention time similar to propane on the analytical column used can be expected to interfere.

4. APPARATUS

- 4.1 Adsorption Tube: Pyrex tubing (1/4 inch OD) formed into a U-tube approximately 8" long by 2" wide. The tube is charged with 5 grams of activated alumina which is held in place with plugs of glass wool.
- 4.2 Cold Bath: A Dewar flask large enough to accommodate the lower half of the adsorption trap and maintained a -80 to -100 degrees Celsius with either dry ice/acetone or a refrigerant probe such as the Neslab CC-100, or equivalent.
- 4.3 Compressed Gases: Cylinders of hydrogen, nitrogen, and compressed air. Follow the recommendation of the gas chromatograph manufacturer to select the grade of each gas.
- 4.4 Drying Tubes: Pyrex tubing (1/2 inch OD) cut to 8-inch lengths. The tubes are filled with Drierite which is held in place with plugs of glass wool or cotton.
- 4.5 Hot Bath: A heating mantle for a 1-L round bottom flask filled with sand and powered by a variable voltage transformer. The voltage is adjusted to maintain the sand at approximately 130 degree Celsius.
- 4.6 Gas Chromatograph: Tracor 560, or equivalent, equipped with a 6' x 1/4" glass column packed with Porapak N, a flame ionization detector, a gas sampling valve, a digital integrator, and capable of operating isothermally at 90 degrees Celsius. Use nitrogen for the carrier gas.

- 4.7 Gas Sampling Valve: Six port valve, Valco V-6-HPa, or equivalent.
- 4.8 Sample Vial: Glass (40 mL), screw-cap, fitted with a teflon-lined septum. Pierce Cat. No. 13075, or equivalent.
- 4.9 Stripping Chamber:
- 4.10 Syringes: Two syringes, 30 mL and 5 mL, glass, Luer-Lock, equipped with stopcocks (Becton-Dickinson #3152, or equivalent).
- 4.11 Syringe Needles: 19 gauge, 3-inch long, to fit 4.10 syringes.
- 4.12 Syringes, Gas-Tight: Gas-tight syringes of 1.0, 2.5, 10, and 50 mL capacities, Hamilton, or equivalent, used for delivery of calibration gas and equipped preferably with sideport needles.
- 4.13 Teflon Tubing: Teflon tubing (1/8 inch OD) used for the connecting lines.
- 4.14 Timer: Stopwatch capable of reading to the nearest second, or equivalent.

5. REAGENTS

- 5.1 Alumina: Neutral aluminum oxide, activity grade I, Woelm.
- 5.2 Calibration Gas: A Certified gas mixture containing 10 parts per million of propane in nitrogen. The regulator valve must be equipped with a stainless steel diaphragm. Equip the outlet from the regulator with an injection septum to facilitate withdrawal of aliquots of calibration gas with a gas-tight syringe.
- 5.3 Drying Agent: Indicating Drierite, 8-mesh. Anhydrous magnesium perchlorate (granular) is also suitable.
- 5.4 Porapak N: Waters Associates, or equivalent. Porapak Q and QS may also be used.

6. PROCEDURE

Samples should be collected in vials (4.8) containing one mL of formalin as a preservative and in a manner that precludes headspace formation. Samples need not be refrigerated since formalin prevents bacterial decomposition for at least three weeks, and probably longer. Rapid loss of propane will occur if the preservative is omitted.

- 6.1 Adjust the flow of hydrogen and air to the flame ionization detector to achieve a linear response over the desired concentration range.
- 6.2 Set the flow of nitrogen through the path encompassing the stripping chamber, the drying tube, and the adsorption tube to 30 to 35 mL/min. This is conveniently measured at the outlet port of the gas sampling valve (see Fig. 2).
- 6.3 Place the adsorption tube in the cold bath and set the gas sampling valve.
- 6.4 Calibration Procedure
 - 6.4.1 Inject an aliquot of calibration gas mixture into the stripping chamber using a gas-tight syringe.

- 6.4.2 Start the timer and allow 12 minutes for complete adsorption of propane by the alumina trap.
NOTE: The minimum time required to completely strip the gases depends upon the volume of the stripping line (stripping chamber, drying tube, adsorption tube, and connecting lines) and the flow through it. This parameter must be determined experimentally and should be re-established when any changes are made in the stripping line.
- 6.4.3 Turn the gas sampling valve to the position that conducts the flow from the adsorption tube into the analytical column of the gas chromatograph. Immediately place the adsorption tube in the hot bath and begin digital integration. Record integrated peak areas.
- 6.4.4 Repeat steps 6.4.1 to 6.4.3 for as many other aliquots of calibration gas mixture as are necessary to cover the expected range of the samples.
- 6.5 Sample Analysis
- 6.5.1 Open a sample vial and fill a 30 mL glass syringe by closing the stopcock and pouring the sample gently into the barrel. Do not attempt to fill the syringe by suction.
- 6.5.2 Introduce 10 mL of sample into the stripping chamber through the injection port.
- 6.5.3 Start the timer and allow the sample to be stripped for 12 minutes (see note in 6.4.2).
- 6.5.4 Turn the gas sampling valve to the position that conducts the flow from the adsorption tube into the analytical column of the gas chromatograph. Immediately place the adsorption tube in the hot bath and begin digital integration. Record integrated peak areas.
- 6.5.5 Drain the sample from the stripping chamber while gas chromatographic analysis proceeds.

7. CALCULATIONS

- 7.1 Use the data from step 6.4.4, together with the known concentrations of the components in the calibration gas, to prepare a graph of integrated peak area vs amount of component (in nanograms) injected into the stripping chamber.
- 7.2 Use the integrated peak area of an identified sample peak (sec. 6.5.4) to determine the amount of component present by referring to the graph obtained in 7.1.
- 7.3 Calculate the concentration of the component in the original water sample from the equation:

$$\text{Concentration (ug/L)} = A / V$$

where A = the amount of component determined in 7.2, expressed in nanograms.

and V = the volume of sample injected into the stripping chamber, expressed in milliliters.

8. REPORT

Report concentrations of purgeable propane as follows: concentrations below 0.05 ug/L as 0.05 ug/L; 0.05 ug/L and above, two significant figures.

9. PRECISION

Solutions of propane were prepared in deionized water and stored in sample vials (see 4.8) containing one milliliter of formalin as preservative. About ten replicates were prepared at each concentration level and the levels were chosen to cover the concentration range of the method. All of the samples were analyzed within 3 weeks of preparation.

The following table summarizes the precision (as measured by the standard deviation,) obtained by a single operator and includes the precision of (1) the analytical methodology and (2) the sample preparation technique.

PROPANE CONCENTRATION (ug/L)	S.D. ¹ (ug/L)	NUMBER ²	C.V. ³ (percent)
0.099	.004	(7)	4.0
0.257	.015	(12)	5.8
2.52	.05	(11)	2.0
12.9	.4	(12)	3.1
24.5	.4	(12)	1.6
53.5	.9	(12)	1.7
110	2.6	(11)	2.4
171	4.0	(11)	2.3

¹Standard deviation of analyses.

²Number of analyses performed.

³Coefficient of variation of analyses.

APPENDIX B
TIME-CONCENTRATION DATA FOR DYE AND PROPANE FROM FIELD MEASUREMENTS

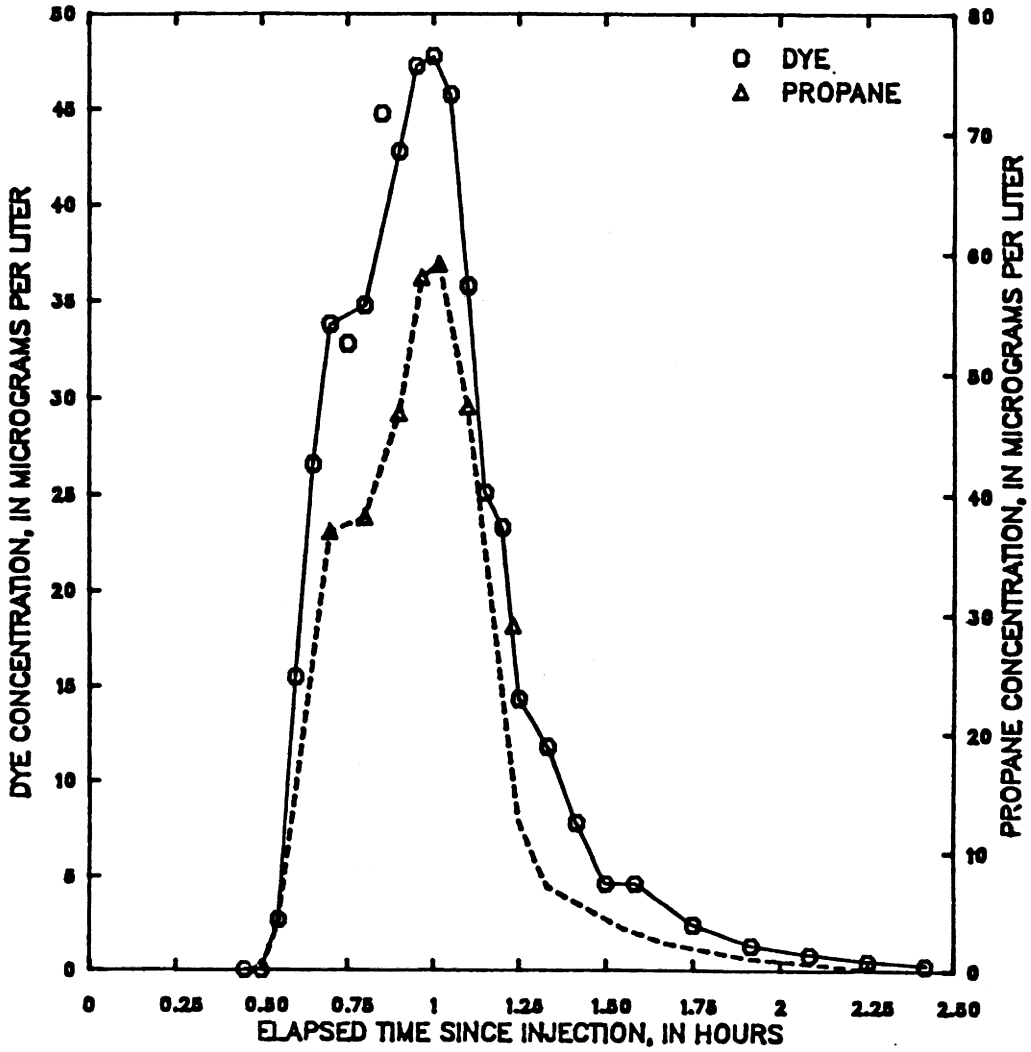


Figure 47 -- Dye and propane concentration from hydrocarbon gas tracer measurements made on Middle Fork Beargrass Creek, upstream end of reach A (upstream end of reach C), April 18, 1985 tracer injection

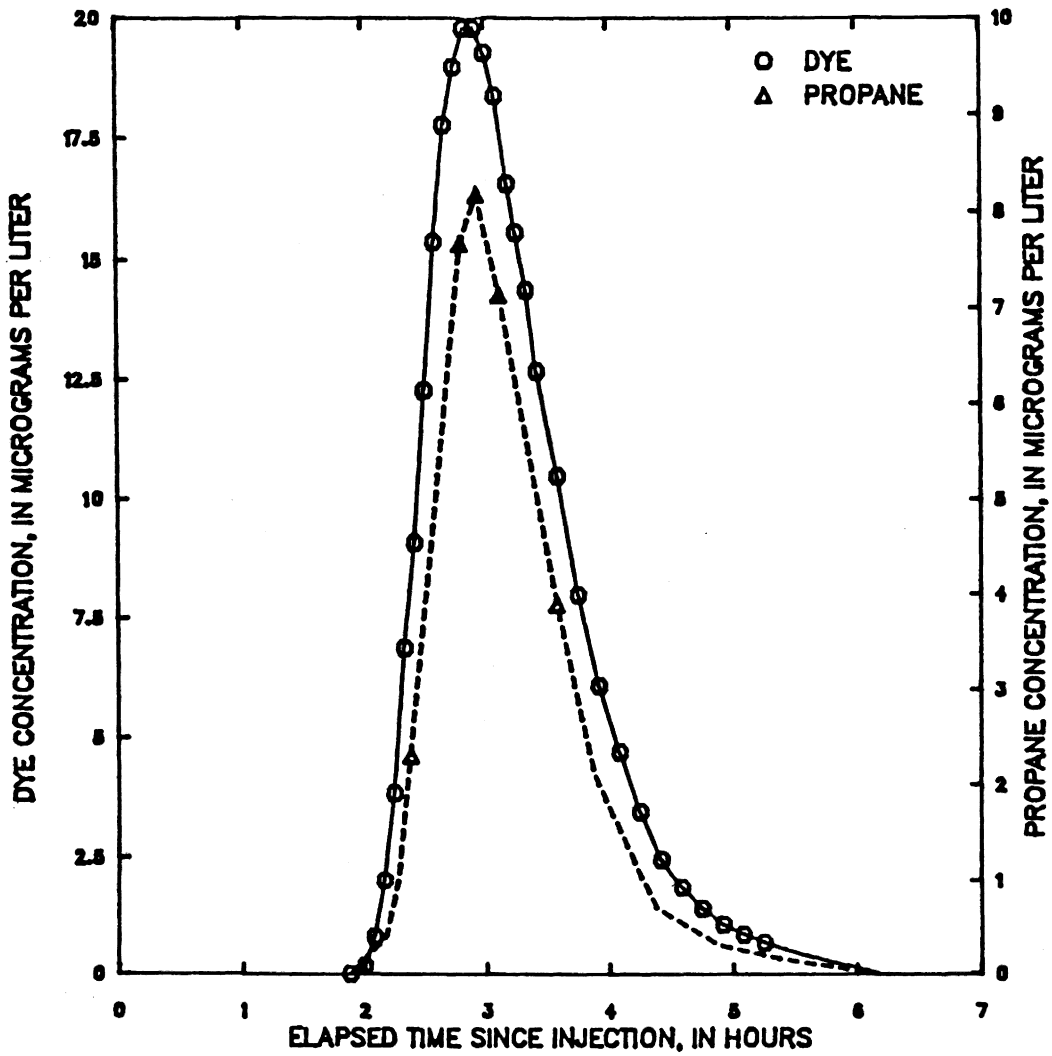


Figure 48 -- Dye and propane concentration from hydrocarbon gas tracer measurements made on Middle Fork Beargrass Creek, downstream end of reach A (upstream end of reach B), April 18, 1985 tracer injection

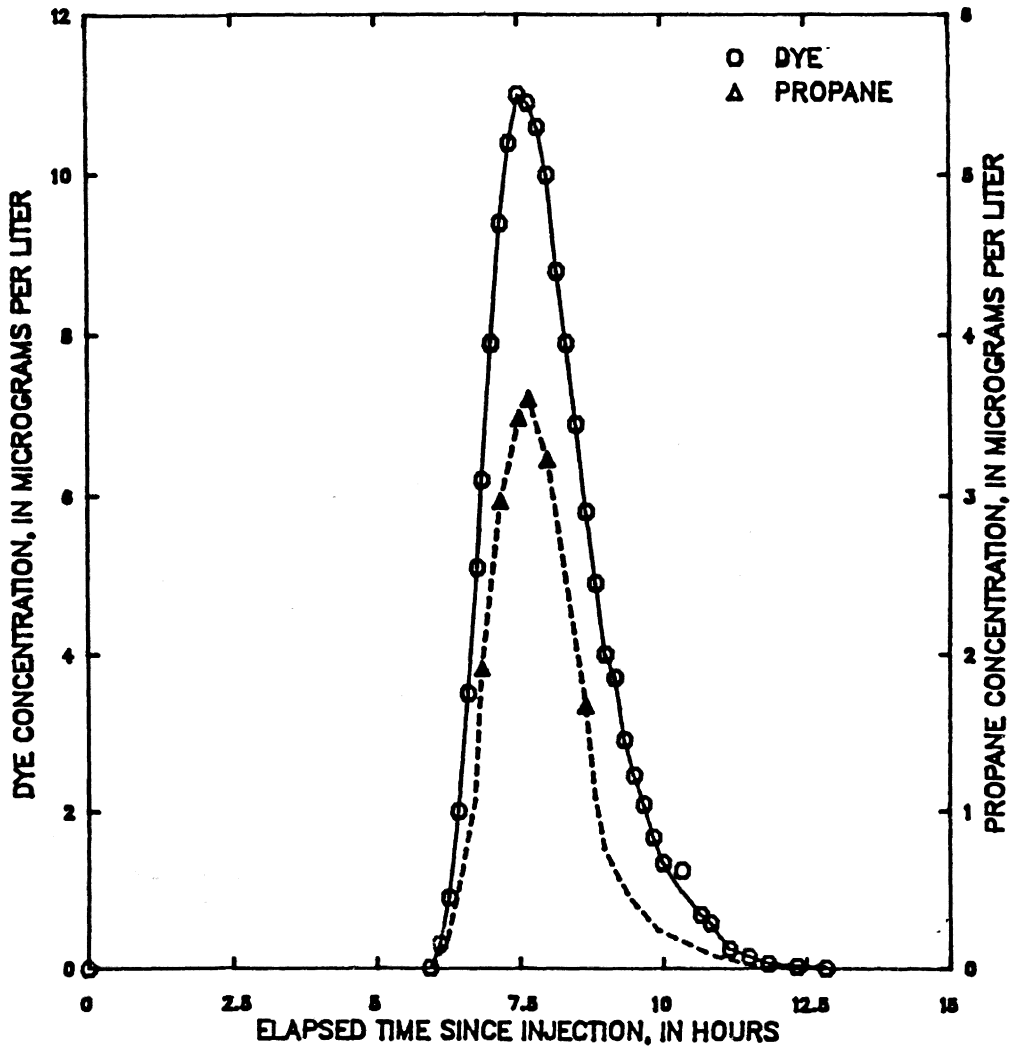


Figure 49 -- Dye and propane concentration from hydrocarbon gas tracer measurements made on Middle Fork Beargrass Creek, downstream end of reach B (downstream end of reach C), April 18, 1985 tracer injection

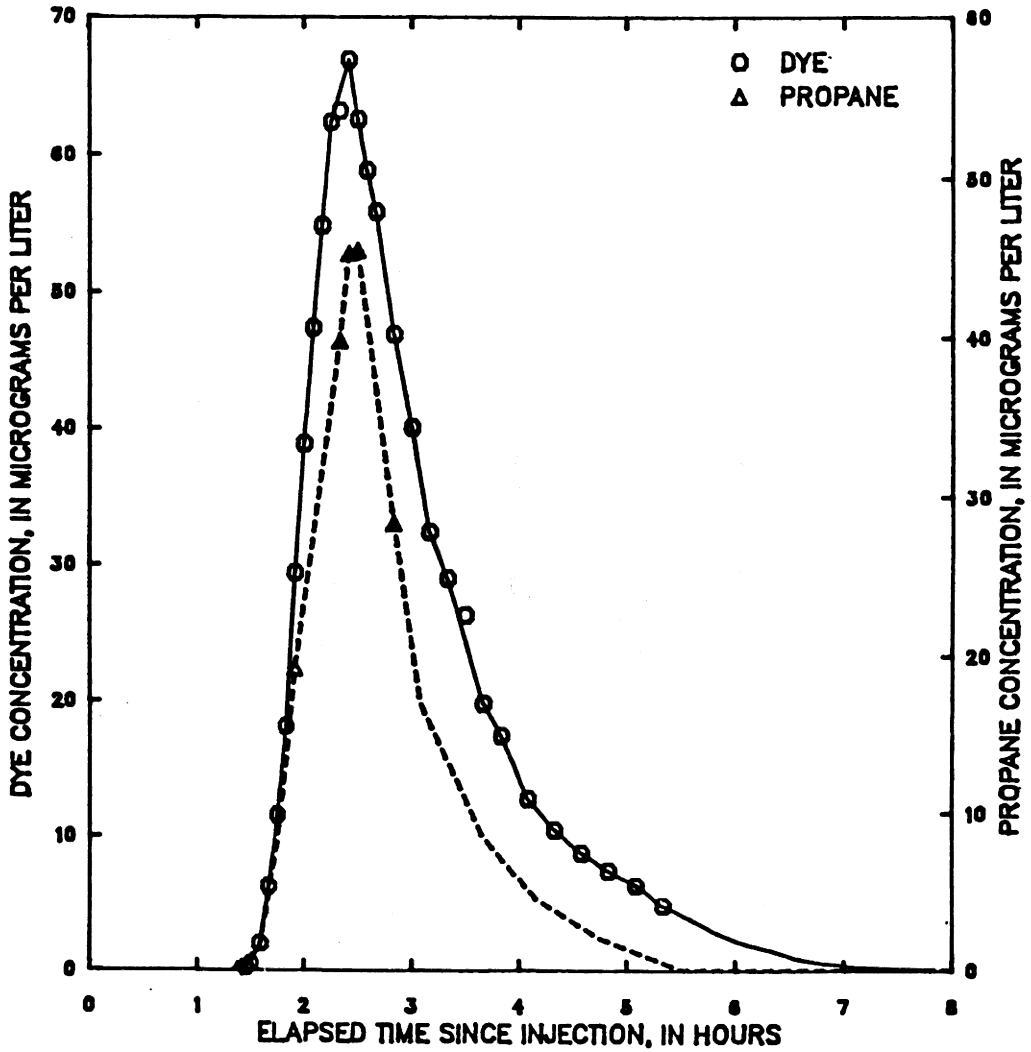


Figure 50 -- Dye and propane concentration from hydrocarbon gas tracer measurements made on Middle Fork Beargrass Creek, upstream end of reach A (upstream end of reach C), May 8, 1985 tracer injection

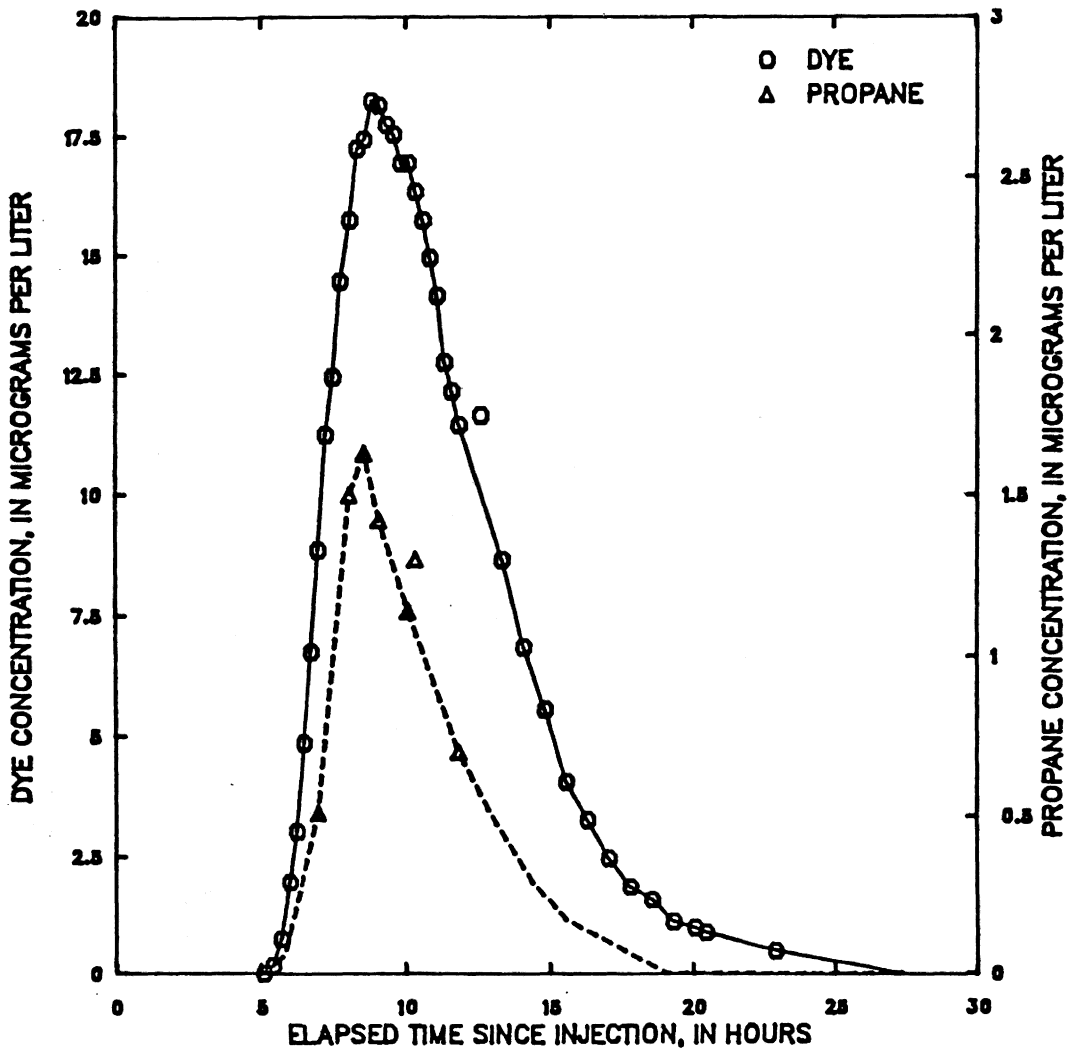


Figure 51 -- Dye and propane concentration from hydrocarbon gas tracer measurements made on Middle Fork Beargrass Creek, downstream end of reach A (upstream end of reach B), May 8, 1985 tracer injection

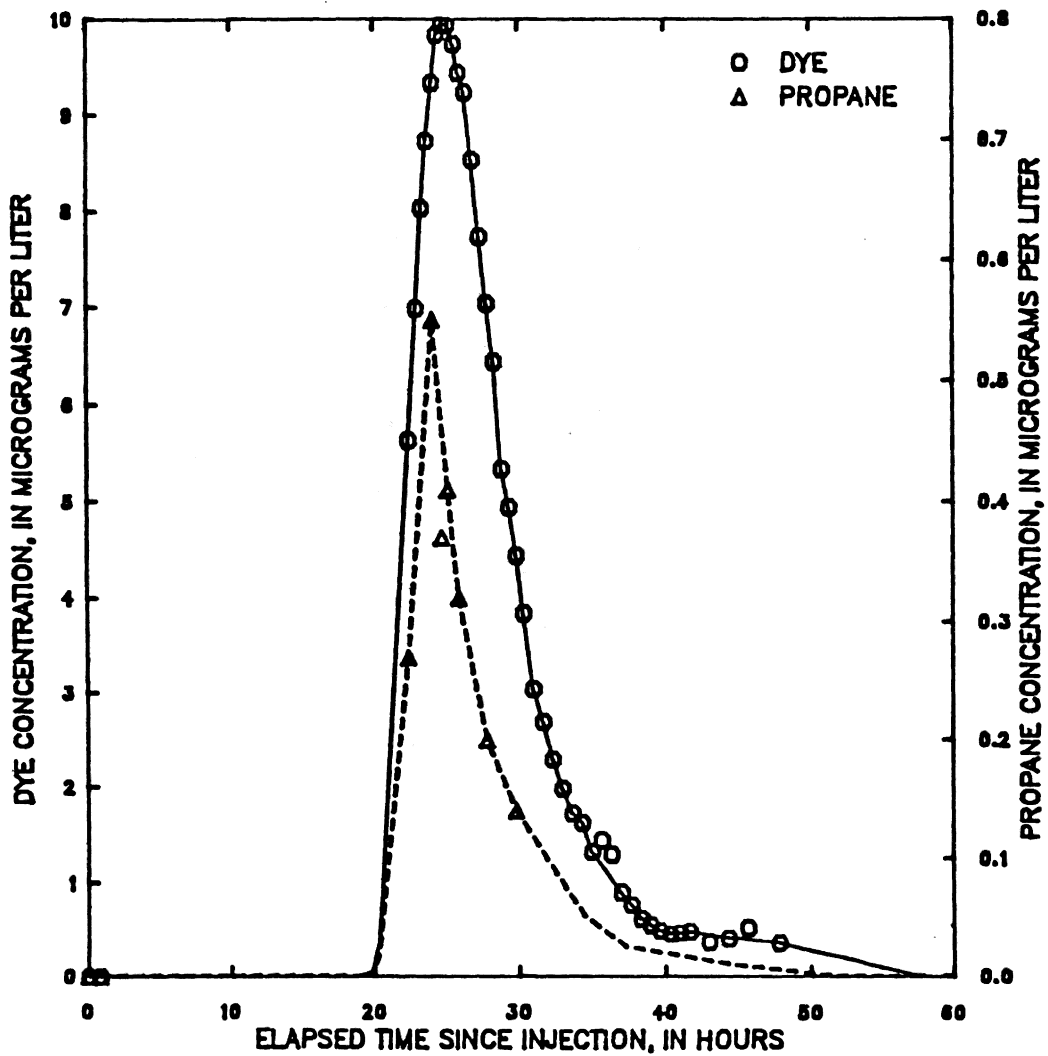


Figure 52 -- Dye and propane concentration from hydrocarbon gas tracer measurements made on Middle Fork Beargrass Creek, downstream end of reach B (downstream end of reach C), May 8, 1985 tracer injection

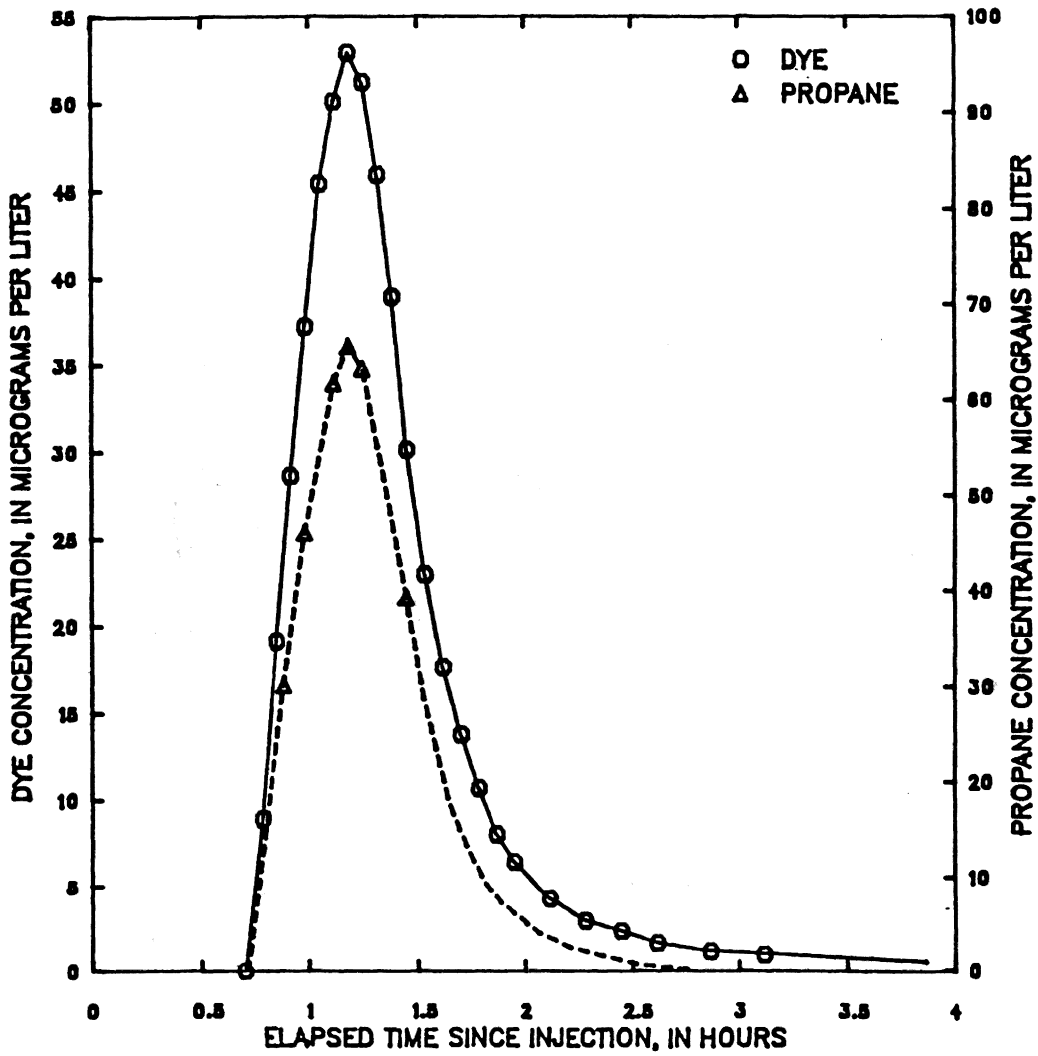


Figure 53 -- Dye and propane concentration from hydrocarbon gas tracer measurements made on Middle Fork Beargrass Creek, upstream end of reach A (upstream end of reach C), May 16, 1985 tracer injection

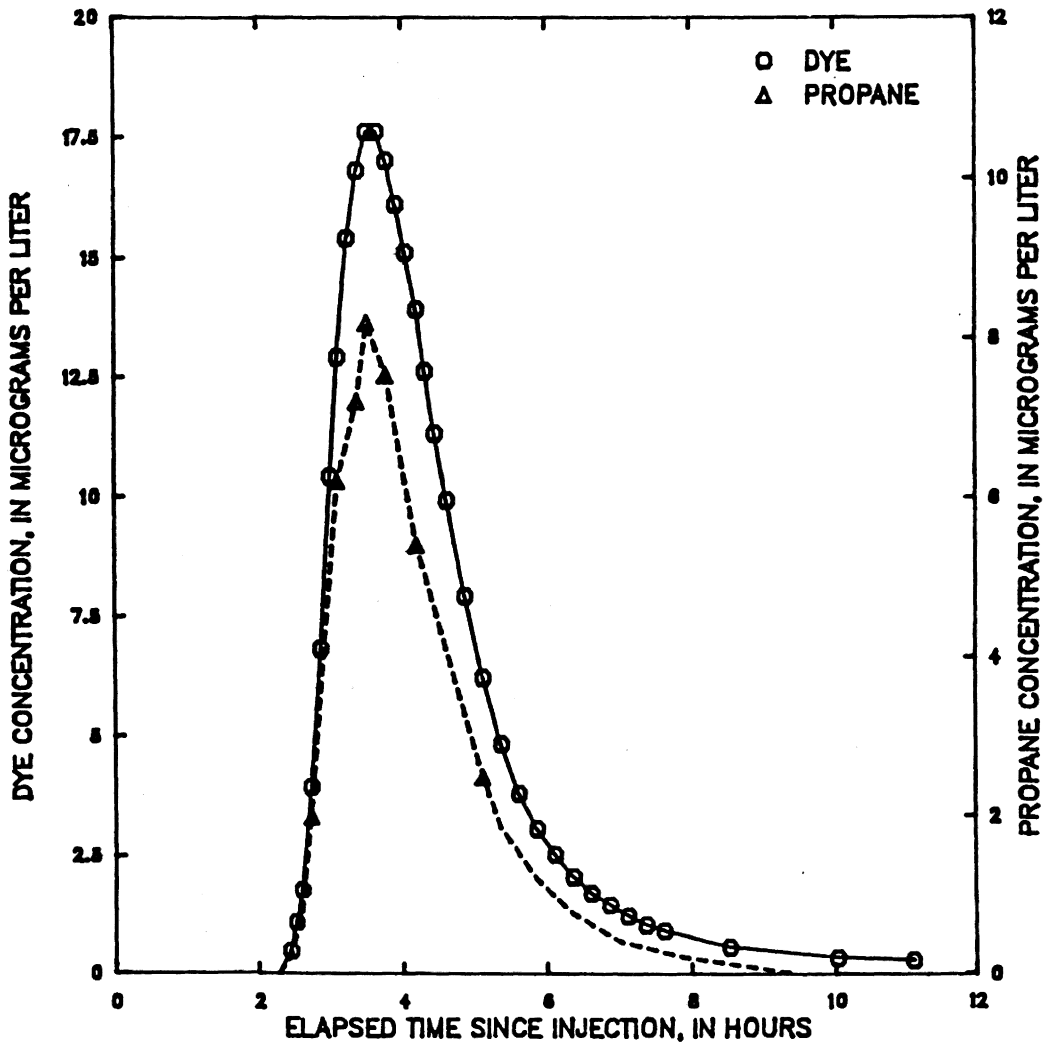


Figure 54 -- Dye and propane concentration from hydrocarbon gas tracer measurements made on Middle Fork Beargrass Creek, downstream end of reach A (upstream end of reach B), May 16, 1985 tracer injection

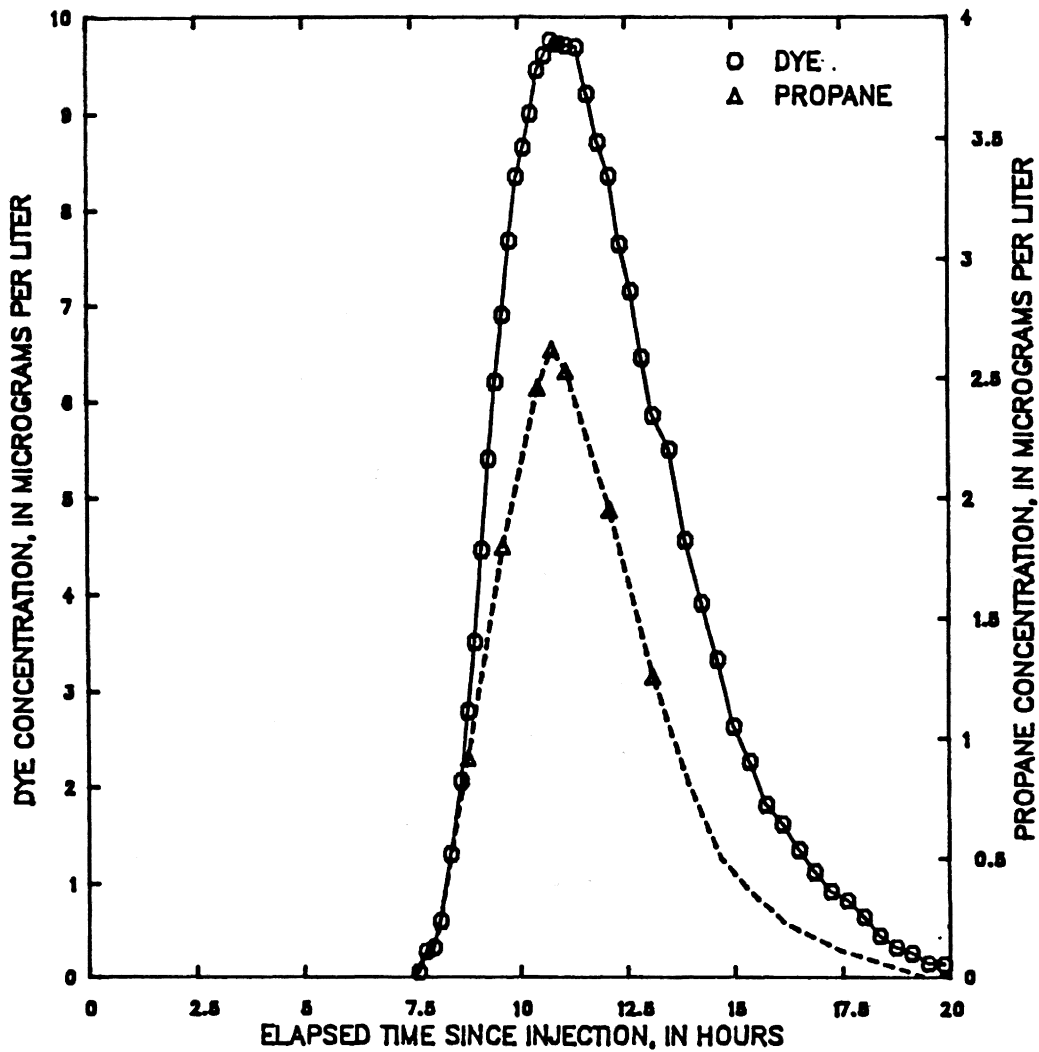


Figure 55 -- Dye and propane concentration from hydrocarbon gas tracer measurements made on Middle Fork Beargrass Creek, downstream end of reach B (downstream end of reach C), May 16, 1985 tracer injection

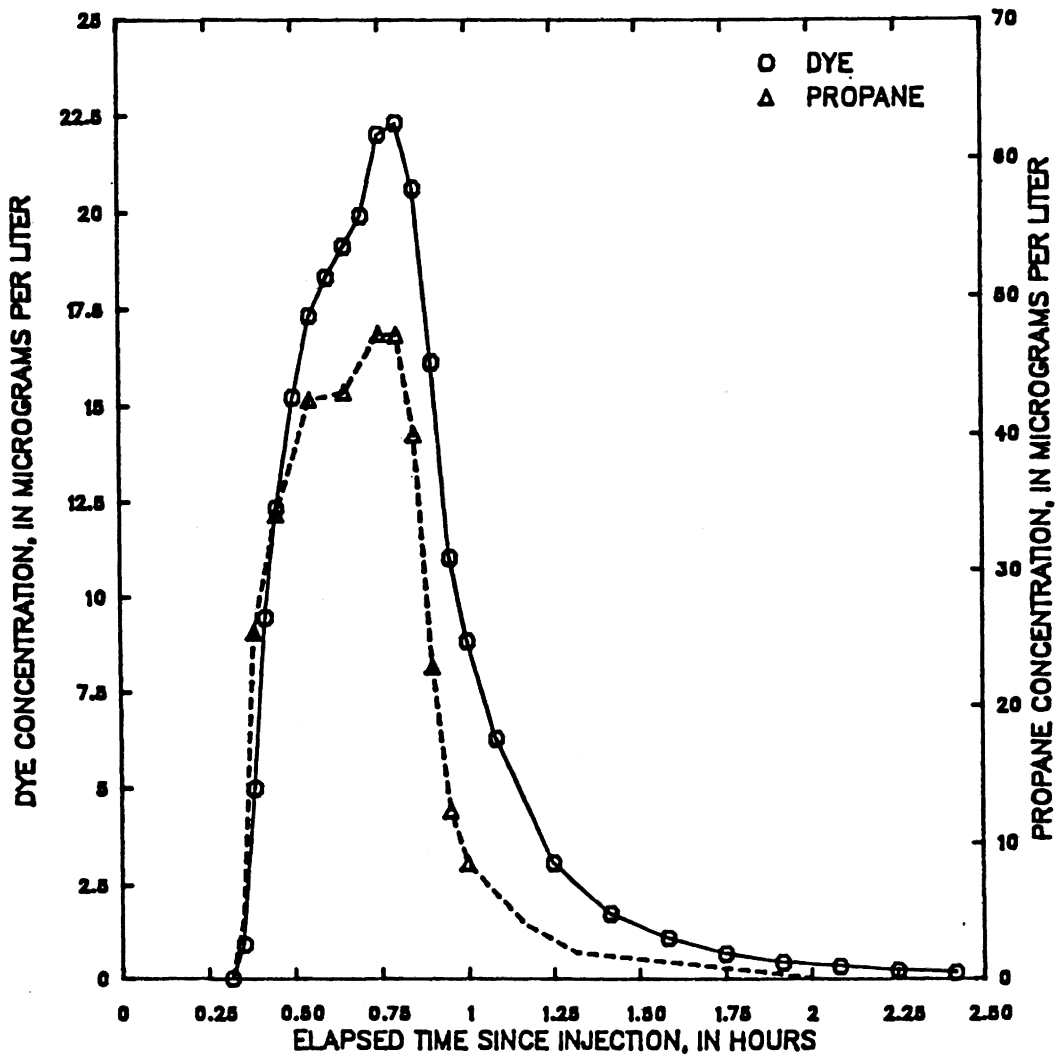


Figure 56 -- Dye and propane concentration from hydrocarbon gas tracer measurements made on Middle Fork Beargrass Creek, upstream end of reach A (upstream end of reach C), May 24, 1985 tracer injection

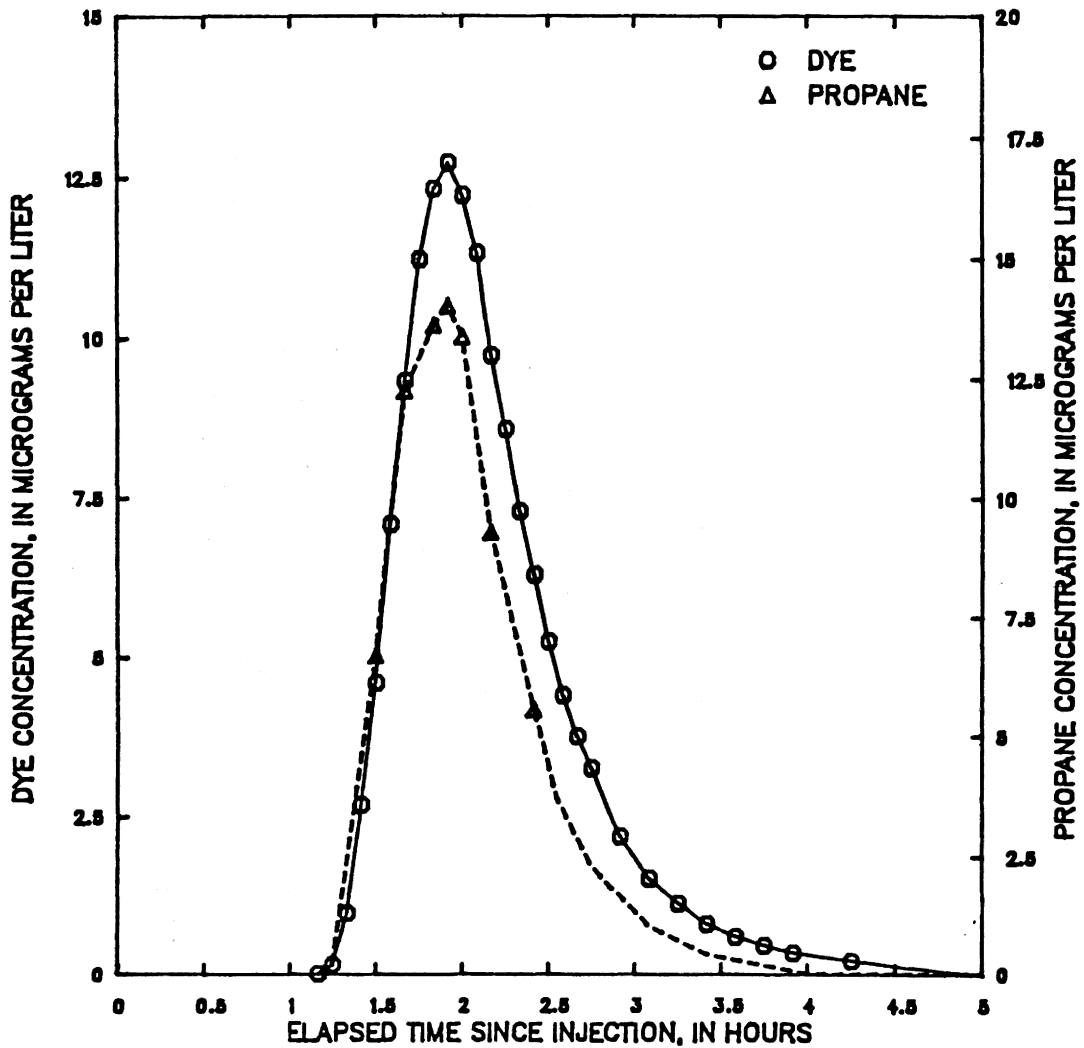


Figure 57 -- Dye and propane concentration from hydrocarbon gas tracer measurements made on Middle Fork Beargrass Creek, downstream end of reach A (upstream end of reach B), May 24, 1985 tracer injection

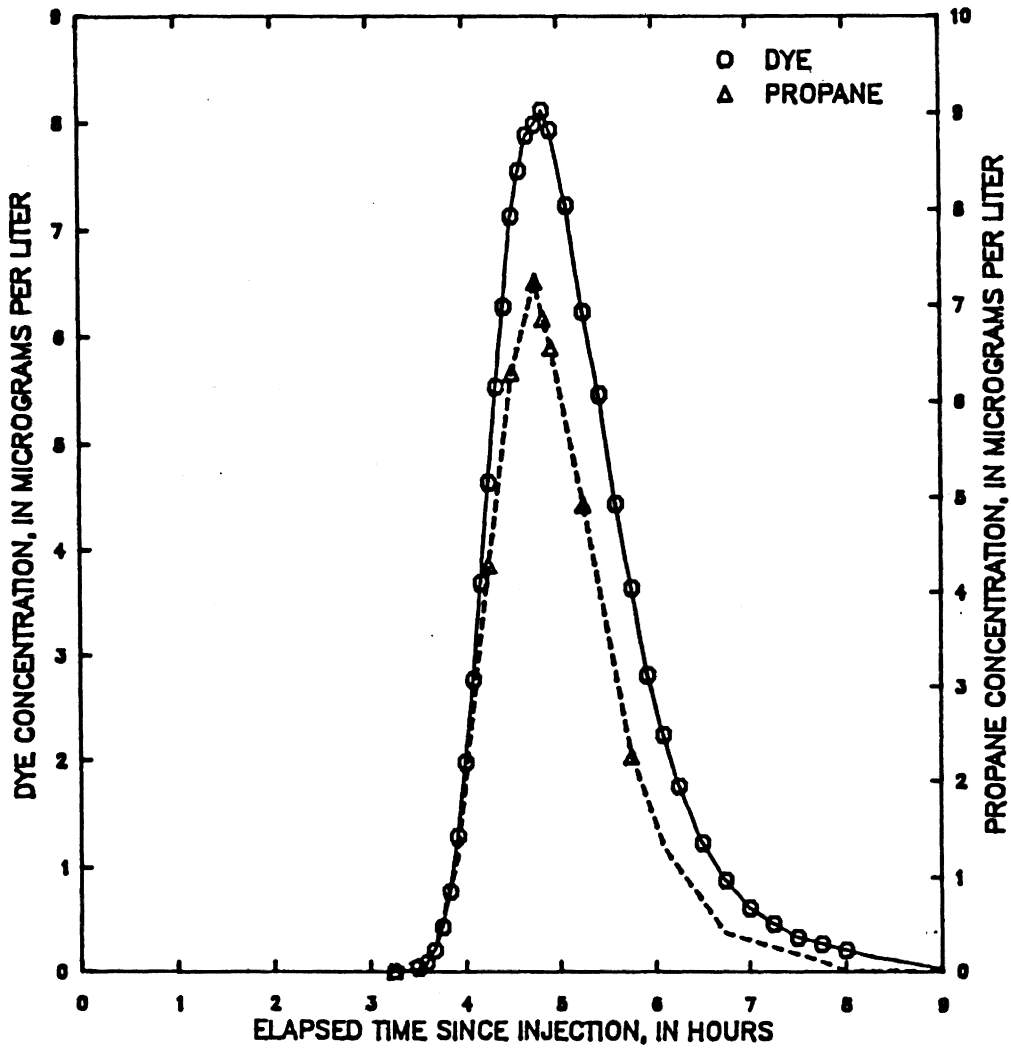


Figure 58 -- Dye and propane concentration from hydrocarbon gas tracer measurements made on Middle Fork Beargrass Creek, downstream end of reach B (downstream end of reach C), May 24, 1985 tracer injection

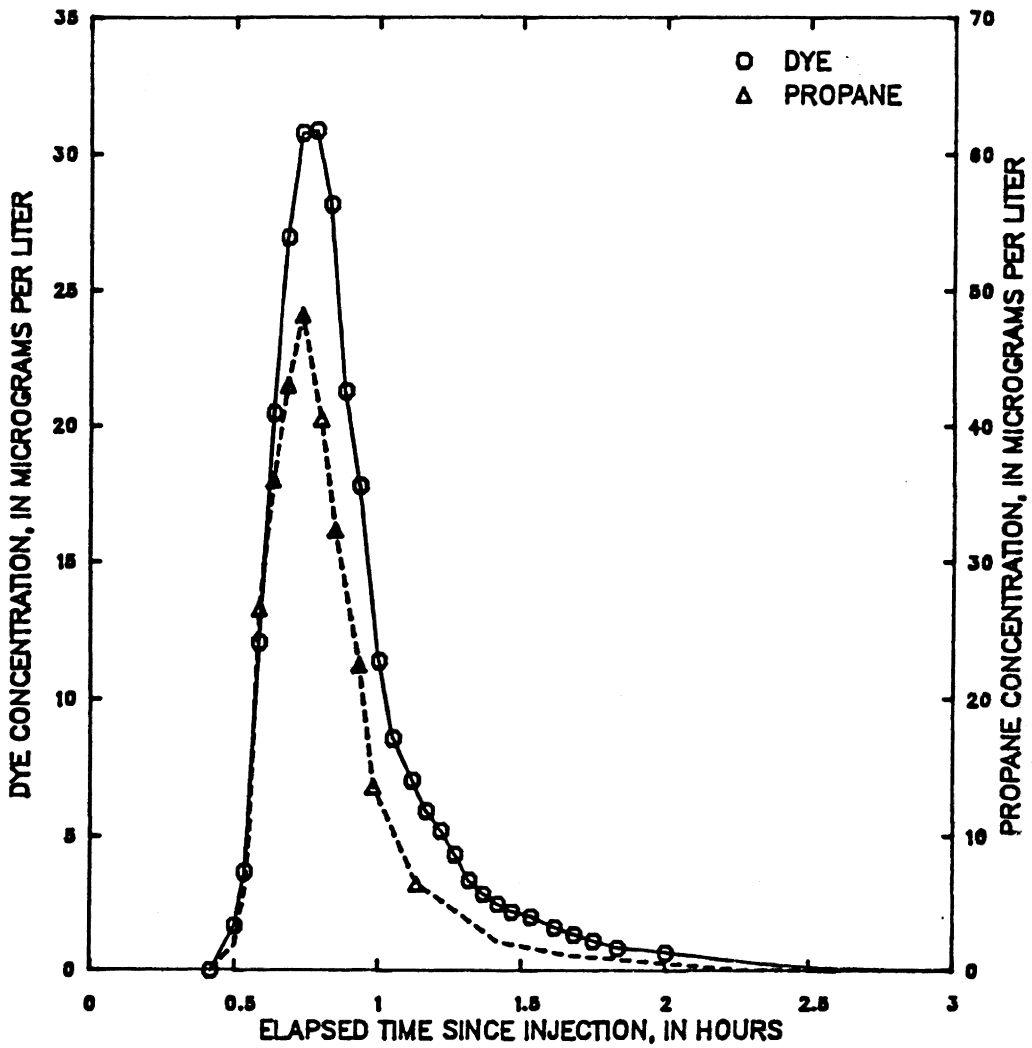


Figure 59 -- Dye and propane concentration from hydrocarbon gas tracer measurements made on Middle Fork Beargrass Creek, upstream end of reach A (upstream end of reach C), June 14, 1985 tracer injection

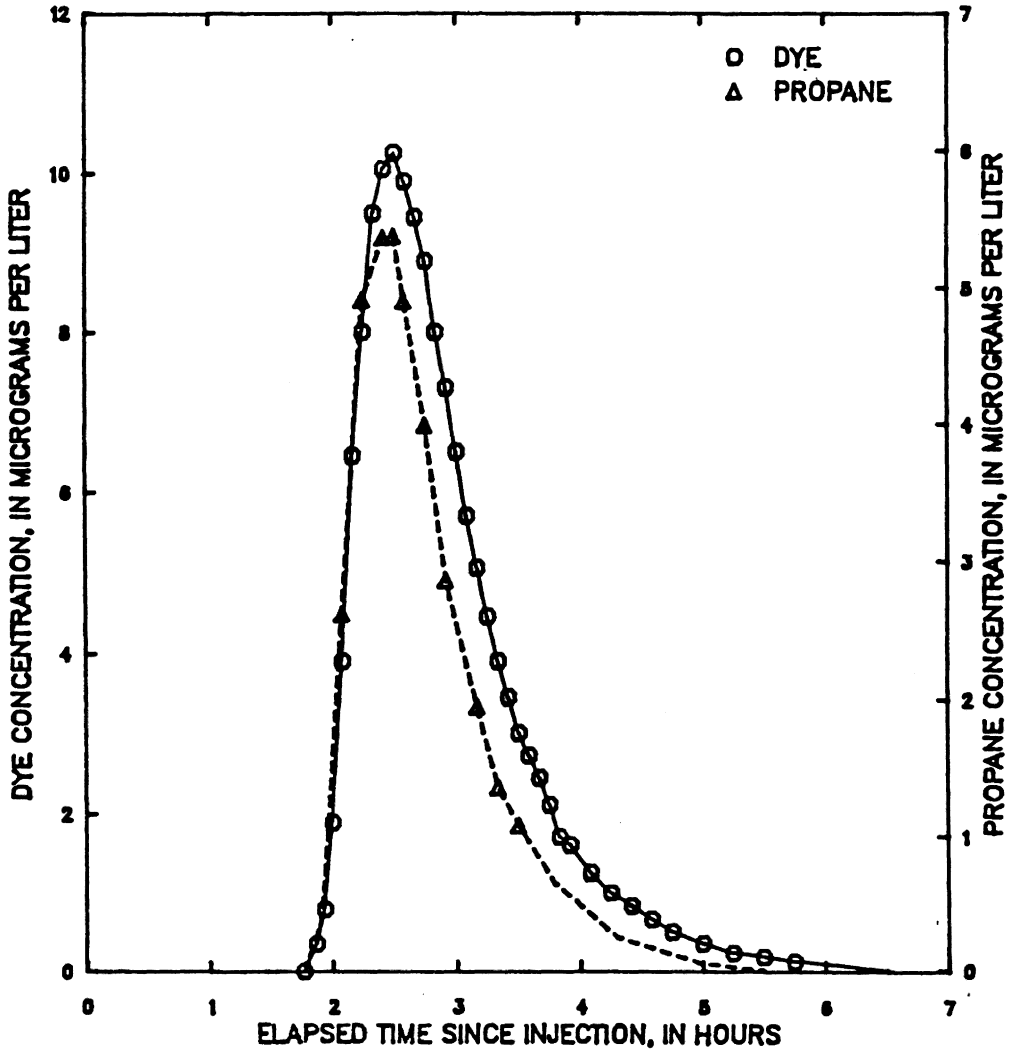


Figure 60 -- Dye and propane concentration from hydrocarbon gas tracer measurements made on Middle Fork Beargrass Creek, downstream end of reach A (upstream end of reach B), June 14, 1985 tracer injection

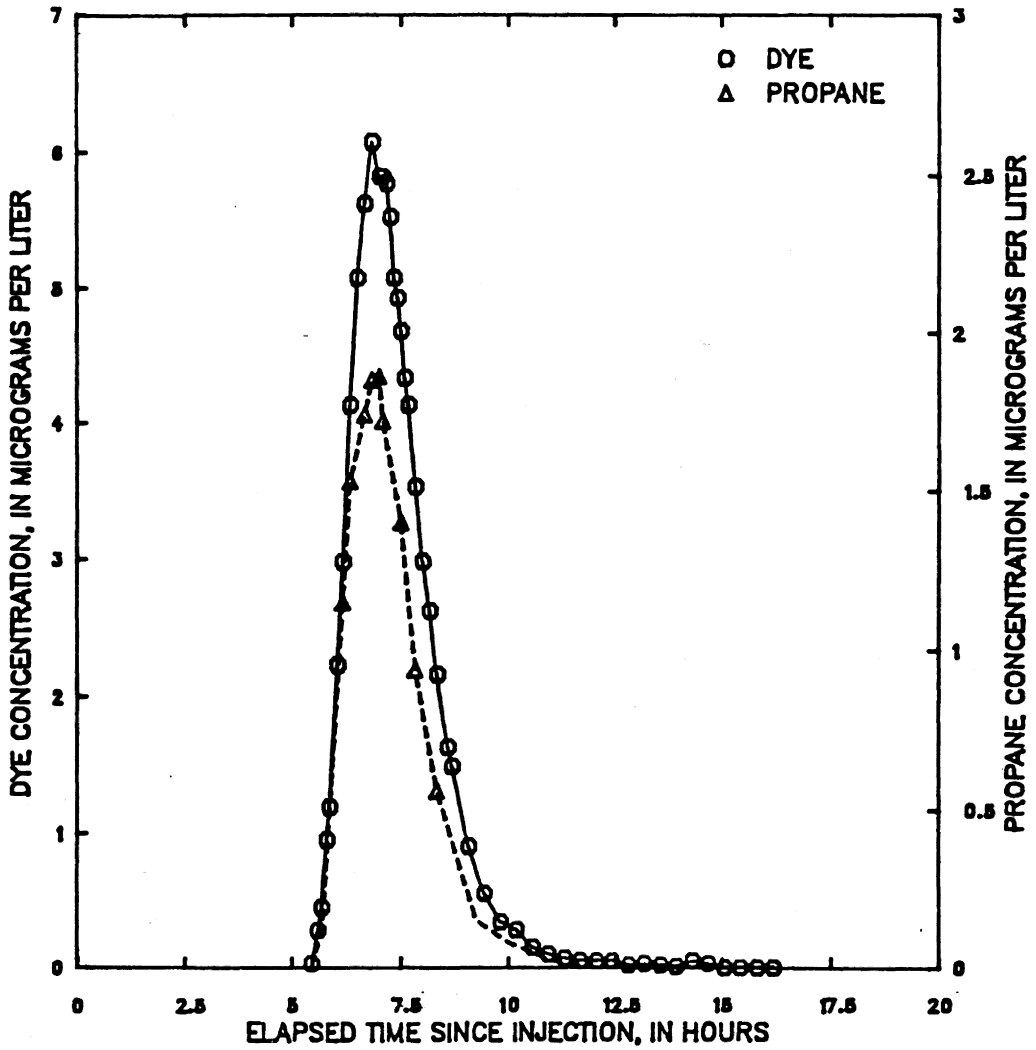


Figure 61 -- Dye and propane concentration from hydrocarbon gas tracer measurements made on Middle Fork Beargrass Creek, downstream end of reach B (downstream end of reach C), June 14, 1985 tracer injection

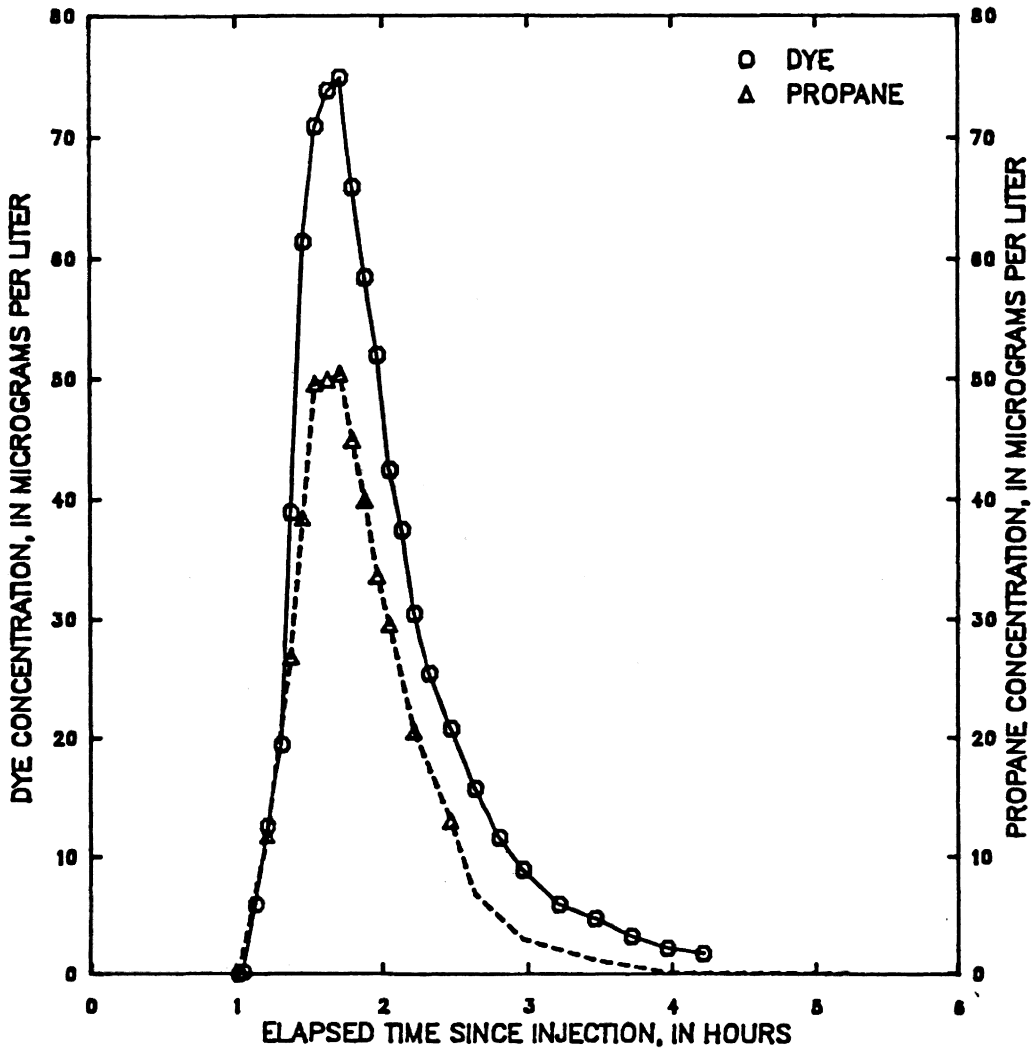


Figure 62 -- Dye and propane concentration from hydrocarbon gas tracer measurements made on Middle Fork Beargrass Creek, upstream end of reach A, August 19, 1985 tracer injection

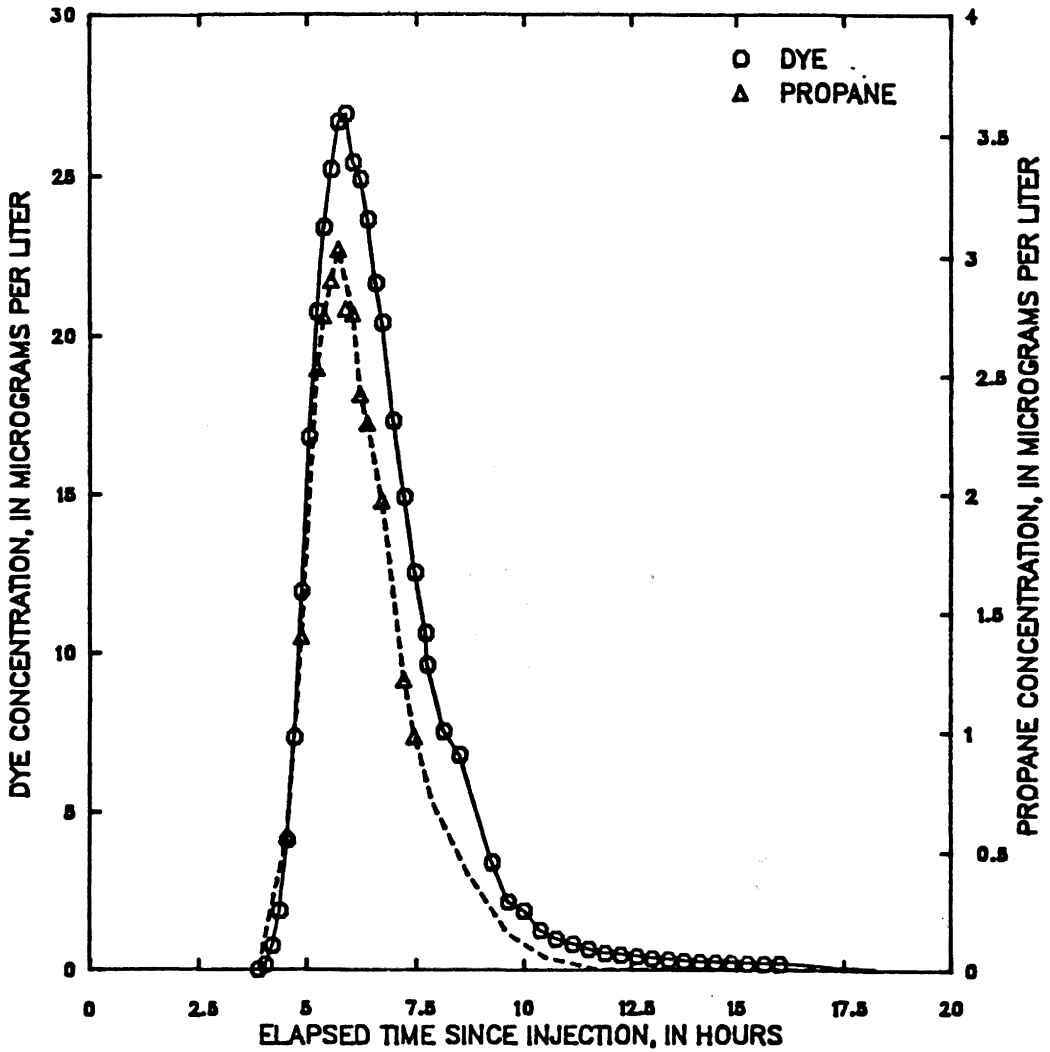


Figure 63 -- Dye and propane concentration from hydrocarbon gas tracer measurements made on Middle Fork Beargrass Creek, downstream end of reach A, August 19, 1985 tracer injection

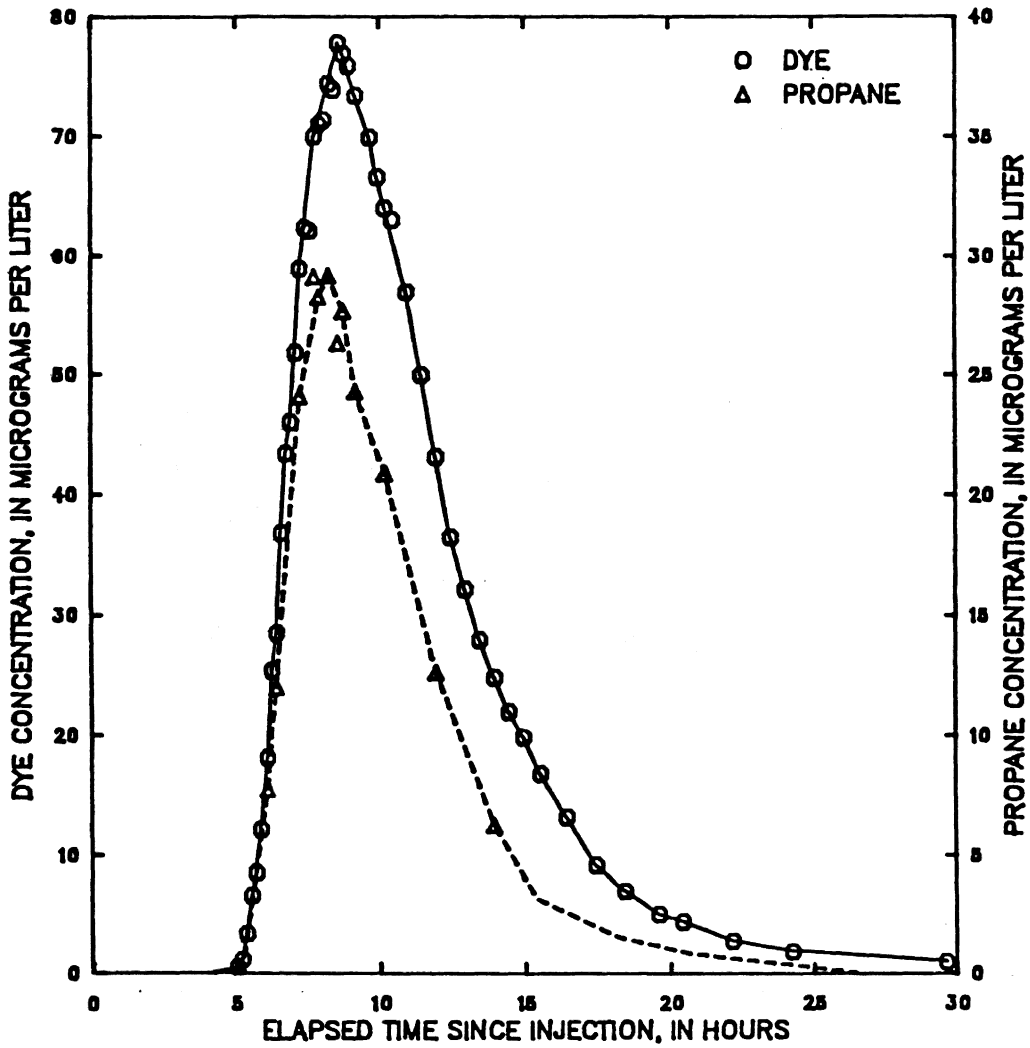


Figure 64 -- Dye and propane concentration from hydrocarbon gas tracer measurements made on Middle Fork Beargrass Creek, upstream end of reach A, September 17, 1985 tracer injection

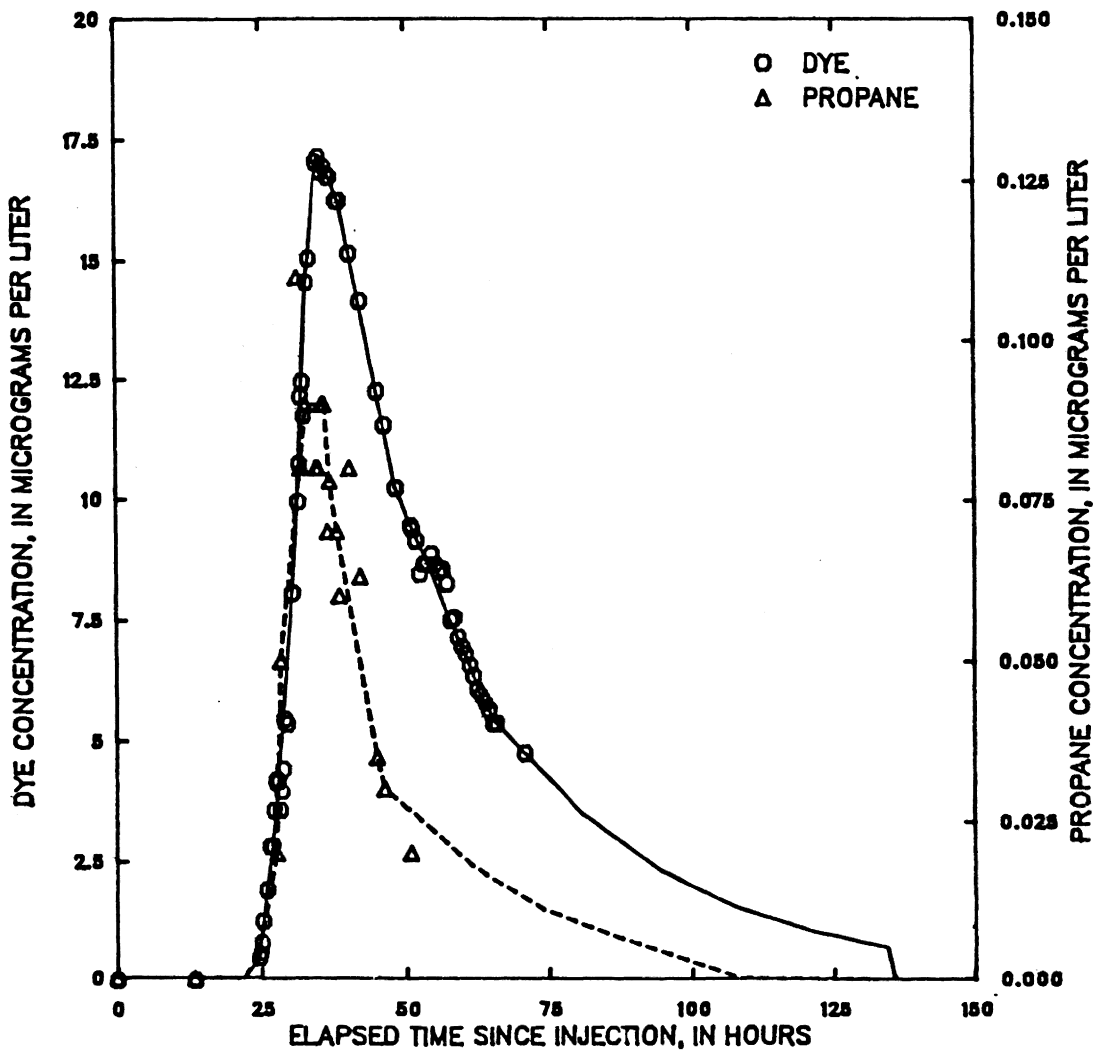


Figure 65 -- Dye and propane concentration from hydrocarbon gas tracer measurements made on Middle Fork Beargrass Creek, downstream end of reach A, September 17, 1985 tracer injection

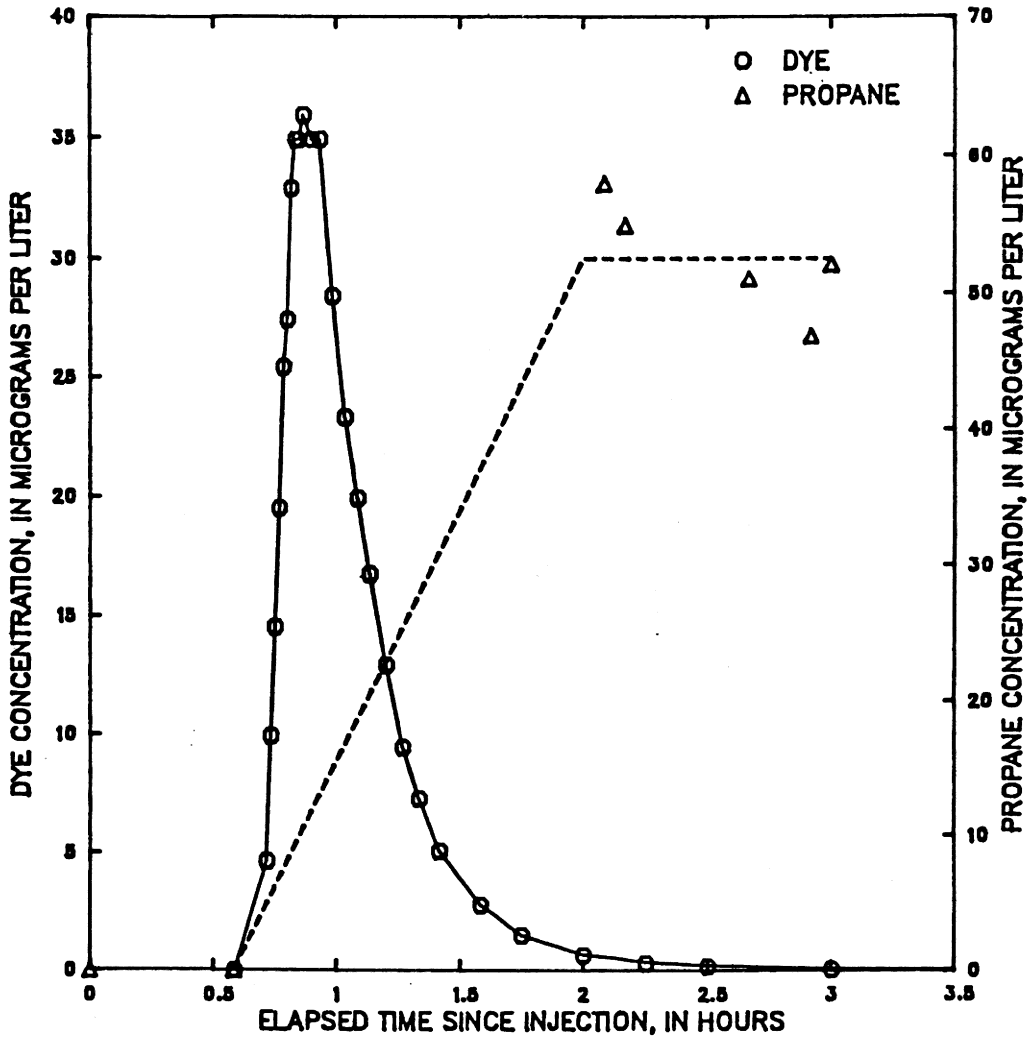


Figure 66 -- Dye and propane concentration from hydrocarbon gas tracer measurements made on Middle Fork Beargrass Creek, upstream end of reach D, April 19, 1985 tracer injection

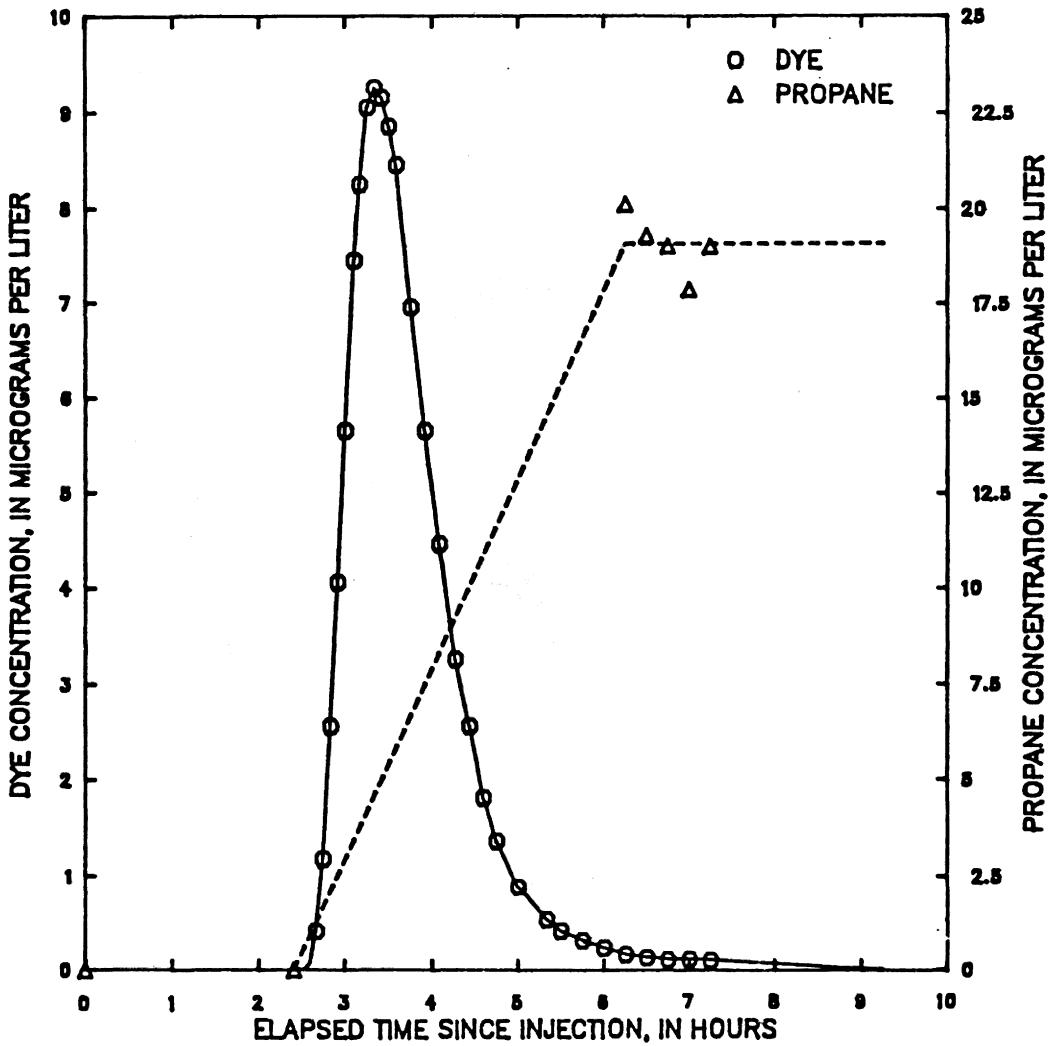


Figure 67 -- Dye and propane concentration from hydrocarbon gas tracer measurements made on Middle Fork Beargrass Creek, downstream end of reach D, April 19, 1985 tracer injection

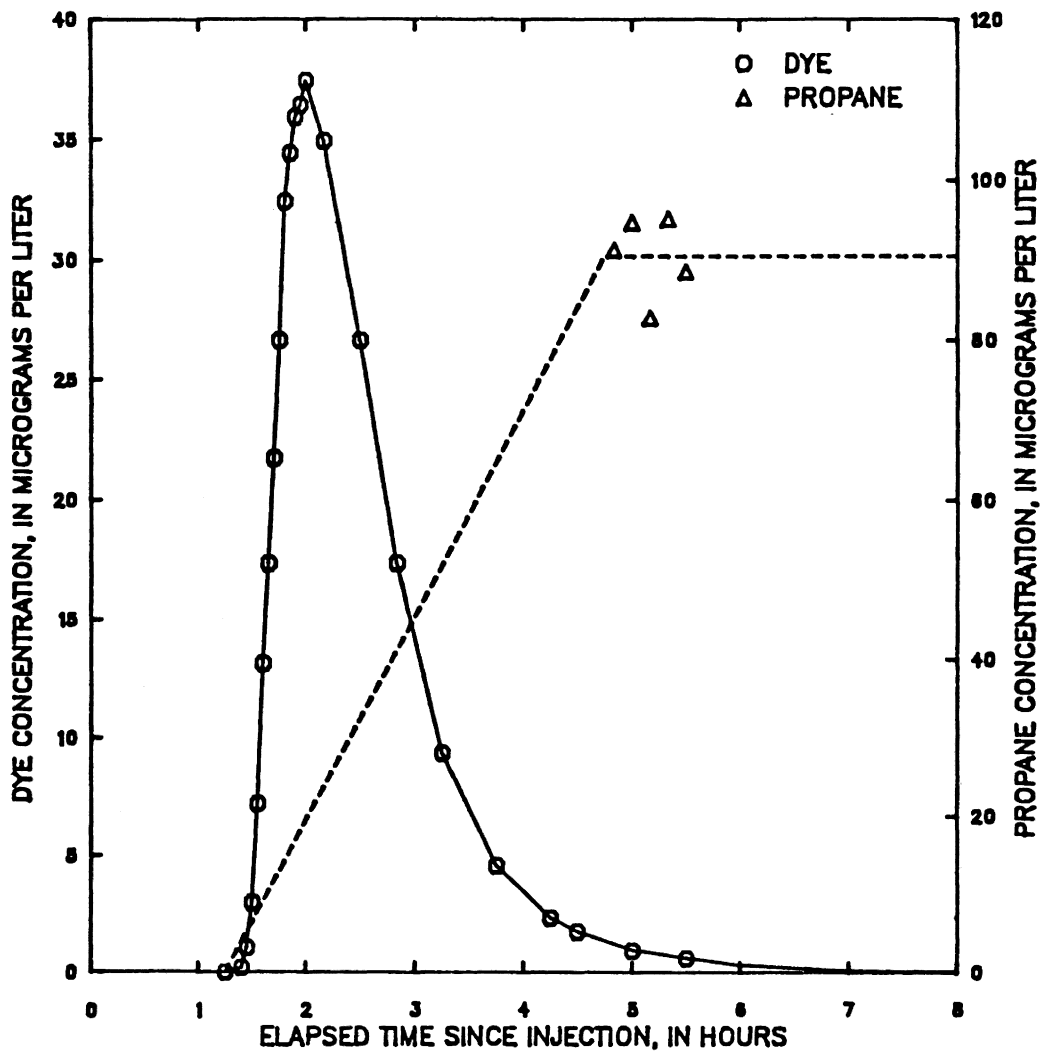


Figure 68 -- Dye and propane concentration from hydrocarbon gas tracer measurements made on Middle Fork Beargrass Creek, upstream end of reach D, May 7, 1985 tracer injection

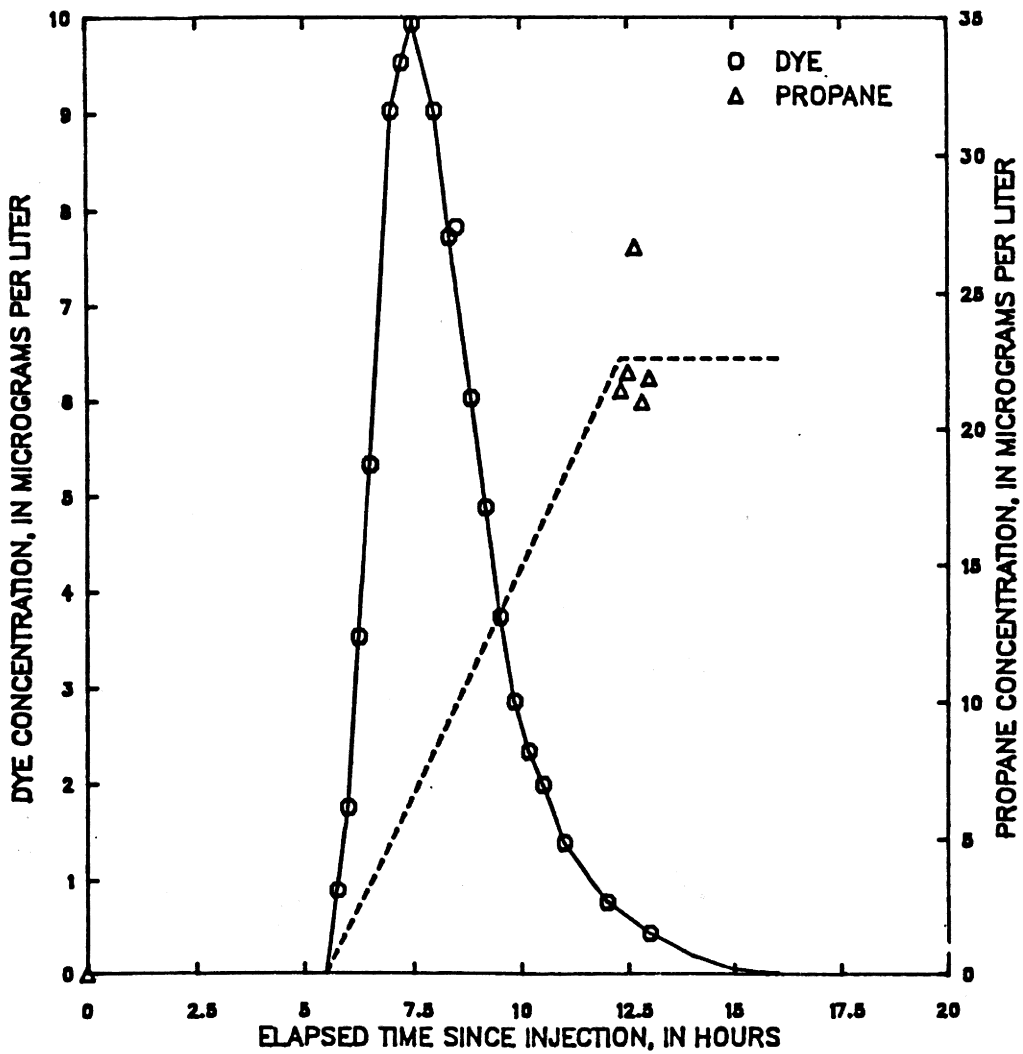


Figure 69 -- Dye and propane concentration from hydrocarbon gas tracer measurements made on Middle Fork Beargrass Creek, downstream end of reach D, May 7, 1985 tracer injection

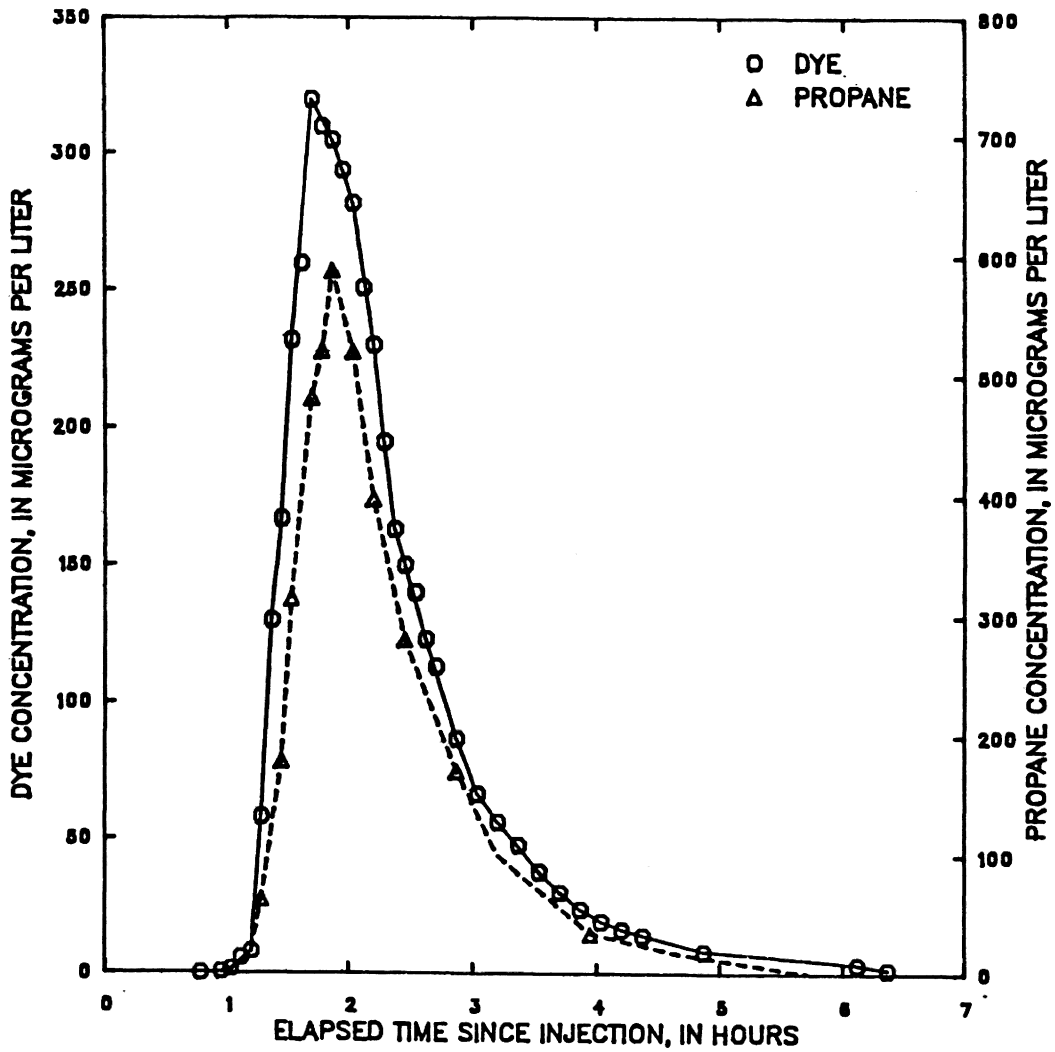


Figure 70 -- Dye and propane concentration from hydrocarbon gas tracer measurements made on Middle Fork Beargrass Creek, upstream end of reach D, September 18, 1985 tracer injection

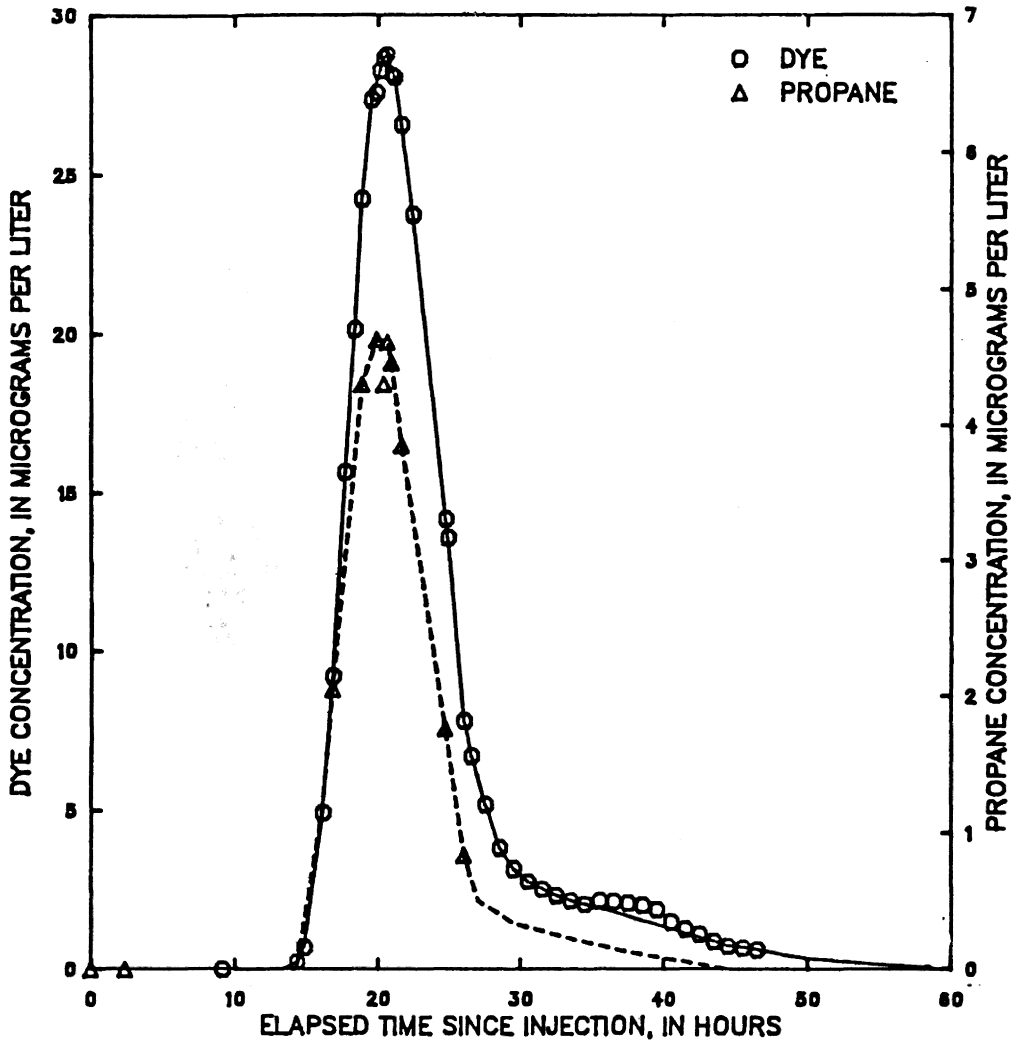


Figure 71 -- Dye and propane concentration from hydrocarbon gas tracer measurements made on Middle Fork Beargrass Creek, downstream end of reach D, September 18, 1985 tracer injection

APPENDIX C
PLOTS OF REAERATION COEFFICIENT VERSUS SELECTED HYDRAULIC PARAMETERS

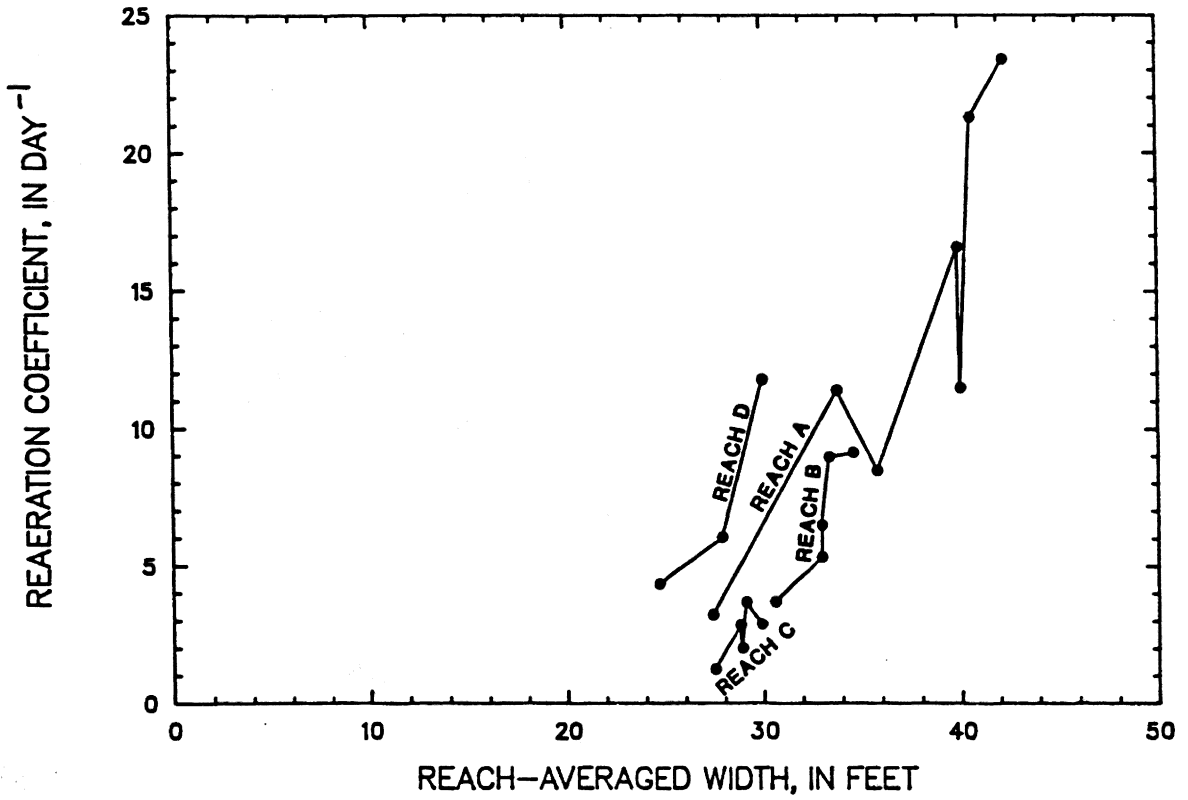


Figure 72 -- Reaeration coefficient shown as a function of reach-averaged width for reaches of Middle Fork Beargrass Creek, from tracer measurements made from April 18, 1985 through September 18, 1985

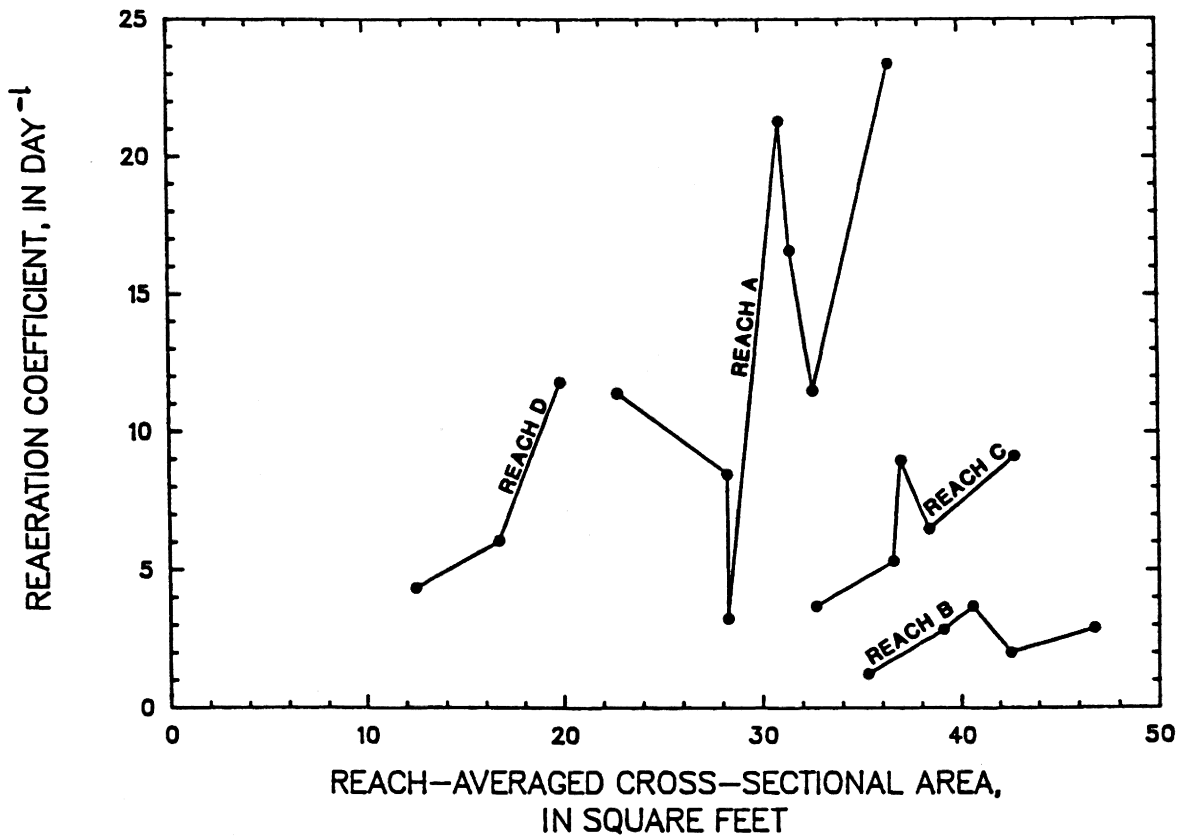


Figure 73 -- Reaeration coefficient shown as a function of reach-averaged cross-sectional area for reaches of Middle Fork Beargrass Creek, from tracer measurements made from April 18, 1985 through September 18, 1985

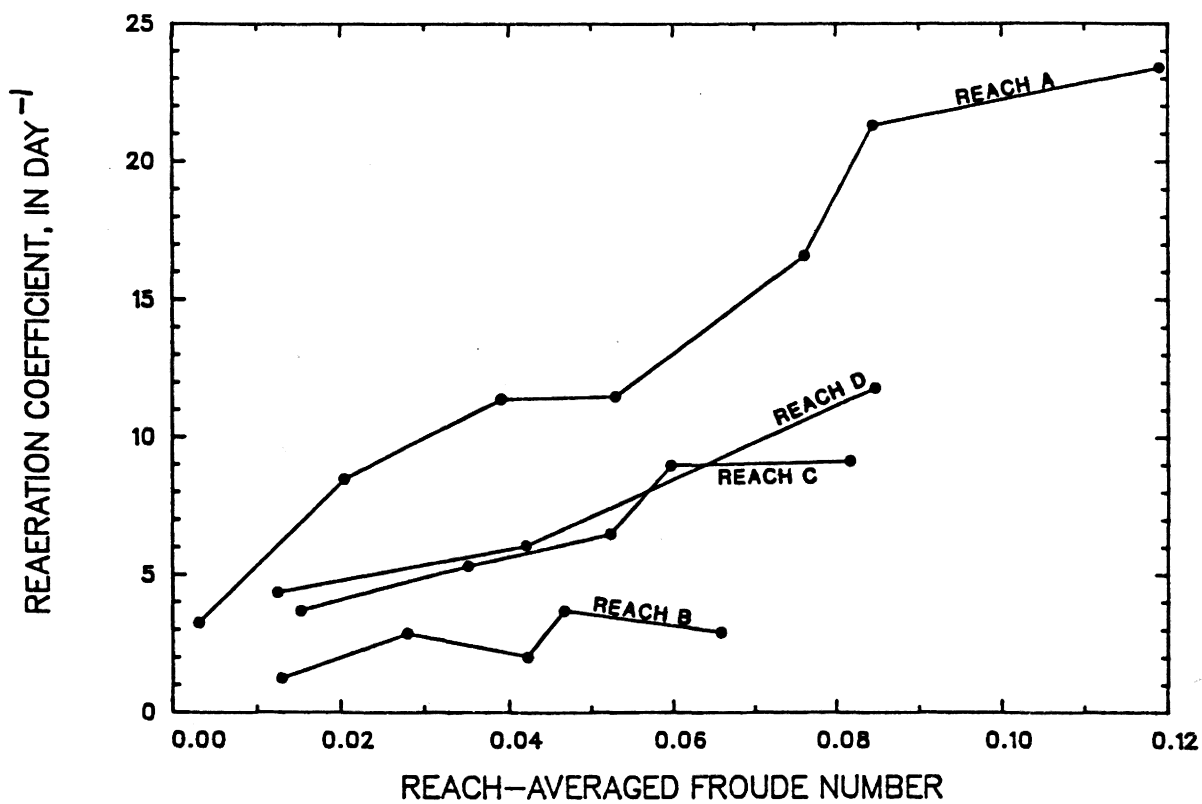


Figure 74 -- Reaeration coefficient shown as a function of reach-averaged Froude number for reaches of Middle Fork Beargrass Creek, from tracer measurements made from April 18, 1985 through September 18, 1985

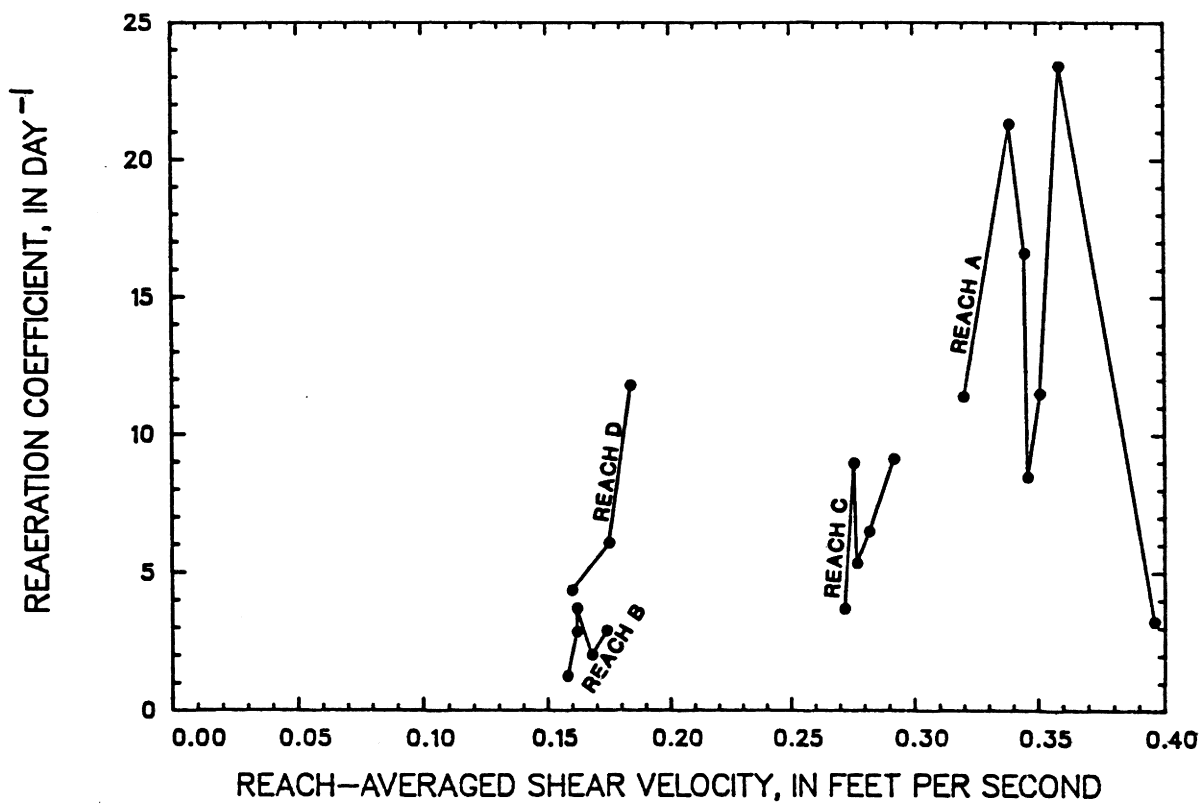


Figure 75 -- Reaeration coefficient shown as a function of reach-averaged shear velocity for reaches of Middle Fork Beargrass Creek, from tracer measurements made from April 18, 1985 through September 18, 1985

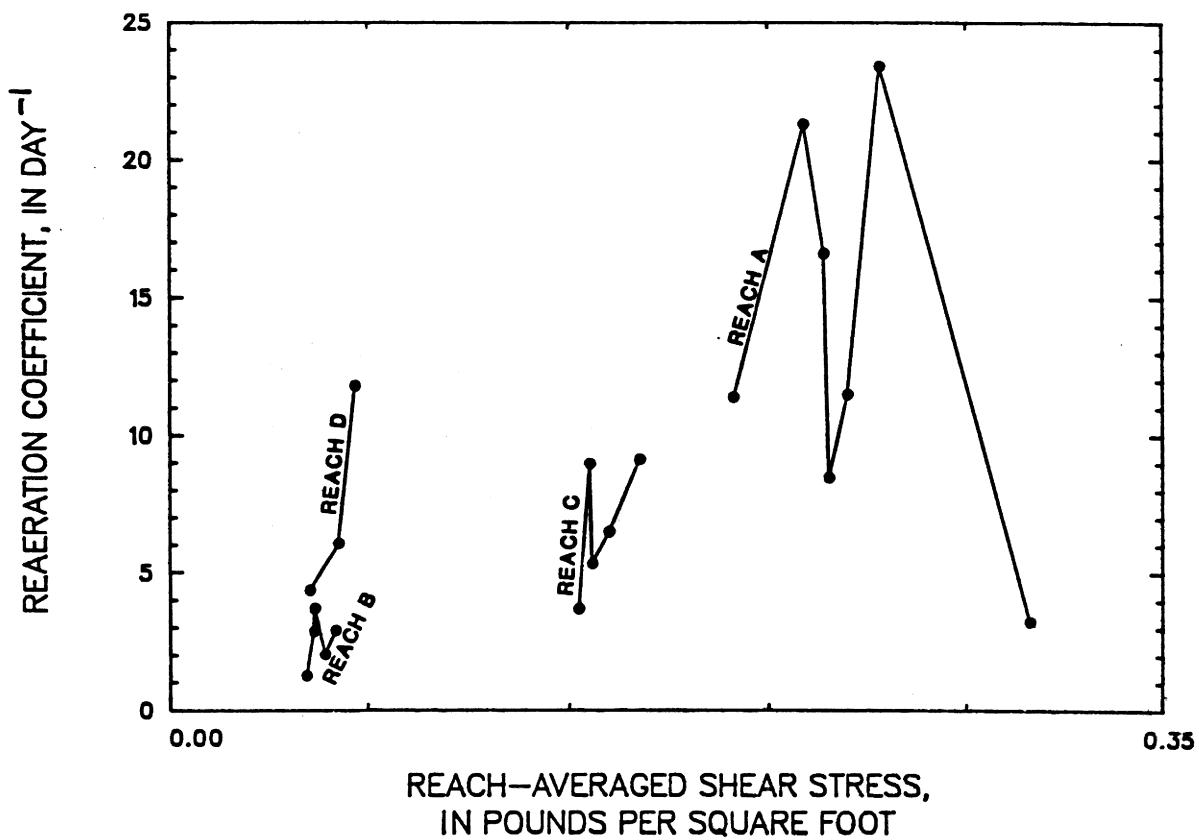


Figure 76 -- Reaeration coefficient shown as a function of reach-averaged shear stress for reaches of Middle Fork Beargrass Creek, from tracer measurements made from April 18, 1985 through September 18, 1985

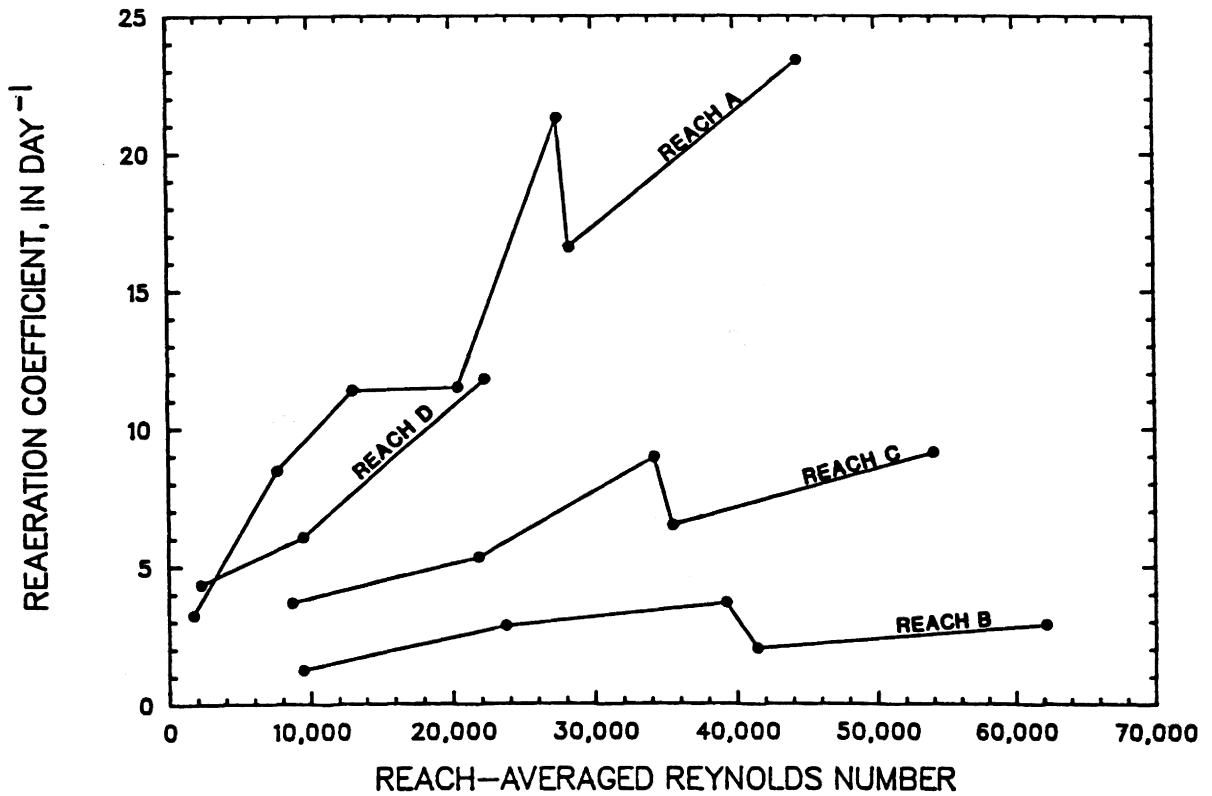


Figure 77 -- Reaeration coefficient shown as a function of reach-averaged Reynolds number for reaches of Middle Fork Beargrass Creek, from tracer measurements made from April 18, 1985 through September 18, 1985

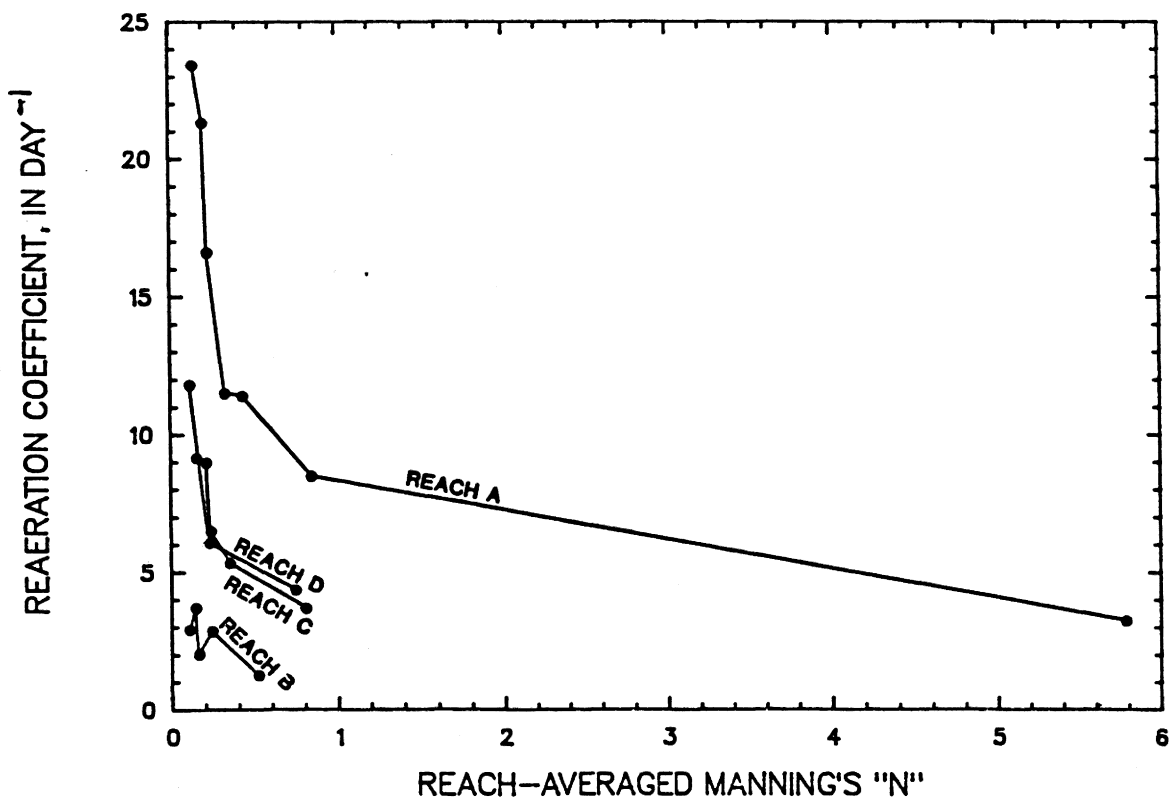


Figure 78 -- Reaeration coefficient shown as a function of reach-averaged Mannings "n" values for reaches of Middle Fork Beargrass Creek, from tracer measurements made from April 18, 1985 through September 18, 1985

APPENDIX D
REAERATION PREDICTION EQUATION VERIFICATION DATA SETS

Table 24 -- Verification data set from results of 39 hydrocarbon gas tracer measurements on 23 stream reaches in Kentucky and Massachusetts¹

DATA SOURCE	DISCHARGE (ft ³ /s)	SLOPE (ft/ft)	VELOCITY (ft/s)	DEPTH (ft)	WIDTH (ft)	K ₂ (day ⁻¹)
KY	0.270	0.010300	0.0929	0.202	14.4	31.10
KY	1.580	0.003960	0.2520	0.340	18.4	17.50
KY	37.300	0.000133	0.2630	2.360	60.1	1.32
KY	60.200	0.000138	0.3380	1.800	98.9	1.64
KY	68.200	0.000136	0.4580	1.690	88.1	1.93
KY	69.900	0.000317	0.4830	1.610	90.1	1.91
KY	72.600	0.000558	0.5210	1.500	92.7	1.89
KY	95.100	0.000138	0.4480	2.150	98.9	0.90
KY	168.000	0.000317	0.8980	2.080	90.1	1.89
MA	3.383	0.010100	0.1308	1.049	24.4	14.48
MA	4.979	0.015000	0.3061	0.569	28.3	26.70
MA	5.898	0.006960	0.4430	0.440	30.1	25.32
MA	6.000	0.008800	0.2690	0.931	24.0	36.79
MA	8.221	0.000390	0.3300	2.189	11.3	4.21
MA	8.723	0.008100	0.4491	0.469	41.2	17.80
MA	10.206	0.001800	0.3730	1.439	19.0	10.09
MA	13.490	0.004500	0.1750	1.013	76.3	19.18
MA	18.402	0.008220	0.4780	0.728	52.7	15.75
MA	21.507	0.000170	0.2411	1.490	60.0	4.18
MA	21.807	0.004360	0.3809	1.069	53.6	10.02
MA	22.107	0.006380	1.1040	0.419	47.4	42.95
MA	25.197	0.015000	0.9970	0.759	33.3	67.66
MA	25.215	0.001850	0.5679	1.109	39.9	12.33
MA	28.605	0.004430	0.3330	2.700	31.8	14.12
MA	29.912	0.000440	0.4279	3.660	19.1	5.07
MA	31.995	0.001800	0.8310	1.840	20.9	3.72
MA	47.904	0.006940	0.4038	1.030	115.5	17.16
MA	50.405	0.004350	0.4701	1.259	85.0	14.31
MA	57.704	0.009820	1.1778	1.319	36.9	43.60
MA	81.210	0.001830	1.0551	1.748	44.0	7.91
MA	87.316	0.004350	1.0830	1.200	67.3	20.36
MA	88.612	0.004070	0.8100	1.889	58.0	15.30
MA	136.014	0.008050	1.5771	1.680	51.3	32.99
MA	144.013	0.006910	0.9229	1.279	121.4	20.67
MA	151.006	0.000550	0.3061	3.490	141.2	0.35
MA	152.524	0.007000	1.6499	1.400	65.9	22.80
MA	322.529	0.004500	2.1460	1.840	81.5	40.01
MA	403.046	0.000470	0.4330	6.289	147.9	1.56
MA	446.060	0.000360	1.3690	3.730	87.4	11.10

¹Data from Parker and Gay (1987) and Ruhl and Smoot (1987).

Table 25 -- Reaeration coefficient prediction results for the Kentucky and Massachusetts verification data set

DATA SOURCE	DISCHARGE (ft ³ /s)	K ₂ (day ⁻¹)	PREDICTED REAERATION COEFFICIENT ¹ (day ⁻¹)			
			P1	P2	P3	P4
KY	0.270	31.100	9.215	48.957	10.652	35.512
KY	1.580	17.500	9.610	29.703	10.937	22.811
KY	37.300	1.320	0.337	0.801	1.331	0.689
KY	60.200	1.640	0.449	1.213	1.595	0.980
KY	68.200	1.930	0.600	1.493	1.913	1.196
KY	69.900	1.910	1.474	2.457	3.367	2.160
KY	72.600	1.890	2.800	3.634	5.038	3.369
KY	95.100	0.900	0.595	1.169	1.904	1.001
KY	168.000	1.890	2.741	2.593	4.972	2.496
MA	3.383	14.482	12.729	11.071	13.050	12.729
MA	4.979	26.708	44.216	38.013	28.540	39.903
MA	5.898	25.321	29.693	40.259	22.222	36.257
MA	6.000	36.794	22.799	16.694	18.823	18.696
MA	8.221	4.213	1.240	1.656	3.019	1.605
MA	8.723	17.807	35.035	41.101	24.657	38.380
MA	10.206	10.094	6.466	5.752	8.526	6.030
MA	13.490	19.184	7.584	8.849	9.425	9.206
MA	18.402	15.751	37.839	27.514	25.879	29.098
MA	21.507	4.184	0.395	1.373	1.471	1.070
MA	21.807	10.027	15.993	12.181	15.063	13.137
MA	22.107	42.956	67.829	63.891	37.346	57.860
MA	25.197	67.668	144.023	51.454	59.943	60.733
MA	25.215	12.337	10.118	9.336	11.297	9.268
MA	28.605	14.125	14.206	4.547	13.983	6.307
MA	29.912	5.070	1.813	1.198	3.835	1.369
MA	31.995	3.721	14.405	6.717	14.105	7.730
MA	47.904	17.166	26.992	16.429	20.929	18.610
MA	50.405	14.312	19.695	11.475	17.169	13.030
MA	57.704	43.609	111.383	26.049	51.003	34.133
MA	81.210	7.911	18.594	8.033	16.560	9.205
MA	87.316	20.367	45.368	18.274	29.005	21.040
MA	88.612	15.300	31.749	9.713	23.177	12.443
MA	136.014	32.993	122.259	21.440	54.079	29.565
MA	144.013	20.676	61.413	19.953	35.085	24.625
MA	151.006	0.354	1.621	1.188	3.574	1.362

(continued)

Table 25 (continued) -- Reaeration coefficient prediction results for the Kentucky and Massachusetts verification data set

DATA SOURCE	DISCHARGE (ft ³ /s)	K ₂ (day ⁻¹)	PREDICTED REAERATION COEFFICIENT ¹ (day ⁻¹)			
			P1	P2	P3	P4
MA	152.524	22.802	111.222	24.525	50.957	31.671
MA	322.529	40.012	92.997	17.069	45.537	22.686
MA	403.046	1.566	1.960	0.725	4.027	0.969
MA	446.060	11.100	4.746	1.902	7.021	2.213

¹P1, P2, P3, and P4 refer to developed prediction equations and are shown in table 22.

**The three page vita has been
removed from the scanned
document. Page 1 of 3**

**The three page vita has been
removed from the scanned
document. Page 2 of 3**

**The three page vita has been
removed from the scanned
document. Page 3 of 3**